OULU 2015
C 520

ACTA UNIVERSITATIS OULUENSIS

Heikki Karvonen

ENERGY EFFICIENCY IMPROVEMENTS FOR WIRELESS SENSOR NETWORKS BY USING CROSS-LAYER ANALYSIS

UNIVERSITY OF OULU GRADUATE SCHOOL;
UNIVERSITY OF OULU,
FACULTY OF INFORMATION TECHNOLOGY AND ELECTRICAL ENGINEERING,
DEPARTMENT OF COMMUNICATIONS ENGINEERING;
CENTRE FOR WIRELESS COMMUNICATIONS;
INFOTECH OULU

ACTA UNIVERSITATIS OULUENSIS
C Technica 520

HEIKKI KARVONEN

ENERGY EFFICIENCY IMPROVEMENTS FOR WIRELESS SENSOR NETWORKS BY USING CROSS-LAYER ANALYSIS

Academic dissertation to be presented with the assent of the Doctoral Training Committee of Technology and Natural Sciences of the University of Oulu for public defence in the OP auditorium (L10), Linnanmaa, on 12 March 2015, at 12 noon

UNIVERSITY OF OULU, OULU 2015

Acta Univ. Oul. C 520, 2015

Supervised by
Professor Jari Iinatti
Professor Carlos Pomalaza-Ráez
Doctor Matti Hämäläinen

Reviewed by
Doctor John Farserotu
Associate Professor Mehmet Can Vuran

Opponents
Doctor John Farserotu
Associate Professor Kimmo Kansanen

ISBN 978-952-62-0749-0 (Paperback)
ISBN 978-952-62-0750-6 (PDF)

ISSN 0355-3213 (Printed)
ISSN 1796-2226 (Online)

Cover Design
Raimo Ahonen

JUVENES PRINT
TAMPERE 2015

Karvonen, Heikki, Energy efficiency improvements for wireless sensor networks by using cross-layer analysis.
University of Oulu Graduate School; University of Oulu, Faculty of Information Technology and Electrical Engineering, Department of Communications Engineering; Centre for Wireless Communications; Infotech Oulu
Acta Univ. Oul. C 520, 2015
University of Oulu, P.O. Box 8000, FI-90014 University of Oulu, Finland

Abstract

This thesis proposes cross-layer approaches which enable to improve energy efficiency of wireless sensor networks and wireless body area networks (WSN & WBAN). The focus is on the physical (PHY) and medium access control (MAC) layers of communication protocol stack and exploiting their interdependencies. In the analysis of the PHY and MAC layers, their relevant characteristics are taken into account, and cross-layer models are developed to study the effect of these layers on energy efficiency. In addition, cross-layer analysis is applied at the network level by addressing hierarchical networks' energy efficiency. The objective is to improve energy efficiency by taking into account that substantial modifications to current standards and techniques are not required to take advantage of the proposed methods.

The studied scenarios of WSN take advantage of the wake-up radio (WUR). A generic WUR-based MAC (GWR-MAC) protocol with objective to improve energy efficiency by avoiding idle listening is proposed. First, the proposed cross-layer model is developed at a general level and applied to study the forward error correction (FEC) code rate selection effect on the length of the transmission period and energy efficiency in a star topology network. Then an energy efficiency model for intelligent hierarchical architecture based on GWR-MAC is proposed and performance comparison with a duty-cycle radio (DCR) approach is performed. Interactions between different layers' devices are taken into account, and the WUR and DCR approaches are compared as a function of event frequency. The third cross-layer model focuses on the effect of the FEC code rate and data packet payload length on the energy efficiency of the IEEE Std 802.15.6-based WBANs using IR-UWB PHY.

The results acquired by using analytical modelling and simulations with the Matlab software clearly illustrates the potential energy gains that can be achieved with the proposed cross-layer approaches. The developed WUR-based MAC protocol, analytical models and achieved results can be exploited by other researchers in the WSN and WBAN field. The contribution of this thesis is also to stimulate further research on these timely topics and foster development of short-range communication, which has a crucial role in future converging networks such as the Internet of Things.

Keywords: cross-layer design, forward error correction, hierarchical network, medium access control, wake-up radio, wireless body area network

Karvonen, Heikki, Langattomien sensoriverkkojen energiatehokkuuden parantaminen kerrosten välistä analyysiä käyttämällä.

Oulun yliopiston tutkijakoulu; Oulun yliopisto, Tieto- ja sähkötekniikan tiedekunta, Tietoliikennetekniikan osasto; Centre for Wireless Communications; Infotech Oulu

Acta Univ. Oul. C 520, 2015

Oulun yliopisto, PL 8000, 90014 Oulun yliopisto

Tiivistelmä

Tässä väitöskirjassa ehdotetaan protokollakerrosten välistä tietoa hyödyntäviä (cross-layer) lähestymistapoja, jotka mahdollistavat energiatehokkuuden parantamisen langattomissa sensori- ja kehoverkoissa. Työ kohdistuu fyysisen- ja kanavanhallintakerroksen välisen vuorovaikutuksen tutkimiseen. Fyysisen- ja kanavanhallintakerrosten analyysissä huomioidaan niiden tärkeimmät ominaisuudet ja tutkitaan kerrosten yhteistä energiatehokkuutta. Lisäksi kerrosten välistä analyysiä sovelletaan verkkotasolle tutkimalla hierarkkisen verkon energiatehokkuutta. Tavoitteena on energiatehokkuuden parantamisen mahdollistaminen siten, että merkittäviä muutoksia nykyisiin standardeihin ja tekniikoihin ei tarvitse tehdä hyödyntääkseen ehdotettuja menetelmiä.

Tutkitut sensoriverkkoskenaariot hyödyntävät heräteradiota. Väitöskirjassa ehdotetaan geneerinen heräteradiopohjainen kanavanhallintaprotokolla (GWR-MAC), jolla parannetaan energiatehokkuutta vähentämällä turhaa kanavan kuuntelua. Kerrosten välinen malli kehitetään ensin yleisellä tasolla ja sen avulla tutkitaan virheenkorjauskoodisuhteen valinnan vaikutusta lähetysperiodin pituuteen ja energiatehokkuuteen tähtitopologiaan pohjautuvissa sensoriverkoissa. Sitten väitöskirjassa ehdotetaan energiatehokkuusmalli älykkäälle GWR-MAC -protokollaan perustuvalle hierarkkiselle arkkitehtuurille ja sen suorituskykyä vertaillaan toimintajaksoperiaatteella toimivaan lähestymistapaan. Eri kerroksilla olevien laitteiden väliset vuorovaikutukset huomioidaan heräteradio- ja toimintajaksoperiaatteella toimivien verkkojen suorituskykyvertailussa tapahtumatiheyden funktiona. Kolmas malli kohdistuu virheenkorjauskoodisuhteen ja datapaketin hyötykuorman pituuden energiatehokkuusvaikutuksen tutkimiseen IEEE 802.15.6 -standardiin perustuvissa langattomissa kehoverkoissa.

Analyyttinen mallinnus ja Matlab-ohjelmiston avulla tuotetut simulointitulokset osoittavat selvästi energiatehokkuushyödyt, jotka saavutetaan ehdotettuja menetelmiä käyttämällä. Kehitetty GWR-MAC -protokolla, analyyttiset mallit ja tulokset ovat hyödynnettävissä sensori- ja kehoverkkotutkijoiden toimesta. Tämän väitöskirjan tavoitteena on myös näiden ajankohtaisten aiheiden jatkotutkimuksen stimulointi sekä lyhyen kantaman viestinnän kehityksen vauhdittaminen, sillä niillä on erittäin merkittävä rooli tulevaisuuden yhteen liittyvissä verkoissa, kuten esineiden ja asioiden Internetissä.

Asiasanat: heräteradio, hierarkkinen verkko, kanavanhallinta, kerrosten välinen suunnittelu, langaton kehoverkko, virheenkorjaus

To my family

Preface

This doctoral thesis work has been carried out as a part of research projects implemented at the Centre for Wireless Communications (CWC), Department of Communications Engineering (DCE), University of Oulu, Finland. These projects have been funded by different sources: the Finnish Funding Agency for Innovation (Tekes), European Union (EU), industry companies, Academy of Finland and CWC. The research started in the Tekes and industry-funded Concepts for Ultra wideband Systems (CUBS) project. The work continued in the EU-funded SENSEI project and in the Tekes and industry-funded WAS project. The CWC and Academy of Finland project Dependable Wireless Healthcare Networks (DWHN) has funded the final phase of this doctoral thesis. In each of the amentioned projects, research related to this doctoral thesis has always been performed when the project scope has matched up with the author's thesis topic. The author has also received personal grants to support and stimulate this doctoral research work from the Tauno Tönning Foundation (Tauno Tönningin säätiö), Seppo Säynäjäkangas Science Foundation (Seppo Säynäjäkankaan tiedesäätiö), Finnish Foundation for Technology Promotion (Tekniikan edistämissäätiö, TES), Ulla Tuominen Foundation (Ulla Tuomisen säätiö) and Riitta and Jorma J. Takanen Foundation (Riitta ja Jorma J. Takasen säätiö), which are gratefully acknowledged.

I want to acknowledge the persons who acted as CWC (and currently DCE) leaders during my postgraduate studies: Professor Matti Latva-aho, Dr. Ari Pouttu and Professor Jari Iinatti. They successfully lead our research unit and gave me the opportunity to perform doctoral research work. I want to gratefully acknowledge my supervisor, Professor Jari Iinatti, for invaluable guidance during the postgraduate research, in the thesis manuscript writing phase and in the preparation of the joint publications. I want to thank Jari for the patience, trust and support he has shown towards my research work and also for affording me the opportunity to work in interesting projects as well as participate in teaching duties during my postgraduate studies. I want to give my sincere thanks to Professor Carlos Pomalaza-Ráez (University of Purdue, Indiana, US) for the supervision of my research. Carlos has always been sincerely willing to discuss the research problems and to do cooperation and joint publications related to my postgraduate studies. Dr. Matti Hämäläinen also supervised my research work and he is a co-author in the majority of the publications related to this thesis. He has

also successfully lead our short-range communication research group and given me opportunities to perform research work in projects in that area. He was also the project manager of the CUBS project and the responsible leader in the WAS project, where I worked as the project manager. Thank you, Matti, for those efforts and also for being a friendly colleague in daily work and during working trips. I am also gratefully thankful to Dr. Timo Bräysy, who gave me the topic for my master's thesis which finally lead to a continuation towards the doctoral thesis research. I also want to thank Zach Shelby, who helped me a lot to get introduced with WSNs already during my master's thesis work and in the early phase of my postgraduate studies. Dr. Jussi Haapola is greatly acknowledged for being my project manager during the SENSEI project; he has always been willing to discuss and share his knowledge related to WSNs during my doctoral thesis research.

I want to greatly thank the pre-examiners of this thesis, Dr. John Farserotu (CSEM, Neuchâtel, Switzerland) and Associate Professor Mehmet Can Vuran (University of Nebraska-Lincoln, US). Their professional and valuable comments helped me to improve the thesis in many ways.

I am also gratefully thankful to all the other, not yet mentioned, co-authors of my publications. Particularly, I want to thank Juha Petäjäjärvi for the cooperation on wake-up radio-related research. Thanks belongs also to all the colleagues at the CWC (DCE) who have made the working environment pleasant and inspiring. Particularly, I would like to thank the most frequent lunch companions during the years, daily work and travelling companions, and office mates: Harri Viittala, Juha Petäjäjärvi, Jani Saloranta, Dr. Jussi Haapola, Martti Huttunen, Lic. Tech. Timo Kumpuniemi, Dr. Timo Bräysy, Dr. Harri Saarnisaari, Tuomas Paso, Lic. Tech. Visa Tapio, Dr. Marko Sonkki, Ville Niemelä, Ikram Ashraf, Hasnain Virk and Dr. Xiaojia Lu. Great thanks also goes to all of our management staff, who have been very helpful and friendly in daily work-related issues as well as in general, in particular, I want to acknowledge Hanna Saarela, Kirsi Ojutkangas, Eija Pajunen, Elina Komminaho, Timo Äikäs and Jari Sillanpää.

In my personal life, there are many important persons who have supported me and given enjoyable content to my life. First, my father Pertti, mother Tuula and sister Johanna are greatly acknowledged for always being a trusted family backbone network in my life. Then I want to thank my wife Paula for support, patience, and being beside me during the entire doctoral research carrier. Very big thanks to our great sons, Eetu and Ilmari, for all the good they have brought to my life and for reminding me what is really important in life. Very great sincere thanks belong to my closest friends, who have been

very important to me since childhood. We have shared many unforgettable free-time moments, activities and trips whose importance to my life is invaluable. Thanks belongs also to our family's acquaintances for sharing free time and to all other close people who have become important to me in various different ways during this journey. There are many friends who have been important with respect to my hobbies, which have been crucial to maintaining a good physical condition and fresh mind. Therefore, I want to thank all the guys in my Finnish baseball and rink ball teams as well as my hunting and golf friends, who have been important during the hobbies and some of whom have become my very good friends also outside the hobbies. Very warm thanks also to all, in particular, Petra and Heikki, who have made our family life much easier by taking care of our kids many times. That has helped us a lot to organize our working tasks and free-time activities.

Finally, I want to thank Outi Hiltunen for reviewing the language of the thesis manuscript.

Symbols and Abbreviations

α	power delay profile coefficient
β	raw bit error probability of the channel
ε	the number of events during the operation time t_{o}
$\varepsilon_{\mathrm{EL}}$	number of events at elementary layer (EL)
$\varepsilon_{\mathrm{IL}}$	number of events at intermediate layer (IL)
$\varepsilon_{\mathrm{AL}}$	number of events at advanced layer (AL)
$\varepsilon_{\mathrm{add}}$	addition operation energy consumption
$\varepsilon_{\mathrm{mult}}$	multiplication operation energy consumption
$\varepsilon_{\mathrm{inv}}$	inversion operation energy consumption
$\varepsilon_{\mathrm{b},0}$	energy per uncoded bit
$\varepsilon_{\mathrm{b},i}$	energy per bit for i:th code rate
ε_{s}	energy per symbol
$\varepsilon^{i}_{\mathrm{enc}}$	encoding energy consumption for i:th BCH code rate
$\varepsilon^{i}_{\mathrm{dec}}$	decoding energy consumption for i:th BCH code rate
η	energy efficiency metric
η_i	energy efficiency for i:th code rate
η_0	energy efficiency for uncoded case
η_{r}	energy efficiency for reference case
η_{new}	energy efficiency after code rate adaptation
η_{old}	energy efficiency before code rate adaptation
η^{i}_{norm}	normalized energy efficiency
$\eta^{i}_{\mathrm{ov,norm}}$	overall normalized energy efficiency
$\eta^{i}_{\mathrm{dis,norm}}$	energy efficiency normalized at each distance point
λ	payload length
λ_{dc}	duty-cycle value
$\hat{\lambda}_{\mathrm{dc}}$	set of duty-cycle values
λ_{max}	maximum payload length
$\lambda_{x,y}$	elements of fundamental matrix when $x, y = 0, 1, \cdots, N-1$
γ_{CRA}	code rate adaptation threshold
ς	number of arrival(s) according to a Poisson distribution

ζ	duty-cycle factor for the IEEE Std 802.15.6-based IR-UWB communication
$\Delta^{(u)}$	burst hopping position for user u
Γ_0	average number of steps to absorption when the initial state $S_t = 0$
γ_l	signal-to-noise ratio of the l:th multipath component
κ	number of nodes with a new packet arrival(s)
μ	non-centrality parameter of chi-square distributed random variable (RV)
Ψ_μ	characteristic function of chi-square distributed RV with non-centrality parameter μ
ρ	arrival rate for Poisson process
σ_0	two-sided noise power spectral density
τ	time period for Poisson process
Θ	time to absorption
Θ_i	time to absorption for i:th code rate
$\mathbf{A}$	fundamental matrix for absorbing chain
$\mathbf{P}$	state transition probability matrix
b	b:th symbol of OOK modulated signal
C	number of resolvable multipath components
CP	channel contention probability
$CP_{\max}$	maximum channel contention probability
$CP_{\min}$	minimum channel contention probability
d	distance
d_0	maximum distance for error free communication in the uncoded case
d_c^b	c:th code word component over the b:th symbol
E_{b}	energy per bit
$E_{\mathrm{b}}^{\mathrm{I}}$	integrated energy per bit
$E_{\mathrm{Imp}}^{\mathrm{MAC}}$	MAC layer imperfections part in the energy consumption
$E_{\mathrm{rx}}^{\mathrm{MAC}}$	MAC layer part in the energy consumption of receiver
$E_{\mathrm{tx,f}}^{\mathrm{MAC}}$	MAC layer part in the energy consumption of transmitter in failed communication case
$E_{\mathrm{tx,s}}^{\mathrm{MAC}}$	MAC layer part in the energy consumption of transmitter in successful communication case
$E_{\mathrm{rx}}^{\mathrm{PHY}}$	PHY layer part in the energy consumption of receiver
$E_{\mathrm{tx}}^{\mathrm{PHY}}$	PHY layer part in the energy consumption of transmitter

$E_{\mathrm{tx},i}^{\mathrm{PHY}}$	PHY layer part, for i:th code rate, in the energy consumption of transmitter
$E_{\mathrm{rx},i}^{\mathrm{PHY}}$	PHY layer part, for i:th code rate, in the energy consumption of receiver
E_{b}/N_0	energy per bit-to-noise ratio
E_{TP}	network energy consumption during a transmission period
$E_{\mathrm{TP},i}$	network energy consumption during a transmission period for i:th code rate
E_{link}^{i}	energy consumption for the communication link for i:th code rate
$E\{X_j\}$	expected number of transmissions occurred during a step, at state j
$E_{\mathrm{TOT,WUR}}^{\mathrm{EL}}$	total energy consumption of elementary layer when using WUR
$E_{\mathrm{TOT,WUR}}^{\mathrm{IL}}$	total energy consumption of intermediate layer when using WUR
$E_{\mathrm{TOT,WUR}}^{\mathrm{AL}}$	total energy consumption of advanced layer when using WUR
$E_{\mathrm{TOT,DCR}}^{\mathrm{EL}}$	total energy consumption of elementary layer when using DCR
$E_{\mathrm{TOT,DCR}}^{\mathrm{IL}}$	total energy consumption of intermediate layer when using DCR
$E_{\mathrm{TOT,DCR}}^{\mathrm{AL}}$	total energy consumption of advanced layer when using DCR
$E_{\mathrm{TX,WUS}}$	energy consumption of wake-up signal transmissions
$E_{\mathrm{RX,WUS}}$	energy consumption of wake-up signal receptions
$E_{\mathrm{TX,BC}}$	energy consumption of beacon transmission
$E_{\mathrm{RX,BC}}$	energy consumption of beacon receptions
E_{C}	constant energy consumption of wake-up radio
E_{clk}	energy consumption of the transceiver's clock
E_{s}^{x}	energy consumption of sensing when x is EL, IL or AL
E_{MCU}^{x}	energy consumption of MCU when x is EL, IL or AL
$E_{\mathrm{TX,D}}^{x}$	energy consumption of data packet transmission when x is EL, IL or AL
$E_{\mathrm{RX,D}}^{x}$	energy consumption of data packet receptions when x is EL, IL or AL
$E_{\mathrm{RX,DC}}^{x}$	energy consumption of channel listening when x is EL, IL or AL
$E_{\mathrm{TX,DE}}^{x}$	energy consumption of DE message transmission when x is EL, IL or AL
$E_{\mathrm{RX,DE}}^{x}$	energy consumption of DE message reception when x is EL, IL or AL
$E_{\mathrm{TOT}}^{\mathrm{NET}}$	total energy consumption of the network
$E_{\mathrm{wait,BC}}$	energy consumption of beacon listening
E_{ε}	energy consumption per event
f	parameter of interest for a function

f_c	central frequency of a signal
G	offered traffic load
G_j	offered traffic load at state j
$g_0^{(u)}$	transmitted data bit for user u
h	time hopping sequence
$h(t)$	channel impulse response
h_l	l:th multipath component
I	implementation losses
i	code rate index
I_{clk}	clock current consumption
$I_{CL,DCR}$	current consumption of channel listening
$I_{C,WUR}$	WUR constant idle mode current consumption
$I_{TX,EL}$	transmission mode current consumption at EL node
$I_{TX,IL}$	transmission mode current consumption at IL node
$I_{TX,AL}$	transmission mode current consumption at AL node
$I_{RX,EL}$	receiving mode current consumption at EL node
$I_{RX,IL}$	receiving mode current consumption at IL node
$I_{RX,AL}$	receiving mode current consumption at AL node
$I_{TX,WUR}$	WUR transmission mode current consumption
$I_{RX,WUR}$	WUR reception mode current consumption
$I_{MCU,EL}$	micro-controller current consumption at EL node
$I_{MCU,IL}$	micro-controller current consumption at IL node
$I_{MCU,AL}$	micro-controller current consumption at AL node
$I_{s,EL}$	sensor current consumption at EL node
$I_{s,IL}$	sensor current consumption at IL node
j	state of the Markov chain model
K	number of information bits in waveform coding mapping
k	number of information symbols (or bits) in a code word
k_i	number of information symbols (or bits) in a code word for i:th code rate
L	packet length in bits
l	multipath component index
L_i	length of the data packet in bits for i:th RS code rate
l_i	length of the data packet in bits for i:th BCH code rate
L_{ACK}	ACK frame length

L_{D}	length of the data packet
$L(d)_{\mathrm{dB}}$	path loss in dB as a function of distance d
L_{DE}	length of detected event (DE) packet
$L_{\mathrm{D,EL}}$	length of data packet for an EL node
$L_{\mathrm{D,IL}}$	length of data packet for an IL node
$L_{\mathrm{D,AL}}$	length of data packet for an AL node
L_P	length of particular packet type
L_{PH}	PHY header length
L_{PMH}	payload and MAC header length
L_{PRE}	preamble length in symbols
L_{W}	length of wake-up signal
m	Nakagami distribution severity index
m_{bch}	number of bits in Galois field ($2^{m_{\mathrm{bch}}}$) operation
m_{bs}	number of bits in RS coded symbol
$MAXi$	maximum number of code rates
n	number of symbols (or bits) in a code word
n_i	code word length for i:th code rate
$n(t)$	zero-mean white Gaussian noise component of a signal
n_{TX}	average number of transmissions required for success
N	number of sensor nodes in the network
NF	receiver noise figure
N_{bs}^{i}	number of bits for filling the last codeword for i:th code rate
N_{cpb}	number of chips per burst
N_{CW}^{i}	number of code words in frame for i:th code rate
N_{EL}	number of nodes at EL
N_{IL}	number of nodes at IL
N_{AL}	number of nodes at AL
N_0	one-sided thermal noise power per Hz
$N_{\mathrm{tx}}^{\mathrm{fail}}$	number of failed transmissions
N_{FCS}	number of octets in the frame check sequence
N_{idle}	total number of idle slots spent in a transmission period
N_j	number of nodes competing for channel access at state j
N_{MH}	number of octets in the MAC header
N_{MFB}	number of octets in the MAC frame body
$N_{\mathrm{tx,MC}}$	average number of transmissions to reach absorption state

N_{pad}	number of bits needed to align with symbol boundary at modulation
N'_{PSDU}	number of bits in the PSDU
N^{i}_{PSDU}	total number of bits before encoding for *i*:th code rate
$N^{\text{succ}}_{\text{tx}}$	number of successful transmissions
$N_{\text{steps},j}$	average number of steps required for success at state j
N^{i}_{T}	number of bits to be transmitted for *i*:th code rate
$N_{\text{tx},i}$	average number of transmissions required for *i*:th code rate
N_{w}	number of time hopping positions in the IR-UWB symbol structure
p	probability to transmit in a slot for a node
$p(t)$	IR-UWB pulse waveform
P_{a}	probability of new packet arrival(s) for a node during a transmission slot
P_{b}	bit error probability
$P_{\text{b},i}$	bit error probability before decoding for *i*:th code rate
$P^{\text{BCH}}_{\text{b},i}$	bit error probability after decoding for *i*:th BCH code rate
$P^{\text{RS}}_{\text{b},i}$	bit error probability after decoding for *i*:th RS code rate
$P_{\text{cw},i}$	code word error probability for *i*:th code rate
P_{idle}	power consumption in the idle mode
$P^{\text{MAC}}_{\text{fail}}$	probability of unsuccessful channel access (MAC layer)
$P^{\text{MAC}}_{\text{succ}}$	probability of successful channel access (MAC layer)
$P^{\text{PHY}}_{\text{fail}}$	probability of unsuccessful transmission (PHY layer)
$P^{\text{PHY}}_{\text{succ}}$	probability of successful transmission (PHY layer)
$P_{(x)}$	probability of event (x={1,2,...,6}) during the transmission period
P_{Ω}	probability that Ω nodes have a new packet to transmit
$P_{j,j+1}$	probability of transition from state j to state $j+1$ in a Markov chain model
$P^{\text{RS}}_{\text{s},i}$	symbol error probability after decoding for *i*:th RS code rate
P_{sd}	power spectral density
P_{q}	probability of no new packet arrival(s) for a node during a transmission slot
P_{rx}	power consumption in the receiving mode
$P_{\text{s},i}$	symbol error probability before decoding for *i*:th code rate
$P_{\text{tx,circ}}$	circuitry component of the transmitter power consumption
$P_{\text{tx,RF}}$	RF component of the transmitter power consumption
P_{tx}	power consumption in the transmission mode

P_{packet}	packet error probability
$P_{\text{packet},i}$	packet error probability for i:th code rate
$P^{i}_{\text{tx,RF}}$	transmitter RF power consumption factor for i:th code rate
$pSIFS$	short interframe spacing time
Q	alphabet size of waveform coding
$Q(\cdot)$	Q-function
r	code rate
r_i	i:th code rate
$\tilde{r}(t)$	received signal after band-pass filtering
$r^{(u)}(t)$	received signal for user u
R	physical uncoded bit rate
RT	radio type
R_{W}	data rate of the WUR
R_{EL}	data rate of the EL node's radio
R_{IL}	data rate of the IL node's radio
R_{AL}	data rate of the AL node's radio
S_t	Markov chain state value
$s^{(u)}(t)$	transmitted signal for user u
SNR_{DV}	signal-to-noise ratio at the decision variable for uncoded case
SNR^{i}_{DV}	signal-to-noise ratio at the decision variable for i:th code rate
t	error correction capability in symbols (or bits)
t_{c}	duration of a chip
t_{D}	duration of the data packet
t_i	error correction capability for i:th code rate
t_{o}	operation duration
t_{W}	duration of the wake-up signal
$T_{\text{s,IL}}$	sensing time per event at IL
$t^{\text{CL}}_{\text{rx}}(\lambda_{\text{dc}})$	DCR receiver channel listening duration as a function of duty cycle
$t^{\text{tot}}_{\text{s}}(\varepsilon)$	total time used for sensing as a function of number of events
$t^{\text{event}}_{\text{s}}$	sensing duration per event
$t^{\text{tot}}_{\text{MCU}}(\varepsilon)$	total MCU active time as a function of number of events
$t^{\text{event}}_{\text{MCU}}$	MCU active time per event
$t^{\text{tot}}_{\text{tx,W}}(\varepsilon)$	duration of wake-up signal transmissions as a function of number of events

$t^{\mathrm{tot}}_{\mathrm{rx,W}}(\varepsilon)$	duration of wake-up signal receptions as a function of number of events
$t^{\mathrm{tot}}_{\mathrm{tx,D}}(\varepsilon)$	transmission time of data packets as a function of number of events
$t^{\mathrm{tot}}_{\mathrm{rx,D}}(\varepsilon)$	receiving time of data packets as a function of number of events
T_{ACK}	ACK packet duration
T_{ACKW}	ACK packet waiting time
T_{BPM}	duration of burst position modulation bit period
T_{f}	data frame duration for uncoded transmission
$T_{\mathrm{f},i}$	data frame duration for i:th code rate
T_{idle}	length of the idle slot
T_{int}	integration time
$T_{\mathrm{MaxAckWait}}$	maximum waiting time for ACK packet
T_{p}	pulse duration
$T_{\mathrm{slot},i}$	slot length for i:th code rate
T_{sym}	symbol period duration
T^{i}_{packet}	transmitted UWB frame duration for i:th code rate
T_{SHR}	duration of synchronization header
T_{PHR}	duration of physical layer header
T^{i}_{PSDU}	PSDU transmission time for i:th code rate
T_{w}	duration of a IR-UWB pulse waveform
u	u:th user
U	operating voltage
W	signal bandwidth
$w(t)$	IR-UWB symbol waveform
x	number of nodes that attempt to transmit in a slot
X_i	number of code symbols in a packet for i:th code rate
Y_c	c:th bit decision in ED receiver
Z_a	a:th decision variable
Z_1	decision variable for the first symbol period in ED receiver
Z_2	decision variable for the second symbol period in ED receiver
z	channel access slot index
ACK	acknowledgement
ADSL	asymmetric digital subscriber line
A/D	analogue-to-digital
AFECCC	adaptive forward error correction code control technique

AL	advanced layer
ALPL	adaptive low-power listening
AODV	ad hoc on-demand distance vector
APP	application
ARQ	automatic repeat request
ASK	amplitude shift keying
AWGN	additive white Gaussian noise
A-MAC	adaptive medium access control (MAC)
BEP	bit error probability
BER	bit error rate
BC	beacon
BCH	Bose-Chaudhuri-Hocquenghem
BM	Berlekamp-Massey
B-MAC	Berkeley medium access control
BPM	burst position modulation
BPSK	binary phase-shift keying
BPZF	band pass zonal filter
CA	collision avoidance
CAP	contention access period
CCA	clear channel assessment
CDMA	code division multiple access
CF	characteristic function
CFP	contention-free period
CLMAC	cross-layer medium access control
CMOS	complementary metal-oxide semiconductor
CP	contention probability
CRA	code rate adaptation
CSMA	carrier sensing multiple access
CTS	clear-to-send
DC	duty cycle
DCR	duty-cycle radio
DE	detected event
DPS-MAC	dual preamble sampling MAC
DSP	digital signal processing
DSSS	direct sequence spread spectrum

EA	Euclid's algorithm
EAP	exclusive access phase
ECC	error control coding
ECG	electrocardiogram
EEG	electroencephalogram
ED	energy detection
EIRP	effective isotropically radiated power
EL	elementary layer
EPD	embedded partial decoding
ET-MAC	energy efficient and high throughput MAC
EWMA	exponential weighted moving average
FCC	Federal Communications Commission
FDMA	frequency division multiple access
FEC	forward error correction
FFD	full function device
FHSS	frequency hopping spread spectrum
FLAMA	a flow-aware medium access
FM	frequency modulation
FM-UWB	frequency modulated ultra wideband
FSK	frequency-shift keying
GFSK	Gaussian frequency-shift keying
GTS	guaranteed time slot
GWR-MAC	generic wake-up radio-based medium access control
HARQ	hybrid automatic repeat request
HBC	human body communications
HDD	hard decision decoding
ICT	information and communications technology
IEEE	Institute of Electrical and Electronics Engineering
IL	intermediate layer
IoT	Internet of Things
IWSN	industrial wireless sensor networks
IR-UWB	impulse radio ultra wideband
ISI	inter-symbol interference
ISO	International Organization for Standardization
LDGM	low-density generator-matrix

LE	low energy
LEACH	low energy adaptive clustering hierarchy
LED	light-emitting diode
LPD	low probability of detection
LPDC	low density parity check
LPL	low power listening
MAC	medium access control
MAP	managed access phase
MCU	micro-controller unit
MEMS	micro-electro-mechanical system
MERLIN	MAC and energy efficient routing with localization support integrated
MISO	multiple-input single-output
MRC	maximal ratio combining
MRE	maximum residual energy
MUI	multi-user interference
MQAM	M-ary quadrature amplitude modulation
NC-MFSK	non-coherent M-ary frequency-shift keying
NET	network
OL	outer layer
OOK	on-off keying
O-QPSK	offset quadrature phase-shift keying
OSI	open system interconnection
PEP	packet error probability
PER	packet error rate
PHR	physical layer header
PHY	physical
PIR	passive infrared
PMAC	pattern-MAC
PPM	pulse position modulation
PSD	power spectral density
PSDU	physical-layer service data unit
QoS	quality of service
QPSK	quadrature phase-shift keying
RAP	random access phase
ReTx	retransmission

RF	radio frequency
RFD	reduced function device
RFID	radio frequency identification
RMAC	routing enhanced MAC
RTS	ready-to-send
RTWAC	radio triggered wake-up with addressing capabilities
RS	Reed-Solomon
RSSI	received signal strength indicator
RV	random variable
Rx	reception
SDD	soft decision decoding
SEC/DED	single error correction/double error detection
SHR	synchronization header
SmartBAN	smart body area networks
SNR	signal-to-noise ratio
S-Aloha	slotted Aloha
S-MAC	Sensor-MAC
SMAC-DCC	S-MAC with dynamic duty-cycle adjustment
TDMA	time division multiple access
TDMA-ASAP	TDMA scheduling with adaptive slot stealing and parallelism
T-MAC	Timeout-MAC
TRAMA	a traffic-adaptive MAC
Tx	transmission
UP	user priority
UWB	ultra wideband
WBAN	wireless body area network
WiseMAC	medium access control protocol based on low-power listening
WiseMAC-HA	WiseMAC high availability
WISP	wireless identification and sensing platform
WMSN	wireless multimedia sensor network
XOR	exclusive or
WPAN	wireless personal area network
WSN	wireless sensor network
WS&AN	wireless sensor and actuator network
WUR	wake-up radio

WUS	wake-up signal
XLP	cross-layer protocol

Contents

1 Introduction

Diverse sensing of the environment combined with autonomous wireless networking enables various application possibilities, e.g., in the areas of habitat monitoring, surveillance scenarios, industrial automation, smart home, medical care and intelligent traffic applications. Ubiquitous sensing is nowadays possible due to rapid development of digital electronics, which enables implementation of cheap, tiny and low-power sensor nodes with wireless communication interface(s) and autonomous networking capabilities. These features enable the applications of distributed wireless sensor networks (WSN) even to non-accessible targets for long periods of time [1–3].

Wireless sensors can replace the traditional wired ones and enables to build more user-friendly and versatile sensing applications. For example, elderly and sick people can be remotely monitored at home, and medical actions can be triggered when seen necessary. Surveillance networks can be used to detect intruders in critical infrastructures or consumers' private areas. Home lighting, heating and air conditioning can be controlled depending on the human presence and surrounding environmental conditions, which are detected by sensor nodes. Consumer vehicles include a variety of sensors and a large number of wires. Therefore, wireless communication of the sensor data will make the vehicles lighter and provide more versatile possibilities for sensing and controlling, which enables lower fuel consumption. Sensors can also be used to monitor traffic and enable intelligent traffic light control as well as to provide information to drivers about the driving conditions. State-of-the-art smart phones also include many types of sensors which produce data to be used by the device itself but the data can also be sent forward using the wireless communication interface(s). Futhermore, the timely research concept called the Internet of Things (IoT) takes advantage of the huge amount of wireless sensor data available in the current and future networks [4–7]. The enormous amount of wireless sensor data coming from the various sources can be stored to back-end system servers and used for different application purposes. Therefore, the short-range wireless sensing devices will enable countless application possibilities which can be deployed individually and through the IoT.

An autonomous network based on wireless sensor nodes can be called by different names depending on the context. A wireless body area network (WBAN) consists of wireless sensor nodes deployed on and in the human (or animal) body. A wireless

personal area network (WPAN) consists of body sensors and other wireless devices in the close proximity ($\leq$ 10 m) of the human body. WSNs can also include actuator nodes, which perform dedicated actions depending on the application, e.g., automatically switch lights or heating on or off if sensors detect that the level of lightning or temperature is above or below a certain threshold. This kind of a network is often called wireless sensor and actuator network (WS&AN). The term wireless multimedia sensor network (WMSN) is used in some contexts if the network includes devices that take pictures or videos and transmit multimedia content by using wireless communication. Sometimes the term also includes a reference to the application scenario, as in the case of industrial wireless sensor network (IWSN). All these networks utilize short-range communication devices which communicate autonomously with each other and provide data directly to the end-user and/or to the backbone network. In this thesis, the abbreviation WSN will be used to describe the network consisting of short-range communication devices with sensors (and possibly actuators) in general. In addition, the abbreviation WBAN will be used when discussing specifically a network which is deployed on or in the human body.

1.1 Wireless sensor networks

Figure 1 shows examples of wireless sensor network application scenarios and a high-level topology of a network connecting WSNs and the end-user through a backbone network. This topology illustrates that sensor nodes are used to collect data from the target by using their sensors to measure some physical quantity. Sensor node observations are then sent to the sink node, which acts as a gateway between the WSN and the backbone network. Backbone communication can be based, e.g., on wireless/wired broadband, a cellular network or a private network infrastructure (military and public security authorities). The combination of a public backbone network and sensor networks can also be called the Internet of Things [4–7]. Remote users can access the sensor data through the backbone and/or directly, depending on the deployment, since not all WSNs will need to allow their data to be available in the backbone network. Inside a WSN, in many applications one-hop communication is used between the sensor nodes and the sink, but multi-hop communication is also efficient (or required) in some scenarios. The end-user can remotely access the data and give control commands to the WSN, via the backbone, basically from anywhere and anytime ubiquitously when a connection to the network is available.

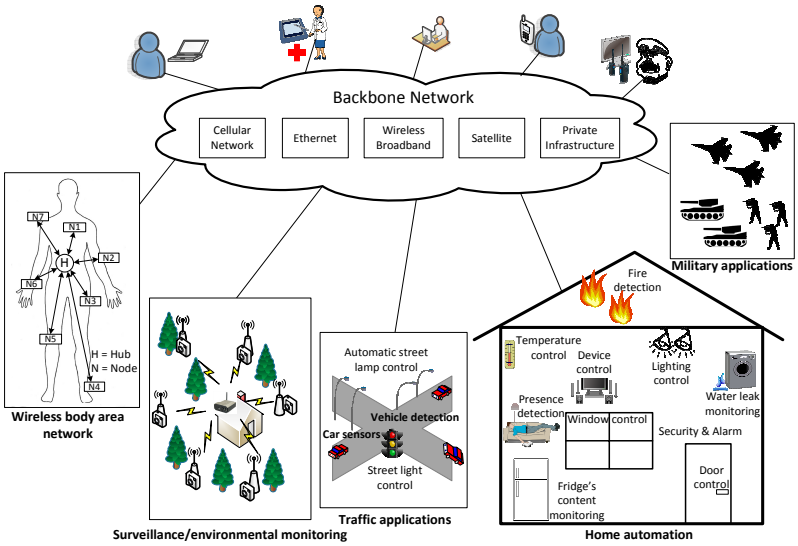

Fig. 1. Examples of WSN applications and a high-level network topology.

The sensor nodes' transmission, over the physical medium, can be based on radio frequency (RF), infrared or optical communication. Most of the WSNs are based on RF communication, which is also the focus of this thesis while infrared and optical communication are outside of the scope of the thesis.

In RF communication-based WSNs, the sensor node's main components are the processing unit (micro-controller unit (MCU) & memory), power source, sensor(s) and radio transceiver, which are illustrated in Figure 2 by using a well-known Crossbow TelosB as an example node [8]. The processing unit is the intelligence of the sensor node. It performs calculations and controls the other components of the node. The power source is typically an AA sized battery (or two of them), but smaller batteries or energy scavenging can also be used, depending on the node characteristics. Sensor nodes can be made to be very small, only a few millimetre in size [9]. However, then the problem is that the battery and antenna size are larger than the sensor node's core hardware. Depending on the application, sensor nodes can include many different types of sensors, some examples are listed in Table 1.

The RF transceiver takes care of the wireless communication coming to and from the sensor node. Figure 2 shows the communication protocol stack layers of the transceiver.

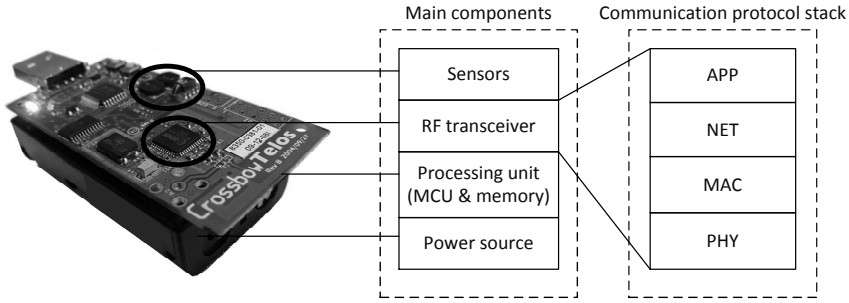

Fig. 2. Sensor node (TelosB [8]) main components and communication protocol stack layers.

Table 1. Examples of different type of sensors for sensor nodes.

MEMS[1] sensors	CMOS[2] sensors	LED[3] sensors	Medical sensors
acoustic	temperature	ambient light	Electrocardiography (ECG)
gyroscope	humidity	proximity	Electroencephalogram (EEG)
accelerometer	capacitive proximity	chemical composition	Electromyography (EMG)
magnetometer	chemical composition		oxygen saturation
pressure			body temperature

[1](micro-electro-mechanical system) MEMS
[2](complementary metal-oxide semiconductor) CMOS
[3](light-emitting diode) LED

The protocol stack does not include all the layers of the open system interconnection (OSI) standard [10] stack, because the transport, session and presentation layers' functionalities are not usually needed in WSNs. In some works also the higher layers, particularly the transport layer, are taken into consideration [11]. However, usually only the layers shown in Figure 2 are addressed in the WSN communication design.

The physical (PHY) layer takes care of the actual signal transmission and reception via the wireless channel. The PHY layer performs functions such as forward error correction coding, frequency selection and modulation and produces the electromagnetic signal to the wireless medium. The PHY layer communicates, via an interface, with the medium access control (MAC) layer, which takes care of efficient channel resource sharing, i.e., organizes channel competition or scheduled access and manages the duty cycling (sleep/awake periods) of the transceiver. The networking (NET) layer's main task is to handle communication routing between the network nodes. The application (APP) layer includes application-related functionalities and sets requirements for the communication and networking that will be handled by the PHY, MAC and NET layers.

1.2 Techniques for lower layers

Many PHY layer techniques have been developed for RF communication-based WSNs, a few common ones are shown in Table 2. The technologies listed in Table 2 can provide low-power operation by using different data rates and communication distances. These PHY layer solutions are based on different signalling methods: narrowband ([12] [13]), wideband ([14][15]) and impulse radio ultra-wideband (IR-UWB) [16].

The IEEE Std 802.15.4 [15], which focuses on low-power and short-range communication, is the well-known and widely used technique for the PHY and MAC layers of sensor nodes' transceivers. The PHY layer of the IEEE Std 802.15.4 supports three different bands (2.4 GHz, 915 MHz and 868 MHz) with direct sequence spread spectrum (DSSS) access mode. Offset quadrature phase-shift keying (O-QPSK) modulation is used in the highest frequency band while binary phase-shift keying (BPSK) is used in the lower frequency bands. The PHY layer supports channel selection, link quality estimation, energy detection measurements, clear channel assessment (CCA) and radio on/off operation.

The IEEE Std 802.15.4a [17] adds an alternative IR-UWB PHY technique to the original standard [15]. IR-UWB PHY is designed to enable coherent and non-coherent detection. Non-coherent receivers have a simple structure which can be made to be very low-power consuming. Other advantages of UWB communication are good localization accuracy and noise-like communication, which creates low interference to other wireless

Table 2. Common physical layer techniques for wireless sensor node transceivers.

	IEEE 802.15.4[5]	Z-Wave	DASH7	Bluetooth LE	IEEE 802.15.6[6]
Frequency [GHz]	2.45	0.868 / 0.915	0.433	2.45	3.9936 / 7.987
Modulation	O-QPSK	GFSK	GFSK	GFSK	OOK / DPSK
Spreading	DSSS	–	–	FHSS	Impulse radio
Data rate [kbps]	250	9.6 / 40	≤ 200	1000	487.5
Range[4] [m]	30–100	100	250	10–100	< 10
Release year	2003	2008	2009	2010	2012

[4]These are typical approximate values to enable a rough comparison between different technologies. The actual communication distance depends highly on the specific transceiver technology parameter setup and the characteristics of the communications environment.

[5]Characteristics for the higher frequency band defined in the standard [15].

[6]IR-UWB physical layer mandatory mode values.

devices and makes the detection of the signal difficult for malicious users [18, 19]. IR-UWB PHY has later been merged into the revised version of the IEEE Std 802.15.4 - 2011 [20].

The IEEE Std 802.15.6 [16] is designed for WBAN purposes. It defines three different PHY options and a dynamic MAC above them. The physical layer options are narrowband, human body communications (HBC) and UWB, which includes a mandatory impulse radio and an optional frequency-modulated PHY definition (IR-UWB and FM-UWB, respectively). The IR-UWB PHY mandatory mode characteristics are introduced in Table 2.

The International Organization for Standardization (ISO) [21] has defined a 18000-7 standard [12] called DASH7. It is based on Gaussian frequency-shift keying (GFSK)-modulated narrowband communication in the 433 MHz industrial, scientific and medical (ISM) band. Z-Wave is a very low data rate (< 40 kbps) solution using GFSK-modulated narrowband communication in the 868/915 MHz ISM band [13]. The latest Bluetooth Special Interest Group (SIG) specification (currently v4.1) also includes a low-energy (LE) version specification for physical and link layers [14]. The Bluetooth LE physical layer is using GFSK modulation and frequency hopping spread spectrum (FHSS) in the 2.4 GHz ISM band. The Bluetooth radio interface is well known and has been widely used in smart phones and portable handsets. Bluetooth LE's power consumption is much lower in comparison to the original Bluetooth. Therefore, it has been found to be a good candidate for smart home, healthcare, sport and fitness applications.

Each PHY layer technology has its own advantages and disadvantages depending on the particular application characteristics. Narrowband and wideband radios can provide longer communication ranges than the UWB technology. IR-UWB has the potential for energy-efficient implementations because frequency up or down conversions are not needed for carrierless signalling. Furthermore, FM-UWB can be used for low-data rate and low-power communication [19, 22, 23]. FM-UWB PHY is an analogue implementation of a spread spectrum system. The transmitter comprises an oscillator whose triangular subcarrier signal is digitally FSK-modulated by the data symbols, and the analogue wideband FM creates a constant envelope spread spectrum signal. The receiver can be implemented with low-complexity components, and carrier synchronization is not required, which is an important characteristic for distributed ad hoc networks. UWB signalling has good characteristics for certain applications (e.g., medical and military) where very precise localization or noise-like signal with low interference to other devices, good resilience to interference and low probability of

detection (LPD) are desired. All these introduced PHY layer techniques can be used to deploy low-power WSN applications, but there is still room for further optimizations which will enable more energy-efficient implementations.

For the WSN transceiver's MAC layer there are various proposals. Different MAC protocol proposals can be divided into three categories: contention-based, contention-free (scheduled) and hybrid. In the contention-based method, the nodes compete for the channel access according to the protocol definitions. The nodes can, for example, send directly when they have a packet to transmit, or at first listen to the channel and then transmit if the channel is free. If collision occurs, the nodes will send again after certain back-off time, depending on the protocol. In contention-free methods, the channel resource is scheduled (centrally or distributed) for the nodes, so that every node has resources available (time slot, frequency or code) for transmission. Hybrid protocols include features from the contention-based and contention-free methods. MAC protocols can also be divided into asynchronous and synchronous categories depending on which method they use for the duty-cycling (sleep/awake schedule) management. In the synchronous protocols, the nodes' listening periods are synchronized so that the target receivers are listening when the transmitter is sending the packet. In the asynchronous protocols, the nodes wake-up to listen to the channel based on their own schedule. Because the transmitter and receiver awake periods are not synchronized, the transmissions must include, e.g., a sufficiently long preamble so that the receiver will wake up and detect the incoming transmission with a high-enough probability.

In recent years, the wake-up radio (WUR) concept has also gained researchers attention [24–29]. A WUR can be used for channel listening instead of the actual data radio because this can save energy in particular types of applications. The idea is that WUR is continuously in a very low-power idle (standby) mode, in which it is able to detect a wake-up signal and to trigger the wake-up of the main transceiver. WURs can be designed to be ultra low-power consuming, and therefore they can be considered to outperform duty-cycle radios' (DCR) energy efficiency, particularly in applications which have a low event frequency.

The IEEE Std 802.15.4 defines a superframe-based MAC, above the PHY layer, including contention-based and contention-free periods. In the narrowband case, carrier sensing multiple access (CSMA) with collision avoidance (CA) is used in the contention-based transmission. In the IR-UWB PHY case, the slotted Aloha (S-Aloha) is used for the channel access. The IEEE Std 802.15.6 defines a MAC with three different modes and is therefore dynamic for different applications. Furthermore, in this case there are

contention-based and contention-free modes. The WSN design phase is so wide that obviously the standard solutions cannot be optimal for every different applications with varying characteristics. Therefore, the research has led to a large amount of MAC protocol proposals, which are often intended for particular types of applications under the author's design scope. The different MAC protocols will be discussed in more detail in Chapter 2.

1.3 Protocol design approaches

In order to enable the implementation of a long lifetime and user-friendly wireless sensing system, the sensor nodes must be designed to be energy efficient because they usually have very limited energy resources. Usually, battery replacement or recharging is not feasible in WSNs. The communication environment has varying conditions due to the wide applications space. Typically, wireless transceiver consumes most of the sensor nodes' energy resources [2, 30–34].

Traditionally, the communication protocol stack layers are designed separately, as was also done in the beginning of WSN research and development. However, it was found that the layered approach does not lead to an optimal solution because different layers' interdependencies affect the overall performance. Therefore, the cross-layer design research area emerged. In that case, the different layers' effect is taken into account in order to find a more optimal solution. It has appeared to be a very interesting and challenging research area, leading to a huge number of publications which introduce performance improvement solutions for different layer combinations and using different types of approaches.

There are various drivers for the cross-layer design. Wireless communication media characteristics affect signal attenuation and multipath fading, which influence the communication bit error rate (BER). At the link level, packet collisions may occur, e.g., due to a hidden terminal problem and/or synchronization errors, and multi-user interference may be caused by non-optimal protocol design. Typically, the packet must be retransmitted if the receiver's decoder cannot correct the errors. Retransmissions generate more traffic to the channel and reduce the sleep period duration of the sensor nodes, which affect energy efficiency negatively. For that reason, there is a direct interdependence between the PHY and MAC layers. Therefore, it is important to take these both layers into account in the performance optimization. Information exchange between the PHY and MAC layers is important because in that way the layers can in

cooperation adjust their parameters in order to achieve better overall performance. If the MAC layer experiences that there is heavy competition for channel resources, then it would be important to get the packet transmitted successfully through the physical channel at the first trial once channel access is acquired at the MAC level. For that reason, the MAC layer could, for example, indicate that the PHY layer should use as reliable transmission method as possible. The PHY layer could then use, for example, the highest transmission power, strongest error correction code or lowest modulation level (number of bits per symbol) as possible to perform successful communication. Looking from the other direction, the PHY layer can inform the MAC layer that the channel conditions are poor and therefore channel access should take a back-off and put the node to sleep mode. Due to the poor channel conditions, a lower modulation index or stronger code could be used, and therefore the packet length would be increased, which requires more channel resources for transmission. The adaptive parameter reconfiguration, however, affects the control overhead, calculational complexity and energy consumption. Therefore, there is a tradeoff between the added complexity and achieved energy consumption gain.

In order to perform optimal routing decisions at the network layer, the PHY and MAC layer conditions and success probabilities should be taken into account. Namely, if the route selection can take into account the reliability and energy efficiency of the available individual links, then optimal routes can be selected, e.g., based on their cost value. For this reason, the cross-layer information exchange from the lower layers to the NET layer is also valuable. In addition, routing should, for example, take into account that the routing load is not accumulated too much for certain nodes (avoid bottlenecks) in the network. Again, there is a tradeoff between the added complexity, when taking all the issues into account in routing design, and the achieved gain.

The application layer sets important design requirements for the lower layers of the protocol stack. If, for example, the delay and data rate requirements are strict, the cross-layer design should enable the solution to be as low energy consuming as possible while still fulfilling the application requirements. If the application does not have strict delay and data rate requirements, in the cross-layer design the protocol parameters which maximize energy efficiency while sacrificing other communication performance metrics should be selected. Applications also set different requirements for the network topology, node density and communication frequency. In order to take all these factors into account, the cross-layer protocol and architecture design are required to satisfy the application requirements while maintaining the energy efficiency and performance of the wireless communications.

Cross-layer design can be done using many different types of approaches and has been defined in a variety of ways. In this thesis, the previous works are divided into two categories: *merging of layers* and *information exploitation between layers*. In fact, both of the categories take advantage of the information exploitation between the layers but the difference between them is that the former additionally uses the merging of two or more layers. Therefore, the following definition for cross-layer design is proposed in this work: *Protocol design using information exploitation between the layers of the reference layered architecture either in the design phase or during run-time − with or without merging of layers*. More details about the categorization and justification of the cross-layer definition are given in Section 2.2.

In this thesis, the cross-layer approach will be used for the PHY and MAC layers. Analytical models and a generic wake-up radio-based medium access control (GWR-MAC) protocol are developed to improve energy efficiency of wireless communication in WSN and WBAN scenarios. Analytical models are developed for a typical star-topology network and for a hierarchical network consisting of heterogeneous devices. The IEEE Std 802.15.6-based WBANs are addressed by developing an analytical model which can be used to find out the most energy efficient forward error correction (FEC) code rate and payload length. FEC is typically required in wireless communication to detect and correct errors. The objective of error correction is to increase reliability, which decreases the number of required retransmissions and consequently can enable lower power consumption. In traditional wireless communication optimization, the maximum data rate and spectrum efficiency (bits/s/Hz) have been the main design goals. In the case of WSNs and WBANs, it is important to minimize the number of transmissions in order to maintain low power consumption. However, the coding cannot be too complex because the network nodes have limited computational capacity, and the energy consumption gain achieved by decreased number of retransmissions may diminish due to the decoding and transmission overhead. Therefore in order to enable energy consumption gains, it must be taken care that FEC does not cause too much overhead.

The target of most of the previous cross-layer research works has been to improve the performance at the node and/or link level. However, it is also important to take into account the network total energy consumption in order to find an efficient solution from the network point of view. Therefore, in this thesis, the focus is also on the network-level architecture and energy efficiency model development for a hierarchical network by taking cross-layer interactions between the architecture layers into account. The purpose of the architecture energy saving strategy is to improve the overall energy

efficiency of heterogeneous networks by enabling the most power consuming nodes to sleep as much as possible. Therefore in this work, a novel network-level architecture energy efficiency comparison model is developed for a wake-up radio and duty-cycle radio-based approaches.

1.4 Motivation

The wireless sensor network research area has been very active for over a decade. The first and most widely cited survey about WSNs was published in 2002 by Akyildiz *et al*. [1]. Akyildiz *et al*. describe the basic features of WSNs and outline various open design problems and possible applications of WSNs. Since then, many protocols and algorithms have been studied and proposed for WSNs. Practical applications have also emerged but the wide breakthrough of consumer applications is still to be seen. There are still research problems to solve in order to improve the WSN applications' energy efficiency, reliability, quality of service (QoS), ease of use, and cost.

WSN communication protocols must be designed carefully to support energy efficiency and reliability of communication in order to improve the lifetime of the sensor nodes, which have scarce energy resources. Some sensor nodes can operate even by using only the energy harvested/scavenged from the environment, e.g., by generating energy from temperature differences, kinetic motion, vibration or using photovoltaic cells to capture sunlight. These kinds of devices requires very well optimized solutions from the energy consumption point of view. In order to make deployment of many envisaged applications possible, the lifetime of a sensor network application must typically be several years because the recharging of batteries is often not possible in practice due to difficult installation location or high number of nodes. Another important aspect, when improving the energy usage, is the environment. It has been predicted that the number of sensor nodes will grow rapidly in coming years to be billions worldwide [35], and thus even a very small energy saving in a single node will have a non-negligible cumulative effect on the global energy consumption. Energy efficiency also extends the life cycle of the sensor nodes, which decreases the environmental pollution caused by the manufacturing of devices.

In this thesis, the focus is on wireless communication energy efficiency improvement by using cross-layer analysis. The goal is to foster the development of very low-power consuming WSNs and WBANs, which have an enormous amount of possible applications, as outlined in Section 1.1. It has been found in previous research that

cross-layer designed solutions are needed to enable the envisaged applications. The design can be done by taking into account many layers of the stack, but then problem becomes very complex and typically does not lead to a scalable solution. In this work, a cross-layer approach will be applied to the PHY and MAC layers because they create the basis for efficient communication and networking. In addition, the cross-layer approach is applied to a hierarchical network which consists of heterogeneous devices. The research methods of this doctoral research include a literature survey, analytical modelling and simulations using the Matlab software. The acquired results can be exploited by other researchers in the field, transceiver designers and bodies responsible for short-range communication standard preparation. The proposed models have been developed with the objective to achieve performance gains with moderate changes to the current standards. In that way the implementation complexity is kept manageable and modularity is maintained. Namely, there is a huge number of cross-layer design protocol proposals available, but they are often too difficult to implement and substantial changes to the standard solutions are required.

Figure 3 illustrates the flow diagram used in this doctoral research approach. At the beginning, the state-of-the-art of wireless sensor network solutions were reviewed. It was found that energy efficiency needs to be improved and cross-layer design is required since there are many interdepencies between the protocol stack layers which affect the performance of wireless communication. Therefore, methods to enable possible energy savings were defined and models for the evaluation of the performance of these methods were developed. The results were analysed and the proposed methods, which enable to improve the energy efficiency of the state-of-the-art of WSNs and WBANs were published. Possibilities for future research related to the proposed methods were also outlined to stimulate further research and development by the research community. Next section introduces in details the author's contribution to the original publications and summarizes the contributions of this doctoral thesis.

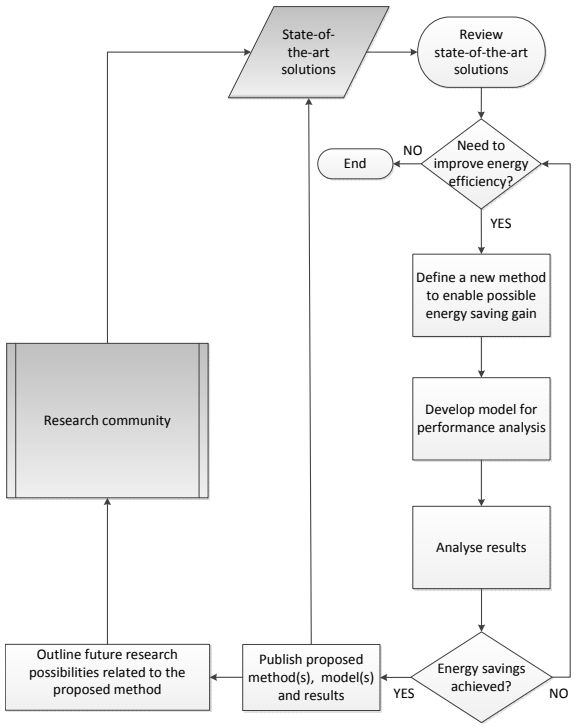

Fig. 3. Research approach diagram for the doctrol thesis work.

1.5 Author's contribution

In this doctoral thesis research, three different cross-layer approaches has been developed and introduced in international peer-reviewed journal publications [36–38]. The models presented in those publications provide a coherent contribution with an objective to improve the energy efficiency of state-of-the-art low-power short range communication. The proposed models and results introduced in the journal papers [36–38] are incorporated into the body of this thesis. In addition, the international conference papers [39–43] published by the author are results of the author's research work introduced in this thesis, as will be detailed below.

Publications [39] and [40] are based on the Markov chain analysis and simulations which are used to study the FEC coding effect on the length of the sensor node transmission period and energy efficiency. In [39], the focus is on the IEEE Std 802.15.4-type radios, while in [40], the focus is on the ultra wideband communication

when using Bose-Chaudhuri-Hocquenghem (BCH) and Reed-Solomon (RS) codes for error correction. In the journal article [36], the analytical and simulation model introduced in the author's conference publications [39] and [40] is developed further in order to provide a more comprehensive study of the topic. In [36], [39] and [40], the author developed the research problem and analytical model in collaboration with the co-authors. Furthermore, the author has implemented a Matlab script to produce analytical and simulation results for those works ([36], [39] and [40]).

In the journal work [37] and conference paper [41], the energy efficient BCH code rates and data payload lengths are explored for IR-UWB transceivers based on the recently published IEEE Std 802.15.6 [16] for WBANs. Journal article [38] introduces the defined hierarchical WSN architecture and provides the energy efficiency comparison results for the networks based on wake-up and duty-cycle radios. For the research work introduced in publications [37], [38] and [41], the author invented an energy efficiency improvement approach, developed an analytical model and implemented a Matlab script to acquire results for the analysis.

A generic wake-up radio-based MAC protocol, which is proposed in this thesis, has been published in [42]. In [43], the GWR-MAC is applied to a two-tier WBAN and its energy efficiency is also analysed therein. The author has developed the GWR-MAC protocol and its energy consumption analysis during this doctoral research. Additional results, compared to the previous publications, are also included in this thesis.

This thesis provides a coherent monograph-form description of the author's research work introduced in the original publications [36–43]. In summary, the main contributions of this thesis are:

- Extensive survey of energy efficient communication techniques for short-range communication
  - Layered approaches
  - Cross-layer approaches
- Proposal for a generic-level wake-up radio-based MAC protocol
- Proposal for three cross-layer modelling approaches to explore energy efficiency
  1) Analysis of the PHY & MAC layers in a star-topology WSN case
  2) Analysis of a hierarchical architecture with a focus on a wake-up scheme
  3) Analysis of an IEEE Std 802.15.6-based WBAN using IR-UWB
- Discussion about the usefulness of the results and summary of future research possibilities.

By proposing three different analytical models, this thesis provides tools for energy efficiency improvements which can be achieved through a cross-layer design exploiting the information exchange between the protocol stack layers. Each model is defined for different types of scenarios: star-topology WSN, hierarchical WSN with heterogeneous devices, and star-topology WBAN. However, in the modelling the generality and coherence between the different models has also been a design goal, as will be shown in this thesis. Namely, the proposed generic-level wake-up radio-based MAC protocol is defined to be scalable for various WSN and WBAN scenarios, and it is applied to the analysis of the proposed models 1 and 2. In addition, in the cross-layer approach for the PHY & MAC layers, the energy consumption model has been derived first at the general-level and then it is applied to the analysis in models 1 and 3.

1.6 Outline of the thesis

Chapter 2 introduces related work proposals for the improvement of WSN communication protocols' energy efficiency using layered and cross-layer design approaches. Chapter 3 introduces a generic wake-up radio-based MAC protocol and the cross-layer approach developed for the lower layers of the protocol stack. An energy efficiency model for a hierarchical WSN is explained in Chapter 4, and energy-efficient payload length and code rate selection model for IR-UWB-based WBANs is introduced in Chapter 5. In Chapter 6, conclusions from the thesis are presented and possibilities for future work are outlined.

2 Background of energy efficient communication

In the wireless sensor network research, energy efficiency has gained most of the attention because the sensor nodes must operate with very limited energy resources. The low energy consumption requirement comes from the characteristics of typical target applications based on the deployment of autonomous nodes, which can be located in various difficult locations and should operate long periods of time on a single tiny battery or even by using only energy harvested from environment. The transceiver components of a typical WSN node have been found to consume most of the energy budget because the sensor observations must be communicated in a wireless fashion [2, 30, 32–34]. Therefore, most of the WSN research has focused on communication protocols' energy efficiency.

The strict energy consumption requirement has led to an emergence of cross-layer design proposals for different parts of the communication protocol stack. In order to create a successful cross-layer design, it is important to understand the functionalities and design problems of each layer. Therefore, here different methods for communication energy efficiency improvement proposed in the literature will be reviewed. Figure 4 shows the taxonomy used for the related work review introduced in this chapter. Section

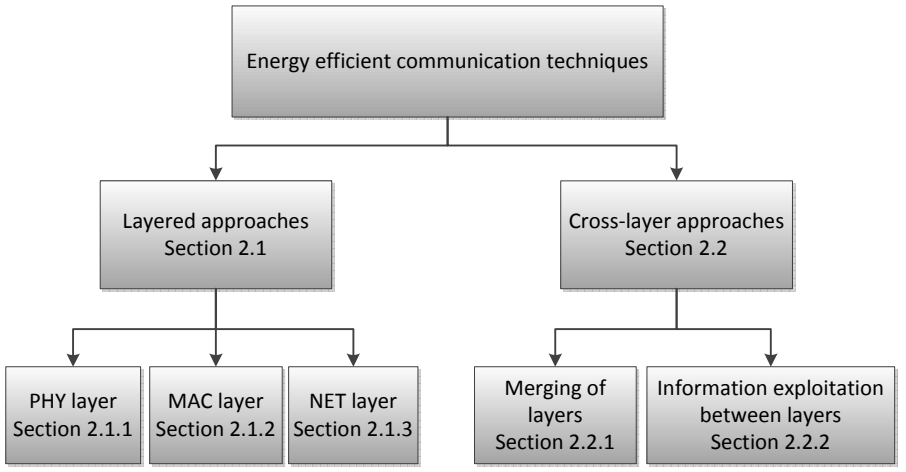

Fig. 4. Taxonomy of the background of energy efficient communication in Chapter 2.

2.1 introduces the works that focus on energy efficiency improvement by using the layered approach because it is important to understand the main design problems of different layers before performing cross-layer design. Then, Section 2.2 reviews works that use a cross-layer approach to enable energy efficiency improvements. In this thesis, the cross-layer approaches are divided into two different categories, as shown in Figure 4, and their definition's are explained in Section 2.2.

In this survey, the main focus is on the PHY and MAC layers because the research carried out in this thesis focus on these lower layers of the OSI model [10]. However, it is also important to understand the interdependencies between the network layer routing and the lower layer protocols. Typically, the higher layers, such as transport, session and presentation, of the traditional OSI stack are not used in WSN transceivers. Therefore they are not addressed in this literature review. The application requirements affect drastically the selection of the network communication techniques and parameter configuration to achieve high energy efficiency. Namely, the system energy consumption depends, e.g., on the application's required sampling frequency, communication reliability, bit rate and delay requirements. The application sets guidelines regarding how often the sensor nodes must perform sensing and reporting and how much data they need to communicate. Therefore, the application's requirements must be taken into account and the lower layers' communication protocols must be designed to fulfil the requirements while remaining as minimum energy consuming as possible. In this thesis, the focus is to design energy efficient communication which enables different types of applications with varying characteristics. However, application design is out of the scope of this thesis and therefore application layer issues will not be addressed in this review.

2.1 Layered approaches

2.1.1 Physical layer

In Section 1.2, the common PHY layer techniques used in WSNs were introduced. This section reviews in more detail the energy efficiency studies concerning the PHY layer techniques. At the physical layer, energy efficiency gains are typically found by optimizing, e.g., the error correction coding rate, modulation method (bits per transmitted symbols) or transmission power. Therefore, this section is structured accordingly. In addition, at the end of the section, the example works that focus on the IR-UWB and WURs are introduced separately because IR-UWB communication and

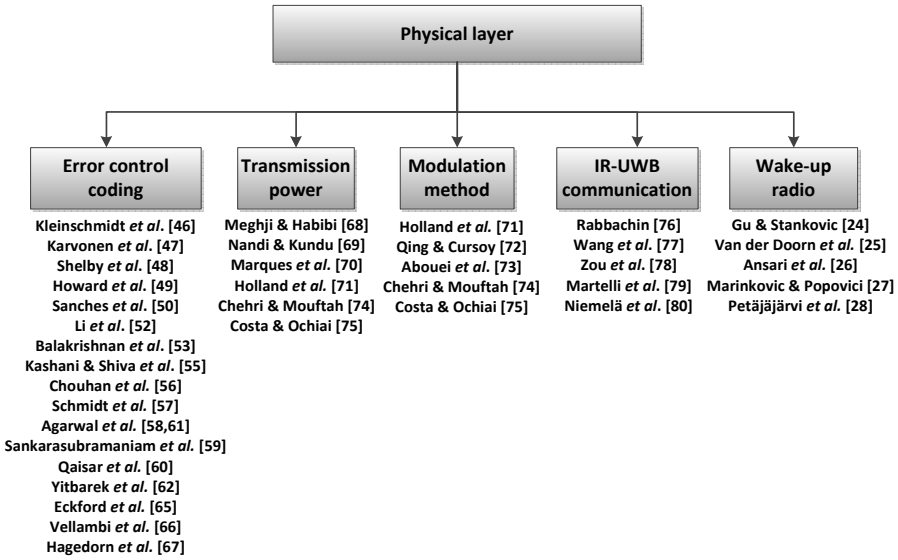

Fig. 5. Taxonomy of the review of physical layer and addressed previous works.

WUR are the main physical layer techniques addressed in this thesis. Figure 5 illustrates the topics addressed in this section and outlines the introduced related works for each topic.

Error control coding

Error control coding (ECC) can be based on FEC, automatic repeat request (ARQ) or hybrid-ARQ (HARQ) [44], [45]. FEC and HARQ are viable methods for energy efficiency improvement because they can be used to increase the reliability by detecting and correcting errors and consequently to decrease the number of retransmissions. The ARQ method can be used to detect errors and request retransmission when required. ECC produces additional overhead, which must be less than the achieved energy efficiency gain through increased reliability. Therefore, there are many previous works that have studied the tradeoff between the added overhead and the achieved energy consumption gain for different types of ECC methods.

An analytical comparison of different ECC methods in Bluetooth technology-based WSNs using a Nakagami-*m* fading channel has been done in [46]. The authors propose an adaptive error control method which is based on adaptation to the number of hops

that a packet needs to travel in the network before reaching its destination. If the packet must be transmitted using many hops to reach the destination, then more energy is wasted if the packet is not received correctly at the sink. Therefore, the authors propose that a stronger code might be used for packets that need to travel more hops. The authors illustrate a clear dependence between the channel conditions, number of hops and the energy efficiency in their performance evaluation for the custom, Hamming and BCH codes in the case of a Bluetooth radio [46]. The authors conclude that a low coding level is efficient in good channel conditions, while when the signal-to-noise ratio (SNR) is low, the studied BCH codes are the most energy efficient. The coding energy efficiency dependence on the channel conditions and number hops the packet needs to travel to the sink has also been shown in [47] and [48]. In [49], the authors found that the critical distance after which ECC becomes energy-efficient in WSN communication varies highly according to the application's characteristics and environment. In [50], the authors evaluate the performance of classic FEC codes in the IEEE Std 802.15.4-based transceivers (CC2420 [51]). The authors show, by simulations, that a simple (15,7) cyclic code can improve BER and provide energy gains for those transceivers. The authors also evaluate the proposed FEC algorithm execution time by using implementation and conclude that the decoding time effect is negligible in the case of typical WSN data rates [50]. In [52], it is shown that an augmented hardware implementation of FEC for the PHY layer provides from 24.8% to 31.4% energy saving for the IEEE Std 802.15.4-based radios.

Binary-BCH, non-binary RS and convolutional codes' performance in WSNs are studied in [53] for a densely deployed WSN with short communication distances using μAMPS sensor nodes. The authors implement and simulate different codes by using the very high speed integrated circuits (VHSIC) hardware description language (VHDL). The power consumption of different codes is evaluated based on a field-programmable gate array (FPGA) and application-specific integrated circuit (ASIC) implementation. Euclid's algorithm (EA) is used for error polynomial coefficient calculation with hard decision decoding (HDD) because soft decision decoding (SDD) requires complex circuitry [54]. The authors found that BCH codes with ASIC implementation provide lower power consumption than RS or convolution codes. Moreover, the authors conclude that BCH and RS codes provide lower power consumption than in an uncoded case but convolutional codes require too much power consuming decoders for WSN transceivers [53]. BCH, RS and convolutional codes' energy efficiencies are studied for WSNs in [55]. The authors found that in the studied scenario, the RS codes provide the lowest

energy consumption. An energy consumption analysis for different length RS codes and modulation methods has been done in [56]. The authors found that RS coding can provide significant energy savings, which depend highly on the communication distance. In [57], it is stated that FEC can be used to decrease the number of retransmissions, which leads to better energy efficiency. Furthermore, it is shown that the optimal tradeoff between the coding energy efficiency gain and coding overhead varies strongly from one node to another because of changes in the channel quality.

There exist also studies on other types of ECC methods for WSN transceivers because it must be kept in mind that WSNs have many different types of applications for different environments where some other codes than BCH or RS can be more efficient. In [58], the authors show that ARQ methods can be efficient in particular conditions. However, there are studies, e.g., [59–61], which do not recommend ARQ methods for WSNs due to their usage of retransmission and overheads. A novel embedded partial decoding (EPD) scheme, where relay nodes perform partial decoding of low density parity check (LDPC) coded packets before forwarding the packets to the next node in the route, is proposed in [60]. The authors found that the proposed method improves the throughput significantly. An adaptive universal FEC (AuFEC) scheme, which is based on the RS codec, has been introduced in [61]. The results of [61] show that significant energy gains can be achieved with coding level adaptation depending on the channel conditions. Convolutional codes are found to require too complex decoders for typical WSN transceivers [53], [59]. The software implementation complexity of different types of codes for industrial WSNs has been studied in [62]. The authors found that LPDC and Turbo codes are too complex for WSNs because they require too much memory and time for decoding. The RS (15,11) code was found to be the most suitable of the codes studied, because it does not require too much memory and the decoding can be done within timing limits of the WSN transceiver [62]. The Hamming and repetition codes were also found to be feasible but not as suitable as the RS codes.

Rateless codes can also be used to mitigate errors in varying channel conditions because they do not possess any fixed rate and the coding redundancy can be increased when the channel conditions change [63–67]. Rateless codes can offer reliable and low latency communication with relatively low complexity and coding overhead leading to low energy consumption. Therefore, they are good candidates to be used in WSNs. In [65], the authors studied rateless and low-density generator-matrix (LDGM) codes in cooperative WSNs. However, the cooperativity is not a binding requirement for the proposed scheme [65] because it can also be used for independent and relay

transmissions. In [67] rateless codes are used to improve the reliability of the proposed over-the-air programming (OAP) approach.

Transmission power

Transmission power adaptation is also an important method to guarantee the performance of communication. Power control can improve connectivity, throughput and delay. From the energy efficiency point of view, power control can be used to minimize transmission power in order to save energy used for transmissions and to decrease the multi-user interference. Transmission power adaptation is widely used in networks which include more capable devices, e.g., in cellular network. However, also power control has additional computational and power consumption costs, which must be evaluated for the WSN case in order to explore the actual energy efficiency gain that can be achieved.

In [68], the authors investigate the impact of transmission power control on the energy efficiency of IEEE Std 802.15.4-based communication in single-hop and multi-hop scenarios. The authors found that by using power control, single-hop communication can provide energy savings compared to multi-hop communication. In addition, the authors point out that single-hop communication should be preferred because multi-hop communication will increase the number of collisions and packet end-to-end delay.

A transmit power optimization model for WSNs using space diversity is proposed in [69]. The authors target to find the minimum power that is needed to achieve the required BER in order to save energy and decrease interference in WSNs. The authors found that when using maximal ratio combining (MRC) to take advantage of the space diversity, the required transmission power can be decreased. The proposed method requires multiple antenna implementation at the receiver.

In [70], the authors focus on transmit power minimization in WSNs using coherent detection with finite-rate feedback. The authors assume a multiple-input single-output (MISO) communication system where sensor node transmissions arrive coherently at the sink node. The transmit power minimization is done by taking into account the rate and BER constraints. The authors propose adaptive modulation/coding, power loading and beamforming strategies to achieve energy consumption savings. The proposed method requires synchronization to maintain coherency, and channel quantizers are also needed to achieve the optimal solution.

Modulation method

Modulation method constellation can be adapted to increase or decrease the number of transmitted bits during one symbol. When the number of bits in a symbol is increased, a higher SNR is required for successful detection. On the other hand, the bit rate increases and the transmission duration is then shorter, which can lead to energy savings if transmission is enough reliable. If the SNR is not high enough, the erroneous packets need to be retransmitted, which can lead to energy inefficiency.

The work done in [71] focuses on the physical layer parameters optimization for a WSN transmitter. The authors focus on the transmission distance, transmission power and modulation level optimization from the energy efficiency point of view. The findings in [71] show that it is important to adapt the parameters according to channel conditions and communication distance in order to achieve the minimum energy consumption per bit in a typical WSN transceiver. In [72], the authors introduce an optimization model for a M-ary quadrature amplitude modulation (MQAM) constellation size to minimize the energy consumption per bit when taking into account the BER constraints. The authors use log-normal shadowing and Rayleigh fading model for the wireless channel and take into account energy consumed in the circuitry, transmissions and retransmissions. The optimization is done for single-hop and multi-hop cases and for fixed and variable power schemes. The results show the optimal constellation size for different communication distances. Also from the results shown in [72], it can be concluded that adaptation of constellation size and transmission power is required to minimize energy consumption as a function of communication distance. The energy efficiency of popular modulation methods for IEEE Std 802.15.4-based communication has been studied in [73]. The introduced model enables to find the optimal modulation method as a function of distance in the case of Rayleigh and Rician fading channels with path loss. The authors found that non-coherent M-ary frequency-shift keying (NC-MFSK) is energy efficient in sparse WSNs while on-off keying (OOK) provides more energy savings in dense WSNs. These results also highlight the importance of adaptive selection depending on the WSN communication distance and channel conditions. The adaptation of modulation and transmission power has been found to be important from the energy efficiency point of view also in [74] and [75].

IR-UWB communication

IR-UWB communication with non-coherent detection has been found to be a good candidate for low-power sensor node transceivers and has therefore gained a lot of attention among WSN researchers. However, it is not as widely studied as, for example, the IEEE Std 802.15.4-based physical layer [20]. Therefore, it will be studied in this thesis and the relevant standards and previous works will also be introduced here.

IR-UWB has been selected as one PHY-layer option to the main WSN-related IEEE standards, 802.15.4 [20] and 802.15.6 [16]. During the development of the IR-UWB technique and those standards, various studies have been published and improvements to the standards have been proposed. In [76], the performance of IR-UWB energy detector receivers was studied in detail for the uncoded case. In [77], the authors computed the link energy consumption of coherent and non-coherent IR-UWB communications using RAKE receivers. Relevant work about non-coherent IR-UWB receiver implementations and performance measurement has been published in [78]. The results shown in [78] substantiate that energy-efficient non-coherent IR-UWB receiver implementations can be done. In the analysis of [77, 78], the performance study was done for uncoded communication. In [79, 80], the performance of non-coherent receivers using UWB technology for medical information and communications technology (ICT) scenarios and fixed RS code was investigated.

Wake-up radio

Wake-up radios are seen very potential solutions to improve the energy efficiency of WSNs. There already exist WUR solutions which can be used for short-range wake-up signalling. For example, Austria Microsystems has developed a commercial AS3933 3D LF wake-up receiver, which uses amplitude-shift keying (ASK) demodulation in three different channels [81]. The maximum wake-up distance is about 6 metres and the power consumption in an idle mode is 17.1 µW. In [82], a wireless identification and sensing platform (WISP) that is a fully programmable, passive computing platform is introduced. The platform includes rectified voltage, temperature and light sensors. WISP design is similar to the passive radio-frequency identification (RFID) tags, which are already in use in many applications, e.g., as door keys. A radio triggered wake-up with addressing capabilities (RTWAC) solution prototype was able to wake up a node from a distance of 10.1 metres with 500 mW transmit power, while the power consumption of

the receiver was 12.5 μW in an idle mode [26]. Relevant WUR solutions have also been proposed, e.g., in [24, 25, 27, 28]. However, the state-of-the-art wake-up radios have some limitations. Namely, the achieved wake-up distance is relatively short (< 10 m) for very low-power implementations, and some solutions are missing the addressing feature. Many state-of-the-art solutions focus on minimizing the power consumption of the wake-up receivers, and the transmitter has more energy resources. However, the wake-up signal transmitter power consumption should also be kept low in networks where wake-up is initiated by energy-constrained devices. Therefore, there is a need to design a wake-up transceiver solution that could improve the achievable distance and still include addressing capability and low power consumption, which is the design goal of the solution proposed in [28]. The addressing feature is also important because it enables that only the target nodes will be awakened instead of all the network nodes within the communication range.

2.1.2 Medium access control layer

There are different types of MAC protocols which try to improve energy efficiency. Their efficiency depends on the application characteristics since different types of networks requires different types of solutions. Indeed, the scalability and adaptivity to network changes are important MAC protocol design objectives because in that way the protocol performance can be ensured in many type of scenarios. Medium access control protocols must be designed to take care of the packet collision avoidance, idle listening and overhearing with minimum control overhead. Packet collisions must be avoided to keep the number of retransmissions low. Idle listening occurs when radios listen to the channel redundantly, when there are no incoming transmissions. Retransmissions and control overhead decrease data throughput and increase energy consumption because redundant bits need to be transmitted. The nodes' potential sleep time also decreases. Overhearing should be avoided so that only the target nodes will receive and decode the packets.

Most of the proposed MAC protocols are duty-cycle based, i.e., the radios have a sleep/awake scheduling which they are following. The MAC protocols can be divided into synchronous and asynchronous categories. Duty-cycling principle is illustrated in Figure 6 (a) for synchronous case, and in Figure 6 (b) for asynchronous case.

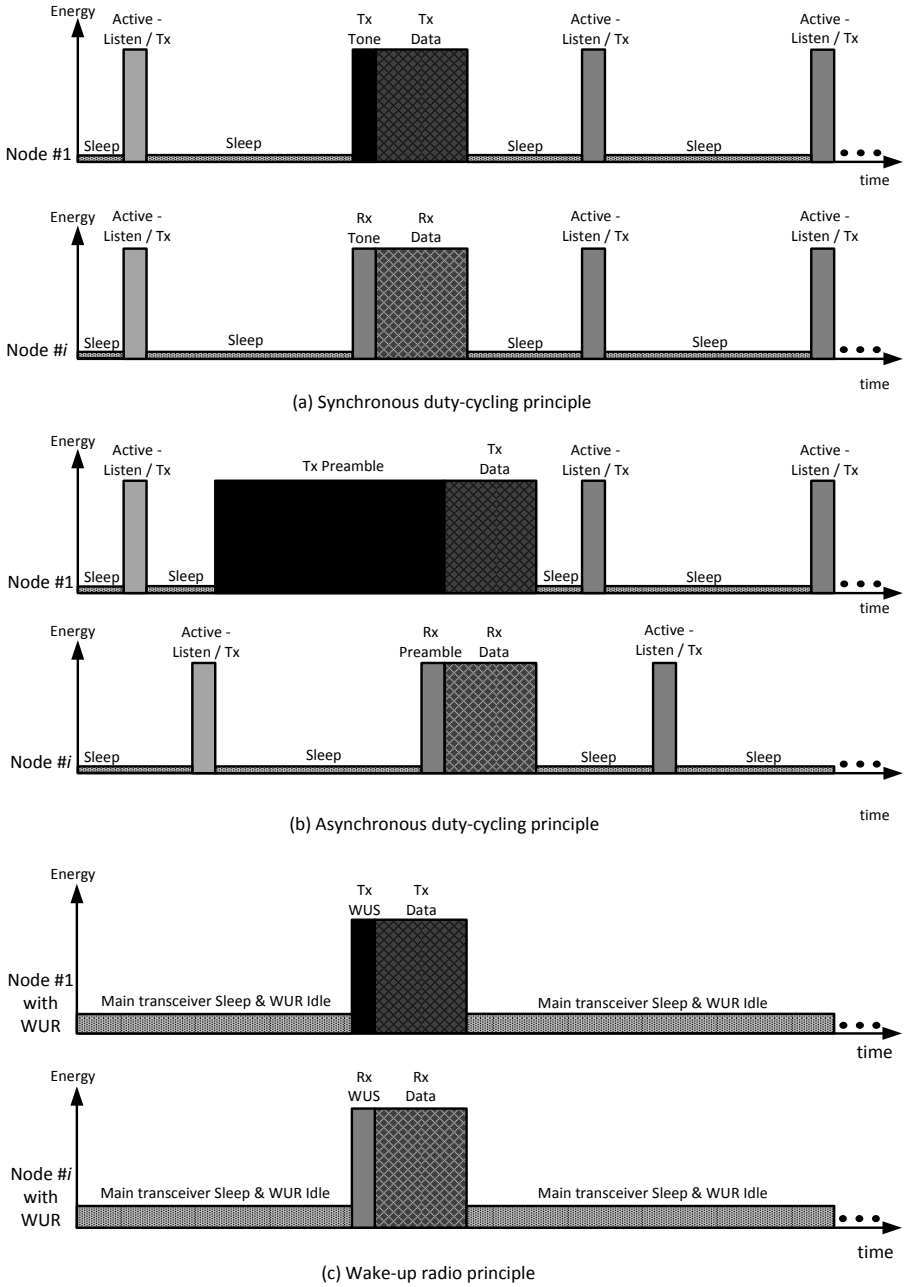

Fig. 6. (a) Synchronous duty-cycling, (b) asynchronous duty-cycling, and (c) wake-up radio principle for data transmission.

Synchronous protocols schedule the sleep/awake periods so that the nodes which are expected to communicate with each other are awake at the same time. Synchronous protocols typically require a centralized control and use clustering of nodes, and inside each cluster there is a common sleep/awake schedule which is controlled by the cluster head. Asynchronous protocols include methods for communication between the nodes which have different sleep/awake schedules. Asynchronous communication is enabled by using a sender or receiver initiated communication. In the sender initiated case, the data source will send a preamble before data transmission. Once the receiver detects the preamble, it will continue the listening to receive the data packet that will follow the preamble, as illustrated in Figure 6 (b). If the receiver does not detect a preamble, it will go back to the sleep mode. In the receiver initiated case, the receiver will use probing to query for potential transmissions. In each case, the idle listening will occur if there is no incoming transmission when the nodes wake up to listen to the channel according their schedule. Idle listening is expensive from the power consumption point of view because the transceivers should be in the sleep mode as much as possible in order to save power.

Recently, wake-up radio-based MAC solutions have also gained attention due to their energy efficiency superiority, particularly in applications with rare events and transmissions [83–85]. Therefore, also WUR MAC approaches will be discussed here. The wake-up radio principle has been illustrated in Figure 6 (c). I.e, in this case the data transceiver can be in the sleep mode until there is incoming data packet to be received from some other node. The WUR of the source mode will notify the target node(s) by sending a wake-up signal (WUS). After receiving the WUS, target node's WUR will wake-up the main transceiver for data packet reception.

The purpose of this MAC review is to introduce relevant example protocols which are addressing the main design problems in WSNs by using different approaches. The example protocols are selected so that by understanding their solutions and features, a thorough view of the MAC design problems is acquired. The existing MAC protocols will be introduced here by organizing them into three groups: contention-based (slotted or unslotted), contention-free (time division multiple access (TDMA) or guaranteed time slots (GTS), etc.), and hybrid (e.g. combination of contention-based and contention-free methods). Figure 7 illustrates the taxonomy of this section and outlines the introduced related works for each category.

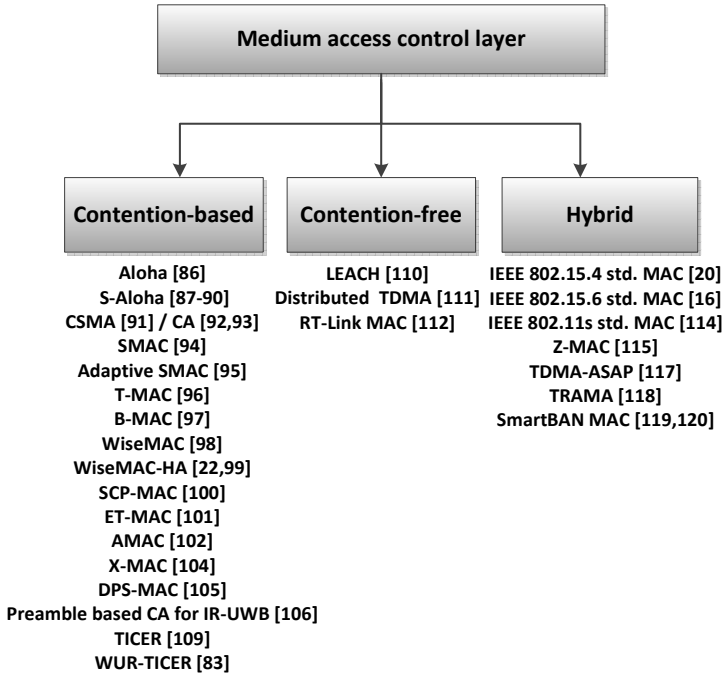

Fig. 7. Taxonomy of the review of MAC layer and addressed previous works.

Contention-based protocols

Contention-based protocols can be divided into two categories: slotted access (synchronous) and unslotted access (asynchronous). The difference is roughly that in the slotted access, the nodes' transmission starting times are pre-determined, while in the unslotted access, the nodes can individually decide the starting time of transmission.

Aloha is the first contention-based random access protocol whose principle is that if the radio has a packet to transmit, it will send it right away without checking whether there is ongoing transmissions in the channel [86]. If a collision occurs, the radio takes back-off and sends the packet later after a random period of time. The slotted Aloha protocol is an improvement to the pure Aloha because it defines discrete time slots for packet transmissions [87]. Radio transmission can start only at the beginning of a time slot, and the packet duration cannot exceed the slot duration. In that way, collisions are reduced because the packet vulnerability period is the same as the packet duration, while in the original Aloha case, the vulnerability periods is two times the packet duration. Therefore, S-Aloha provides higher throughput than the pure Aloha. However, also the

S-Aloha maximum throughput is quite low because it does not use carrier sensing or collision avoidance methods before transmission. The S-Aloha MAC protocol is widely studied, e.g., in [87–90]. Due to its simple implementation and low communication overhead, S-Aloha is a suitable choice for many WSNs scenarios which do not have a heavy traffic load. S-Aloha has also been chosen for standards [16, 17, 20] to be used with IR-UWB PHY.

In order to improve throughput, a CSMA method was invented for channel listening before transmission [91]. In addition, collision avoidance methods, e.g., ready-to-send (RTS) and clear-to-send (CTS) message transmissions before data transmission, are used to reserve the channel and mitigate the hidden-node problem [92, 93]. A hidden node may corrupt the ongoing transmission if it does not notice it by using carrier sensing. Therefore, RTS and CTS broadcasts can be used to notify the nodes, within the range of the transmitter and receiver, about the upcoming transmission. Later on, a large number of MAC protocols has been proposed, but they typically apply the basic methods introduced by Aloha, S-Aloha, CSMA and CA.

Sensor-MAC (S-MAC) [94] is a duty cycling-based protocol and focuses on energy efficiency improvement by avoiding idle listening. S-MAC uses synchronization to organize the communication between the nodes. At the beginning of the active period, the network nodes will exchange synchronization and RTS / CTS messages before data transmissions. The original S-MAC protocol has been improved by adding an adaptive listening feature to save energy by changing the duty cycle depending on the network traffic conditions [95]. S-MAC is quite a complex protocol because of the synchronization procedure and does not therefore scale to a networks with high number of nodes. Timeout-MAC (T-MAC) protocol provides energy efficiency improvement, compared to the S-MAC protocol, by adding a short listening period for possible RTS/CTS messages [96]. If there is no activity, the nodes can go to the sleep mode. That enables adaptivity to changing network traffic conditions. However, the T-MAC protocol has similar complexity and scalability weaknesses as the S-MAC protocol.

Berkeley MAC (B-MAC) [97] is an asynchronous protocol which uses preamble transmissions to enable the receivers to detect the incoming transmission when they wake up to sample the channel. The preamble sampling method of the B-MAC protocol supports adaptivity to the traffic load experienced in the network. Before the transmitter sends the preamble, it will perform a clear channel assessment (CCA) to avoid collision with an already ongoing transmission. The receiver node performs periodic channel sampling that is called low-power listening (LPL). Accurate channel assessment is

critical from the B-MAC energy efficiency performance point of view. To enable accurate CCA in the B-MAC protocol, the noise floor is estimated by sampling the channel when it is assumed to be free of transmissions, e.g., right after the packet reception. The authors show that B-MAC is more flexible, simpler to implement and can save energy in comparison with S-MAC and T-MAC. However, it must be noted that B-MAC is just a link layer protocol, and S-MAC and T-MAC also provide hidden terminal avoidance, synchronization with neighbours and message fragmentation, which may be useful or required in the network operation when taking into account also other layers of the protocol stack.

WiseMAC [98] is another protocol which uses LPL, i.e., the receiver nodes wake up for a short period of time to sample the channel for potential oncoming transmissions. WiseMAC reduces the wake-up preamble length by exploiting the knowledge of the neighbours' channel sampling schedules. In [22, 99], the authors have proposed a WiseMAC high availability (WiseMAC-HA) protocol intended to be used with FM-UWB PHY in WBAN applications based on the IEEE Std 802.15.6 [16]. The WiseMAC-HA protocol extends the original protocol to operate on multiple channels (can be separate frequency band, sub-carrier or a CDMA code) in order to increase the robustness to interference and enable adaptivity to varying traffic loads. WiseMAC-HA includes a basic WiseMAC mode for low-power communication and a CSMA mode to enable low-latency communication. LPL-based protocols are also called channel polling protocols, which save energy because the nodes do not need to listen to the channel longer if a preamble is not detected. In LPL methods, the preamble transmission duration must be long enough to enable that all potential receivers will wake up during the preamble and can detect the preamble. For this reason, the duty cycle must be at least 1-2% so that the preamble length can be kept reasonable [100]. Therefore, [100] proposes a scheduled channel polling MAC protocol (SCP-MAC), which enables extremely-low duty cycles (< 0.1 %). SCP-MAC synchronizes the neighbours' channel polling time and therefore eliminates the usage of long preambles. Only a short wake-up tone is required to be sent by the transmitter. SCP-MAC is designed to handle bursty and varying traffic loads [100].

The energy-efficient and high throughput MAC (ET-MAC) protocol is proposed in [101]. ET-MAC is based on added information to a long preamble and uses collision avoidance signalling and handshaking. The ET-MAC design is based on B-MAC [97], and the goal is to maximize the node's sleep time by avoiding idle listening, collisions and overhearing. The authors show by simulations that ET-MAC improves energy

efficiency and throughput, in comparison with the B-MAC protocol, by decreasing the idle listening time and number of collisions.

In [102], the authors propose an asynchronous MAC (AMAC) protocol which has a quorum-based asynchronous feature and which is based on the pattern-MAC (PMAC) protocol [103]. The principle of AMAC is that nodes can decide a sleep schedule plan based on their own traffic amount. AMAC is well scalable because it has good adaptation capability for communication environment changes and different traffic data rates. X-MAC [104] and dual preamble sampling MAC (DPS-MAC) [105] also propose modifications to B-MAC. They are asynchronous and duty-cycled MAC protocols. The X-MAC protocol is based on a shortened preamble approach whose goal is to improve energy efficiency and latency. X-MAC has also a flexible adaptation capability for both bursty and periodic data traffic. The DPS-MAC protocol reduces idle listening to increase energy efficiency. The efficiency of DPS-MAC depends on the traffic load and preamble length.

A preamble-assisted modulation for impulse radio UWB sensor networks based on the IEEE Std 802.15.4a [17] is proposed in [106]. The protocol enables the usage of clear channel assessment for UWB communication. The idea of the CCA method proposed in [106] is that preamble symbols are periodically inserted into the frame payload in the time domain so that receivers can detect ongoing transmissions. In [107], the performance analysis of the IEEE Std. 802.15.4a MAC protocol for energy detection (ED) receivers was done using the fixed RS code rate proposed in the standard [17].

Wake-up radio-based MAC solutions can be positioned to the contention-based category because they are asynchronous and do not require transmission period scheduling. Recently, the authors of [83] have proposed a MAC protocol based on a WUR for ultra low-power WSNs which can operate by using only energy harvested from the environment. The protocol is based on a nano-Watt wake-up receiver [108], which is used in cooperation with the main transceiver. The main transceiver will be awakened when the WUR receives the wake-up signal from the transmitter. In that way, the energy waste caused by idle listening of the main radio can be avoided [83]. The authors show by simulations that a WUR-based MAC improves throughput remarkably and provides 53% energy saving in comparison with TICER MAC [109], which is a transmitter initiated duty-cycled protocol but does not use a WUR. The authors have named their solution WUR-TICER [83]. Similar approaches consisting of a WUR working in cooperation with the main transceiver have been discussed in [84] and [85], which

also show that WUR-based solutions have remarkable potential to decrease power consumption and delay in short-range applications.

Contention-free protocols

Contention-free MAC protocols arrange the transmissions so that there are dedicated channel resources for different radios. That requires synchronization among the network nodes. The transmission medium can be shared among nodes, for example, by using frequency division multiple access (FDMA), time division multiple access (TDMA) and/or code division multiple access (CDMA). Usually, the WSN is divided into clusters so that the cluster head can coordinate the transmission scheduling for the nodes that belong to the cluster. In a star-topology network, the sink node takes care of the synchronization and resource sharing. However, distributed scheduling algorithms have also been proposed.

Low energy adaptive clustering hierarchy (LEACH) is a TDMA-based MAC protocol [110]. LEACH is based on clustering including cluster head rotation and is intended for energy consumption minimization. Nodes that are selected to be cluster heads send advertisement messages by using the CSMA MAC protocol. Based on the received signal strength of the advertisement messages received, other nodes can then decide which cluster head to join. A node will send an assignment information message to the selected cluster head by using the CSMA MAC protocol. The cluster head then takes care of the transmission scheduling inside the cluster in a TDMA fashion. LEACH has been widely studied and various improvements have been proposed in the literature.

In [111], the authors propose a protocol for a distributed assignment of collision free transmission schedules (comparable to the TDMA method) for self-organizing sensor networks. The authors introduce the usage of a super frame for transmissions scheduling. The method proposed in [111] requires a neighbour discovery phase, which is done using message exchange based on random access. After the discovery phase, the neighbour nodes organize their communication time schedules in a distributed fashion. The proposed super frame structure includes a TDMA period for data transmissions and a BOOTUP period for neighbour discovery. The proposed method is scalable only to flat network topologies.

The RT-Link MAC protocol proposed in [112] is based on TDMA and supports mobility. It has been designed to provide a low end-to-end latency and good throughput

and to decrease energy consumption, leading to increased lifetime. RT-Link is designed particularly for applications which require low-latency real-time communication [113].

Hybrid protocols

There are also hybrid MAC protocols, which include features of the contention-based and contention-free methods. One good example is the MAC layer solution of the IEEE Std 802.15.4, which is designed for the star topology and peer-to-peer communication [20]. In that solution, there are superframe-based modes and modes without a superframe. The superframe begins with a beacon message transmitted by the cluster head, which is defined to be a full function device (FFD). Reduced function devices (RFD) are basic sensor nodes which should receive the beacon to acquire synchronization, a superframe structure and control information. The superframe structure is divided into active and inactive periods. The communication from RFD to FFD takes place during an active period and RFD radios can be in a sleep mode during inactive periods because then they cannot communicate to FFD. The active period is divided into the contention-access period (CAP) and contention-free period (CFP). During the CAP, the nodes can access the channel randomly, in a slotted fashion, using the CSMA/CA protocol. During the CFP, the nodes can get guaranteed time slots when they can transmit in a contention-free TDMA fashion. The GTS mode is more flexible than the traditional TDMA since the length of a GTS period can be dynamically adjusted by the FFD. If the FFD has something to send to an RFD, then it will announce the pending packet in the beacon message. The RFD must then request the pending packet from the FFD during the CAP. If the FFD wants to communicate with another FFD, then it must act as an RFD associated with that FFD. In a mode without a superframe structure, communication is carried out using the unslotted CSMA/CA protocol. Communication from the FFD to an RFD is carried out so that the RFD must periodically poll pending packets from the FFD. In this mode, FFDs can communicate with each other easily because they are active all the time.

The IEEE Std 802.15.4 includes many features that support low power consumption. The CSMA/CA scheme does not involve RTS/CTS message exchange, which reduces energy consumption and provides higher channel utilization in certain situations but suffers from the hidden-terminal problem in multihop networks. The standard enables to turn off the radios, which reduces energy consumption. The IEEE Std 802.15.4 has also

a battery life extension mode, which limits the back-off exponent to take values between zero and two [20].

The MAC layer of the IEEE Std 802.15.6 also defines different modes, which include contention-free and contention-based channel access [16]. The WLAN mesh protocol IEEE Std 802.11s [114] also defines channel access which includes contention based on contention-free transmission slots. The reason for the fact that many of the recent WSN and ad-hoc MAC protocols include different modes must be the characteristic of these networks and varying applications scenarios which require dynamic and scalable protocols.

The Z-MAC protocol [115] incorporates the CSMA method to TDMA-based scheduling. The CSMA method is intended for low-traffic cases, and TDMA is a good option for high traffic loads. Z-MAC does time slot assignment so that two nodes within a two-hop communication range have assignment to the same slot. The local frame size is also adapted according to the node's neighbourhood size to enable dynamic channel utilization. The CSMA method is used so that a node can compete for the channel access in a slot which is not used by the slot owner. Before competing for the access in a slot, the node must first listen for a certain time to make sure that the slot is not used by the owner. Each node must also listen to the channel during a neighbour's time slot in order to be able to receive possible upcoming transmissions. Therefore, the channel competition option (slot stealing) increases energy consumption [116]. In [117], the authors propose TDMA scheduling with adaptive slot stealing and parallelism (TDMA-ASAP) for WSNs. The TDMA-ASAP protocol enables longer sleep times and therefore reduces energy consumption in comparison with Z-MAC.

A traffic-adaptive MAC protocol (TRAMA) is proposed in [118]. TRAMA targets to avoid collisions and save energy by enabling nodes to be in a low-power idle state whenever they are not participating in communication. TRAMA uses distributed election for channel slot assignment to nodes which have data to send.

A recently proposed smart body area networks (SmartBAN) MAC protocol was defined for medical, wellness, leisure and sport application purposes [119, 120]. The SmartBAN MAC protocol uses separate channels for data and control messages and defines different channel access modes: Scheduled Channel Access, Slotted Aloha Channel Access and Multi-use Channel Access. Multi-use Channel Access enables that the high priority messages can be transmitted with a low delay during each slot when required. In addition, in the Multi-use Channel Access mode, a secondary user can try to

transmit in the scheduled access slot using S-Aloha, if the slot is not used by the node for which it was reserved and there is not a high priority transmission ongoing.

2.1.3 Network layer

The network layer takes care of routing and end-to-end delivery of messages in WSNs. In addition, in the routing protocol design for WSNs, energy efficiency has been seen to be the most important design goal. At the general level, routing protocols can be divided into a proactive and a reactive category [121]. The proactive methods perform route discovery before the request for communication. Therefore, the routes are already established when there is a need to route data messages in the network. In the reactive protocols, the route will be discovered in on-demand fashion after some source node sends a route request message to the network. In addition, there are hybrid protocols, which combine features of the proactive and reactive algorithms.

In WSNs, the route is typically selected based on the link distance, number of hops on the path, nodes' residual energy or transmission power. Usually, routing protocols calculate the cost of the path by using the metric which is the most important from the application requirements point of view. Once the cost of the paths is calculated, the routing protocol selects the minimum cost path for communications. However, if the protocol always selects the same minimum cost path, the nodes along the path will finish their energy sources and become disconnected from the network. Therefore, the routing protocol must take care of load balancing so that the network's overall energy efficiency and lifetime will be maximized and the connectivity will be maintained as good as possible. Another important design goal of the WSN routing protocols is the minimization of control overhead, because that is a redundant energy consumption factor and decreases the amount of bandwidth that can be used for valuable information transmissions.

A well-known standardized routing protoccol for WSNs is defined by the ZigBee Alliance [122], which has developed network and application layers above the IEEE Std 802.15.4 PHY and MAC layers [15]. The ZigBee protocol enables multi-hop mesh networking, and the routing is based on the ad hoc on-demand distance vector (AODV) protocol. ZigBee uses clustered topology, where the cluster head is a FFD and basic nodes are RFDs, according to the IEEE Std 802.15.4 definition. The FFD coordinates the communication inside the cluster and the RFDs can use multi-hop routing towards the FFD.

Recently, a comprehensive survey about energy-efficient routing protocols for WSNs was done in [123]. In that survey, the routing protocols are classified into four categories [123]: network structure, topology-based, communication model, and reliable routing. The network structure-based routing category is further divided into flat and hierarchical categories. In flat networks, all the nodes are assumed to have the same roles and characteristic from the routing point of view. In hierarchical networks, the nodes have different roles, i.e., the network is clustered so that the cluster-head nodes can coordinate the communication and forward messages between the clusters. The communication model is defined to be a query- or negotiation-based. In addition, a distinction is made between coherent- and non-coherent-based protocols depending on whether the data is processed or not processed locally before the transmission. The topology category includes location- and mobile agent-based protocols. Reliable routing protocols are classified into QoS- and multipath-based methods. The work done in [123] provides a thorough discussion about energy-efficient routing protocols for WSNs and analyses their advantages and disadvantages.

2.2 Cross-layer approaches

The limited processing capabilities and energy resources of WSN nodes have led to an emerge of cross-layer designed protocols, which take jointly account of the different layers' characteristics to improve the overall performance of the communication. There are many possible ways to perform joint design of different layers and their interactions. Therefore, there is an enormous amount of research labelled as cross-layer designs.

The following definition for cross-layer design has been given by Srivastava and Motani in [124]: *Protocol design by the violation of a reference layered communication architecture is cross-layer design with respect to the particular layered architecture*. By the violation of a layered architecture the authors mean, e.g., new interface creation between layers, layers' boundaries redefinition, particular layer's protocol design by taking details of another layer into account, and joint tuning of parameters across different layers. In other words, cross-layer design takes advantage of interactions between the layers.

The definition for cross-layer design has been further formulated by Jurdak in [125] to also include algorithm and architecture design in it: *Cross-layer design with respect to a reference layered architecture is the design of algorithms, protocols, or architectures that exploit or provide a set of interlayer interactions that is a superset of*

the standard interfaces provided by the reference layered architecture. Jurdak defines further that the interlayer interactions can be divided into two different categories: *information sharing* and *design coupling* [125]. By using information sharing, the different layers can share information through interfaces which can be implemented between adjacent or non-adjacent layers. The cross-layer designed architecture can also enable that there is a common parameter data base accessible by all the layers. Design coupling means the design of protocols and algorithms which exploit the features or avoid the weaknesses of the existing mechanism. Further, design coupling also includes designs which integrate the functionalities of adjacent layers partially or completely by producing a new cross-layer designed protocol which merges these layers [125]. In [124], the merged layers are referred to as a super layer, which replaces the original layer of the protocol stack.

In this thesis, the following categorization for the cross-layer design approaches is defined:

- *Merging of layers*: The functions of the protocols at two or more layers are jointly designed by merging them to create a single cross-layer designed protocol.
- *Information exploitation between layers*: The information between the different layers is exploited in a cross-layer fashion while maintaining the original layered protocol stack structure.

That definition of categories is used in this thesis because it makes a clear distinction between the cross-layer approaches. The distinction is based on whether the original layered structure is maintained or revised in the cross-layer design, as illustrated in Figure 8. The former approach does not maintain the original layered protocol structure but instead jointly designs the functions of the protocols at two or more layers by merging them into a single cross-layer designed protocol. For example, the PHY and MAC layers can be jointly designed and the upper layers maintain the layered structure, or the entire protocol stack can be merged into a single cross-layer protocol. The latter approach maintains the original layered protocol structure but exploits the information exchange between the different layers, or uses a common data base for all the layers, to improve the performance in a cross-layer fashion. This approach usually includes interface definition between the cross-layer designed layers, but new interfaces are not needed if the required cross-layer information can be exchanged by using the existing interfaces. In addition, the design coupling approach is positioned in this work to the information exploitation category, because in that case the details of a fixed layer(s)

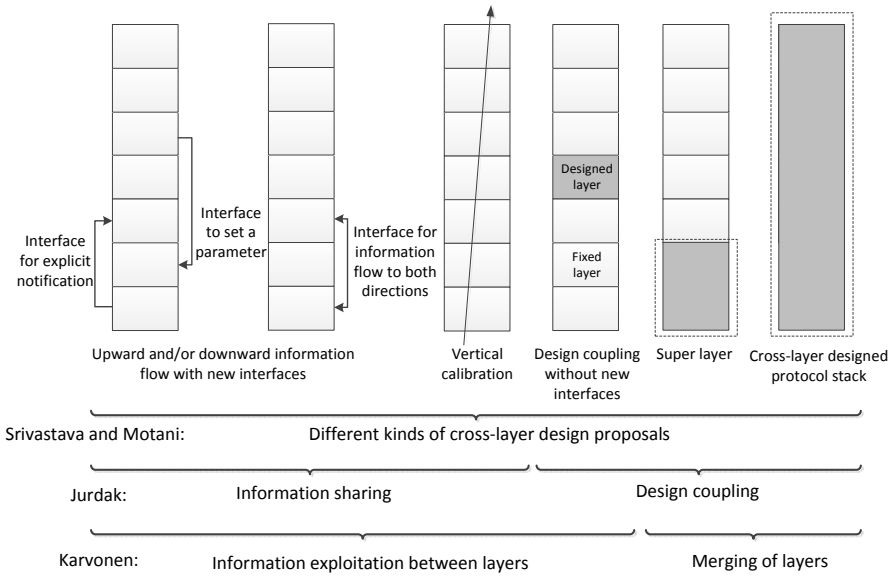

Fig. 8. Illustration of the cross-layer categories defined in this thesis.

are exploited during the design phase. Vertical calibration also uses details of other layer parameters for the adjustment of (cross-layer optimized) parameters across the layers during the design phase or dynamically during the network run-time. Both of the categories, which are defined above, take advantage of the information exploitation between the layers; the difference between them is that the former category also uses the merging of two or more layers. Therefore, the following definition for cross-layer design is proposed here: *Protocol design using information exploitation between the layers of the reference layered architecture either in the design phase or during run-time − with or without merging of layers*. That definition includes both categories and the information exploitation can include new interface(s) design or it can be done with the existing interfaces. In addition, the information exploitation can be performed already in the design phase when using design coupling. Therefore, the proposed definition includes all the cross-layer approaches discussed by Srivastava and Motani [124] and Jurdak [125].

Modularity and scalability are easier to maintain in the information exploitation approach, which maintains the original layered structure. When the different layers are merged, it is difficult to replace those layers by using some other protocol, which means that modularity is lost. In the layered approach, modularity enables that, at least

in principle, a protocol at one layer can be changed without affecting the design of the other layers. On the other hand, cross-layer performance gains usually increase when the layers are merged. However, typically the merged designs are tailored for the target application scenario, and therefore scalability of those designs is weak. Figure 9 illustrates the effect of the different cross-layer approaches on performance, complexity and modularity measures. It is not straightforward to make a strict distinction between these measures for different approaches, but the figure provides a rough illustration of the differences.

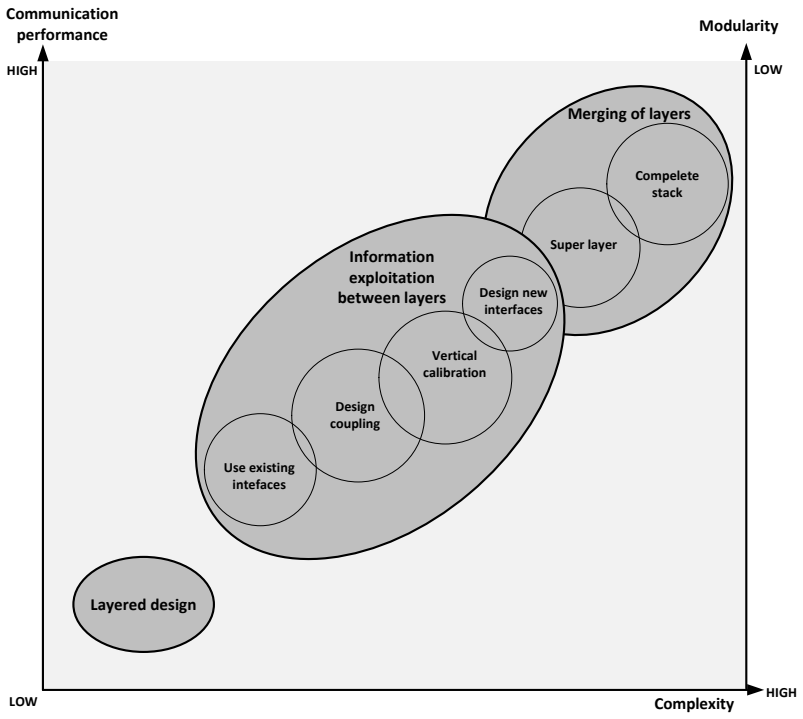

Fig. 9. Illustration of the cross-layer approaches' performance, complexity and modularity.

The main focus of this survey is on the works that address the PHY and MAC layers, because the focus of this thesis is on those layers. However, research on higher layers will also be introduced to get a thorough view of the research work done in the cross-layer design area. In addition, the PHY and MAC layer parameters' selection can also be taken into account in the routing protocol design, and therefore it is important

to understand the interactions between those layers and to discover possibilities for performance improvements throughout the whole stack. Figure 10 illustrates the topics addressed in this section and outlines the introduced related works for each topic.

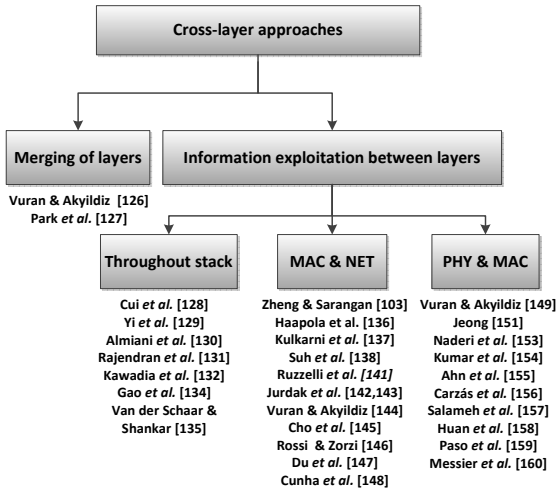

Fig. 10. Taxonomy of the review of cross-layer approaches and addressed previous works.

2.2.1 Merging of layers

Two different designs that merge multiple layers by using a cross-layer design will be described in this section. These approaches violate the layered communication protocol architecture by combining functionalities of the layers to a single cross-layer designed protocol to enable more efficient communication in comparison with the original layered structure.

The cross-layer protocol (XLP), which combines the functions of a traditional layered protocol stack MAC, routing and congestion control into a single protocol is introduced in [126]. The design goal of the XLP is to achieve efficient and reliable communication with minimum energy consumption. The XLP solution relies on traditional RF-transceiver PHY-layer functionalities, which are needed below the proposed cross-layer solution. The XLP is based on the concept of initiative determination as well as receiver-based contention and forwarding, local congestion control and distributed duty-cycle method, i.e., the nodes can set their own sleep/awake schedule asynchronously. The XLP's core idea is that an individual node can decide that is it willing to participate

in communication depending on the link quality, traffic load and energy level. After listening to the channel to ensure that it is free (CSMA), the transmitter node broadcast an RTS packet and then the neighbour nodes make the decision about participating in the communication by using initiative determination based on the state of the node.

According to the definition for XLP initiative determination, the receiver decides to participate in the communication if all the following conditions are satisfied: the SNR of the link is reliable enough; the node does not have too much traffic to relay; the node buffer does have enough space; the node has enough remaining energy. In addition, the nodes must know their location so that they will not participate in the forwarding if they are not closer to the sink than the source is. The receivers compete for channel access if they decide to participate to communication. Before transmitting a CTS packet, the receivers determine their back-off duration based on their location in the network with respect to the source nodes and the sink node. The first node which sends the CTS will acknowledge to the source that it is willing to forward the packet. Other receiver nodes that are competing will also receive the CTS and therefore they can go back to the sleep mode because there is already a forwarding node which will provide better progress (in distance) for the packet. After receiving the CTS message, the source node transmits the data packet.

By taking all the above-mentioned conditions into account, the XLP design addresses important problems of the cross-layer design because reliability, congestion control and energy consumption are taken into account in a distributed fashion. There are some problems that may occur during the procedure: the CTS may collide; there are no neighbours whose initiative conditions are met; there are no nodes closer to the sink. However, XLP proposes solutions for these cases. If the initiative condition is not met, the neighbour sends a keep-alive packet so that the source knows that there is a node which may be willing to forward later on. The source will also reduce the data generation rate if it receives only keep-alive messages, because then it knows that the network is congested. If the CTS is not received, the source assumes that they have collided and retransmits the RTS message until the maximum number of trials is reached. For a case that there are no nodes closer to the sink, XLP defines an angle-based routing solution, which takes care that the packet can be routed around the void.

An energy consumption analysis for a single packet transmission from the source to the sink using multi-hop forwarding according to the XLP principle is also developed in [126]. The model takes account of the packet transmission success probability at the PHY layer. The authors also perform simulations which take into account channel

errors, packet collisions and energy consumption. The design and results in [126] show that a cross-layer designed protocol stack can improve the communication performance with lower implementation complexity when compared to a layered approach and other previous cross-layer protocols. XLP is designed to replace the entire communication protocol stack but, according to the authors, future research is also needed in this area. In particular, the authors mention that future work is needed for cross-layer designed adaptive modulation, error control and topology control.

Breath is an adaptive cross-layer protocol designed for reliable and low-delay communication while taking into account energy efficiency [127]. The protocol is designed for a WSN system where the source nodes send the packet to the sink using multi-hop communication. The authors proposed a constrained energy efficiency optimization model whose constraints are delay and reliability. The protocol is based on randomized routing and MAC with duty cycling, which are jointly optimized to achieve energy efficiency while taking into account the packet latency and reliability requirements. The Breath protocol's optimal working point is enabled by the proposed algorithm, which can be used to adapt the hop distance, sleep period length or transmit power, depending on the traffic load and channel conditions. Each node can go to sleep for a random time duration, which depends on the traffic and network conditions. Breath is based on geographic clustering, and the route selection is done randomly to avoid using fixed routes and routing tables. The messages from the source cluster are relayed via other clusters that are between the source cluster and the sink. Breath uses a CSMA/CA-based MAC, whose operations are jointly optimized with sleep period lengths and randomized routing. The assumption is that nodes have location information, which is calculated from the received signal strength indicator (RSSI) information. Location information is used to select optimally the hop distance and the transmit power of the nodes. The authors found that an exact analytical solution cannot be found because the optimization problem is too complex. Therefore, an approximate solution for constraints and upper bound for energy consumption were used in [127]. For the medium access collision probability, the authors use the Markov chain model for the CSMA/CA method.

The authors have implemented the Breath protocol and found that their solution can outperform the IEEE Std 802.15.4-based implementation in terms of energy efficiency and reliability. Therefore, the authors conclude that the Breath protocol is an ideal candidate for applications which have low delay and high reliability requirements (e.g., control and automation applications). That analysis is done for a specific topology

where only the source cluster can send packets and other clusters act only as relays. This assumption restricts the usage of the results since it does not consider real mesh network characteristics and the results are limited to the considered scenario. However, the results show that cross-layer optimization of physical, MAC and routing layer parameters will improve the energy efficiency in comparison with the IEEE Std 802.15.4-based implementation when using the network topology and assumptions considered in [127].

2.2.2 Information exploitation between layers

The information exploitation approach takes advantage of information sharing between the different layers to improve the performance of the target layers. The purpose is that different layers can exchange information which is important from the communication performance point of view. In this section, the previous works that cover well this wide research area, which has enormous number of potential ways to improve energy efficiency, are introduced.

Throughout stack interaction

A cross-layer energy efficiency optimization model for the physical, MAC and routing layers is proposed in [128]. The uncoded M-ary quadrature amplitude modulation scheme is used at the PHY layer and an interference-free TDMA MAC and a centralized control with a perfect synchronization is assumed. Therefore, the study is restricted to small-scale networks, which include few dozens closely located nodes so that synchronization and interference-free scheduling can be achieved. The authors point out that the energy consumption minimization problem, when taking multiple layers into account, is complex and hard to solve. The authors find an approximate solution to the problem by using convex optimization for the study of delay and energy consumption trade-off. Based on the results, the authors conclude that by using joint optimization and adaptation for different layers, significant energy gains are possible in comparison to a non-optimized layered approach.

In [129], the authors introduce a cross-layer optimization model for link-layer scheduling, power control, and routing in UWB-based large-sized sensor networks. For channel resource allocation, the authors use sensor nodes allocation to different frequency sub-bands. Power control optimizes the transmission power for a given sub-band, and the routing solution selects a path from the source node to the sink. The

authors formulate the problem as non-linear programming (NLP). In [129], the problem is solved by using a branch-and-bound approach. By performing simulations, the authors show the usefulness of their solution and the importance of cross-layer optimization.

An energy-aware cross-layer data gathering protocol (RMC) is proposed in [130]. The RMC integrates the routing, MAC and clustering protocols targeting to collision-free communication. The RMC is based on local scheduling and forwarding decisions which decrease the overhead that would be caused by topology changes. Cluster formation has been seen viable for energy efficiency also in [131] and [132]. A flow-aware medium access (FLAMA) protocol is proposed in [131], where MAC schedules are adapted to traffic flows which are known from application characteristics or using traffic prediction techniques. The FLAMA protocol also determines the receiver mode and sleep mode states for the nodes to save energy. A distributed election algorithm is used in the FLAMA to schedule the transmission through a data forwarding tree which is formed so that some nodes act as a parent node (cluster head) for associated child nodes. A performance evaluation of the CLUSTERPOW [133] and MINPOW protocols, which are cross-layer solutions to the clustering, power control and routing problem, has been done in [132]. A coalition-aided cross-layer optimization approach is presented in [134], where the possible energy efficiency improvements have been explored by studying the interactions between the PHY, MAC and NET layers. Data aggregation and cooperative communication are used to reduce the channel contention, and the MAC layer exploits the physical layer conditions [134] to improve energy efficiency and energy balancing across the sensor nodes. A cross-layer design problem is formulated for the PHY, MAC and APP layers in [135] to improve quality and to reduce the power consumption of wireless multimedia transmissions. The authors provide examples of cross-layer design cases and highlight the importance of the radio parameters' adaptation when taking into account the interactions between the protocol stack layers.

MAC & NET interaction

Cooperation between the MAC and NET layers can improve the route selection because the routing protocol can take into account the channel access competition, resource sharing and sleep scheduling information from the MAC layer. On the other hand, the NET layer can indicate the preferred routes to MAC layer, and channel access can then be scheduled taking that into account. If, for example, the MAC layer does channel

access coordination only between the neighbours and does not do cooperation with the network layer, then end-to-end latency can be large and it cannot be avoided.

The MAC and routing layer interaction for sleep scheduling design has been addressed, e.g, in [103], [136] and [137]. The PMAC protocol, which is based on adaptive sleep/awake schedules, is proposed in [103]. Adaptivity is based on the knowledge of the node's own and its neighbour's traffic knowledge. The nodes exchange information about the upcoming traffic estimate, and the sleep period lengths are determined based on that information. Only the nodes which are on the routing path need to wake up for data forwarding, i.e., there is cooperation between the network and MAC layers. The authors show that PMAC saves energy in comparison with a fixed period-based SMAC. The analysis done in [103] does not take account of the effect of the physical layers transmission success probability, which may affect the actual traffic in the network due to retransmissions. Moreover, PMAC requires strict synchronization, which requires communication and is therefore energy consuming. In [136], cross-layer analysis is used to analyse a single-hop and multi-hop WSN with the focus on the effect of sleep periods on energy consumption. The authors state that even though ideal multi-hop communication outperforms single-hop communication in many scenarios, it is important to develop more realistic energy consumption models which take into account the PHY and MAC layer characteristics to acquire more reliable insight to the performance comparison. The authors show that single-hop communication has 40% lower energy consumption when using their cross-layer energy consumption model. Moreover, the authors show that regular sleep periods can reduce energy consumption significantly, particularly in a low traffic case. An integrated MAC and routing protocol solution for WSNs with rare events is proposed in [137]. The authors' purpose is to decrease communication overhead by light addressing, tiered topology organization for routing, and a power-saving mode enabling the nodes to go directly to the sleep mode independently. The authors found that their protocol outperforms S-MAC [94] in terms of average energy consumption while satisfying the end-to-end latency requirement.

A cross-layer protocol called MAC-CROSS takes advantage of the MAC and NET layer interactions [138]. The protocol uses routing information to schedule maximum sleep periods for the nodes that do not need to participate in the communication. The MAC layer of the MAC-CROSS protocol is based on the existing S-MAC [94], [95] and T-MAC [96], which use CSMA/CA method.

Multipath transmission can be used to improve the communication reliability [139], [140]. In [139], the authors propose a lightweight source coding/decoding algorithm

based on exclusive or (XOR)-operation and fault tolerant routing for WSNs. The algorithm is designed so that it does not require much computational operations and storage capabilities. The coding level is adjusted by using the network state information from the routing algorithm. The routing scheme avoids sending the packet in the paths which are found to be failed. The proposed coding algorithm divides the information into multiple packets that are sent via different paths. From the correctly received packet fragment index numbers, the sink can find which are the successful and failed paths. The sink will send an ARQ message containing information about the failed paths to the source node. The sink node estimates the network communication reliability states from the number of successfully received packets by using the exponential weighted moving average (EWMA) method. If the average loss rate is above the threshold, the sink may send a message containing information about the coding ratio adjustment to the source node. By performing simulations, the authors found that their method improves reliability in comparison with the maximum residual energy routing scheme (MRE) combined with an ordinary FEC algorithm. The tradeoff between the possible increased energy consumption and achieved reliability gain is not evaluated in [139]. A hybrid FEC-feedback transmission mechanism for multi-path transmissions is proposed in [140]. The FEC-feedback algorithm principle is such that the sink will send an acknowledgement (ACK) message to the source once the bitstream is correctly recovered. The source node will then stop the transmission. According to the authors, the proposed feedback mechanism reduces the number of retransmission and therefore improves energy efficiency [140] in comparison with multi-path transmission without feedback. The methods introduced in [139] and [140] are suitable for applications with high reliability requirements. The authors point out that the cross-layer interaction design is highly important and remains to be done in future work for the proposed method [140]. In addition, the evaluation of the tradeoff between increased energy consumption, in comparison with single path transmission, and achieved reliability gain is not addressed in [140].

The cross-layer designed MERLIN (MAC and energy-efficient routing with localization support integrated) protocol has been proposed and evaluated in [141]. The MERLIN protocol uses multicast upstream and downstream relaying for packets transmitted to and from the gateway. The network topology is divided into different time zones and a scheduling policy is used for routing the packets efficiently and reliably to the closest gateway. The MERLIN protocol is designed for low duty-cycle sensor networks using multi-hop topologies with designated sink nodes.

In [142], local and neighbour state information is used in a cross-layer fashion to adapt the MAC and routing layer behaviour. The proposed method improves the global energy efficiency and enables to fulfil the application requirements. The used MAC protocol is based on B-MAC [97], which adapts the duty cycle with the adaptive low-power listening (ALPL) method [143], [142]. ALPL is based on a cost function which decreases routing costs and adapts the listening mode lengths of the B-MAC protocol to save energy. However, the optimization framework proposed in [142] is independent of the underlying MAC or routing protocol and is scalable to large and dense networks.

The adaptive medium access control (A-MAC) protocol for heterogeneous wireless networks is proposed in [144]. A-MAC is based on a two-layer architecture, which selects the most suitable network, for a terminal, always when it gets a flow and provides QoS-based scheduling in case of multiple flows. The authors state that A-MAC is the first adaptive MAC proposal which takes care of the mentioned functionality without requiring any modifications to the existing network structures. A virtual cube concept for comparison of different networks, in terms of desired performance metrics, is also introduced in [144].

In [145], the authors propose the cross-layer medium access control (CLMAC) protocol. CLMAC is based on the network and MAC layer interaction so that routing distance is added to the preamble field of B-MAC. The solution reduces routing control traffic and enables energy-efficient routing. The MAC and network layer interaction is also used in [146] to improve energy efficiency in WSNs. The authors consider hop count coordinates-based routing algorithms and propose a MAC technique that is designed to efficiently find the minimum cost nodes within node radio coverage. The routing algorithm uses MAC layer information to find cost-efficient routes. The cross-layer designed routing enhanced MAC protocol (RMAC) is introduced in [147]. RMAC is duty cycle-based and improves end-to-end latency in comparison with existing protocols such as S-MAC. RMAC also mitigates the traffic contention problem more efficiently than S-MAC while maintaining energy efficiency and high throughput. The dynamic duty-cycle adjustment method for the S-MAC protocol (SMAC-DCC) is proposed in [148]. SMAC-DCC adapts the duty cycle based on the network traffic load information from the network layer. Based on the simulation results, the authors conclude that latency and energy consumption can be decreased by using the proposed cross-layer approach [148].

In wireless communication, errors that occur in the transmission medium due to thermal noise, multi-path fading effect, multi-user interference and/or collisions must be mitigated. The PHY and MAC layers have an important role in avoiding errors caused in transmissions and channel access. In WSNs, it is important to avoid retransmissions and idle listening, because the radio transceivers consume most of the nodes' power budget. However, the retransmission and idle listening avoidance must be done so that the added overhead is not too large in comparison with the energy consumption decrement that can be achieved by using it. Therefore, there is a tradeoff to explore, which has been addressed in previous works that are surveyed here.

In [149], the authors study the effect of ECC methods on energy efficiency in WSNs by using a cross-layer analysis which takes the effects of the MAC and physical layers into account. The studied MAC is contention-based (with CSMA and handshake), and broadcast transmissions are used. The authors derive models for energy consumption, latency and packet error rate (PER) calculation, which can be used to compare the performance of the FEC, ARQ and hybrid-ARQ schemes. The authors do not study the convolutional codes because they have been found to be energy inefficient in typical WSN communication scenarios [53], [59], [149]. In addition, the rateless codes are neglected because they are efficient only for very long payloads, which are not used in WSNs, and therefore the authors focus on the block codes (BCH and RS) [149]. In [149], the performance evaluation is done for Mica2 and MicaZ nodes [150]. The authors mention in [149] that ECC is highly important in WSNs due to strict energy constraints. HARQ and FEC coding can be used to improve error resiliency and enable lower transmit power or hop length extension, which is useful when combined with a channel-aware routing protocol. In [149], the authors found that hop length extension, achieved by using HARQ and/or certain FEC codes, can decrease energy consumption and end-to-end latency in comparison with ARQ. Furthermore, the authors found that transmit power control can be used for energy efficiency improvement, particularly in a scenario where low end-to-end latency is not required. The authors also conclude that the selection of a suitable ECC scheme (FEC, ARQ or HARQ) depends highly on the characteristics of the sensor nodes and the application characteristics (e.g., end-to-end distance and target BER).

Potential communication improvement techniques for WSN transceivers have been evaluated in [151] using a practical approach by performing outdoor measurements with

a wireless sensor network platform, which was using a CC1000 transceiver [152]. The authors added single error correction/double error detection (SEC/DED) coding and a retransmission mechanism which mitigates the packets lost due to multipath effect and collisions. The measurement results show that the use of this simple SEC/DED code improves the transceiver packet reception rate performance, but the energy efficiency analysis was not done in this work [151].

In [153], the performance of different error control strategies for WSNs intended for multimedia communication has been studied. The authors compare the performance of ARQ, link-level FEC, application-level erasure coding, hybrid-ARQ, and cross-layer hybrid schemes. The studied cross-layer schemes include: erasure coding combined with link-level ARQ; erasure coding combined with link-level FEC; and erasure coding combined with hybrid-ARQ. By simulations, the authors show that these cross-layer methods improve reliability in multimedia transmission. The authors found that simple RS coding consumes less energy than the other schemes and cross-layer hybrid schemes have the highest energy consumption [153] because in their setting they allow too high number of retransmissions. On the other hand, the results show that from the delay point of view, the cross-layer schemes performs best. According to the authors, the results show that the energy consumption and reliability tradeoff must be improved further in future studies. They mention that there is a need to design an adaptive QoS-aware error control scheme that takes account of both energy efficiency and reliability in the case of delay-constrained communication in WSNs [153].

A cross-layer approach for the PHY and MAC layers of the IEEE Std 802.15.4-based WSNs with LEACH clustering algorithm is proposed in [154]. The authors compare the clustered and non-clustered network delay, throughput and power consumption performance. By performing simulations, the authors found that a cross-layer approach with clustering decreases the communication delay, but further optimization for the optimal number of clusters is needed to achieve also energy efficiency gain.

In [155], the authors propose for mobile WSNs an adaptive FEC code control technique (AFECCC), which dynamically sets the amount of FEC redundancy per packet based on the arrivals of ACK packets. The proposed method does not therefore require the information of the SNR or BER. In [155], the main performance metric is throughput, and also the overhead of different algorithms is estimated. The authors show by simulations and implementation that their adaptive method performs better than fixed code rate FEC algorithms. However, the authors do not evaluate the energy efficiency performance of the proposed method.

An adaptive method for MQAM modulation level selection at the PHY layer and time slot assignment at the MAC layer with a goal to minimize transmission energy in WSNs has been proposed in [156]. The model takes account of the application bit rate requirement and symbol error rates in the modulation and time slot allocation adaptation for a particular user. The optimization model is based on SNR gap approximation with focus on the bit rate and reliability so that the symbols' error rate is maintained for the required bit rate by using adaptive modulation. The energy minimization model introduced in [156] is simplified one because it is based only on the transmitted symbol energy and the relation between the duration of the symbols transmitted in the slot and the duration of the time slot.

An adaptive selection of the MAC protocol back-off probability and PHY layer MQAM modulation order, which depends on the packet retransmission delay constraint and traffic load, is proposed in [157]. This adaptive cross-layer scheme improves energy consumption per successfully communicated bit.

A PHY/MAC cross-layer model, which can be used to study the energy efficiency of orthogonal modulations in variable-length TDMA-based WSNs, is introduced in [158]. The authors studied the pulse position modulation (PPM) and frequency-shift keying (FSK) modulation methods and found that PPM is more energy efficient in dense WSNs. Moreover, they showed that the cross-layer approach provides energy gains in both modulation cases.

A modulation adaptation method for IEEE Std 802.15.4a UWB communication is proposed in [159]. The authors use a cross-layer approach to the physical and MAC layers to adapt the modulation based on the QoS requirement and channel information. Based on the results, the overall system throughput and delay can be halved by using the proposed modulation adaptation method [159].

A transmission power control algorithm for WSNs is proposed in [160]. The authors uses a cross-layer approach so that the transmission power at the PHY layer is adapted by using the multiple access interference information given by the MAC layer. The authors find that when using cross-layer information, significant energy efficiency gain can be achieved with a feasible low-complexity increment.

2.3 Summary and discussion

From the literature review, it can be found that there is a large number of works which target to enable energy efficient communication in WSNs. The reason is that transceivers have been found to consume most of the energy in typical sensor nodes. There are different methods, at different layers of the protocol stack, which can be considered for possible energy savings.

It can be observed from the previous works that at the physical layer, error correction coding, modulation method and transmission power adjustment were found to provide energy savings. Transmission power optimization is a straightforward way to improve energy efficiency. If transmission power can be decreased while still achieving successful communications, energy consumption decreases. On the other hand, transmission power can be increased, if reliability is not at the desired level, in order to avoid retransmissions. However, power can be increased only until the regulated maximum power in the given band is reached. In addition, the transmission power increment will also increase transmission energy consumption and interference to other nodes. Modulation method adaptation (bits per symbol) can be used to improve reliability and energy efficiency. However, typically low modulation levels (often binary modulation) are used in WSNs, and therefore the adaptation possibilities are limited. Error correction coding can be used to increase reliability, which decreases the number of retransmissions and energy consumption. There are many types of codes that can be used to improve reliability. Error correction strength, and consequently also complexity, can be increased, if the reliability requirements are not met. However, in energy efficiency optimization, the tradeoff between coding overhead and energy saving gain must be evaluated. In comparison with transmission power increment, the difference is that when coding complexity is increased, it does not directly generate more interference to other nodes in the vicinity. However, it must be taken into account that because stronger coding increases the packet lengths, more traffic will be generated to the channel, causing higher probability of collisions and decrease of the data throughput.

At the MAC layer, idle listening, collision, overhearing and control overhead minimization have gained a lot of attention, and many protocols have been proposed to solve the problems. Most MAC protocols use duty cycling for scheduling the nodes' sleep/awake periods to save energy. Recently, wake-up radio-based MAC solutions have been proposed because they have potential to save energy, particularly when the event frequency is low. It depends on the application characteristics, mainly on the

traffic intensity, which one should be favoured. Performance comparison has not been widely studied, and therefore there is a need for cross-layer models which enable the selection between the duty cycling and wake-up radio methods. There is also a need for a MAC protocol which takes advantage of wake-up radios and is scalable to different application scenarios.

Network layer routing protocols' most important design goal from the energy efficiency point of view is to minimize the protocol overhead and the energy consumption cost of the selected path. In path selection, it must also be taken into account that the network may not be congested (to avoid bottlenecks) and that the network connectivity will be maintained by taking fairness into account so that energy resources will not be finished in particular nodes. The routing performance depends highly on the lower layers because the link state (experienced channel condition and competition) affects to the communication success probability on the selected routes.

During the evaluation of the WSN research, the cross-layer design has gained attention because it has been found to provide more energy-efficient solutions than the traditional layered design. Numerous different cross-layer models have been proposed, focusing on different parts of the protocol stack. The survey introduced different types of cross-layer design approaches. Some of them violate the layered structure by using merging of layers, while others take advantage of the information exploitation between the layers. Both approaches require the development of cross-layer models which can be used to evaluate and enable the design of protocols characteristics and the required information exchange.

The WSN application field is so wide that it is difficult, or even impossible, to develop a general cross-layer designed protocol stack solution. Furthermore, in the related work, e.g., about error control coding, it has been found that it is very difficult to find a method which is adequate for different applications that have varying channel conditions, resource constraints, multi-user interference, and application requirements. In some cases, BCH or RS codes were found to be the most efficient while, in some other applications more complex codes, e.g., convolution or LDPC, could be considered. In addition, rateless codes are found to be efficient, particularly in a dynamic environment, because the coding algorithm enables that the redundancy will be adapted according to the channel conditions without a need for channel estimation. Adaptive coding based on fixed code rates requires knowledge of the channel state or received SNR. The general conclusion regarding error control coding is that it cannot be very complex because

low-power transceivers set limitations to the decoding complexity. Therefore, block codes are preferred in majority of the previous studies.

Each proposed model has its own valuable contribution to the development of future wireless sensor and body area networks. However, there is still room and need for further optimization in many scenarios. Particularly, when using a cross-layer design, there are wide-range of performance improvement possibilities when taking into account the interactions between the different layers. However, in the cross-layer design there are also many challenges because that can lead to unintended consequences [161], [162], [163]. Violation of the traditional architecture will lead to non-modular solutions, which are difficult to update, also their scalability is usually weak because the designs are typically tailored for some particular application scenario. Table 3 provides a summary of the conclusions made after the related work review.

In this thesis, three different models will be introduced to enable energy efficiency improvements in WSNs. The focus is on the PHY and MAC layers because these layers are the most important in that they provide efficient communication media for the upper layers. The cross-layer approaches are developed so that they do not require redesign of the protocol stack, therefore maintaining modularity. Indeed, too complex cross-layer designs are often not useful because they are too tailored for a particular case and generalization is difficult. Therefore, the target has also been to develop a general-level cross-layer approach for lower layers intended for different types of application scenarios. Here the main focus is on a star-topology WSN and WBAN, which is based on relative fresh standard, making it valuable to explore potential energy gains. In addition, the objective has been to take advantage of the wake-up radios in order to improve energy efficiency at the link and at the network level by avoiding idle listening, which is found to be important problem. There is also a need for a model for hierarchical architecture energy consumption evaluation while taking into account the effect of the lower layers. That will enable to achieve energy efficiency gains at the network level when the network includes heterogeneous devices. In addition, the network level model focuses on the wake-up radio-based network architecture, which is a potential method for idle listening avoidance and high energy efficiency.

Table 3. Summary of the conclusions from the related work review.

Related works	Conclusion
PHY: ECC [46–50, 52, 53, 55–67]	FEC coding is found to enable significant energy gains. Even simple codes (e.g. Hamming) can improve energy efficiency in good channel conditions, while when the SNR is low, BCH and RS codes are found to be the most energy efficient. Adaptive coding is found useful since performance depends highly on the number of hops, communication distance and varying channel conditions. Convolutional, LDPC and Turbo codes have been found to require too complex decoders for typical WSN receivers. However, in the future they may be feasible when the nodes' capabilities increase. Rateless codes have been found to be a good option for varying channel conditions with relatively low complexity.
PHY: Tx power & Modulation [68–75]	Tx Power and modulation adaptation are straightforward ways to decrease energy consumption of transmission or to increase reliability. They provide an option to prefer single-hop communication instead of multi-hop by adapting transmit power and/or modulation constellation. Regulations and radio transmission power resources set limitations. Typically, simple modulation is used in WSNs due to low data rate and difficult channel conditions, which limits the adaptation possibilities.
PHY: IR-UWB [16, 20, 76–80]	Selected physical layer option for IEEE Std 802.15.4(a) and IEEE Std 802.15.6. IR-UWB with energy detection receiver enables high energy efficiency with low implementation complexity. IR-UWB PHY is not as widely studied and implemented as narrowband versions of the standards.
PHY: WUR [24–28, 82]	Wake-up radios can be used to enable continuous very low-power listening, and the nodes can be awakened with a wake-up signal. The constant power consumption of wake-up receivers can be made so low that WURs have potential for higher energy efficiency than duty-cycle radio-based networks, particularly when the event frequency is low.
MAC: Contention based [22, 83–85, 94–107, 109]	Asynchronized and synchronized protocols are proposed. Synchronization increases complexity and energy consumption. Simplicity is a feasible characteristic for WSNs and performs well for low traffic load applications. Throughput is low, and collisions increase with traffic load. Idle listening avoidance using duty cycling, also with adaptivity to increase performance for varying traffic load. These solutions enable good energy efficiency for target applications. WUR-based solutions can avoid idle listening to improve energy efficiency further.

Related works	Conclusion
MAC: Contention free [110–112]	Synchronization is required to enable contention-free channel access. They enable high reliability and throughput, which makes them suitable for high traffic load and low latency applications. Enables prioritization of transmissions. Energy consumption increases with the added complexity in comparison with contention-based protocols. Duty cycling is used to save energy. These solutions typically require a central coordinator but there are also distributed versions available.
MAC: Hybrid [16, 20, 114, 115, 117–120]	Enables scalability to different applications due to different modes (contention-free and contention-based). Different modes enable suitability for low and high data traffic load also with prioritizing the transmissions. There are standards available for WSNs (e.g., IEEE 802.15.4) and for WBANs (e.g., IEEE 802.15.6). Duty cycling is used to save energy in these solutions, which enables good energy efficiency.
NET: Routing [15, 121–123]	Routing protocols can be classified into following categories: network structure, topology-based, communication model, and reliable routing. Energy efficiency is an important goal and depends highly on the lower layers' performance, which can be taken into account by calculating the routes' cost. Many algorithms are available for multi-hop networks. Small-scale WSNs and WBANs are typically based on a single-hop star topology, which does not require optimized routing protocols. Large networks require multi-hop communication and clustering with well-designed routing to enable energy efficiency.
Merging of layers [126, 127]	Designs include joint design of the PHY/MAC/NET layer characteristics. The merging of layers approach can provide high energy efficiency for tailored applications. The optimization problem and implementation typically becomes too complex when each layer characteristic is taken into account. Modularity is weak in these solutions since different layers are merged using abstraction and a single layer protocol cannot be replaced.
Information exploitation throughout stack [128–135]	Can provide high energy efficiency gains in comparison with the layered design. Modularity can be maintained but is typically lost due to heavy interactions between the layers. The solutions are tailored for particular application scenarios since a scalable solution is difficult to achieve when considering the multiple layer characteristics.

Related works	Conclusion
Information exploitation between MAC & NET layers [103, 137, 138, 141, 142, 144–148]	There are lots of possibilities to improve performance by designing MAC and NET layer interactions. Routing performance can be improved when the channel competition conditions are known at the MAC layer. Channel access can be made more efficient when knowing the routing plan. That also enables longer sleep periods for the nodes which are not on the routing path. Therefore, there are many protocols proposed which improve energy efficiency by jointly designing these layers. Modularity can be maintained but requires carefull design without creating new compulsory interfaces.
Information exploitation between PHY & MAC layers [149, 151, 153–160]	These layers provide the basis for efficient communication through the channel. There are straightforward ways to improve energy efficiency by adapting the layers' parameters via information exploitation. Lower-layer information is typically useful also for the NET layer and can be shared via common layer state information data base. Modularity can be maintained if new interfaces are not required.

3 Cross-layer approach for lower layers

In this chapter, a cross-layer energy efficiency analysis for the lower layers (PHY & MAC) of the sensor node transceiver protocol stack will be introduced. This analytical cross-layer approach is originally proposed by the author and his co-authors in peer-reviewed publications [36], [39] and [40]. Here, these original works are revised and extended to also include description of a generic wake-up radio-based medium access control protocol, which is defined in this doctoral thesis and also published in [42].

The target scenario is a star-topology WSN, where sensor nodes send data packets to a sink node, as illustrated in Figure 11. In the star-topology network, the sink node coordinates the communication and receives data from the sensor nodes [20]. In the IEEE Std 802.15.4 [20], it has been defined that the sink node (coordinator) is a full function device which is able to act as a manager of the network and can also communicate with other FFDs within its range. Furthermore, the standard [20] defines that the sensor nodes are reduced function devices which can communicate only with the FFD acting as the coordinator for the network. That is, the network can be clustered so that a single cluster is based on a star topology and the sink nodes can send forward

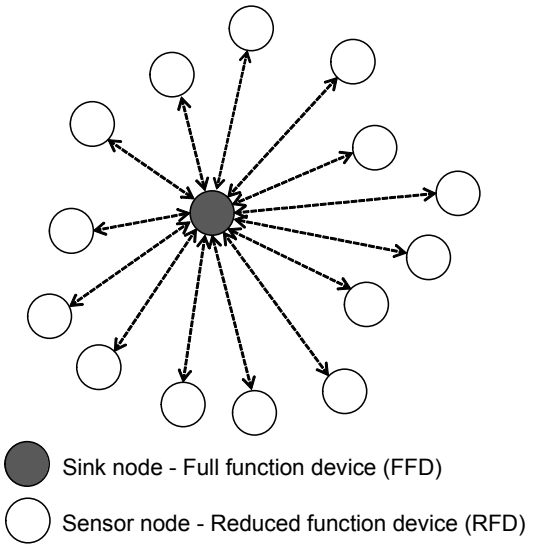

Fig. 11. Star topology network.

the data collected from the cluster. In that case, the sink nodes may have another radio interface which can be used for longer range communication between cluster heads or directly to the backbone network. This network topology is suitable for many types of sensor network applications, e.g., environmental monitoring and surveillance scenarios. In these type of scenarios, the low-power sensor nodes are continuously monitoring the environment, and once an event (e.g., a pollution level or an intruder appearance) is detected, the nodes will send a notification to the sink node, which will then take care of any further actions, as defined by the application characteristics. Another common feature of environmental monitoring and surveillance scenarios is that events typically occur rarely, which requires specific attention to the radios' sleep period management to enable energy-efficient operation while still being able to fulfil the event reporting delay requirements.

The objective of the proposed model is to enable energy efficiency improvements for star-topology network communication in the case where sensor nodes observe an event and transmit data to the sink node. Before data transmission, the sensor nodes wake up the sink node according to the GWR-MAC protocol principles, which will be introduced in Section 3.1. The design objective of the GWR-MAC protocol have included energy efficiency, flexibility and scalability to typical WSN and WBAN scenarios. GWR-MAC defines guidelines for the transmission period initialization and data packet transmission procedure for network nodes equipped with WURs. Energy efficiency is addressed by using wake-up signalling to avoid idle listening. Flexibility and scalability are enabled by defining a general framework with a bi-directional wake-up procedure and transmission period for which different types of channel access methods can be used depending on the application scenario. Namely, depending on the application, there are various channel access control methods that can be used according to the GWR-MAC design. In this chapter, one example scenario will be defined in detail and analysed.

Because the application space is wide, also the developed analytical modelling approach is first defined at the general level, so that it can be applied to various scenarios. In this work, a mathematical analysis supported by Matlab simulation is used for a detailed performance evaluation by using the proseded modelling approach. A Markov chain [164] model is used to evaluate the average number of steps (time slots) needed by sensor nodes to transmit a packet successfully to a sink node during a transmission period of GWR-MAC, when taking into account the probability of channel access success, packet success probability at the PHY layer and new packet arrivals probability, which affect the network traffic load. Markov chain modelling has been used in many

previous works addressing MAC protocol performance analysis, e.g., in [165–169]. Here, the purpose is not to propose a novel Markov chain model for MAC protocol analysis but instead the Markov chain modelling is used as a tool to enable proposed cross-layer analysis of the energy consumption. A supporting simulation model is built to verify the analytical model and to obtain a more complete view of the network behaviour during a transmission period. The simulation results provide information about the number of channel access collisions, idle slots and unsuccessful and successful transmissions, which are then used in the energy consumption analysis. The proposed model can be used to select the physical and MAC layer parameters jointly so that energy efficiency gains can be achieved. The analytical model is developed so that it can be applied to explore the energy efficiency of different lower layer techniques as long as the required event probabilities can be derived or measured for the target technology.

The model proposed in this chapter is used to explore the potential energy savings that can be achieved by selecting the forward error correction code rate of IR-UWB radios using non-coherent energy detection during the transmission period of a GWR-MAC-based WSN, where data packets are transmitted using the S-Aloha contention access. IR-UWB PHY and S-Aloha are the selected techniques for the IEEE Std 802.15.4 [20] as well for the IEEE Std 802.15.6 [16] for WBANs. In addition, an energy consumption comparison between a contention-free MAC (TDMA) and the S-Aloha protocol is carried out. The communication bit error probability at the PHY layer is derived by using a Nakagami-*m* fading channel model, which has been found to be realistic for UWB signalling [170, 171].

The following sections describe the system model, including the GWR-MAC protocol, analytical model derivation at the general level, and the PHY and MAC layer characteristics. Then the model for the transmission period length and an energy consumption analysis and results for the IR-UWB PHY combined to an S-Aloha-based transmission period are introduced with comparison to a TDMA method-based transmission period. In the end, a summary of this chapter is provided.

3.1 A generic WUR-based MAC protocol

As was found in the literature review in Chapter 2, it is important to maximize the sleep period length of the sensor nodes to save energy. Typically, the sleep periods are controlled in WSNs by using a duty cycle-based MAC protocol. In duty-cycled protocols, radios are listening to the channel for part of the time, according to their

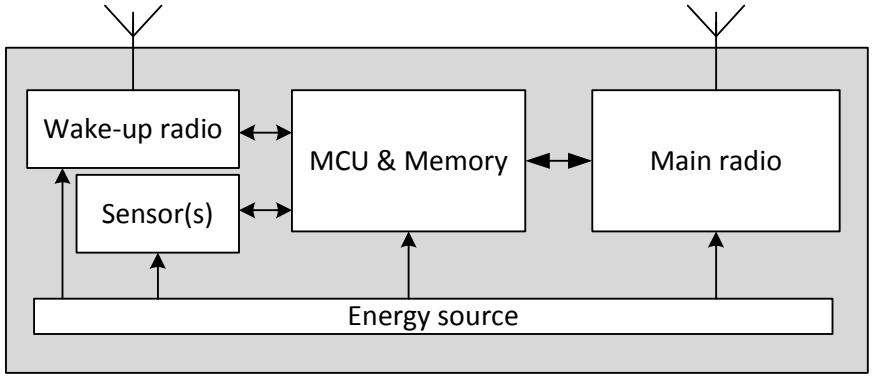

Fig. 12. WSN node architecture with WUR and main radio.

schedule (or randomly), and they go to the sleep mode if incoming transmissions are not detected. Duty cycle-based MAC protocols work well in many WSN applications but not in applications where the monitored events, and consequently communication, occur rarely. A drawback of the duty-cycle approaches is idle listening, which increases energy consumption and should thus be avoided if possible. Idle listening can be decreased by setting the duty cycle very low when the traffic load is low. Adaptive duty cycle protocols have been proposed for that purpose. However, low duty cycle will increase the communication delay and may not be able to satisfy the application requirements.

An alternative approach is to use a wake-up radio [24–29] to avoid the idle listening problem while allowing energy-efficient and low latency operation. As was explained in Chapter 2, the wake-up receiver is continuously able to detect the wake-up signal when it is in the ultra low-power standby mode. Therefore, the communication delay can be avoided when the event occurs and there is data to transmit.

In this work, it is assumed that the WSN nodes are equipped with wake-up radios to avoid idle listening. In addition, the nodes include the main data radio, as illustrated in Figure 12. A generic WUR-based MAC protocol is proposed here to enable idle listening avoidance in sensor network applications. The GWR-MAC protocol is not restricted to any specific WUR technology or data radio technology. Two different options for the wake-up procedure are defined for the GWR-MAC protocol: source-initiated and sink-initiated. The data transmission period of GWR-MAC can be implemented by using different types of channel access methods, as will be explained below.

In the source-initiated mode, the sensor node(s) will wake up the sink node from the sleep mode by transmitting a wake-up signal (WUS), as illustrated in Figure 13.

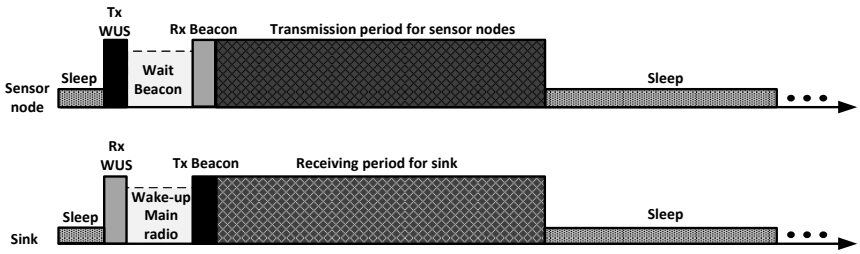

Fig. 13. GWR-MAC protocol source-initiated mode.

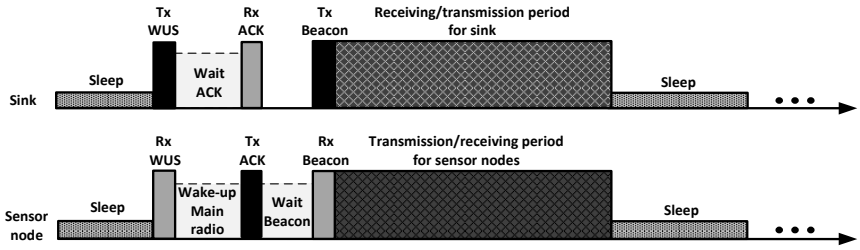

Fig. 14. GWR-MAC sink-initiated mode.

To decrease the probability of WUS collisions, a random (or predefined) delay for WUS transmissions can be used. The WUR of the sink node will receive the WUS and generate a wake up via MCU to the main radio. The sink node's main radio will then broadcast a beacon (BC) message to initiate transmission period for the sensor node(s) according to the channel access procedure, which can be based on different methods suitable for different scenarios. The beacon message is, at the same time, an acknowledgement to the sensor node(s) that the WUS has been received by the sink. If the sensor node does not get the beacon message, it will retransmit the WUS after a random back-off period. The WUS transmission procedure is therefore similar to the Aloha channel access with a random (or predefined) delay for the first transmission. Once the beacon message is received, the sensor node(s) will send the data packet(s) to the sink during the transmission period by using the channel access method informed in the beacon message. This mode of the GWR-MAC protocol is therefore a combination of the source-initiated wake-up procedure and following channel access control method for the transmission period.

In the sink-initiated mode, illustrated in Figure 14, the sink node will wake up the sensor nodes from the sleep mode by sending the WUS using broadcast, uni-cast or multi-cast. It depends on the used WUR technology whether it is possible to use

addressing to wake up only certain sensor nodes or whether broadcast should be used. When the sensor node receives the WUS, it will send an ACK message to the sink. The sink node knows that the WUS has been detected correctly and sends the beacon containing information about the following transmission period. Data transmissions are then performed during the transmission period, and once they are finished, all the nodes have entered the sleep mode.

Typically, the data flow is from the sensor nodes to the sink node. However, the transmission period can also be dedicated to the sink node to transmit data to the sensor node(s), if, for example, a wireless software update or reconfiguration of sensor node(s) requires it. Therefore, in Figure 14, it is illustrated for the sink-initiated case that the transmission period can be dedicated to the sensor node(s) or to the sink node to transmit data packets. The sink node can determine in the beacon the upcoming transmission period channel access mechanism, timing and scheduling information. Different channel access methods can be used for the transmission period management. When the transmission period is finished, all the nodes have entered the sleep mode and the next transmission period will take place after the next wake-up procedure.

For the transmission period channel access, one option is to use a contention-based MAC. In that case, the nodes compete for channel access and transmit packets according to the contention-based MAC principle. For example, in the Aloha case, nodes transmit when they have a packet to transmit. If the packet is not successfully received, then the retransmission policy defines either that the packet is discharged or retransmitted. For example, in the Aloha case, the unsuccessful packet will be retransmitted again after a random backoff period if the ACK is not received during a certain time. In addition, other contention-based methods, e.g., CSMA/CA, etc. can be used during the transmission period. Another option is to use contention-free scheduled methods, e.g., TDMA-based protocols or guaranteed time slots defined in the IEEE Std 802.15.4 [20]. The requirement for the usage of contention-free methods is that the sink node assigns dedicated time slots for each sensor node. The sink node does not have information about which nodes have a packet to transmit, and therefore the channel resources may be wasted. In the ideal contention-free case, no collisions will occur if the nodes are perfectly synchronized and follow the schedule.

The described GWR-MAC protocol principle is suitable for different types of application since it defines a bi-directional wake-up procedure between the sensor nodes and the sink. In addition, it enables the usage of different channel access methods for the transmission period. However, note that the GWR-MAC protocol is not defined here

in a detailed manner (wake-up collision avoidance, packet formats, turn-around times, etc.). Instead, the described GWR-MAC is a general-level framework for short-range networks which take advantage of the wake-up radios. It depends on the application scenario which mode of the GWR-MAC protocol should be used. For example, in some applications only the source-initiated case may be used, and then only the sink node should be equipped with a WUR. In some scenarios, there can be a need that only the sink node must be able to wake up sensor nodes. In that case, the sink-initiated mode would be used and only the sensor nodes must be accompanied with a WUR. Some application scenarios require both modes of the GWR-MAC protocol. In such cases all the network nodes must be equipped with a WUR and data radio as illustrated in Figure 12.

In this chapter, the focus is on the energy efficiency analysis of the transmission period, and the GWR-MAC protocol defines how the transmission period establishment will be done. Therefore, in this section, a model for the transmission period energy efficiency analysis will be derived. In Chapter 4, the GWR-MAC protocol is used in the context of a hierarchical network, and the energy efficiency comparison with a duty-cycle radio-based network is performed. Therefore, the focus is therein on the evaluation of the effect of the wake-up procedure on the network energy efficiency.

3.2 System model

Here will be defined the system model and assumption for the developed transmission period length and energy efficiency model. During the analysed transmission period, the sensor nodes send data packets to the sink node as in typical WSN applications.

The total number of sensor nodes in the star topology network is N, which are assumed to have a packet to transmit to the sink node. As shown in Figure 15, the transmission period establishment of the GWR-MAC protocol begins so that one of the N sensor nodes (#1 in this case) sends a wake-up signal once it has seen it necessary according to the particulars of an actual application; i.e., the triggering reason for the wake-up procedure depends on the application scenario. Figure 15 illustrates the wake-up procedure of the source-initiated mode of the GWR-MAC protocol, but the proposed transmission period analysis is applicable also to the sink-initiated mode. Here it is assumed that sensor node #1 sends the WUS because it has detected a critical event (e.g., sensor value is above the predetermined threshold). A wake-up signal can also be generated if, e.g., a certain timer has expired after the previous transmission period. The

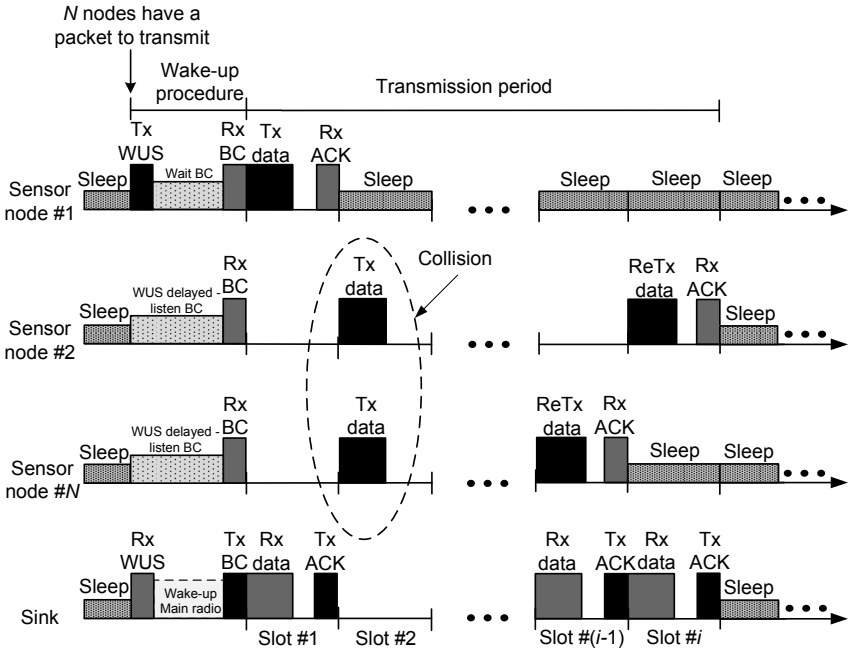

Fig. 15. Wake-up procedure and transmission period message diagram for GWR-MAC based on slotted contention-based channel access.

other $N-1$ sensor nodes, which have data to transmit, have added random delay to the WUS transmission and are, in the meantime, listening for a possible beacon message from the sink in order to detect whether the wake-up has already been performed by some other sensor node. It must be noted that the wake-up signals may collide if multiple sensor nodes send the signal at the same time. However, a wake-up message is typically very short, which decreases the probability of collision. In addition, it will be assumed that a suitable randomization is used, and therefore the WUS collision probability is assumed to be zero and the sink node's WUR will decode the WUS from node #1 successfully. The wake-up procedure will not be analysed here in more detail since the focus is on the data radio energy efficiency during the transmission period.

After the successful reception of the WUS, the sink node turns on its main radio and broadcast a beacon message to the sensor nodes. This beacon message is at the same time an acknowledgement to the sensor nodes that the WUS has been received. The beacon message includes information about the upcoming transmission period channel access starting time, channel access method and possible scheduling. It is

assumed that the N sensor nodes receive the beacon message successfully, achieve perfect synchronization with the sink and can start sending their data packets during the transmission period in a contention-based or contention-free fashion, as was explained in the GWR-MAC protocol description.

In this work, the slotted channel access during the transmission period will be defined and analysed in more detail. As shown in Figure 15, N sensor nodes with a packet to transmit will transmit (Tx) it in a randomly selected slot during the transmission period. Despite the used channel access method during the transmission period, unsuccessful transmission may occur due to errors introduced by the wireless channel fluctuations or due to collisions occurred during the channel access. In the analysis hereafter, it is assumed that if data transmission is not successful, the sensor node will retransmit (ReTx) the packet until it has been successfully received (Rx) by the sink. In other words, it is assumed that the sink node sends an ACK message after a successful packet reception. If a data packet collision or erroneous detection for some other reason occurs, and consequently the ACK message will not be received, the sensor nodes have to transmit their packets again according to the used MAC protocol features.

In addition, in the analysis, it is taken into account that new packets can arrive to each of the N nodes during the transmission period. However, the sensor node does not generate a new packet for transmission until the previous one is successfully delivered; i.e., it is assumed that buffering is not supported by the nodes, which is a reasonable assumption in many WSN applications.

3.3 Transmission period

This section describes the mathematical model developed to analyse the transmission period in the described WSN scenario. A Markov chain [164] model is used to enable the estimation of the length of the transmission period taking the PHY and MAC layer characteristics and new packet arrival probability into account.

The objective of the Markov chain model is to evaluate how many steps are needed that every node has successfully reported its observation (data packet) to the sink node. The number of steps to absorption can be translated into time to absorption when the average length of step is known. The model enables to explore the protocol stack parameter tuning effect on the transmission period length. As was introduced in Chapter 2, e.g., the transmission power, modulation method, error correction coding rate, or channel access method can be adapted to decrease the number of retransmissions. The

objective of the model is then to provide a tool to find out the parameter setting which shortens the length of the transmission period. Furthermore, the eventual goal is to use the model for energy efficiency evaluation.

For the Markov model analysis, the possible actions that can occur during the transmission period must be defined. In the above-described star-topology network scenario, the following actions can take place:

1. A sensor node wakes up the sink node by sending a wake-up signal. This type of a message is assumed to be delivered error free since the focus here is on the data radio part.
2. Once the sink node is awakened, it will send a beacon message to the sensor nodes so that they can synchronize with the sink, and know when and how they must try to access the channel. At this point, there are N nodes which have a data packet to transmit.
3. To transmit data, the sensor nodes can use a contention-based or a contention-free channel access method. In the former case, the sensor nodes choose a transmission slot z with probability p. In the latter case, each sensor node transmits in a slot determined by the sink node.
4. If there is only one transmission in a slot, a collision will not occur and the success probability depends on the bit error probability (BEP) at the receiver detection process. If there are multiple transmissions in the same slot, a collision will occur and the packets will be lost. In the case of an unsuccessful transmission due to channel errors or collisions, the node(s) try to retransmit the packet in a new slot, as described in step 3. If the node has a successful transmission, it will enter the sleep mode.
5. During the transmission period, new packets can arrive to each node with a certain probability. The nodes do not support buffering of packets but a new packet can replace the old packet, in which case the node transmits only the latest sensor observation.
6. The transmission period ends when every node has successfully transmitted data packet and entered the sleep mode.

For the purpose of the transmission period process analysis, in this work, the Markov chain model which have states between 0 and N, illustrated in Figure 16, has been developed. The initial state value, at time $t = 0$, is defined to be $S_t = 0$. The absorption state, where all the N nodes have successfully completed their transmissions is defined as $S_{t+\Theta} = N$, where Θ is the time required to reach the absorption state. In the j:th state,

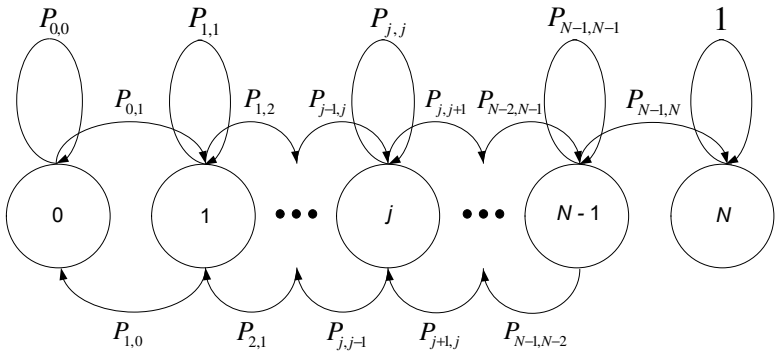

Fig. 16. Markov chain model for the transmission period analysis ([36] ©ACM 2014).

$N-j$ nodes have a packet to transmit and j nodes have already successfully transmitted a packet and entered the sleep mode.

For the state transition probability calculation, the factors which affect the probability of state transitions must be defined. To compute the state transition probabilities for the different actions in the described Markov chain model, the following probabilities must be known; (1) the probability of successful channel access, (2) the packet transmission success probability, and (3) the probability of new packet arrivals at each node. The first one depends on the MAC protocol features, the second one depends on the PHY layer features and the wireless channel characteristic, and the third one depends on the network traffic model. In addition, the corresponding probabilities must be known for the unsuccessful channel access and packet transmission and no new packet arrivals for each node. Therefore, the probability of successful (unsuccessful) channel access $P_{\text{succ}}^{\text{MAC}}$ ($P_{\text{fail}}^{\text{MAC}}$) and the probability of successful (unsuccessful) wireless transmission $P_{\text{succ}}^{\text{PHY}}$ ($P_{\text{fail}}^{\text{PHY}}$) are defined. Furthermore, let's define $P_{\Omega}(\Omega=\kappa)$ to be the probability that $\kappa=0,1,...,j$ node(s) will have a new packet arrival during the j:th state.

Next, the events that can occur in the Markov chain model and corresponding probability for them will be defined.

Event 1 :

Successful channel access & successful transmission & no new arrivals => move from state j to state $j+1$; Probability for event (1) is defined as

$$P_{(1)} = P_{\text{succ}}^{\text{MAC}} P_{\text{succ}}^{\text{PHY}} P_{\Omega}(\Omega=0) \tag{1}$$

Event 2 :

Successful channel access & successful transmission & κ node(s) have a new packet => move from state j to state $j-\kappa+1$; Probability for event (2) is defined as

$$P_{(2)} = P_{\text{succ}}^{\text{MAC}} P_{\text{succ}}^{\text{PHY}} P_{\Omega}(\Omega = \kappa) \tag{2}$$

Event 3 :

Unsuccessful channel access & no new arrivals => stay in state j; Probability for event (3) is defined as

$$P_{(3)} = P_{\text{fail}}^{\text{MAC}} P_{\Omega}(\Omega = 0) \tag{3}$$

Event 4 :

Unsuccessful channel access & κ node(s) have a new packet => move from state j to state $j-\kappa$; Probability for event (4) is defined as

$$P_{(4)} = P_{\text{fail}}^{\text{MAC}} P_{\Omega}(\Omega = \kappa) \tag{4}$$

Event 5 :

Successful channel access & unsuccessful transmission & no new arrivals => stay in state j; Probability for event (5) is defined as

$$P_{(5)} = P_{\text{succ}}^{\text{MAC}} P_{\text{fail}}^{\text{PHY}} P_{\Omega}(\Omega = 0) \tag{5}$$

Event 6 :

Successful channel access & unsuccessful transmission & κ node(s) have a new packet => move from state j to state $j-\kappa$; Probability for event (6) is defined as

$$P_{(6)} = P_{\text{succ}}^{\text{MAC}} P_{\text{fail}}^{\text{PHY}} P_{\Omega}(\Omega = \kappa) \tag{6}$$

The Markov chain model described above can then be used to study different PHY and MAC layer protocol combinations when the defined probabilities can be derived or measured for the techniques of interest. In Section 3.5, it is shown in detail how these probabilities are derived for a particular combination of PHY and MAC layers studied in this work by using the proposed approach.

3.4 Energy consumption

The energy consumption model is introduced here at the general level without going into details of particular protocols at the PHY and MAC layers. The number of transmissions

required for success is a very important factor in the sensor network overall energy consumption. There are many protocol design features and parameters which affect the number of transmissions. The effect of any protocol parameter tuning must be explored in an orderly way to find possible energy gains. Therefore in this work, the number of unsuccessful and successful transmissions has been used as a key factor which depends highly on the lower layer protocol features.

The energy consumption, E_{TP}, of wireless communication during a transmission period is defined here as

$$E_{\mathrm{TP}} = N_{\mathrm{tx}}^{\mathrm{fail}}\left(E_{\mathrm{tx}}^{\mathrm{PHY}} + E_{\mathrm{tx,f}}^{\mathrm{MAC}}\right) + N_{\mathrm{tx}}^{\mathrm{succ}}\left(E_{\mathrm{tx}}^{\mathrm{PHY}} + E_{\mathrm{tx,s}}^{\mathrm{MAC}} + E_{\mathrm{rx}}^{\mathrm{PHY}} + E_{\mathrm{rx}}^{\mathrm{MAC}}\right) + E_{\mathrm{Imp}}^{\mathrm{MAC}}, \quad (7)$$

where $N_{\mathrm{tx}}^{\mathrm{fail}}$ is the number of failed transmissions, $E_{\mathrm{tx}}^{\mathrm{PHY}}$ is the PHY layer part on the energy consumption of a transmitting node, $E_{\mathrm{tx,f}}^{\mathrm{MAC}}$ is the MAC protocol effect on the energy consumption of a transmitting node in the failed transmission case, $N_{\mathrm{tx}}^{\mathrm{succ}}$ is the number of successful transmissions, $E_{\mathrm{tx,s}}^{\mathrm{MAC}}$ is the MAC protocol effect on the energy consumption of a transmitting node for a successful transmission, $E_{\mathrm{rx}}^{\mathrm{PHY}}$ and $E_{\mathrm{rx}}^{\mathrm{MAC}}$ are the PHY and MAC layer portions on the energy consumption of the receiving (sink) node, respectively. The energy consumption caused by the MAC protocol imperfections during the transmission period is taken into account by adding a factor $E_{\mathrm{Imp}}^{\mathrm{MAC}}$, which depends on the MAC protocol characteristics. For example, for a slotted random-access MAC, this parameter can model the effect of the idle slots present in the transmission period due to the used channel access and back-off strategy. In an ideal TDMA MAC case, there are no unused slots during the transmission period, and therefore $E_{\mathrm{Imp}}^{\mathrm{MAC}}$ would be zero. $E_{\mathrm{Imp}}^{\mathrm{MAC}}$ can also be used to take account of other energy consumption overheads caused by the MAC protocol, e.g., beacon transmission or synchronization and slot scheduling required in the contention-free MAC protocol case.

The energy consumption model expressed in (7) can be used as a starting point for the analysis of different combinations of PHY and MAC layer protocols. The more detailed energy consumption factors must be derived for the protocols of interest. For example, depending on the studied protocol characteristics, the MAC factors can either include or not include the ACK message transmission and reception after a successful data packet detection. The next section describes detailed derivations for the IR-UWB-based WSN case.

3.5 Analysis of a WSN based on IR-UWB

This section describes how the proposed cross-layer approach can be used for the transmission period analysis and consequently energy efficiency evaluation of WSN transceivers using IR-UWB PHY and S-Aloha for channel access during data transmissions. The approach is used to evaluate how the error correction code rate affects the average number of transmissions required for success, and therefore the length of the transmission period. Finally, an analysis is developed to evaluate the achieved energy consumption savings.

The parameter values assumed for the analysed IR-UWB network (if not otherwise declared) are given in Table 4. These parameters are defined to be adequate for the IR-UWB transceivers based on the standard [20]. The transmitter and receiver power consumption approximate typical values of state-of-the-art designs [78, 172, 173].

3.5.1 PHY layer

Impulse radio based ultra-wideband communication has desired characteristics for several WSN applications. IR-UWB transmissions are based on very short-duration pulses, which have very wide power spectrum in the frequency domain with low energy level. Indeed, the Federal Communications Commission (FCC) regulations have specified that the maximum power emission for an IR-UWB transmitter should not exceed -41.3 dBm/MHz at the unlicensed $3.1-10.6$ GHz band [174]. Furthermore, the FCC defines that UWB signals should have fractional bandwidth greater than 20%, or a bandwidth (W) greater than 500 MHz [174]. The fractional bandwidth is defined as [174][175]

$$B_f = 2\frac{f_H - f_L}{f_H + f_L}, \tag{8}$$

where f_L and f_H are the lower and higher frequencies corresponding to upper and lower -10 dB points in the signal spectrum.

Depending on the modulation method, IR-UWB signals can be detected by using either coherent or non-coherent techniques. Coherent receivers are not well suitable for low-cost and low-power WSNs since they require complex analogue-to-digital (A/D) conversion and digital signal processing (DSP) operations. Therefore, the non-coherent receivers based on energy detection are favoured in sensor networks, since they allow simple and low-cost implementations enabling energy-efficient operation. Common

Table 4. Parameters assumed for IR-UWB based WSN analysis ([36] ©ACM 2014).

Parameter	Definition	Value
W	bandwidth	499.2 MHz
f_c	central frequency	4492.8 MHz
m	Nakagami fading severity index	3
α	power delay profile coefficient	0.3
N_{cpb}	number of chips per symbol	16
t_c	chip duration	2 ns
T_{int}	integration time	20 ns
R	uncoded bit rate	0.98 Mbps
m_{bs}	bits per coded symbol	6
N	number of sensor nodes in the network	20
p	probability to transmit in a slot	$0.05, 0.1, 0.2, 1/(N-j)$
ρ	arrival rate for Poisson process	0.03 events/s
L_{PMH}	payload and MAC layer header	127 bytes
L_{PH}	PHY layer header	2 bytes
L_{ACK}	ACK frame size	7 bytes
$T_{MaxAckWait}$	maximum wait time for ACK frame	151 µs
L_{PRE}	preamble length	64 preamble symbols
P_{rx}	receiver power consumption	20 mW
$P_{tx,circ}$	transmitter circuitry power consumption	2 mW
P_{idle}	idle mode power consumption	1 mW
P_{sd}	power spectral density	-41.3 dBm/MHz
$P_{tx,RF}$	transmitter RF power component	37 µW

modulation schemes used in non-coherent transceivers are binary pulse (or burst) position modulation and on-off keying.

IR-UWB communication does not require the use of a carrier signal, hence it does not require up or down frequency conversion, which is an important issue for a simple and low-cost transceiver implementation. Due to wideband signals with low power emission, the main advantages of IR-UWB PHY are noise-level communication, resistance to severe multi-path/jamming and very accurate time resolution of the multipath components [18]. Commercial UWB communication-based products have been developed, for example, by DecaWave [176], Zebra Technologies [177] and

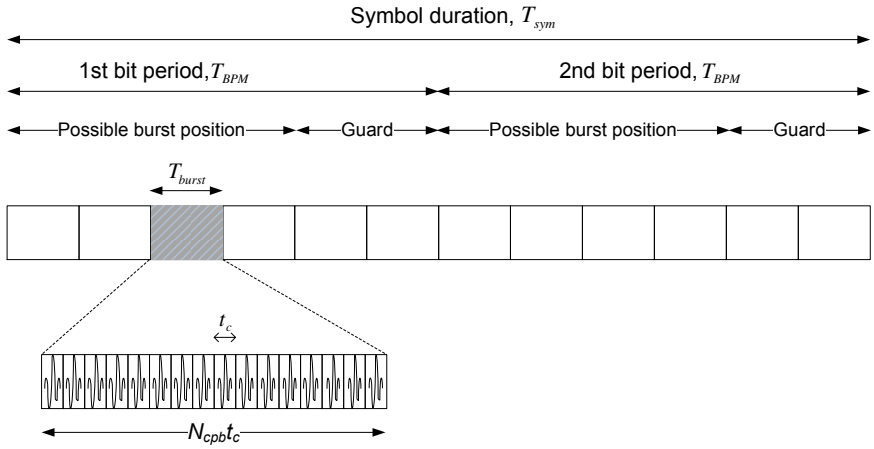

Fig. 17. Symbol structure of the IEEE Std 802.15.4a-compliant IR-UWB communication ([36] ©ACM 2014).

Ubisense [178]. The IEEE Std 802.15.6 (published in Feb. 2012) [16] has a remarkable potential for WBAN applications that will most probably lead to an emergence of new UWB-based products.

The IR-UWB symbol structure, as defined in [20], is shown in Figure 17. In the binary burst position modulation (BPM) case, the transmitted signal consists of a burst of chips, i.e., each bit is transmitted using N_{cpb} chips of duration t_c. One chip consists of a single UWB pulse of duration T_p, i.e., here it is assumed that $t_c = T_p$. There are different pulse types available for transmission, e.g., a Gaussian pulse or one of its derivatives is typically used [18]. As can be seen from Figure 17, the symbol period of duration T_{sym}, defined in the IEEE Std 802.15.4, is divided into two periods, which enables a burst (and pulse) position modulation. The burst is transmitted either during the first or second period, depending on the input bit. Depending on the hopping sequence, the burst can reside at a different location inside a bit period to avoid multi-user interference (MUI), as illustrated in Figure 17. In addition, each symbol period includes guard periods to avoid inter-symbol interference (ISI).

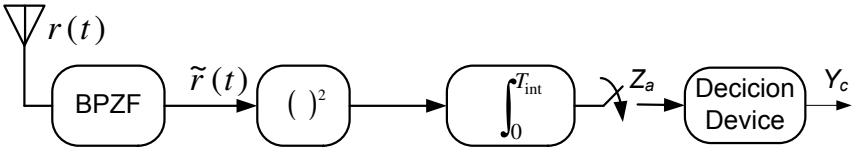

Fig. 18. Architecture of a non-coherent ED receiver ([37] ©Springer Science+Business Media 2014).

The transmitted IR-UWB signal, in the case of the described symbol structure and binary modulation, for the u:th user is defined as [20]

$$s^{(u)}(t) = \sum_{d=0}^{N_{cpb}-1} \sqrt{\frac{\varepsilon_{\mathrm{s}}}{N_{cpb}T_p}}\, p\left(t - g_0^{(u)} T_{\mathrm{BPM}} - \Delta^{(u)} T_w - dt_c\right), \tag{9}$$

where ε_{s} is the energy of the transmitted symbol, $g_0^{(u)} \in \{0,1\}$ is the transmitted bit for the u:th user, $T_{\mathrm{BPM}} = T_{\mathrm{sym}}/2$ is the bit period duration for the binary BPM case, $\Delta^{(u)}$ is the burst hopping position inside the symbol period for the u:th user, $T_{\mathrm{w}} = N_{\mathrm{cpb}} T_{\mathrm{p}}$ is the duration of the signal waveform (burst). The transmitted pulse waveform $p(t)$ of duration T_{p} is such that $(1/T_{\mathrm{p}}) \int_0^{T_{\mathrm{p}}} p^2(t)dt = 1$ and the bandwidth W is approximately $1/T_{\mathrm{p}}$.

The basic architecture of the non-coherent ED receiver is shown in Figure 18. First the antenna receives a signal, which then goes through a band pass zonal filter (BPZF). The filter removes the out-of-band noise from the signal. The output of the filter includes therefore only in-band noise and signal energy, which go through a squaring operation. The squared signal is integrated using specific integration time, T_{int}, to acquire knowledge of the received signal energy. The integration time is a very important parameter of the ED receiver because it determines the amount of signal and noise energy affecting the decision on a received bit. In the additive white Gaussian noise (AWGN) case without multipath effect, the ideal integration time is the same as the duration of the transmitted burst, T_{w}, because in this case all the signal energy can be collected. If T_{int} is longer than the burst duration, a superfluous noise energy would also be collected. In the multipath channel case, the selection of T_{int} is more difficult because a sufficient amount of delayed signal components should also be collected by the integrator. However, T_{int} should not be unnecessary long to avoid collection of additional noise. When selecting adequate T_{int}, the integration time and bandwidth product ($T_{\mathrm{int}} \cdot W$) is often used as a measure. The effect of integration time on the receiver performance has been previously studied, e.g., in [76, 80, 179, 180]. After the

integrator, a sampling operation produces the decision variable Z_a, which is input for a decision device which determines whether the transmitted bit was a one or a zero. Depending on the modulation method, the decision device does the decision (Y_c) based on a threshold or by comparing the received energies in different symbol periods. The former method can be used, e.g., for OOK, and the latter is used for the pulse (and burst) position modulation. In the next sections, the BEP derivation for the uncoded and coded transmissions, when using binary burst position modulation in a multipath fading channel case, will be introduced.

Uncoded Transmission

Here will be introduced the bit error probability derivation for the uncoded transmission in a Nakagami-*m* fading channel when using binary BPM and non-coherent ED receiver. In the channel, the transmitted signal $s^{(u)}(t)$ will travel through multiple paths, which will cause that signal components will arrive to the receiver with different delays and power levels. The Nakagami-*m* distribution [181] can be used to characterize the statistics of the multipath faded signal [45] and is well suitable for ad hoc and sensor network environments [46], [182]. It is also found to be sufficient for IR-UWB communication BEP derivation [170, 171]. The received signal, after the multipath fading, for the u:th user is defined as

$$r^{(u)}(t) = s^{(u)}(t) \otimes h(t) + n(t), \tag{10}$$

where $\otimes$ is the convolution operator, $h(t)$ is the channel impulse response and $n(t)$ is the zero-mean white Gaussian noise term with two-sided power spectral density (PSD) $\sigma_0 = N_0/2$.

The following derivation is used to calculate the bit error probability for the detection of the signal from the fading channel. The derivation for BEP calculation is based on the models originally introduced in [76] and [183], and here it is only shortly introduced.

In the Nakagami-*m* channel case, the instantaneous power of the signal components varies according to gamma distribution. The gamma distribution has a closed form characteristic function (CF), which is useful in the derivation of the BEP because it can be used to define the CFs of the decision variables at the ED receiver. Let's define that in the case of the bit $'0'$, the transmitter will transmit signal waveform on the first symbol interval, and in the case of the bit $'1'$, the signal waveform will be transmitted on the second symbol interval. For the BEP derivation explanation, let's further assume that a

signal waveform for the bit $'0'$ is transmitted, i.e., $g_0 = 0$ in (9). In the case of burst position modulation, the ED receiver produces one decision variable for both symbol periods in order to compare them. In this case, the decision variables can be modelled as non-central chi-square distributed random variables (RVs) [76]. For the first symbol period, the CF for the chi-square decision variable Z_1 with non-centrality parameter $\mu_1 = \mu$, composed of C resolvable multipath components, can be defined as

$$\Psi_{\mu}(j\nu) = \prod_{l=1}^{C} \Psi_{|h_l^2|}(j\nu) = \prod_{l=1}^{C} \frac{1}{(1 - j\nu\frac{\gamma_l}{m})^m}, \tag{11}$$

where γ_l is the SNR of the l:th multipath component h_l and m is the fading severity index [76]. For the second symbol period, the decision variable Z_2 has a non-centrality parameter $\mu_2 = 0$ because the corresponding symbol period includes only a zero-mean noise component.

Because the $'0'$ bit is transmitted on the first symbol interval, the bit error probability is defined as $P_{\mathrm{b}} = P_{\mathrm{r}}\{Y_c = Z_1 - Z_2 < 0\}$. By deriving the difference between two non-central chi-square RVs and averaging with respect to the non-centrality parameter μ, the BEP is given by [76]

$$P_{\mathrm{b}} = \frac{1}{2} + \frac{1}{\pi}\int_0^{\infty} \left(\frac{1}{1+\nu^2}\right)^{N_{\mathrm{cpb}}WT_{\mathrm{int}}} \Re\left\{\frac{\Psi_{\mu}(\frac{-j\nu}{1+j\nu})}{j\nu}\right\} d\nu, \tag{12}$$

where $N_{\mathrm{cpb}}WT_{\mathrm{int}}$ is the degree of freedom of the non-central chi-square distributed RVs. Equation (12) can be evaluated by using numerical techniques, and the packet error probability for the uncoded case can then be calculated as

$$P_{\mathrm{packet}} = 1 - (1 - P_{\mathrm{b}})^L, \tag{13}$$

where L is the packet length in bits.

Coded Transmission

In this section, it is shown how the BEP can be calculated when using the Reed-Solomon (n,k,t) codes, which have an error correction capability of $t = (n-k)/2$. The IEEE Std 802.15.4 defines that the IR-UWB PHY-based radios will use a RS code with a total number of symbols in a code word $n = 63$, number of information symbols in a code word $k = 55$, bits per symbol $m_{\mathrm{bs}} = 6$, and code rate $r = 0.87$ [20]. Here, the introduced cross-layer model will be used to study also the other code rates of the RS

code performance with parameters $n = 63$ and $m_{\mathrm{bs}} = 6$. By selecting the same code word length and number of bits per symbol, the implementation complexity with respect to the standard will not change drastically.

In the FEC coding case, the transmitted energy per information bit will be reduced, in comparison to the uncoded case, because the encoder generates parity bits, which also needs to be transmitted. Therefore, it must be taken into account that the energy per bit in a coded packet depends on the code rate and can be calculated as $\varepsilon_{\mathrm{b},i} = r_i \varepsilon_{\mathrm{b},0} \leq \varepsilon_{\mathrm{b},0}$, where r_i is the i:th code rate and $\varepsilon_{\mathrm{b},0}$ is the energy per uncoded bit [45]. This assumption leads to a fair comparison because the energy per packet will be the same for the uncoded and coded packets despite the used code rate.

The decoded symbol error probability, in the case of a hard decision decoding, for the i:th code rate, can be calculated as [44, 45]

$$P_{\mathrm{s},i}^{\mathrm{RS}} = \frac{1}{n} \sum_{e=t+1}^{n} e \binom{n}{e} (P_{\mathrm{s},i})^e \left(1 - P_{\mathrm{s},i}\right)^{n-e}, \tag{14}$$

where e is the number of erroneous symbols in a code word, $P_{\mathrm{s},i} = 1 - \left(1 - P_{\mathrm{b},i}\right)^{m_{\mathrm{bs}}}$ is the symbol error probability of the code word before decoding and $P_{\mathrm{b},i}$ is the bit error probability, when using a code rate r_i. $P_{\mathrm{b},i}$ can be calculated using (12) by substituting the energy per bit for the i:th code rate case. The packet error probability in the case of i:th code rate can be calculated from the symbol error probability as

$$P_{\mathrm{packet},i} = 1 - (1 - P_{\mathrm{s},i}^{RS})^{X_i}, \tag{15}$$

where $\lceil X_i = L_i / m_{\mathrm{bs}} \rceil$ is the number of RS code symbols in a packet and $L_i = L / r_i$ is the packet length when using a code rate r_i.

The decoded bit error probability for the i:th RS code rate can be approximated by using [45]

$$P_{\mathrm{b},i}^{\mathrm{RS}} \approx \frac{2^{(m_{\mathrm{bs}}-1)}}{2^{m_{\mathrm{bs}}} - 1} P_{\mathrm{s},i}^{\mathrm{RS}}. \tag{16}$$

This approximation is used to illustrate coding performance with the uncoded case in Figure 19, which shows the BEP versus energy per bit-to-noise ratio results in a Nakagami-m fading channel. The fading channel parameters used in the calculations are a Nakagami factor $m = 3$, a power delay profile (PDP) coefficient $\alpha = 0.3$ and bandwidth integration time product $W \cdot T_{\mathrm{int}} = 10$, which is a sufficient value based on the results shown in [76]. More detailed parameters for this performance evaluation are given in Table 4. In [184], a SNR gap analysis for the same receiver architecture, and

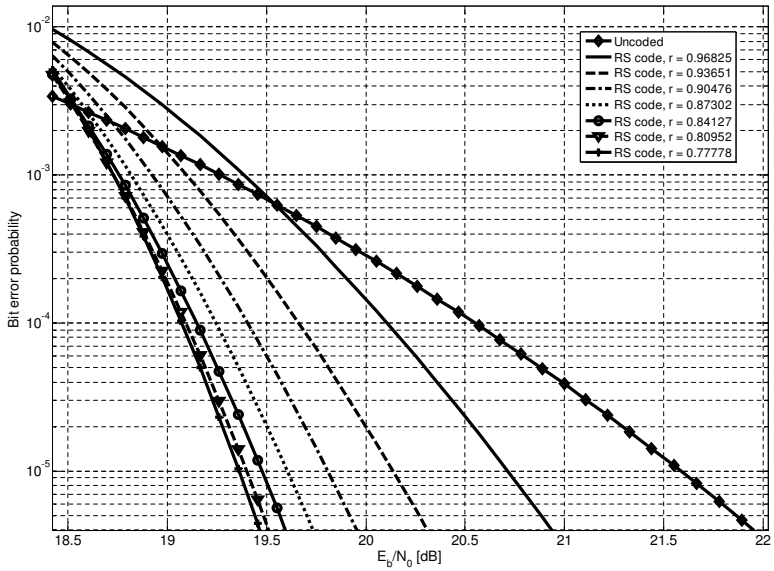

Fig. 19. BEP versus E_b/N_0 in dB at the receiver in a Nakagami-m fading channel ([36] ©ACM 2014).

with the same channel model, as the one used here was proposed. The RS code rates from $r = 0.78$ to $r = 0.97$ were found to be the most potential energy saving enablers [184]. Therefore, the focus in this work is on those code rates. Figure 19 clearly shows that all the studied code rates can lead to reduced required values for E_b/N_0, e.g., when the target BEP$= 10^{-4}$. However, Figure 19 also shows that there is an E_b/N_0 region where coding leads to a worse BEP performance than in the uncoded case. As mentioned earlier, for a fair comparison, it must be taken into account that when using FEC coding, a smaller amount of energy is used for each transmitted bit. In the low E_b/N_0 case, the coding cannot anymore correct the bit errors, and therefore, it would be better to transmit an uncoded signal with higher energy per bit. It is however not desirable to communicate in the low E_b/N_0 region since it leads to a high packet-loss rate, and consequently, increases the number of retransmission, which leads to energy inefficiency.

3.5.2 MAC layer

The S-Aloha random access method is simple to implement, it has low overhead, and it is also chosen to the standards [16] and [20] to be used with the IR-UWB physical layer.

In addition, the conventional clear channel assessment cannot be performed when using UWB signalling. Therefore, the focus here is on an S-Aloha method analysis for the transmission period of the GWR-MAC protocol. However, an energy consumption comparison with a TDMA method-based transmission period will also be shown in Section 3.5.7.

For a finite S-Aloha case, the probability that any node has successfully accessed the channel in a slot is

$$P_{succ}^{MAC}(p) = Np(1-p)^{N-1}, \tag{17}$$

where N is the number of nodes competing for channel access in a slot with probability p. The maximum channel access efficiency can be found by computing the derivative of (17) at the zero value

$$P_{succ}^{MAC}(p^*)' = 0, \tag{18}$$

which occur when $p^* = 1/N$, i.e., when the number of slots in a transmission period is the same as the number of competing nodes. That case corresponds with a traffic load $G = 1$. Therefore, the maximum channel access success probability can be calculated as

$$P_{succ}^{MAC}(p^*) = (1-1/N)^{N-1}. \tag{19}$$

It must be noticed that the code rate affects the packet duration due to coding overhead, by a factor $(1/r_i)$, and therefore the slot length must be adapted accordingly. The slot length must be long enough so that the synchronization header, the preamble, the data packet and ACK messages can be delivered within it.

Figure 20 shows the packet success probability for transmissions over a Nakagami fading channel and the combined success probability, at a given slot, that takes the effects of both the PHY and MAC layers into account. The results for two different code rates, $r = \{0.96, 0.87\}$, and the uncoded case are shown to illustrate the performance difference between the uncoded and coded scenarios. In the traditional MAC layer analysis, the PHY layer success probability is assumed to be one (i.e., ideal receiver), which corresponds with the result shown in Figure 20 "PHY & MAC" curves, at their maximum value, where the PHY layer packet success probability is one, because E_b/N_0 is high enough for error-free transmission. Similarly, in the traditional PHY layer studies, the medium access success probability is not taken into account, which corresponds with the "PHY" curves shown in Figure 20. The results show that in the combined success probability ("PHY & MAC" curves), there is a transition region (between zero and maximum) with E_b/N_0 values that do not guarantee error-free communication at

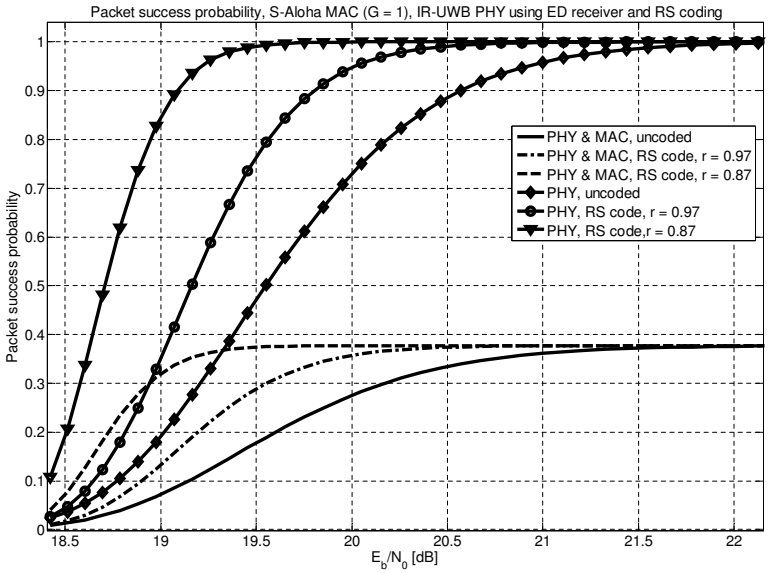

Fig. 20. Packet success probabilities vs. E_b/N_0 in dB for the uncoded and coded cases ([36] ©ACM 2014).

the PHY layer level. This illustrates that the joint analysis of PHY and MAC layers takes this transition region into account. Moreover, it can be observed that when the PHY layer provides error-free communication, the joint packet success probability is at maximum only 0.368. The reason is that the S-Aloha MAC protocol cannot provide a higher throughput [87, 88]. This simple comparison illustrates the importance of the joint analysis of PHY and MAC layers.

3.5.3 State transition probabilities

Section 3.3 introduced a Markov chain model at the general level for the analysis of the transmission period. In this section, the state transition probabilities for Markov chain events $(1)-(6)$ are derived for the combination of IR-UWB PHY and S-Aloha channel access during the transmission period.

Assume that $a = \varsigma$ new packets arrive at each node during a time period τ. In this work, the new packet arrival probability calculation, the traditional Poisson probability distribution, is used. Poisson probability distribution is selected here as an example case because it enables straightforward analysis and is enough to illustrate the features of the

proposed model. However, the proposed model allows for that different probability distributions can be used on particular application scenarios. For example, exact traffic modelling of a surveillance scenario has been discussed in [185].

According to a Poisson probability distribution with ρ events per second, the probability for $a = \varsigma$ arrivals during the time period τ can be calculated as

$$P_{\mathrm{r}}(a = \varsigma) = \frac{(\rho\tau)^{\varsigma}}{\varsigma!} e^{\rho\tau}. \tag{20}$$

Furthermore, let's define that $P_{\Omega}(\Omega = \kappa)$ is the probability that $\kappa = 0, 1, ..., j$ node(s) will have at least one new packet to transmit according to a Poisson probability distribution.

Assume that the system is at the initial state, which is defined as $S_t = 0$. The state transition probability for moving to the next state $S_{t+1} = 1$ is

$$P_{0,1} = P_{\mathrm{r}}\{S_{t+1} = 1 | S_t = 0\} = Np(1-p)^{N-1} P_{\mathrm{q}} P_{\mathrm{succ}}^{\mathrm{PHY}}, \tag{21}$$

where N is the number of nodes competing for the channel access at the initial state. The PHY layer success probability $P_{\mathrm{succ}}^{\mathrm{PHY}} = 1 - P_{\mathrm{packet}}$, can be calculated by using (13) for the uncoded case and by using (15) for the coded case. The probability that a new packet does not arrive to the queue of a node is defined here as $P_{\mathrm{q}} = P_{\mathrm{r}}(a = 0) = 1 - P_{\mathrm{a}}$, where $P_{\mathrm{a}} = P_{\mathrm{r}}(a > 0)$ is the probability of a new arrival(s) to the node's queue.

The probability of staying at the initial state is

$$P_{0,0} = P_{\mathrm{r}}\{S_{t+1} = 0 | S_t = 0\} = 1 - P_{0,1} = 1 - Np(1-p)^{N-1} P_{\mathrm{q}} P_{\mathrm{succ}}^{\mathrm{PHY}}, \tag{22}$$

i.e., the system remains at the starting state if none of the nodes is successful, which is the complement of the probability that any of the N nodes is successful.

The transition probability from state j to state $j+1$ is defined as

$$P_{j,j+1} = P_r\{S_{t+1} = j+1 | S_t = j\} = (N_j) p(1-p)^{(N_j - 1)} [P_{\mathrm{q}}]^{j+1} P_{\mathrm{succ}}^{\mathrm{PHY}}, \tag{23}$$

where N_j is the number of nodes competing for channel access at state $S_t = j$. In this case, one of the N_j nodes is successful in accessing the channel, transmits successfully the packet and new arrivals do not happen for the nodes that have an empty queue.

If the system is at state j and one node successfully transmits a packet, then $\kappa = j+1$ nodes can have a new packet arrival. But if the chain is at state j and no successful transmission takes place, then at most $\kappa = j$ nodes can have a new packet arrival.

Therefore, the transition probability for moving κ steps backwards is defined as

$$
\begin{aligned}
&P_{j,j-\kappa} = P_{\mathrm{r}}\{S_{t+1} = j-\kappa | S_t = j\} = \\
&(N_j)p(1-p)^{N_j-1}\binom{j+1}{\kappa+1}[P_{\mathrm{a}}]^{\kappa+1}[P_{\mathrm{q}}]^{j-\kappa+1}P_{\mathrm{succ}}^{\mathrm{PHY}} \\
&+(1-(N_j)p(1-p)^{N_j-1}P_{\mathrm{succ}}^{\mathrm{PHY}})\binom{j}{\kappa}[P_{\mathrm{a}}]^{\kappa}[P_{\mathrm{q}}]^{j-\kappa},
\end{aligned}
\tag{24}
$$

where $\kappa = [1,...,j]$. For the case $\kappa = 0$, the above equation is the probability $P_{j,j}$ for staying at the same state.

Using the state transition probabilities for the Markov chain, one can evaluate how many steps are needed to move from initial state $S_t = 0$ to state $S_{t+\Theta} = N$, where each node has successfully transmitted its packet(s). In addition, from the number of steps, the time to absorption Θ can be derived, as it will be described in the next section.

3.5.4 Time to absorption

A discrete-time Markov chain analysis [164][186] is used here for the derivation of the average number of steps to absorption, using the state transition probabilities introduced in the previous section. The expected time to absorption can then be calculated from the average number of steps, because the average length of the step is known.

At first, let's define the probability transition matrix $\mathbf{P} = [P_{x,y}]$ as

$$
\mathbf{P} = \begin{pmatrix}
P_{0,0} & P_{0,1} & 0 & \cdots & 0 & 0 \\
P_{1,0} & P_{1,1} & P_{1,2} & 0 & \cdots & 0 \\
\vdots & \vdots & \ddots & \ddots & \vdots & \vdots \\
P_{(N-2),0} & P_{(N-2),1} & P_{(N-2),2} & \cdots & P_{(N-2),(N-1)} & 0 \\
P_{(N-1),0} & P_{(N-1),1} & P_{(N-1),2} & \cdots & P_{(N-1),(N-1)} & P_{(N-1),N} \\
0 & 0 & 0 & \cdots & 0 & 1
\end{pmatrix},
\tag{25}
$$

which is composed of the state transition probabilities derived in Section 3.5.3. The matrix $\mathbf{P}$ can be decomposed as

$$
\mathbf{P} = \begin{pmatrix} \mathbf{V} & \mathbf{R} \\ \mathbf{O}^{\mathrm{T}} & 1 \end{pmatrix},
\tag{26}
$$

where the matrix $\mathbf{V}$ is composed of elements $V_{x,y} = P_{x,y}$ for $x,y = 0,1,\cdots,N-1$, $\mathbf{R}^{\mathrm{T}} = [0\ 0\ \cdots\ P_{(N-1),N}]$ and $\mathbf{O}^{\mathrm{T}} = [0\ 0\ \cdots\ 0]$. The fundamental matrix for the analysed

absorbing chain can be then defined as

$$\mathbf{A} = [\mathbf{I} - \mathbf{V}]^{-1}, \tag{27}$$

which consist of elements $\lambda_{x,y}$ for $x, y = 0, 1, \cdots, N-1$. If the initial state is $S_t = 0$, then the mean number of steps to absorption is

$$\Gamma_0 = \sum_y \lambda_{0,y}. \tag{28}$$

As stated earlier, the duration of a single step (slot) must be such that the data packet can be transmitted and the following ACK message can be received successfully, i.e., the slot duration is

$$T_{\text{slot},i} = T_{\text{f},i} + T_{\text{MaxAckWait}} + T_{\text{ACK}}, \tag{29}$$

where $T_{\text{f},i} = T_{\text{f}}/r_i$ is the duration of a data frame (including payload and headers) containing the redundancy introduced by the code rate r_i ($r_i = r_0 = 1$ for the uncoded case), $T_{\text{MaxAckWait}}$ is the maximum time a node waits for the ACK frame before retransmitting the data packet and T_{ACK} is the duration of the ACK frame. Therefore, the expected time to absorption when using i:th code rate (r_i) is calculated as

$$\Theta_i = \Gamma_0 T_{\text{slot},i}. \tag{30}$$

3.5.5 Analytical model verification

Different events can occur during the transmission period, as described in the previous sections. From the medium access control point of view, events can lead to collided packets, idle slots and successful channel access. After a successful channel access, the physical transmission over the wireless channel can lead to unsuccessful or successful receptions. Unsuccessful channel access or receptions will cause retransmissions. As introduced above, the Markov chain model described above can be used to find out the average number of steps required to reach the absorption state, which finally follows after the possible events. For the energy consumption derivation, more detailed information about the occurred events must be acquired. Therefore, a Matlab simulation model is developed to find out the number of collisions, total number of transmitted packets and also the number of idle slots spent during the transmission period. The analytically computed BEP values are used in the simulation model to evaluate the transmission success probability of the PHY layer.

In addition, the simulation results are used to verify the analytical results in two ways to confirm the correctness of the models: 1) results from the Markov chain model match the simulation model results regarding the number of steps to absorption; 2) for a boundary scenario case, no new arrivals during the competition period, the simulation results about the expected number of required transmissions to reach absorption also match the analytical results. For the verification (1), the analytical model has been explained in the previous sections. Next, it will be explained how the expected number of transmissions can be derived analytically for verification (2). Then the results of both comparisons (1) and (2) are shown.

The expected number of transmissions required to reach the absorption state can be derived as follows. The average number of steps needed for a node to be successful when at Markov chain state j, can be derived using (23), without taking into account the probability of new arrivals, as

$$N_{\text{steps},j} = \frac{1}{(N_j)p(1-p)^{(N_j-1)}(1-P_{\text{packet},i})}, \tag{31}$$

where the denominator is composed of PHY and MAC layer success probabilities when using i:th code rate. The expected number of transmissions (X_j) occurred during a step, at state j, can be calculated as

$$E\{X_j\} = \sum_x P_{\text{r}}[X = x]x, \tag{32}$$

where $x = [1,...,N_j]$, and the probability that x nodes attempt to transmit at state j can be calculated as [187]

$$P_{\text{r}}[X = x] = \frac{G_j^x e^{-G_j}}{x!}, \tag{33}$$

where $G_j = pN_j$ is the offered traffic load at state j. The average number of transmissions needed to reach the absorption state can then be found by considering all the Markov chain states as

$$N_{\text{tx,MC}} = \sum_{j=0}^{N} N_{\text{steps},j} E\{X_j\}. \tag{34}$$

Equation (34) can be used to find out the average number of transmissions calculated analytically and can be verified with the corresponding simulation results.

Figure 21 shows the average number of steps to absorption for the uncoded and coded, $r = 0.87$, cases. The results in Figure 21 are calculated using the Markov chain

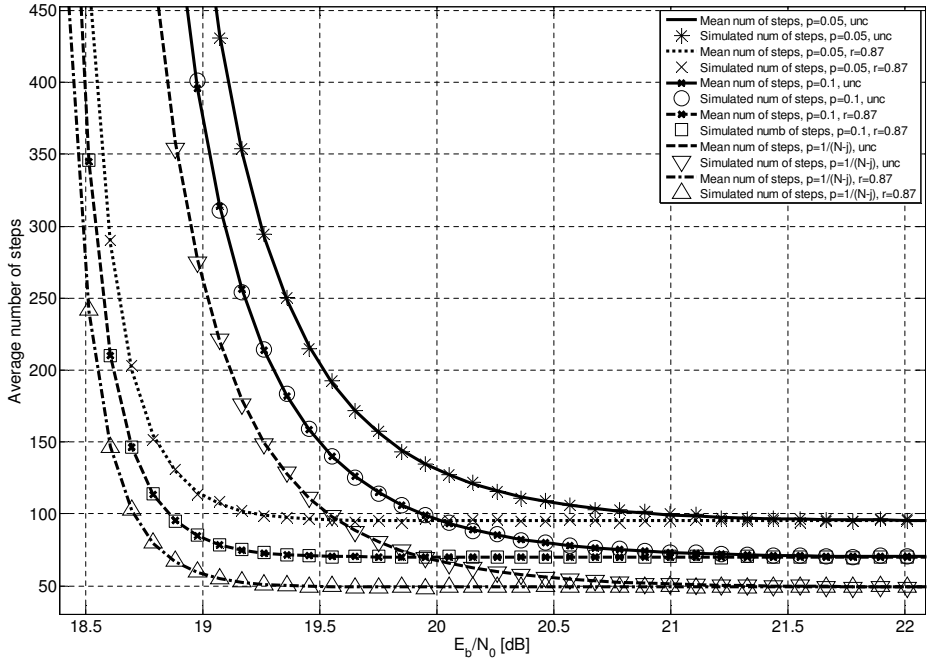

Fig. 21. Average number of steps vs E_b/N_0 in dB calculated using analytical and simulation models with different *p* values ([36] ©ACM 2014).

model and the corresponding simulations for the transmission period. The results are calculated for different channel competition probability values, $p = 0.1$, $p = 0.05$ and $p = 1/(N_j)$. The case $p = 1/(N_j)$ corresponds with the ideal scenario, where the channel competition probability is assumed to be adapted according to the number of nodes participating in the competition at state j. These results show that the Markov chain model produces the same average number of steps to absorption than the simulations. It can also be observed that the average number of steps to absorption is lower for $p = 0.1$ than for $p = 0.05$. The reason being that when $p = 0.05$, more idle steps are spent during the transmission period, since the nodes' probability to participate in the competition is too low. Therefore, when $p = 0.05$, the average number of nodes participating in the channel competition is lower than in the case of $p = 0.1$. The optimum value of p depends on how many sensor nodes are willing to transmit the packet to the sink node. In the studied scenario, at the beginning of the competition period $N_j = N = 20$. At that state, $p = 0.05$ is the optimum value for the S-Aloha protocol. However, during the competition period, when nodes are successful in their transmissions, the number of

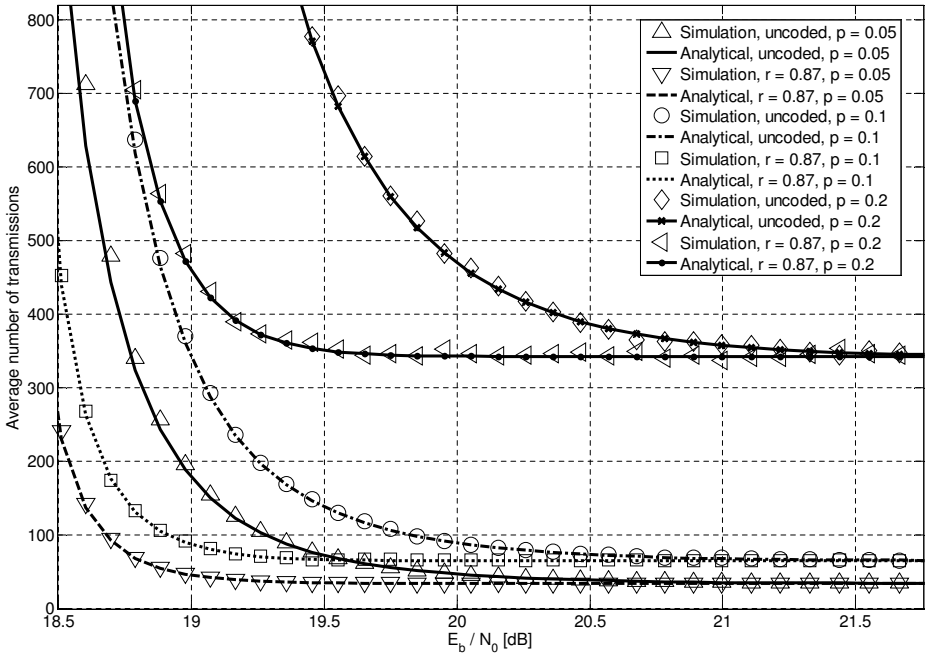

Fig. 22. Average number of transmissions required to reach the absorption state calculated using analytical and simulation models with different *p* values ([36] ©ACM 2014).

competing nodes decreases and the channel competition probability $p = 0.05$ becomes too low. It can be observed from Figure 21 that the average number of steps is the lowest when $p = 1/(N_j)$, because this corresponds with the case $G = 1$ for each step, which is the optimum traffic load for an S-Aloha-based network.

Figure 22 shows the results for the average number of transmissions required to reach the absorption state. These results are calculated using (34) and with simulations using a Matlab model for each corresponding case. It can be observed that the analytically calculated average number of transmissions match very well the simulation results, giving confidence to the use of the simulation model for cases that cannot be verified analytically. From these results, it can be observed that when the channel competition probability p is 0.1 or 0.2, a larger amount of transmissions are required than for the case of $p = 0.05$. The reason for these results is that when the channel competition probability is higher, more collisions will occur during the competition period. A probability $p = 0.2$ is obviously too high in this scenario, since the number of nodes, $N = 20$, is leading to a drastically higher number of transmissions during the competition

period. If there were less nodes in the network trying to transmit, e.g., when $N = 5$, the channel contention probability $p = 0.2$ would lead to a maximum throughput in the S-Aloha case. Figure 22 also shows that the uncoded transmission case with $p = 0.05$ requires less transmissions to reach the absorption state than the coded case with $p = 0.1$, if E_b/N_0 is greater than 19.6 dB. In addition, it can be observed that with higher channel competition probability values, the difference between uncoded and coded transmissions starts to appear with higher E_b/N_0 values. The rationale is that the joint PHY and MAC layer unsuccess probability gets higher already with lower E_b/N_0 values. This result illustrates the cross-layer tradeoff, which depends on the PHY and MAC layer characteristics.

Figures 21 and 22 show that the analytical results match well the simulation model results. Therefore, the additional information about the transmission period events, i.e, the number of collisions, idle slots and retransmissions, collected from the simulations can be reliably used in energy consumption calculations. Moreover, it can be observed that the average number of steps and transmissions can be reduced drastically for certain E_b/N_0 values by using error correction. For example, when $E_b/N_0 = 19.25$ dB and $p = 0.05$, the values are three times higher for the uncoded case.

3.5.6 Steps to absorption

As was shown above, error correction can reduce the average number of steps required to reach the absorption state. Here, will be taken a closer look at the savings which the different code rates can provide. The performance comparison is done here so that results are obtained using the Markov chain model (28) for different code rates and calculating the percentage of improvement in comparison with the uncoded case. From Figure 23, it can be observed that the maximum saving can be around 88% for the code rate $r = 0.81$ at $E_b/N_0 = 18.6$ dB. When $E_b/N_0 = 19.25$ dB and $p = 0.1$, the code rate $r = 0.87$ provides around 67% saving, which matches the results shown in Figures 21 and 22.

Figure 24 shows the time to absorption saving percentages for different code rates in comparison with the uncoded case. These results are calculated by using (30) and deriving the saving percentage in comparison with the uncoded case. It can be observed that the savings in time to absorption can be almost 85%, which is approximately a 3% lower result than in the steps saving case. In addition, the savings diminish at lower E_b/N_0 values than the ones shown in Figure 23. The reason is that coding increases the

packet length to include coding redundancy, leading to a longer slot length. Therefore, strong coding will lead to high redundancy, which makes the slot duration length inefficient. However, note that the time saving percentages can also be large when selecting the correct code rate for a particular E_{b}/N_0 value.

Figures 23 and 24 indicate that the energy savings will most probably be achieved by using error correction, because the number of steps and time to absorption are reduced by using the correct code rate. Therefore, the energy consumption modelling shown in the next section is well-motivated to find out the actual energy saving gain.

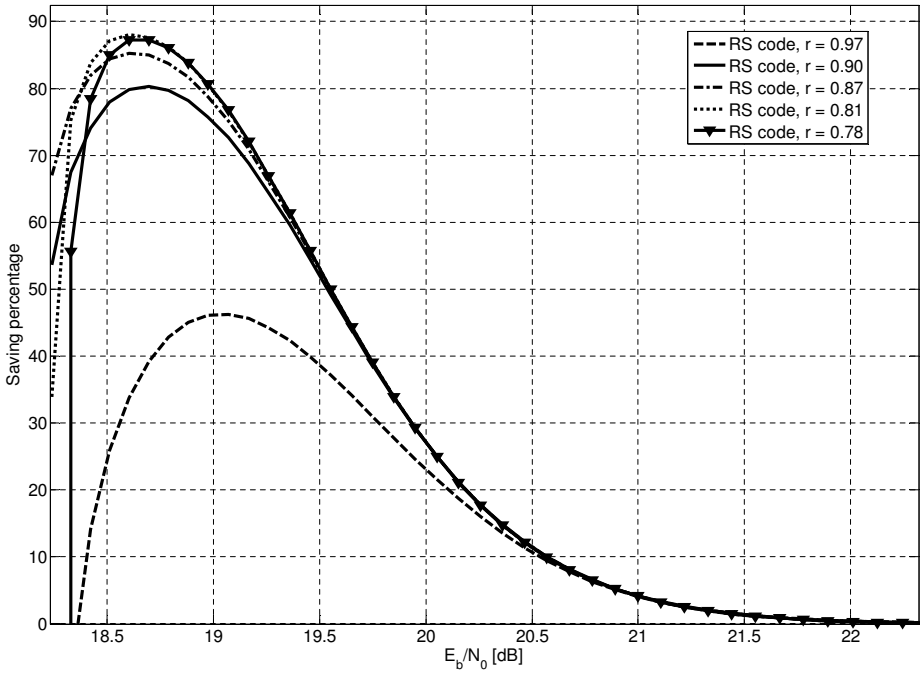

Fig. 23. Saving percentage in average number of steps versus E_{b}/N_0 in dB for different code rates, $p = 0.1$ ([36] ©ACM 2014).

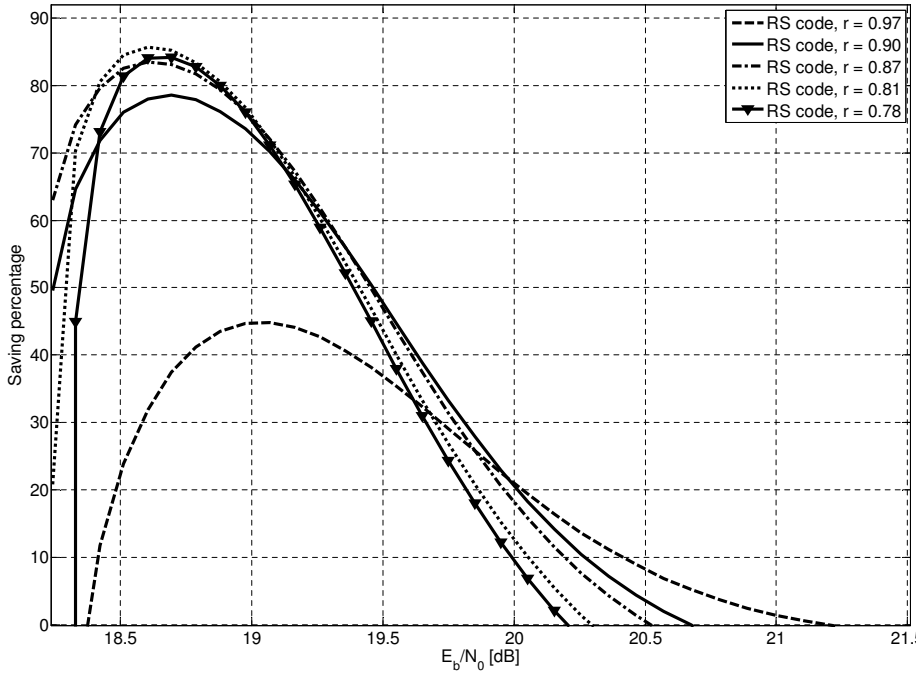

Fig. 24. Average time saving percentage versus E_b/N_0 in dB for different code rates, $p = 0.1$ ([36] ©ACM 2014).

3.5.7 Energy consumption

This section describes the energy consumption model that can be used to evaluate the energy consumption of the studied star-topology network, when using IR-UWB PHY and S-Aloha for channel access during the transmission period. The proposed model can be used to calculate the energy consumed from the beginning of the transmission period until each node has successfully transmitted its packet(s).

For the energy consumption analysis, the starting point is the general-level model introduced in Section 3.4. For the computation of the energy consumption, the transmission and reception power consumption values of IR-UWB PHY and S-Aloha channel access must be derived. The power consumption cost of a transmission at the PHY layer has two components: radio frequency (RF) consumption and internal

circuitry consumption. The transmission power consumption can be then defined as

$$P_{\mathrm{tx},i} = r_i P_{\mathrm{tx,RF}} + P_{\mathrm{tx,circ}}, \tag{35}$$

where $P_{\mathrm{tx,RF}}$ is multiplied by the chosen code rate r_i since the energy per coded bit depends on the used code rate as described in Section 3.5.1. The receiver power consumption is simply P_{rx}, which accounts for the power consumption of all the components at the receiver. The PHY layer energy consumption for a packet transmission and reception can be then calculated for code rate r_i as

$$\begin{aligned} E_{\mathrm{tx},i}^{\mathrm{PHY}} &= (r_i P_{\mathrm{tx,RF}} + P_{\mathrm{tx,circ}}) T_{\mathrm{f},i} \\ E_{\mathrm{rx},i}^{\mathrm{PHY}} &= P_{\mathrm{rx}} T_{\mathrm{f},i}. \end{aligned} \tag{36}$$

The MAC layer energy consumption factors are defined as

$$\begin{aligned} E_{\mathrm{tx,f}}^{\mathrm{MAC}} &= P_{\mathrm{rx}} T_{\mathrm{MaxAckWait}} \\ E_{\mathrm{tx,s}}^{\mathrm{MAC}} &= P_{\mathrm{rx}} (T_{\mathrm{MaxAckWait}} + T_{\mathrm{ACK}}) \\ E_{\mathrm{rx}}^{\mathrm{MAC}} &= P_{\mathrm{tx}} T_{\mathrm{ACK}} \\ E_{\mathrm{Imp}}^{\mathrm{MAC}} &= P_{\mathrm{idle}} T_{\mathrm{idle}}, \end{aligned} \tag{37}$$

where T_{idle} is the length of the idle slot, P_{tx} is the power consumption in the transmission mode for the uncoded case and P_{idle} is the power consumption in the idle mode. For the S-Aloha case, the ACK message transmission and reception energy consumption is taken into account in (37). For other channel access methods, such as the ones that use collision avoidance, the MAC energy consumption factors should also include the handshaking procedure, e.g., the ready-to-send and clear-to-send packet transmission and reception.

By substituting the above derivations, done for the PHY (36) and MAC (37) layers, to the energy consumption model introduced in Section 3.4, (7), the average energy consumption for the network during the transmission period, when using i:th code rate, can be computed as

$$\begin{aligned} E_{\mathrm{TP},i} = N_{\mathrm{tx}}^{\mathrm{fail}} \left(P_{\mathrm{tx},i} T_{f,i} + P_{\mathrm{rx}} T_{\mathrm{MaxAckWait}} \right) + N_{\mathrm{idle}} P_{\mathrm{idle}} T_{\mathrm{idle}} + \\ N_{\mathrm{tx}}^{\mathrm{succ}} \left(P_{\mathrm{tx},i} T_{\mathrm{f},i} + P_{\mathrm{rx}} T_{\mathrm{MaxAckWait}} + P_{\mathrm{rx}} T_{\mathrm{ACK}} + P_{\mathrm{rx}} T_{\mathrm{f},i} + P_{\mathrm{tx}} T_{\mathrm{ACK}} \right), \end{aligned} \tag{38}$$

where $N_{\mathrm{tx}}^{\mathrm{fail}}$ is the number of failed transmissions (due to a MAC layer collision or PHY transmission errors) for the whole network, $N_{\mathrm{tx}}^{\mathrm{succ}}$ is the number of successful

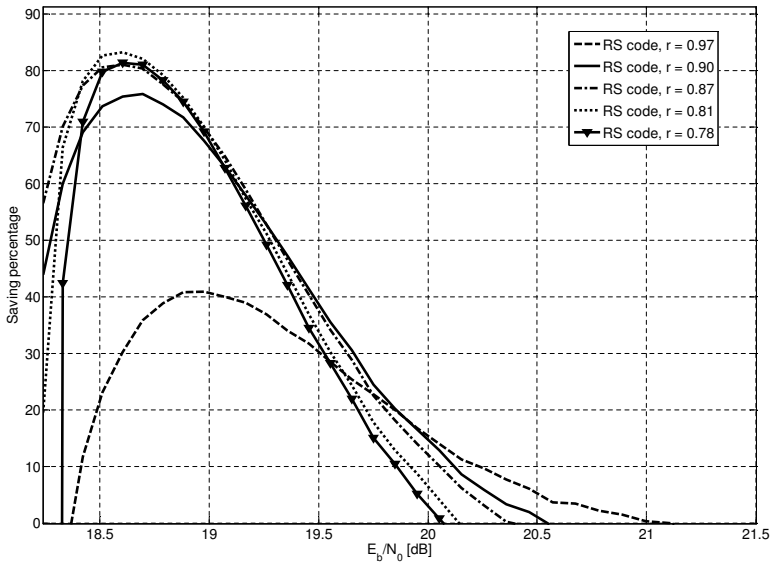

Fig. 25. Energy saving percentage result versus E_b/N_0 in dB when using different code rates, $p = 0.1$ ([36] ©ACM 2014).

transmissions and N_{idle} is the total number of idle slots used during the transmission period. The parameters $N_{\text{tx}}^{\text{fail}}$, $N_{\text{tx}}^{\text{succ}}$ and N_{idle} are provided by the Matlab simulations which model the described transmission period. In the scenario where new arrivals cannot happen, the analytical derivations introduced in Section 3.5.5 are used to find out the average number of $N_{\text{tx}}^{\text{fail}}$ and $N_{\text{tx}}^{\text{succ}}$, which are compared with simulation results to verify the models, as shown in Figures 21 and 22.

Figure 25 shows the energy saving percentage for the communication during the transmission period when different code rates are compared to the uncoded transmission. From the results, it can be observed that the energy savings for N nodes can be around 82% for the most energy-efficient code rate $r = 0.81$. It can also be concluded that the weakest code rate, $r = 0.97$, can provide at maximum a saving of 41%. In addition, the performance for $r = 0.97$ is better than in the other cases when the received E_b/N_0 is greater than 20 dB, and that code rate provides savings for the widest range E_b/N_0 values. For E_b/N_0 values below 20 dB, the stronger codes should be used, as it can be observed from the results shown in Figure 25. It can also be observed that the energy saving decreases drastically when E_b/N_0 is below 18.5 dB because then the coding gain starts to be negative.

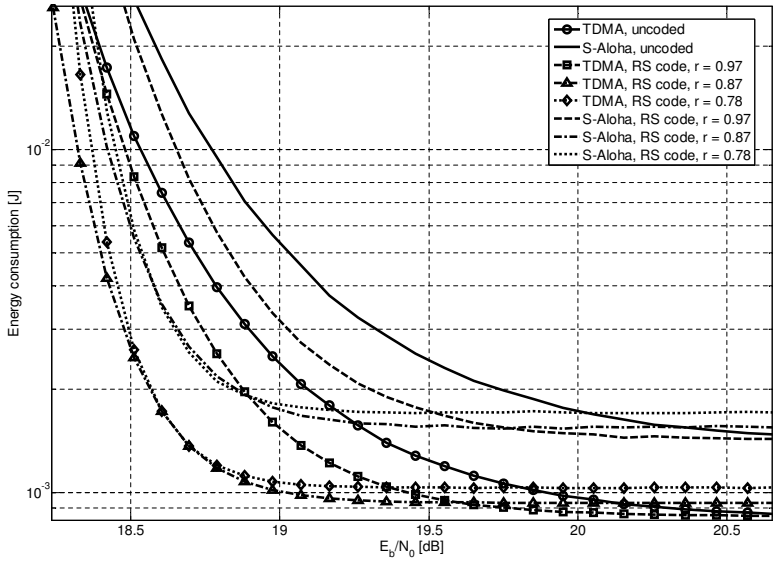

Fig. 26. Energy consumption comparison of TDMA- and S-Aloha-based MAC methods ([36] ©ACM 2014).

As can be observed, by comparing Figures 23 and 25, the percentage of energy saving follows closely the saving percentages of the average number of steps to absorption. The rationale is that the average number of steps is highly correlated with the required average number of transmissions, which is a major contributor to the energy consumption. Therefore, it can be found that the Markov chain model and analytical derivations of the average number of transmissions required for absorption can already provide a reliable inference on which code rates can save energy.

Figure 26 shows the energy consumption comparison of the TDMA and S-Aloha MAC methods when combined with IR-UWB PHY using ED. These results are calculated using (38) for three different code rates and the uncoded case. For the TDMA MAC, it is assumed that the sink node can perfectly synchronize with the nodes and schedule their transmission slots, leading to collision-free channel access. To enable fair comparison, for the S-Aloha case, it is assumed that the node probability to transmit in a slot is optimum, i.e., $p = 1/(N_j)$. From these results, it can be observed that TDMA MAC outperforms S-Aloha because there are no collisions during the channel contention leading to a decreased number of retransmissions, and consequently, lower energy consumption. For $E_\mathrm{b}/N_0 > 20$ dB, it can be observed that by using TDMA, almost 50% lower energy consumption would be achieved in comparison with

S-Aloha. On the other hand, from these results, it can also be observed that for certain E_b/N_0 values, the S-Aloha protocol combined with enough strong coding will lead to lower energy consumption than a combination of TDMA MAC and weak coding. For example, when $E_b/N_0 = 18.7$ dB, S-Aloha with $r = 0.78$ or $r = 0.87$ provides lower energy consumption than TDMA with $r = 0.97$ (or with uncoded transmission). Taking into account that TDMA would require a larger control overhead than S-Aloha, the difference would be even larger in practical implementations. This fairly simple comparison between TDMA and S-Aloha combined with IR-UWB and different error correction code rates highlights the fact that energy efficiency is dependent on the joint characteristics of the physical and MAC layers.

The results of this section show that remarkable energy savings can be achieved by selecting between the uncoded case and different RS code rates. In addition, the channel competition probability was found to have remarkable effect on the number of steps to absorption, which was shown to directly affect the energy consumption. The proposed model can be then used well at the network planning phase to select the configuration for the device's PHY and MAC protocols, if the expected channel conditions and/or communication distances and number of nodes are known, to improve energy efficiency. From the results, it can also be observed that the E_b/N_0 range leading to energy savings by tuning the code rate is quite narrow. If real-time protocol parameter adaptation should be done, it creates a challenge for the accurate and fast channel estimation (or the detection of received signal strength). That may not be possible with current technology, but in the future, computational capabilities of the sensor nodes are expected to increase, which will allow the required level of estimation. In addition, it must be noted that for the simple receiver structure and hard-decision decoding (HDD) case, the maximum coding gain is approximately 3 dB. However, the proposed model can also be used to include soft decision decoding (SDD) or more sophisticated codes that have a wider coding gain. For example, RS codes with SDD receiver can give approximately $2-3$ dB larger coding gains than HDD in the AWGN channel [45],[188–190]. For the fading channel case, the coding gain difference is remarkably larger, more than 6 dB [188], [191]. For larger coding gain, consequently the E_b/N_0 range which leads to energy savings, will be wider. In this work, the focus is on a simple receiver structure, and the studied RS code with HDD is the same as the one chosen in [20] to be used in conjunction with a non-coherent IR-UWB PHY. Therefore, the model studied here provides a tool to obtain energy savings by adjusting the rate of the RS code chosen for that standard and/or the channel access competition characteristics of

the nodes. In addition, the general approach to the PHY and MAC analysis introduced in this work can also be used for different coding methods or, for example, to study the transmission power and modulation effect on the cross-layer performance. In the latter case, the proposed model can be used by substituting the effect of transmission power and modulation adaptation to the physical layer bit error probability derivation and the energy consumption factors.

3.6 Summary

This chapter introduced a cross-layer approach that can be used to study potential energy consumption savings that can be achieved by adapting communication protocol characteristics. First, a generic wake-up radio-based MAC protocol was defined to enable bi-directional wake-up procedure in order to avoid idle listening in WSN applications. The GWR-MAC protocol uses wake-up signalling to trigger the transmission period, in which different channel access methods can be used to manage data transmissions between the sensor nodes and the sink. Then, an analytical and simulation model, which were developed taking relevant characteristics of the PHY and MAC layers into account, was introduced. In this thesis, the proposed model is used to evaluate the energy efficiency of different RS code rates for a WSN using IR-UWB communication with non-coherent energy detection and GWR-MAC, whose transmission period is based on S-Aloha. The introduced approach can also be used to analyse the energy efficiency for other combinations of MAC and PHY protocols. As an example case, this work shows results for a TDMA-based channel access energy consumption comparison with S-Aloha-based channel access.

The results of this chapter show that significant energy savings can be achieved by selecting the proper code rate or uncoded transmission, depending on the channel conditions. The maximum energy savings percentage was found to be over 80% for a particular code rate when compared with the uncoded case. On the other hand, the results also show that in which instances RS coding does not lead to energy savings and the uncoded case should be used instead. In addition, the results showed that the channel competition probability of S-Aloha channel access has a remarkable effect on the transmission period length and consequently on energy consumption.

The proposed model can be used for a protocol characteristics selection at the network implementation phase or adaptively during the run-time. If the channel conditions and the number of nodes competing for the channel are known accurately

enough during the run-time, the transceivers can select the code rate adaptively and tune the channel competition probability, e.g., from a look-up table which is composed of the results given by the proposed model. In addition, the model enables to evaluate the required transmission period length for the star-topology network including sensor nodes and a sink. The transmission period length can be then adjusted to save energy by selecting the protocol parameters correctly. Transmission period length evaluation is useful, e.g., when planning network scheduling and routing for a network which includes multiple clusters composed of sensor nodes and sink nodes. This model is therefore useful for a cross-layer design approach based on information exploitation between the layers to upward and downward direction. In this work, the analysis focuses on the PHY and MAC layers, but joint performance of those layers can also be improved by exploiting the number of nodes information from the network layer. To the other direction, network layer can take advantage of the lower layers' joint performance information, calculated by the proposed model, when performing routing decisions.

4 Energy-efficient hierarchical network

In this section a hierarchical architecture design for WSNs will be discussed and an energy efficiency model will be proposed. In the author's publication [38], the architecture has been originally defined in more detail, and the energy efficiency model discussed and revised in this chapter is also originally proposed therein.

The wireless sensor network architectures can be divided roughly into two categories: flat and hierarchical. In the flat architecture case, all the network nodes are at the same level and they have similar roles and typically also same characteristics. In the hierarchical network case, the nodes have different characteristics and roles at different layers. The flat network structure is simpler but it cannot provide efficient communication, particularly when the network size is large. The hierarchical network structure has been found to provide more efficient communication in the case of heterogeneous networks since the nodes' operations can be designed so that the overall performance will be improved in comparison with a flat architecture.

At the early stage of the WSN research, the target applications included a homogeneous set of sensor devices, which were performing a simple sensing task and reporting sensor observations to a central (sink) node. That network topology is still valid for many applications. However, the development of WSN devices has led to an emergence of heterogeneous networks which include different types of devices with varying capabilities, enabling the implementation of versatile application scenarios. Support for heterogeneous devices is needed in WSNs for energy efficiency, scalability and quality of service purposes. The network of a heterogeneous set of devices must be designed intelligently to enable efficient and reliable operation. The previously proposed hierarchical architectural approaches can be divided into intra-network and in-network hierarchies. In the intra-network proposals, the design goal is efficient communication between the WSN and the rest of the world, see, e.g., [192] and [193]. The proposed in-network hierarchies of WSNs typically limit to two-tier topologies, where the higher tier forms a backbone network. The lower tier nodes can be simpler and they save energy by communicating directly only with a higher tier node [194]. For example, several WSN protocols, e.g., ZigBee [122] and Z-Wave [13], make a distinction between a routing and a non-routing device. The approach also allows energy saving by clustering nodes and designating only one node at a time as an energy-consuming higher tier

node [195], [196]. The multi-tier architectures proposed in the literature are typically designed for a particular application purpose, e.g., hospital environment [197], traffic monitoring system [198], surveillance [199], environmental monitoring [200], smart home [201], or underwater acoustic sensor networks [202]. Therefore, there is a need for an architecture that enables to use different types of heterogeneous devices and can be then applied to several WSN applications, ranging from environmental sensing, surveillance and security to remote health care, military uses and process automation.

The network's total energy consumption can be decreased by taking into account the features of the heterogeneous devices at different layers of the architecture. Different types of devices' functionalities must be designed so that communication requirements can be met while maintaining the low energy consumption. As was noticed in the background discussion regarding energy-efficient communication protocols, it is important to maximize the length of the nodes' sleep mode and minimize the number of transmissions in order to save energy. It is particularly important in a heterogeneous network for the nodes which are the most power consuming.

To enable energy efficiency by putting the nodes into the sleep mode, the heterogeneous hierarchical network requires a method for awakening the nodes when required from the application point of view. For that purpose, there are two different types of radios that can be used for communication between different architecture layers: duty-cycle radio and wake-up radio. Duty cycle-based radio is the traditional approach while wake-up radios have started to gain more and more research attention in recent years, as was introduced in Section 2.1.2.

An energy efficiency evaluation model for a hierarchical WSN whose device's functionalities are designed so that energy savings can be achieved by using a wake-up mechanism will be proposed in this section. The proposed model takes account of sensing, processing and communication layer characteristics and the interdependencies of the different network layers. The physical and MAC layer characteristics affect energy consumption of an individual node, as well as the network-level consumption, particularly in the case of hierarchical network, where the energy savings can be obtained by using a wake-up mechanism. The wake-up mechanism effect on the hierarchical network energy consumption is explored in this work by using the proposed model. The GWR-MAC protocol, which includes the wake-up procedure, and the transmission period were introduced in Section 3.1. The energy efficiency of the transmission period was analysed in Chapter 3. Here the focus is on the evaluation of the wake-up procedure's effect on the energy efficiency of the WSN. However, the

energy consumption of the data packet transmissions is also taken into account in the proposed energy consumption model. The architecture details are explained at the level which is required for understanding the proposed analytical energy efficiency model.

4.1 Architecture for a heterogeneous network

The developed network architecture is based on hierarchical levels of intelligence and usage of wake-up signalling. It can be used in various application scenarios which include heterogeneous devices. The wake-up functionality is seen as a long lifetime enabler, particularly for the wireless long-lasting (e.g., surveillance, structural, environmental and industrial) monitoring systems, which have many possible application scenarios in both private and public sectors. Due to a very wide target application space, the architecture must be designed to be flexible, adaptive and scalable to varying configurations. Therefore, this work is defining a high-level architecture, which is independent of the particular implementation techniques (e.g., radio interfaces), in order to enable that different application scenario designers have flexibility to choose the most suitable implementation technique by using the proposed architecture as a starting point.

The driving factors of the architecture design are the functionalities which the network needs to fulfill. Therefore, the network nodes are categorized here into different architectural layers based on their overall capabilities and functionalities. The division and functionalities of the layers are defined to be meaningful and usable for a wide application space. The high-level architecture and the functionalities offered at the different layers are shown in Figure 27.

The hierarchical layers of the architecture are named as elementary layer (EL), intermediate layer (IL), advanced layer (AL) and outer layer (OL). The complexity, capabilities and performance of the devices at different layers increase from the bottom to the top. Consequently, the devices at the lowest layer (EL) consume the least energy and the energy consumption increases from the bottom up. The idea is to decrease the overall energy consumption by using the low-complexity devices for continuous event monitoring and data collection while keeping the more power consuming higher layer devices in the sleep mode as long as possible.

The elementary layer nodes will wake up the higher-complexity devices (IL and AL) only when required from the application requirements point of view. The EL devices are usually simple sensor nodes providing basic sensing and actuation services. These nodes offer networking services by communicating with the devices at the intermediate

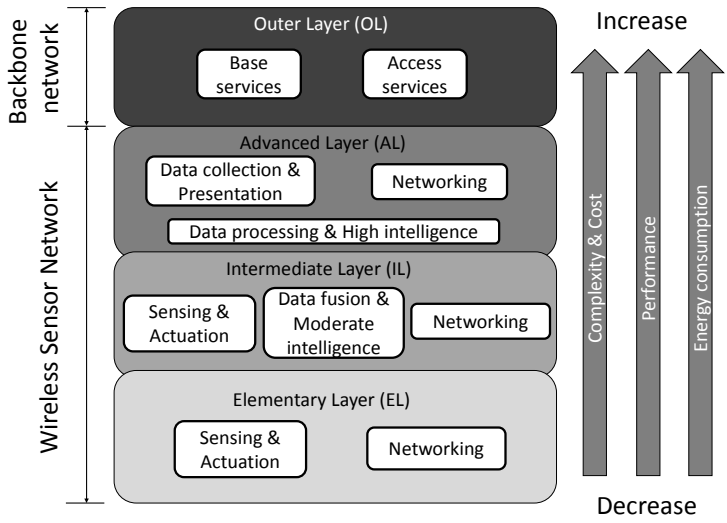

Fig. 27. High-level overview of the hierarchical architecture ([38] ©Springer Science+Business Media 2014).

layer, and in the mesh network case, the EL sensor nodes are communicating also with each other. The simplest networking service which elementary layer node can offer is just to send a simple message containing, e.g., a temperature or humidity value sensed by the node.

The intermediate layer nodes have more capabilities and they can offer higher performance functionalities and sensing, such as recording a video. The IL nodes may also perform data aggregation for information collected from elementary layer nodes and make decisions based on the data by using, e.g., pattern recognition algorithms. Therefore, the intermediate layer nodes can decide whether an event is so critical that also the advanced layer needs to be awakened. The IL nodes also offer important networking services for the architecture because they can communicate both with upper and lower layer devices.

The advanced layer nodes are the most intelligent devices in the architecture, and they will eventually collect all the relevant data from the lower layers. The AL nodes can make intelligent decisions, process data and act as a gateway between the WSN and the backbone network. Therefore, AL devices must provide adequate interfaces so that the sensor network services can be offered to user through service interfaces. The outer layer is the backbone infrastructure, e.g., wireless/wired broadband or cellular network, comprising Internet connection, back-end systems and applications server.

4.1.1 Techniques and components

There are many technologies available that can be used to implement the described hierarchical architecture. As an example, Table 5 shows network components and possible technologies for different layers for three application scenarios. The physical components which implement the logical components in different hierarchical layers, and the interface specifications between them, can change from an application to another. The elementary, intermediate and advanced layer nodes can be, for example, a ZigBee node, laptop and desktop computer, respectively. The components can also reside at the same physical device, which could be, e.g., a smart phone with different sensors, wireless local area network (WLAN) and 3G/4G interfaces. However, here the focus is on a hierarchical network which is composed of different types of physical devices at each layer.

Table 5. Example characteristics of architecture components in different application scenarios ([38] ©Springer Science+Business Media 2014).

	Medical care	Industrial automation	Surveillance scenario
EL sensor	body temperature, blood glucose level	temperature, proximity, pressure	passive infrared (PIR), accelerometer, magnetometer
EL node	IEEE 802.15.6, low-power MCU	WirelessHART, ISA100.11a [203], WUR, low-power MCU	WUR, IEEE 802.15.4(a), DASH7 [12], Bluetooth LE, low-power MCU
IL sensor	electrocardiogram (ECG), electroencephalogram (EEG)	detection and ranging, camera	video/still camera
IL actuator	insulin pump	control robot movements	control camera view angle
IL node	IEEE 802.15.6 / 802.11bgn, MCU	WUR, WirelessHART, ISA100.11a, 802.11bgn, MCU	wake-up radio, IEEE 802.15.4(a) / 802.11bg, MCU
AL node	IEEE 802.11bgn / 802.3, MCU, data base	IEEE 802.11bgn / 802.3, MCU, data base	WUR, IEEE 802.15.4(a) / 802.11bgn, MCU, data base
AL / OL interface	WSN OpenAPI Gateway (WOAG) [204] with Internet connection through cellular network, asymmetric digital subscriber line (ADSL), Fiber, IEEE 802.11bgn etc.		

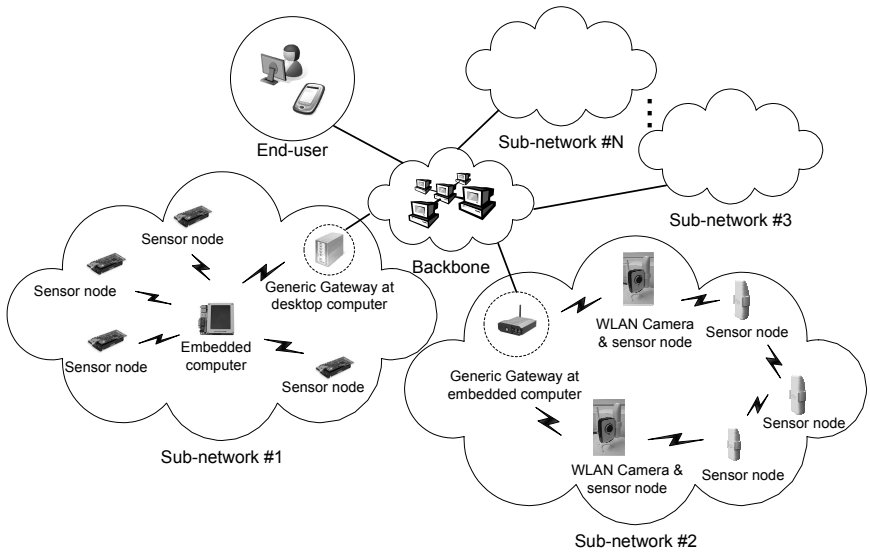

Fig. 28. Hierarchical geographically distributed heterogeneous network implementation example ([38] ©Springer Science+Business Media 2014).

A detailed mapping between logical components and physical components needs to be done separately for each implementation. Figure 28 illustrates an example of application scenarios that have been implemented using the proposed hierarchical architecture principle. Sub-network #1 illustrates a WSN where the sensor nodes (TelosB [8]) collect data from the office environment and send it to the embedded computer (FriendlyARM [205]), which forwards the data to the desktop computer with a connection to the backbone network. Sub-network #2 illustrates a surveillance WSN where the sensor nodes (TUTWSN [206]) detect movements in the monitored area and wake up a WLAN camera node to record a video once the intruder has been detected. The WLAN camera node sends the video to an embedded computer, which forwards the data to the backbone network. An authenticated end-user can access the data from sub-networks through the backbone network and receive, e.g., automatic alarms about intruders in the monitored area.

4.1.2 Wake-up concept

A low-power wake-up concept can be implemented with a specific wake-up radio or by using a duty-cycled MAC protocol. The downside of duty-cycle radios is that they will listen to the channel unnecessarily if the event reporting frequency is lower

than the duty cycle. The energy consumption of WURs is very low in the standby mode, when they can be continuously listening possible wake-up signals. Therefore, WURs have potential to decrease energy consumption in comparison with duty-cycle radio-based networks. Both approaches were introduced in Chapter 2. For both cases, source-initiated communication is assumed, i.e., the focus is on the scenario where the sensor nodes have sensed something and trigger the wake up of the higher layer.

In the DCR approach, each layer's low-power transceivers need to wake up and sleep according to a predefined schedule. It is assumed that the nodes in each network layer have low-power radios (e.g., IEEE Std 802.15.4-based) for duty cycling to enable the wake-up mechanism. In the DCR-based network case, the transmitter sends a detected event (DE) message in order to inform the node at a higher layer that it should stay awake. If a higher-layer node receives a DE message during the duty cycle listening, it will stay on, send an ACK message and wait for a data transmission.

In the WUR-based network, the wake-up signals are used to activate the higher layers when needed. The GWR-MAC protocol introduced in Section 3.1 is used for the WUR-based wake-up mechanism. The lower-layer WUR transmits the wake-up signal and the higher-layer node sends back a beacon message, as described in the GWR-MAC protocol's source-initiated mode definition. Then the lower-layer nodes can send their data to the higher-layer node. The same GWR-MAC wake-up procedure is used for the elementary layer to wake up the intermediate layer and the intermediate layer to wake up the advanced layer.

4.2 Performance evaluation

This section introduces an energy efficiency comparison of the WUR- and DCR-based hierarchical network introduced in Section 4.1. The intelligent hierarchical operation is assumed for both WUR and DCR approaches, i.e., the lower-layer devices are performing continuous sensing and wake up the higher layers when required. The comparison is done with different duty-cycle and event-frequency values in a typical surveillance scenario, which corresponds with the case of sub-network #2 in Figure 28. The used analytical approach can also be applied to other WSN scenarios with layered hierarchical architecture. However, the detailed assumptions must be adjusted to match the particular application under evaluation.

4.2.1 Model assumptions

The energy efficiency comparison takes account of the energy consumption of the nodes' core components: micro-controller unit, transceiver and sensors. A low-power micro-controller has typically the active, standby, and sleep modes. The transceiver has the transmit (Tx), receive (Rx), idle and sleep modes. The active, Tx and Rx modes are the most energy consuming parts. Therefore, it is important to put the nodes into the sleep mode when possible. The sensing component consists of sensors and A/D converters. The sensing component has different modes, which affect energy consumption, e.g., sensor warm-up, active mode and settle time of the A/D converter. The dominating energy consumption factors of each transceiver's components are taken here into account: wake-up signalling, data transmission and reception, and MCU and sensor active mode current consumption. The relevant energy consumption characteristic, affecting the WUR and DCR energy efficiency comparison, are then addressed. However, energy consumption during network initialization and run-time management (e.g., communication required for synchronization and routing) are not taken into account.

In order to perform the analytical calculations for the surveillance scenario, further assumptions for components that affect energy consumption are defined. The assumptions for the elementary layer nodes' are:

- Sensing module: nodes are monitoring the environment continuously with motion detection (e.g., passive infrared (PIR)) sensors.
- Transceiver module: nodes transmit a wake-up signal (or DE) when an event is detected. Then, the main radio will also be awakened in order to transmit and receive information to and from IL.
- MCU module: MCU is turned on when an event is detected in order to switch transceiver states and to react to possible IL commands. MCU goes to the sleep mode once the event is finished.

The intermediate layer nodes' assumptions affecting energy consumption are:

- Sensing module: nodes are in the sleep mode until they are awakened. After they wake up, they will start sensing for 5 seconds, if the event is determined as critical. The main sensor is a video camera which monitors intruders. If the AL is awakened, it is assumed to require additional 10 seconds sensing from the IL layer sensor.

– Transceiver module: WUR is in the listening mode continuously (or DCR according to the duty cycle) to detect a wake-up signal (or DE) from EL and transmit a wake-up signal (or DE) to AL, if a critical event is detected. Then, the main radio is also awakened in order to transmit and receive information to and from AL and EL
– MCU module: MCU is turned on when the WUS (or DE) is detected in order to do processing and aggregation, make decisions and switch transceiver states. MCU goes into the sleep mode once the event is finished.

The advanced layer nodes' assumptions affecting energy consumption are:

– Sensing module: nodes do not include sensors.
– Transceiver module: WUR is in the listening mode continuously (or DCR according to the duty cycle). AL node receives a WUS (or DE) from IL. Then, the main radio will also be awakened in order to receive and transmit information to and from IL. The transceiver also needs to communicate outside the network if the event is critical.
– MCU module: MCU is turned on when a WUS (or DE) is detected in order to do processing and aggregation, make decisions and switch transceiver states. MCU goes into the sleep mode once the event is finished.

The parameter values for the studied network scenarios are shown in Table 6. The parameters are chosen so that they represent typical values for nodes equipped with WUR, IEEE Std 802.15.4 and IEEE Std 802.11b communication interfaces and sensors, as described for the surveillance scenario. The number of nodes at the elementary layer is 100, and the number of nodes at the intermediate layer is 10, i.e., there is in average 10 sensor nodes assumed to be associated with one IL node, which acts as a coordinator node for the sensor nodes. At the advanced layer there are two nodes, i.e., there are five IL nodes associated with one AL node. As can be observed from Table 6, more events are assumed to occur at the elementary layer than at the intermediate or advanced layer. This is due to the intelligent hierarchical network characteristic. It is assumed that IL can make an intelligent decision on whether an event is critical or not, as was discussed above in the architecture description. Only critical events are calculated as events for IL, which requires also AL to be awakened. Similarly, only the events, which cause the alarm to the end-user, are counted as events for AL. The same fixed BEP is assumed for communication at each layer and the used value is mentioned when presenting the results. More detailed modelling for the PHY and MAC layers regarding data transmissions are not used here because the main purpose is to compare the impact of the wake-up mechanisms (WUR vs DCR) on the hierarchical network's energy

efficiency. However, it is important to take the required retransmissions into account to evaluate when the data transmission energy consumption starts to dominate over the wake-up mechanism's energy consumption. Here the average number of transmissions required for success is calculated by using a fixed BEP value, which is used to calculate the packet success probability. However, the proposed model can also be used by using a BEP calculated using dedicated channel models and channel access success probabilities for different layers' communication links.

Table 6. Parameters for performance comparison ([38] ©Springer Science+Business Media 2014).

Parameter	Description	Value
N_{EL}	Number of nodes in EL	100
N_{IL}	Number of nodes in IL	10
N_{AL}	Number of nodes in AL	2
$I_{TX,EL}$	TX mode current consumption, EL	17.4 mA
$I_{TX,IL}$	TX mode current consumption, IL	250 mA
$I_{TX,AL}$	TX mode current consumption, AL	300 mA
$I_{RX,EL}$	RX mode current consumption, EL	19.7 mA
$I_{RX,IL}$	RX mode current consumption, IL	19.7 mA
$I_{RX,AL}$	RX mode current consumption, AL	250 mA
$I_{CL,DCR}$	Current consumption of channel listening (DCR)	19.7 mA
U	Operating voltage	3.0 V
$I_{C,WUR}$	WUR constant idle mode current consumption	60 µA
$I_{TX,WUR}$	WUR transmission mode current consumption	100 mA
$I_{RX,WUR}$	WUR reception mode current consumption	200 µA
I_{clk}	Clock current consumption	2 µA
R_W	WUR data rate	20 kbps
R_{EL}	Data rate, EL radio	250 kbps
R_{IL}	Data rate, IL radio	1 Mbps
R_{AL}	Data rate, AL radio	10 Mbps
ε_{EL}	Number of events in EL	$10 - 31536000$/year
ε_{IL}	Number of events in IL	$2 - 6307200$/year
ε_{AL}	Number of events in AL	$1 - 3153600$/year
λ_{dc}	Duty-cycle percentage	$0.03 - 5\%$
$T_{s,IL}$	Sensing time per event, IL	5 s + 10 s
$I_{MCU,EL}$	Micro-controller current consumption, EL	1 mA
$I_{MCU,IL}$	Micro-controller current consumption, IL	100 mA
$I_{MCU,AL}$	Micro-controller current consumption, AL	300 mA
$I_{s,EL}$	Sensor current consumption, EL	3 µA
$I_{s,IL}$	Sensor current consumption, IL	30 mA
t_o	Operation duration	one year
$t_{wait,BC}$	Beacon waiting time	3.4 ms
L_{DE} / L_{ACK} / L_{BC}	Length of DE/ACK/BC message	50 bits
L_W	Length of wake-up signal	50 bits
$L_{D,EL}$	Length of data packet in EL	1024 bits
$L_{D,IL}$ / $L_{D,AL}$	Length of data packet in IL/AL	4096 bits

4.2.2 Energy efficiency

The analytical energy consumption model for the WUR- and DCR-based networks is proposed here. Furthermore, performance comparison of the WUR and DCR approaches is enabled by defining an energy efficiency metric.

The total energy consumption during the operation time, t_o, as a function of number of events and bit error probability, for WUR-based network layers (EL, IL and AL) can be calculated as

$$
\begin{aligned}
&E^{\mathrm{EL}}_{\mathrm{TOT,WUR}}(\varepsilon,t_o,\beta) = E^{\mathrm{EL}}_{\mathrm{s}}(t_o) + E^{\mathrm{EL}}_{\mathrm{MCU}}(\varepsilon,t_o) + E_{\mathrm{TX,WUS}}(\varepsilon,t_o,\beta) \\
&+ E_{\mathrm{wait,BC}}(\varepsilon,t_o) + E_{\mathrm{RX,BC}}(\varepsilon,t_o) + E_{\mathrm{C}}(t_o) + E^{\mathrm{EL}}_{\mathrm{TX,D}}(\varepsilon,t_o,\beta) + E_{\mathrm{clk}}(t_o), \\
&E^{\mathrm{IL}}_{\mathrm{TOT,WUR}}(\varepsilon,t_o,\beta) = E^{\mathrm{IL}}_{\mathrm{s}}(t_o) + E^{\mathrm{IL}}_{\mathrm{MCU}}(\varepsilon,t_o) + E_{\mathrm{TX,WUS}}(\varepsilon,t_o,\beta) \\
&+ E_{\mathrm{TX,BC}}(\varepsilon,t_o) + E_{\mathrm{wait,BC}}(\varepsilon,t_o) + E_{\mathrm{RX,BC}}(\varepsilon,t_o) + E_{\mathrm{RX,WUS}}(\varepsilon,t_o,\beta) \\
&+ E_{\mathrm{C}}(t_o) + E_{\mathrm{clk}}(t_o) + E^{\mathrm{IL}}_{\mathrm{TX,D}}(\varepsilon,t_o,\beta) + E_{\mathrm{RX,D}}(\varepsilon,t_o,\beta), \\
&E^{\mathrm{AL}}_{\mathrm{TOT,WUR}}(\varepsilon,t_o,\beta) = E^{\mathrm{AL}}_{\mathrm{MCU}}(\varepsilon,t_o) + E_{\mathrm{RX,WUS}}(\varepsilon,t_o) + E_{\mathrm{TX,BC}}(\varepsilon,t_o) \\
&+ E_{\mathrm{C}}(t_o) + E_{\mathrm{clk}}(t_o) + E^{\mathrm{AL}}_{\mathrm{TX,D}}(\varepsilon,t_o,\beta) + E^{\mathrm{AL}}_{\mathrm{RX,D}}(\varepsilon,t_o,\beta),
\end{aligned}
\tag{39}
$$

where ε is the number of events during the operation time t_o, β is the raw bit error probability of the channel, $E_{\mathrm{TX,WUS}}$ is the energy consumption of wake-up signal transmissions, $E_{\mathrm{RX,WUS}}$ is the energy consumption of wake-up signal receptions, $E_{\mathrm{TX,BC}}$ is the energy consumption of beacon transmission, $E_{\mathrm{wait,BC}}$ is the energy consumption of beacon listening, $E_{\mathrm{RX,BC}}$ is the energy consumption of beacon receptions, E_{C} is the constant energy consumption of WUR and E_{clk} is the energy consumption of the clock needed to maintain the time synchronization. E^x_{s} is the energy consumption of sensing, E^x_{MCU} is the energy consumption of MCU, $E^x_{\mathrm{TX,D}}$ and $E^x_{\mathrm{RX,D}}$ are the energy consumption of data transmissions and receptions, respectively, calculated separately for each layer (i.e., x is EL, IL or AL).

The total energy consumption during t_o, as a function of number of events, duty-cycle percentage and bit error probability, for DCR-based network layers (EL, IL and AL) can

be calculated as

$$E^{\mathrm{EL}}_{\mathrm{TOT,DCR}}(\varepsilon,\lambda_{\mathrm{dc}},t_{\mathrm{o}},\beta) = E^{\mathrm{EL}}_{\mathrm{s}}(t_{\mathrm{o}}) + E^{\mathrm{EL}}_{\mathrm{MCU}}(\varepsilon,t_{\mathrm{o}}) + E^{\mathrm{EL}}_{\mathrm{RX,DC}}(\lambda_{\mathrm{dc}},t_{\mathrm{o}}) + E_{\mathrm{clk}}(t_{\mathrm{o}}) + E^{\mathrm{EL}}_{\mathrm{TX,DE}}(\varepsilon,t_{\mathrm{o}},\beta) + E^{\mathrm{EL}}_{\mathrm{RX,BC}}(\varepsilon,t_{\mathrm{o}},\beta) + E^{\mathrm{EL}}_{\mathrm{TX,D}}(\varepsilon,t_{\mathrm{o}},\beta),$$

$$E^{\mathrm{IL}}_{\mathrm{TOT,DCR}}(\varepsilon,\lambda_{\mathrm{dc}},t_{\mathrm{o}},\beta) = E^{\mathrm{IL}}_{\mathrm{s}}(\varepsilon,t_{\mathrm{o}}) + E^{\mathrm{IL}}_{\mathrm{MCU}}(\varepsilon,t_{\mathrm{o}}) + E^{\mathrm{IL}}_{\mathrm{RX,DC}}(\lambda_{\mathrm{dc}},t_{\mathrm{o}}) + E_{\mathrm{clk}}(t_{\mathrm{o}}) + E^{\mathrm{IL}}_{\mathrm{RX,DE}}(\varepsilon,t_{\mathrm{o}},\beta) + E^{\mathrm{IL}}_{\mathrm{TX,BC}}(\varepsilon,t_{\mathrm{o}},\beta) + E^{\mathrm{IL}}_{\mathrm{TX,DE}}(\varepsilon,t_{\mathrm{o}},\beta) + E^{\mathrm{IL}}_{\mathrm{TX,D}}(\varepsilon,t_{\mathrm{o}},\beta) + E^{\mathrm{IL}}_{\mathrm{RX,D}}(\varepsilon,t_{\mathrm{o}},\beta), \tag{40}$$

$$E^{\mathrm{AL}}_{\mathrm{TOT,DCR}}(\varepsilon,\lambda_{\mathrm{dc}},t_{\mathrm{o}},\beta) = E^{\mathrm{AL}}_{\mathrm{MCU}}(\varepsilon,t_{\mathrm{o}}) + E^{\mathrm{AL}}_{\mathrm{RX,DC}}(\lambda_{\mathrm{dc}},t_{\mathrm{o}}) + E_{\mathrm{clk}}(t_{\mathrm{o}}) + E^{\mathrm{AL}}_{\mathrm{RX,DE}}(\varepsilon,t_{\mathrm{o}},\beta) + E^{\mathrm{AL}}_{\mathrm{TX,BC}}(\varepsilon,t_{\mathrm{o}},\beta) + E^{\mathrm{AL}}_{\mathrm{TX,D}}(\varepsilon,t_{\mathrm{o}},\beta) + E^{\mathrm{AL}}_{\mathrm{RX,D}}(\varepsilon,t_{\mathrm{o}},\beta),$$

where λ_{dc} is the duty-cycle percentage, $E^{x}_{\mathrm{RX,DC}}$ is the energy consumption of channel listening according to the duty cycle, $E^{x}_{\mathrm{TX,DE}}$ and $E^{x}_{\mathrm{RX,DE}}$ is the energy consumption of DE message transmission and reception, respectively, when x is EL, IL or AL. Depending on the assumed DCR MAC protocol, the DE message can be replaced, e.g., by using a preamble before the data packet.

The duration of each mode (sensing, MCU active, transmit and receive different type of packets) must be known in order to calculate the consumed energy. The duration of the sensing mode of the EL nodes depends only on the analysed operation duration t_{o} because they are assumed to be sensing the environment continuously. The duration of sensing for the IL nodes depends on the number of events as follows: $t^{\mathrm{tot}}_{\mathrm{s}}(\varepsilon) = \varepsilon t^{\mathrm{event}}_{\mathrm{s}}$, where $t^{\mathrm{event}}_{\mathrm{s}}$ is the duration of sensing per event. Similarly, the duration of MCU awake time depends on the number of events at each layer: $t^{\mathrm{tot}}_{\mathrm{MCU}}(\varepsilon) = \varepsilon t^{\mathrm{event}}_{\mathrm{MCU}}$, where $t^{\mathrm{event}}_{\mathrm{MCU}}$ is the MCU active time per event. The total transmission and reception times of the data packets are a function of number of events as

$$t^{\mathrm{tot}}_{\mathrm{tx,D}}(\varepsilon) = t^{\mathrm{tot}}_{\mathrm{rx,D}}(\varepsilon) = \varepsilon t_{\mathrm{D}} = \frac{\varepsilon L_{\mathrm{D}}}{R}, \tag{41}$$

where R is the data rate of the data radio and t_{D} and L_{D} are the duration and length of the data packet, respectively. The duration of wake-up signal transmission and reception can be calculated as

$$t^{\mathrm{tot}}_{\mathrm{tx,W}}(\varepsilon) = t^{\mathrm{tot}}_{\mathrm{rx,W}}(\varepsilon) = \varepsilon t_{\mathrm{W}} = \frac{\varepsilon L_{\mathrm{W}}}{R_{\mathrm{W}}}, \tag{42}$$

where R_{W} is the data rate of the WUR and t_{W} and L_{W} are the duration and length of the wake-up signal, respectively. In the similar manner, the duration for DE and BC

messages can be derived. In this work, the BC messages are assumed to be delivered error free.

The data, DE and WUS transmission times must be multiplied by the number of retransmissions required for successful detection. The packet error probability (PEP) can be calculated from the BEP as

$$P_{\text{packet}} = 1 - (1-\beta)^{L_P}, \tag{43}$$

where L_P is the length of the particular packet type. The average number of transmissions required for success (n_{TX}) can be calculated from the PEP as

$$n_{\text{TX}} = \frac{1}{1-P_{\text{packet}}}, \tag{44}$$

which must be derived separately for each packet type.

In the WUR case, the receiver is always ready to receive the WUS. Therefore, there is a constant receiver energy consumption component, E_{C}, for the entire duration of the network operation. In the DCR case, the receiver goes on and off according to the duty cycle to listen to the channel for possible oncoming transmissions. Therefore, the DCR receiver channel listening duration is a function of the duty cycle as $t_{\text{rx}}^{\text{CL}}(\lambda_{\text{dc}}) = \lambda_{\text{dc}} t_{\text{o}}$.

Finally, when all the energy consumption components have been defined, the total energy consumption in the network (during t_{o}) can be calculated as

$$\begin{aligned} &E_{\text{TOT}}^{\text{NET}}(\varepsilon, \lambda_{\text{dc}}, t_{\text{o}}, \beta) = \\ &N_{\text{EL}} E_{\text{TOT},RT}^{\text{EL}}(\varepsilon, \lambda_{\text{dc}}, t_{\text{o}}, \beta) + N_{\text{IL}} E_{\text{TOT},RT}^{\text{IL}}(\varepsilon, \lambda_{\text{dc}}, t_{\text{o}}, \beta) + N_{\text{AL}} E_{\text{TOT},RT}^{\text{AL}}(\varepsilon, \lambda_{\text{dc}}, t_{\text{o}}, \beta), \end{aligned} \tag{45}$$

where RT is the radio type (WUR or DCR), N_{EL}, N_{IL} and N_{AL} are number of devices in EL, IL and AL, respectively. In the WUR network $\lambda_{\text{dc}} = 1$ (100%), because it is continuously listening to the channel. In a DCR-based network $0 < \lambda_{\text{dc}} < 1$.

The energy consumption per event can be calculated as

$$E_{\varepsilon}(\varepsilon, \lambda_{\text{dc}}, t_{\text{o}}, \beta) = \frac{E_{\text{TOT}}^{\text{NET}}(\varepsilon, \lambda_{\text{dc}}, t_{\text{o}}, \beta)}{\varepsilon}. \tag{46}$$

Figure 29 shows the energy consumption per event for the example case, when the bit error probability $\beta = 2 * 10^{-3}$. It can be observed that the WUR approach consumes significantly less energy than the DCR approach with a low number of events. For example, when the number of events is less than 1,000 per year, the WUR approach outperforms DCR with $\lambda_{\text{dc}} = 1\%$ more than one order of magnitude. Only a DCR

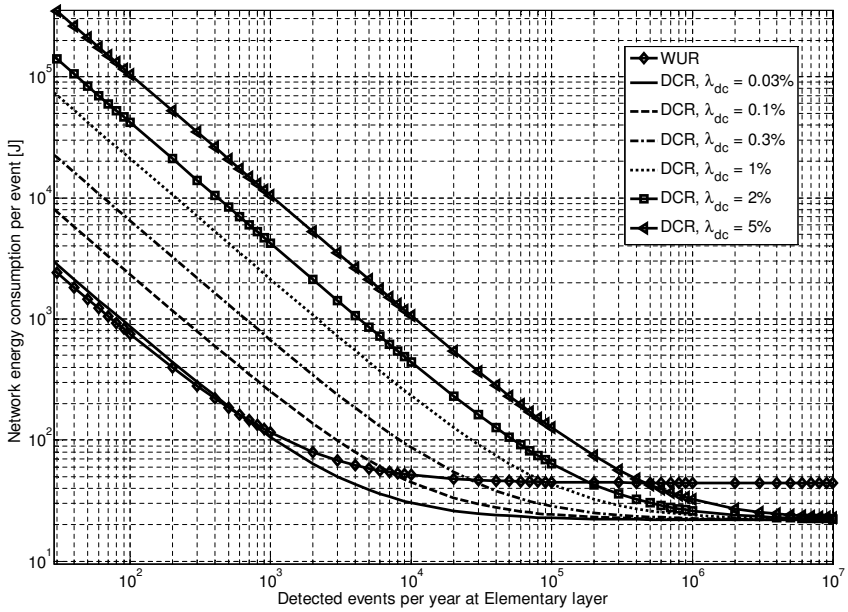

Fig. 29. Network energy consumption per event comparison for WUR- and DCR-based networks, $\beta = 2 * 10^{-3}$ ([38] ©Springer Science+Business Media 2014).

with an extremely-low duty cycle $\lambda_{\mathrm{dc}} = 0.03\%$ will get close to the WUR performance when the number of events is low and outperforms the WUR when the number of events per year increases to 600. However, it must be noted that such an extremely-low duty cycle values are not practical because that would require that the transmission and listening periods of the duty-cycle radios are perfectly synchronized or very long preambles should be used. A DCR with $\lambda_{\mathrm{dc}} = 1\%$ has lower energy consumption than the WUR approach when the number of events per year increases to 90,000 (ten per hour). It can be then concluded that if the events occur more rarely than ten per hour, the GWR-MAC-based approach would provide lower energy consumption in comparison with a DCR based approach with duty cycle values greater than 1%, which can be considered as a typical duty-cycle value for low-power networks [207]. However, also extremely-low duty-cycle ($< 0.1\%$) MAC protocols have been proposed [100, 208]. Therefore, the results are also shown here for an extremely-low duty-cycle values.

The energy efficiency metric is defined here as

$$\eta(\varepsilon, \lambda_{\mathrm{dc}}, t_{\mathrm{o}}, \beta) = \frac{\min(E_{\varepsilon}(\varepsilon, \hat{\lambda}_{\mathrm{dc}}, t_{\mathrm{o}}, \beta))}{E_{\varepsilon}(\varepsilon, \lambda_{\mathrm{dc}}, t_{\mathrm{o}}, \beta)}, \tag{47}$$

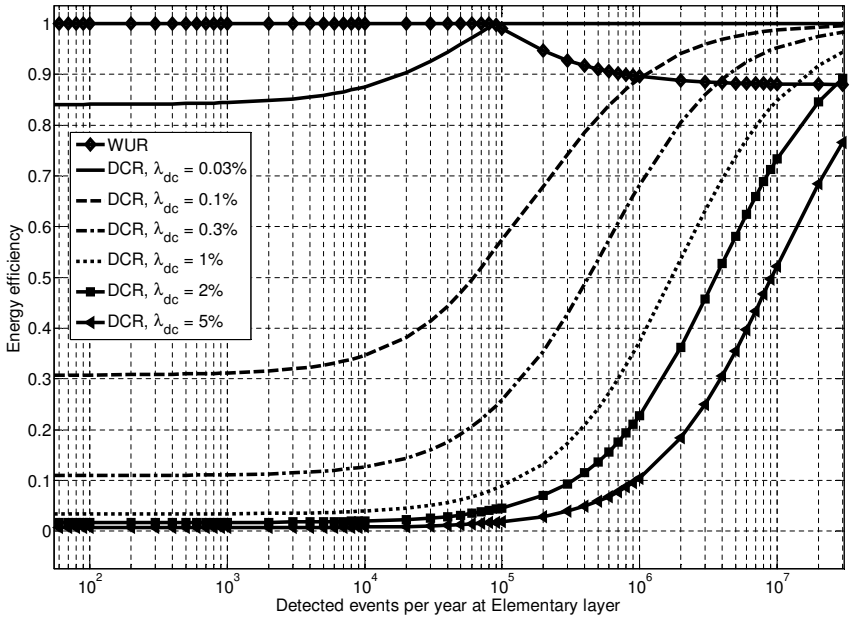

Fig. 30. Network energy efficiency comparison for WUR- and DCR-based networks, $\beta = 10^{-4}$ ([38] ©Springer Science+Business Media 2014).

where the minimum of the energy consumption per event is calculated over the duty cycle value set $\hat{\lambda}_{\mathrm{dc}} = (0, 1]$. That minimum energy consumption per event value is divided by the energy consumption per event for particular ε, λ_{dc}, t_{o} and β combination. Therefore, the metric defined in (47) will lead the maximum energy efficiency to be one and enable clear comparison for the WUR and DCR approaches as a function of number of events, duty-cycle percentage and channel BEP.

Figure 30 shows the energy efficiency comparison of WUR- and DCR-based networks with fixed channel $\beta = 10^{-4}$ as a function of number of events per year at elementary layer. Energy efficiency is calculated by using (47). It can be observed that the WUR-based network architecture will be the most energy efficient until the number of events increases to around ten events per hour ($\approx 90,000$ events per year). After that point, the DCR network with $\lambda_{\mathrm{dc}} = 0.03\%$ would be the most energy efficient. For the case of the highest number of events (one per second), the DCR with $\lambda_{\mathrm{dc}} < 2\%$ would provide higher energy efficiency than the WUR approach.

By comparing results of Figure 29 and Figure 30, it can be observed that when the channel conditions are better, the number of events can be approximately 150 times higher until the DCR with the lowest duty-cycle value starts to be more energy

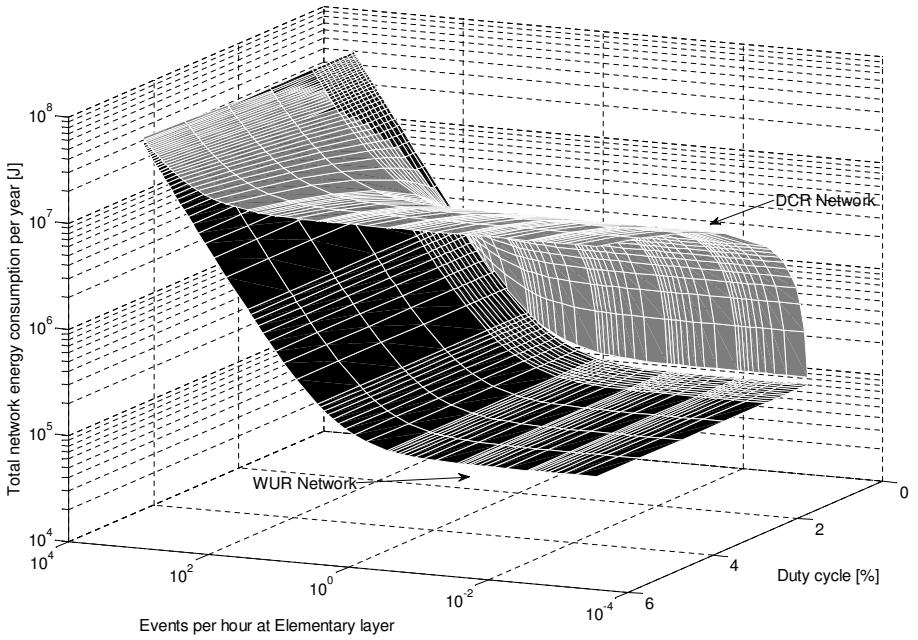

Fig. 31. Network total energy consumption as a function of event frequency and duty-cycle percentage ([38] ©Springer Science+Business Media 2014).

efficient than the WUR approach. The reason is that in the worse channel conditions, the energy used for retransmissions starts to affect more the total energy consumption, also reducing the idle listening in the DCR-based approach. It can be seen that in both channel cases, the energy efficiency of the WUR approach is drastically better than of the DCR approach with $\lambda_{\mathrm{dc}} > 1\%$, for low number of events ($\varepsilon < 10$ per hour).

Figure 31 shows the total energy consumptions for WUR- and DCR-based networks as a function of number of events per hour and duty-cycle percentage values in the error-free case. Note that the purpose of the 3D figures is to show the trend of energy consumption comparison results between the WUR and DCR approach, while the 2D figures show more easily readable results of the selected cases. It can be seen that in the WUR-based network, energy consumption is drastically lower with the whole range of studied duty-cycle values when the event frequency is low. For the lowest number of events case, the energy consumption gain of the WUR approach is more than two orders of magnitude in comparison with a DCR with $\lambda_{\mathrm{dc}} = 5\%$. For the highest number of events per hour, DCR has energy consumption gain of 12% with the smallest duty-cycle percentage value.

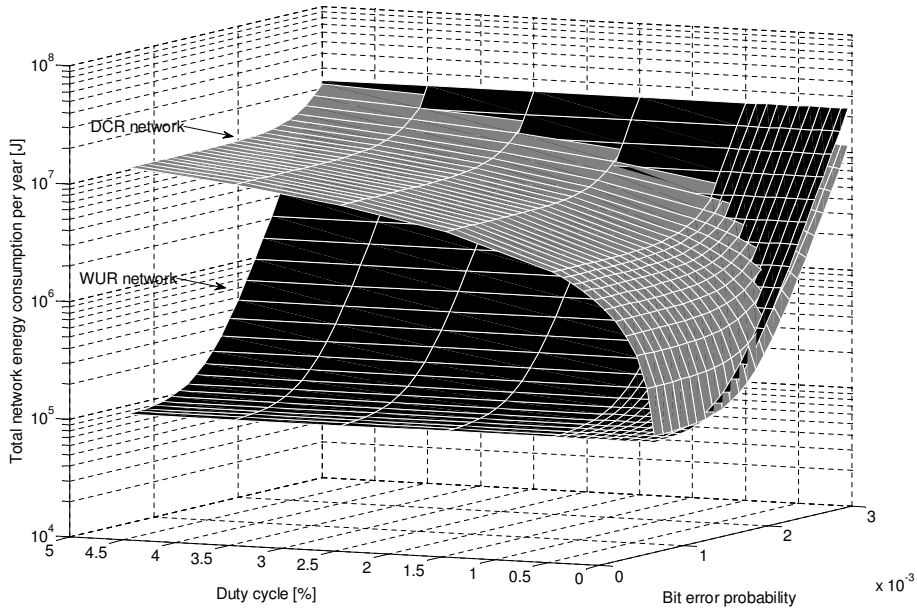

Fig. 32. Network total energy consumption, one event per hour, 100 EL nodes ([38] ©Springer Science+Business Media 2014).

Figure 32 shows the network total energy consumption comparison as a function of BEP and duty-cycle percentage, when the number of events is fixed to one per hour. This figure illustrates that in the DCR approach, energy consumption increases rapidly as the duty-cycle percentage increases from 0.01% to 1%. Moreover, it can be observed that the channel BEP affects relatively more the energy consumption in the WUR approach because higher BEP requires more data packets to be sent and therefore the idle listening of DCR decreases. In addition, data transmissions are more energy consuming and they start to dominate over the wake-up mechanism's energy consumption when the bit error probability increases.

Figure 33 shows the network total energy consumption comparison as a function of BEP and duty-cycle percentage when the number of events is fixed to one per hour and the number of nodes at the elementary layer is increased to 300. It can be observed that when the number of nodes in the network is larger than in the case of Figure 32, the superiority of the WUR over the DCR approach increases; i.e., the importance of the correct wake-up approach increases because more energy is wasted if the DCR approach with too high duty-cycle percentage, with respect to event frequency, is used.

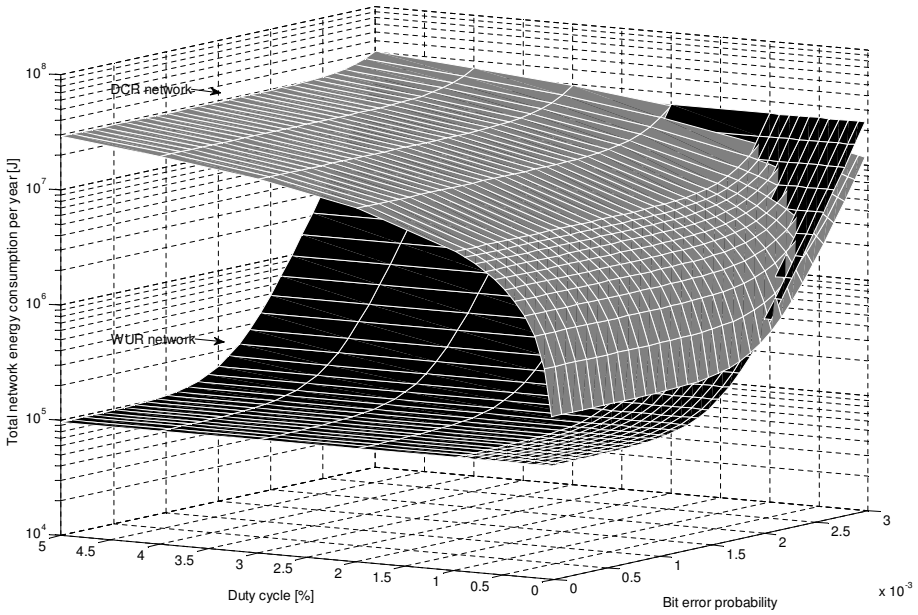

Fig. 33. Network total energy consumption, one event per hour, 300 EL nodes.

The proposed model can be then used to explore the correct radio approach for networks with varying number of different types of devices.

Figure 34 shows the energy efficiency comparison as a function of number of nodes at the elementary layer when the number of events is fixed to one per hour. It can be observed that when the number of nodes at EL is low (less than 75), the DCR approach with $\lambda_{\mathrm{dc}} = 0.03\%$ can outperform the WUR. In comparison with the DCR with $\lambda_{\mathrm{dc}} = 0.03\%$, the WUR is clearly more energy efficient (approximately five times) also with a lower number of devices (ten EL nodes). This result shows clearly that when the number of nodes increases, the importance of an energy-efficient wake-up procedure increases. The energy efficiency of the WUR approach, in comparison with the DCR approach with the lowest duty-cycle percentage, is approximately twice better when the number of EL nodes is larger than 200.

It is also important to discuss about the performance of the WUR- and DCR-based network approaches. In the WUR network case, the delay of communication due to the wake-up procedure is very short and can meet the delay requirements of surveillance as well as most of the other WSN scenarios. The wake-up receiver is continuously listening to the channel and will detect the wake-up message immediately. Therefore, the wake-up will occur in few milliseconds. In the DCR network, the delay depends on the duty

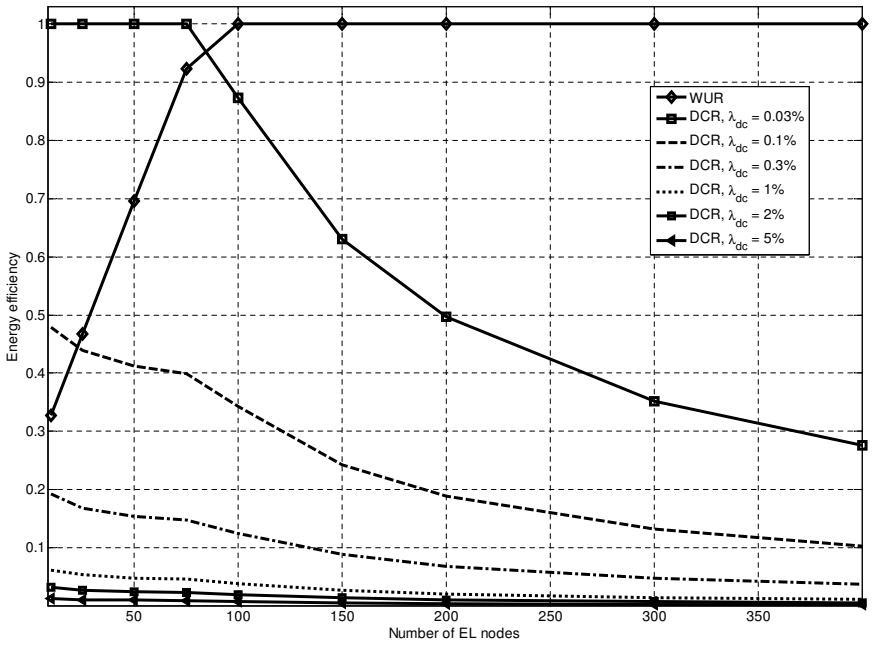

Fig. 34. Energy efficiency comparison as a function of number of nodes at EL, one event per hour, $\beta = 10^{-4}$.

cycle. Using the duty cycle $\lambda_{\text{dc}} = 0.03\%$, the radio can be listening to the channel only for 0.3 ms during one second. During that time it should receive the DE message in order to know that the transmitter has a data packet about the event to transmit. If the event occurs right after the DCR listening period, then the notification regarding the event can be received in the next DCR listening period. Therefore, the delay will be, at minimum, one second. In theory, the duty cycle $\lambda_{\text{dc}} = 0.03\%$ can be used for the studied highest number of events (one per second) but in practice higher duty-cycle values should be used to loosen the synchronization requirement. In addition, when taking into account the sleep-to-listen and listen-to-sleep transition delay and energy consumption, it would be very inefficient to wake up every second to listen to the channel for a 0.3 ms period duration. In practice, in such a low duty-cycle scheduling case, the sleep periods should be longer and the wake-up should occur less frequently (using longer listening duration each time) when taking into account the transceiver transition energy consumption between different modes. That will lead to an increase of the delay of the hierarchical architecture layers' wake-up mechanism in the DCR approach case.

Notice that in the introduced analysis, the transceiver transition delays and energy consumption between different modes are not taken into account. However, they are not assumed to affect the conclusions provided in this work. Instead, when adding transition energy consumption to the analysis, the energy saving gain of the WUR approach will increase when compared with the DCR approach. Because each time the redundant idle listening is performed by the DCR, there will be an additional energy consumption factor due to the fact that the transceiver transition energy consumption occurred during sleep-to-listen and listen-to-sleep mode change. Since in this work the goal is to illustrate the energy saving potential of the WUR, it is justified to state that transition energy consumption will not change the conclusions. In future research, more parameters can be added to the energy consumption model and then more detailed results can be acquired.

4.3 Summary

Energy efficiency of an hierarchical architecture with a wake-up mechanism for wireless sensor networks was discussed in this chapter. The studied architecture is designed to enable the deployment of multiple different technologies in the same network. Therefore, it can be used for different types of WSN and WBAN applications. Energy efficiency is achieved by utilizing a wake-up concept, which can be used to activate the network layers only when required. An analytical model was developed to compare the wake-up radio- and duty-cycle radio-based approaches' energy efficiency in a hierarchical WSN as a function of event frequency. The studied WUR approach is based on the GWR-MAC protocol introduced in Section 3.1.

The results show that a WUR-based hierarchical network can provide remarkably higher energy efficiency than a DCR-based network when the event frequency is low. It was concluded that the WUR approach provides higher energy efficiency in comparison with the DCR approach with duty cycle, $\lambda_{\mathrm{dc}} > 1\%$, when the number of events is less than ten per hour. The reason is that, from the energy consumption point of view, it is very expensive to listen to a channel unnecessarily. The DCR is more energy efficient only when sufficiently low duty cycle is combined with a high number of events. However, in many practical solutions, the duty cycle is fixed and must be large enough to handle the worst-case traffic. Duty cycle should be changed dynamically when the event frequency changes in order to save energy. Furthermore, the very low duty-cycle operation would require very strict synchronization in order to enable that

transmissions would be done exactly at correct times according to the duty cycle. Strict synchronization maintenance requires message exchange between the network nodes, which will cause additional energy consumption.

The proposed analytical model can be utilized, e.g., at the network planning phase to select the most energy-efficient wake-up approach. An adaptation algorithm can also be developed, e.g., based on a look-up table, to check which radio configuration will lead to the highest energy efficiency when the event frequency and channel conditions are known. Therefore, this model provides a tool to explore the physical layer and MAC layer design effects on the network energy consumption. In this work, the physical layer design selection is between the WUR and duty cycle-based radio. The PHY layer selection affects the MAC layer design because the WUR enables that duty cycling does not need to be used if the wake-up signalling leads to higher energy efficiency. In addition, the cross-layer analytical approach is applied here also to the network architecture design since the wake-up mechanism selection affects the interaction between the devices at different hierarchical levels, and consequently the network total energy consumption, as was seen from the results.

5 Code rate and payload length selection for WBANs

In this chapter, an analytical energy efficiency model developed for the IEEE Std 802.15.6-based communication [16] will be proposed. This model has been originally introduced by the author of this thesis and his co-authors in [37] and [41].

In the WBAN applications, the human body creates a very challenging wireless communication environment [209]. Therefore, the communication protocols must be designed carefully to support reliability and energy efficiency. Reliability is important because many WBAN applications require low-latency and secure communication for life-critical data. Energy efficiency of the wireless communication is very important in wireless sensor networks [210–212] and the same applies to WBANs [213], which use a similar type low-power nodes with radio transceivers. Communication reliability and energy efficiency have also interdependencies because retransmissions should be avoided to maintain low energy consumption.

Due to the very wide application space, the IEEE Std 802.15.6 defines three physical layer options (narrowband, IR-UWB and human body communications) and a common MAC protocol with three different modes, whose characteristics are suitable for varying scenarios. As was introduced in the previous sections, the IR-UWB communication using a non-coherent ED receiver has been found to be a good candidate for a very low-power WBAN and WSN nodes. The on-off keying-based signalling, which enables non-coherent detection, has been chosen as the mandatory option for the IR-UWB PHY of the IEEE Std 802.15.6 and it will be explored here. For the very low-power WBAN nodes, the MAC protocols must be designed to include as minimal overhead and complexity as possible. On the other hand, the MAC protocol should enable that the number of retransmissions and the channel access delay can be minimized [214]. Therefore, there is a tradeoff between the protocol complexity and performance. UWB communication creates special challenges for the MAC design because signals are noise-like and traditional carrier-sensing methods cannot be applied. In the IEEE Std 802.15.6 [16], the MAC protocol design challenges have been solved by defining different access phases (contention-free and contention-based) for a superframe and different methods for channel completion. In the IR-UWB case, the S-Aloha protocol is used for contention-based channel access [16], which is therefore under the study here.

There are only few related works addressing networks based on the IEEE Std 802.15.6. In [215], a model for throughput, delay and bandwidth efficiency analysis has been introduced. The authors show results as a function of payload length for an error-free channel case and narrowband communication, but the IR-UWB PHY is not considered in that work. An energy analysis for scheduled access modes of the IEEE Std 802.15.6 has been introduced in [216]. However, also in that work, the UWB PHY is not considered, and an ideal channel condition has been assumed. An IEEE Std 802.15.6-based WBAN using the narrowband PHY has been analysed in [217] and [218] by assuming saturation and non-saturation conditions, respectively. In [219], simulation results for bit-interleaved UWB on-off waveform coded modulation are shown, and a simple receiver architecture is proposed.

According to the author's best knowledge, the proposed model, which is originally introduced in [37] and [41], is the first one developed for the analysis of the energy efficiency of IEEE Std 802.15.6-based IR-UWB communication using ED receiver with different BCH code rates and payload lengths. The forward error correction choice for the mandatory mode of the standard [16] is a binary BCH code with parameters $n = 63, k = 51$ and $t = 2$, leading to a code rate $r = 0.81$. Here, also other code rates are studied to find potential energy efficiency gains jointly with payload length selection. An analytical cross-layer model has been used order to take account of relevant characteristics of the PHY and MAC layers using the aforementioned techniques. The analysis has been done using a path loss model defined by the IEEE P802.15 working group in the additive white Gaussian noise case [220]. The proposed model can be used for packet length and code rate selection as a function of communication distance in order to save energy in the WBAN devices. An example adaptation algorithm, which can utilize the analytical model results, has also been proposed in this work.

The remainder of the chapter is organized as follows. Section 5.1 gives a brief overview of the IEEE Std 802.15.6 and Section 5.2 provides a description of the developed model and acquired results. Section 5.3 introduces the adaptation algorithm. A summary of this chapter is provided in Section 5.4.

5.1 IEEE Std 802.15.6 overview

The IEEE Std 802.15.6 was published in February 2012 and it is intended for low-power devices to be used in wireless body area networks [16]. The standard defines that WBAN includes sensor nodes and one and only one hub (sink). Usually one-hop communication

is used in WBANs, but the standard [16] defines also an option for a two-hop star topology, in which the nodes can also act as a relay.

The three PHY layer options defined for WBANs in [16] are narrowband, ultra-wideband and human body communications (HBC). In this work, the IR-UWB with OOK modulation and ED receiver will be studied because it enables low-cost and low-power implementations [213] with suitable features for secure communication and low interference to other wireless systems. The narrowband- and HBC-based physical layers will not be studied here.

Three different channel access modes for the common MAC for WBANs have been defined in [16]: a beacon mode with superframes, non-beacon mode with superframes and non-beacon mode without superframes. Here the focus is on the beacon mode with superframes, whose structure is illustrated in Figure 35. The hub must establish a time base dividing the time axis into beacon periods, and it can set the lengths for different phases depending on the predominant communication requirements in the network. The second beacon (B2) needs to be send by the hub during a superframe, if the contention access period length is non-zero. The standard [16] defines two different methods for random access: carrier sensing multiple access with collision avoidance (CSMA/CA) and slotted Aloha. The former is intended for a narrowband PHY and the latter one for the IR-UWB and HBC PHY. The superframe includes three contention-based phases shown in Figure 35 [16]: exclusive access phase (EAP1 & EAP2), random access phase (RAP1 & RAP2) and contention access period. EAP1 and EAP2 are dedicated only to the highest user priority (UP) (emergency information) frames. In the managed access phase (MAP), the hub can arrange different types of allocation intervals for uplink, downlink and bi-link [16].

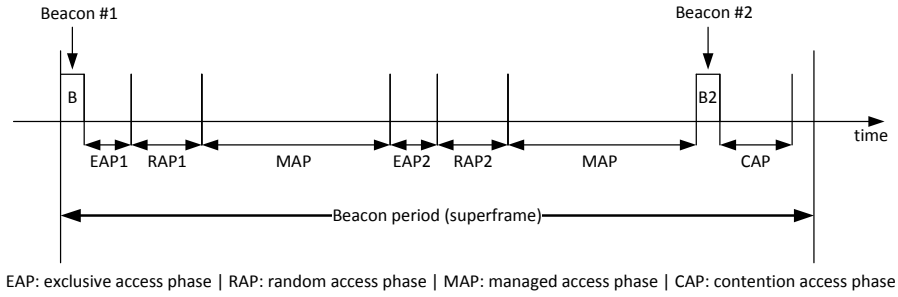

Fig. 35. A beacon period (superframe) with access phases ([37] ©Springer Science+Business Media 2014).

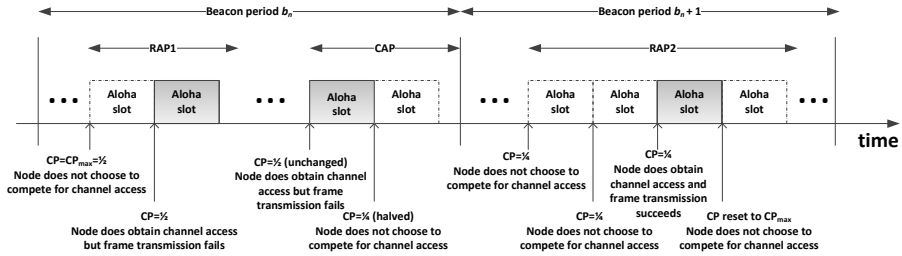

Fig. 36. Slotted Aloha access method example for the IEEE Std 802.15.6-based communication ([37] ©Springer Science+Business Media 2014).

In the slotted Aloha case, the random access period is divided into slots in which the nodes must transmit their frames if they decide to transmit. Node transmission probability in a given slot depends on the channel contention probability (CP). The hub must transmit a beacon message at the beginning of the superframe period so that the nodes know when they should compete for channel access. The slotted Aloha access method example for the IEEE Std 802.15.6 is presented in Figure 36. The standard defines different slotted Aloha channel access contention probabilities $CP_{\min} \leq CP \leq CP_{\max}$ for different access phases, and they depend on the user priority [16]. During the channel competition, the nodes will adapt their *CP* according to the definitions of [16], depending on whether the transmission was successful or not. As illustrated in Figure 36, the node's *CP* is at first 1/2. Due to unsuccessful transmissions, the node will decrease the *CP* to 1/4. Finally, the node has successfully transmitted the frame and it will increase the CP to maximum value $CP_{\max}$ which will be used in the next contention access period.

5.2 Performance improvement analysis

In this section, it will be explained the developed analytical model for a one-hop star topology WBAN composed of *N* sensor nodes and one hub. The model focuses on the energy efficiency of the communication link between a sensor node and a hub, taking PHY and MAC characteristics into account. However, the model is also applicable to the link between a sensor node and a relay node in the two-hop star topology.

First, the IR-UWB PHY signal and path loss model will be presented. The PHY layer success probability derivation for uncoded and coded transmissions follows after

that. Then, the MAC layer success probability will be discussed. Finally, the energy efficiency model will be defined and acquired results analysed.

The parameter values assumed for the studied network (if not otherwise declared) are shown in Table 7. The parameters follow the definitions of the WBAN standard and corresponding network characteristics [16].

Table 7. Parameters assumed for the IR-UWB-based WBAN ([37] ©Springer Science+Business Media 2014).

Parameter	Description	Value
W	bandwidth	499.2 MHz
f_c	central frequency	3993.6 MHz
N_{cpb}	number of chips per burst	16
T_p	pulse duration	2 ns
T	integration time per pulse	2 ns
R	uncoded data rate	0.975 Mbps
I	implementation losses	5 dB
NF	receiver noise figure	10 dB
P_{sd}	power spectral density	-41 dBm/MHz
$P_{tx,RF}$	transmitter RF power consumption	37 µW
$P_{tx,circ}$	transmitter circuitry power consumption	2 mW
P_{rx}	receiver power consumption	20 mW
N_0	thermal noise density	-174 dBm/Hz
N_{MH}	MAC header length	7 octets
N_{FCS}	frame check sequence length	2 octets
T_{SHR}	synch. header duration	40.32 µs
T_{PHR}	PHY header durations	82.052 µs
$pSIFS$	short interframe spacing	75 µs
N	number of nodes in WBAN	10
λ	payload length	10 - 255 octets

5.2.1 IR-UWB PHY

The IR-UWB physical layer symbol structure of [16], which is introduced in Figure 37, is based on pulse waveforms of duration $T_w = N_{cpb} T_p$, which can be formed using a

single pulse or burst of pulses as

$$w(t) = \sum_{i=0}^{N_{\text{cpb}}-1} p(t - iT_{\text{p}}), \tag{48}$$

where $N_{\text{cpb}} \geq 1$ is the number of pulses (chips) per burst and T_{p} is the pulse duration. According to the IEEE Std 802.15.6 definition, the OOK signalling must be used with a Q-ary waveform coding, which maps K information bits onto coded-pulse sequences of length $2K$ using an alphabet of size $Q = 2^K$ [16]. In the mandatory mode of standard, $K = 1$ $(Q = 2)$, and in the optional mode $K = 4$ $(Q = 16)$. Due to half-rate mapping of waveform coding, the symbol time coincides with the burst (pulse) position modulation symbol time for all Q values. Therefore, also in the WBAN standard, the IR-UWB symbol time is divided into two intervals of duration $T_{\text{sym}}/2$, as in the case of BPM introduced in Chapter 3. The UWB symbol structure is shown in Figure 37. The symbol structure also includes the time hopping positions ($N_{\text{w}}/2 - 1$ in the OOK case) in order to support multi-BANs for coexistence. The duty-cycle factor is defined to be the ratio $\zeta = T_{\text{w}}/T_{\text{sym}}$, which shall be 3.125% for every data rate and modulation combination introduced in the standard. That is, in this case the duty-cycle factor during a symbol time is given by the ratio when a pulse waveform is present over the symbol time. A relatively small duty-cycle factor enables low-power consumption and constant pulse power for a given effective isotropically radiated power (EIRP) [16].

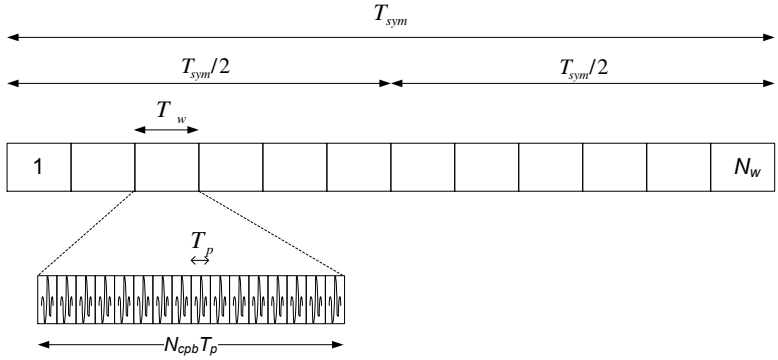

Fig. 37. IR-UWB symbol structure according to the IEEE Std 802.15.6 ([37] ©Springer Science+Business Media 2014).

The IR-UWB signal, for the b:th symbol, when using OOK modulation and 2-ary waveform coding can be then expressed as [16]

$$x^b(t) = \sum_{c=0}^{2K-1} d_c^b w_{2Kb+c}(t - c(T_{\text{sym}}/2) - bKT_{\text{sym}} - h^{(2Kb+c)}T_{\text{w}}), \tag{49}$$

where $b \geq 0$, d_c^b is the c:th code word component over the b:th symbol, $h^{(2Kb+c)}$ is the time hopping sequence and w_{2Kb+c} is from (48). The uncoded data rate for OOK modulation can be calculated as $R = 1/T_{\text{sym}}$. In the standard [16], it has been defined that either static or dynamic scrambling should be used for spectral shaping to reduce spectral lines caused by the consecutive same polarity pulses when using the burst of pulses for IR-UWB signalling. However, because the scrambling and time hopping does not affect the bit error probability derivation of the interference-free AWGN channel used hereafter, they will be ignored for simplicity. In the binary modulation with 2-ary waveform coding ($K = 1$) case, the transmitted signal for the b:th bit is defined as

$$s^b(t) = \sum_{c=0}^{2K-1} d_c^b \sum_{i=0}^{N_{\text{cpb}}-1} \sqrt{\frac{E_{\text{b}}}{N_{\text{cpb}}T_{\text{p}}}} p(t - c(T_{\text{sym}}/2) - bKT_{\text{sym}} - iT_{\text{p}}), \tag{50}$$

where E_{b} is the energy per bit and $b \geq 0$. The code words for 2-ary waveform coding defined in [16] are illustrated in Table 8. If the b:th transmitted bit is '1', then the symbol mapper code word is $d = [d_0\ d_1] = [0\ 1]$ and the pulse waveform will be located on the second half of the symbol period. If the b:th transmitted bit is '0', then the symbol mapper code word is $d = [d_0\ d_1] = [1\ 0]$ and the pulse waveform will be located on the first half of the symbol period.

Table 8. Symbol mapper for 2-ary waveform coding.

Binary data symbol	Code word
0	10
1	01

Path loss model

In order to find out the received signal power as a function of distance, the path loss needs to be derived. The path loss in dB for IR-UWB communication on-body to

on-body scenario (at 3.1 to 10.6 GHz band), can be calculated as [220]

$$L(d)_{\mathrm{dB}} = c_a log_{10}(d) + c_b + \boldsymbol{X}, \tag{51}$$

where c_a and c_b are parameters for linear fitting, d is the distance in millimetres and $\boldsymbol{X}$ is a Gaussian distributed random variable, i.e., $\boldsymbol{X} \sim \mathbf{N}(\mu_x, \sigma^2)$ with mean μ_x and standard deviation σ.

The path loss parameter values for the hospital room case are: $c_a = 19.2$, $c_b = 3.38$, $\mu_x = 0$ and $\sigma = 4.40$ [220]. Figure 38 shows the path loss as a function of distance calculated by using the model defined in (51).

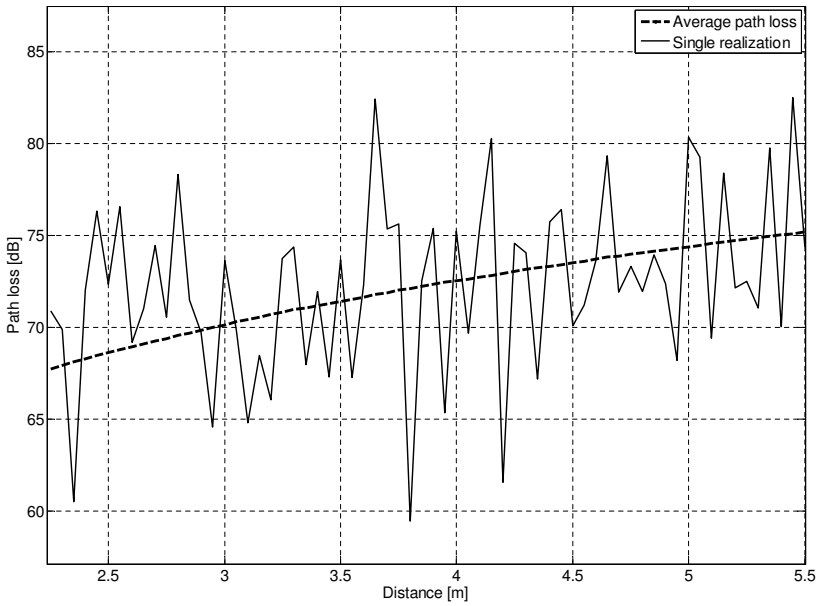

Fig. 38. Path loss as a function of distance for the $3.1-10.6$ **GHz band in the IR-UWB on-body surface to on-body surface scenario ([37] ©Springer Science+Business Media 2014).**

In the IEEE Std 802.15.6 [16], the required sensitivity value derivation model has been defined for receiver in order to achieve the packet error rate (PER) $< 1\%$ for a random physical-layer service data unit (PSDU) of length 24 octets in the AWGN case without interference. The receiver sensitivity values can be used to derive the required energy per bit-to-noise ratio (E_{b}/N_0) by taking into account data rate, receiver noise figure (NF) and implementation losses (I). Figure 39 shows the required E_{b}/N_0, in dB,

versus the communication distance calculated using parameters: uncoded data rate $R = 0.975$ Mbps; NF = 10 dB; and I = 5 dB.

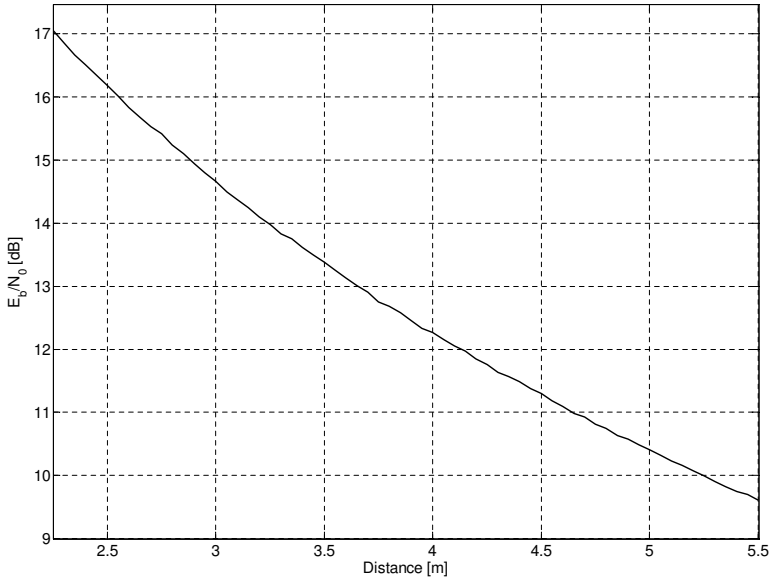

Fig. 39. E_b/N_0 **at the antenna input versus the distance for uncoded data rate** $R = 0.975$ **Mbps ([37] ©Springer Science+Business Media 2014).**

ED receiver

The receiver architecture for non-coherent energy detection was shown in Figure 18 and the principle of the receiver operation was explained therein for the burst position modulation case. In the on-off keying combined with 2-ary waveform coding case, the symbol decision can be done by comparing the amount of integrated energy of symbol intervals in order to determine whether the transmitted bit was one or zero. Therefore, the theoretical bit error probability in the AWGN case can be calculated by using the same approach introduced for the ED receiver with binary burst position modulation. For the BEP derivation purpose, the SNR at the decision variable of the ED receiver can be calculated as [76]

$$SNR_{\mathrm{DV}} = \frac{2\frac{E_{\mathrm{b}}^{I}}{N_0}}{4 + N_{\mathrm{cpb}} 2TW \frac{N_0}{E_{\mathrm{b}}^{\mathrm{I}}}}, \tag{52}$$

where T is the integration time per pulse, W is the signal bandwidth and E_{b}^{I} is the integrated energy per bit. By assuming Gaussian approximation, BEP can be calculated by using (52) and the $Q(\cdot)$ function as [45] [76]

$$P_{\mathrm{b}} = Q\left(\sqrt{SNR_{\mathrm{DV}}}\right). \tag{53}$$

BCH coding

The IEEE Std 802.15.6 defines that the BCH code with parameters $n = 63$, $k = 51$ and $t = 2$ shall be used in the default mode for FEC to mitigate the bit errors occurred in the channel. In this work, BCH coding will be investigated closer by deriving its performance also using other code rates, in order to find possible energy efficiency gains.

As in Chapter 3, a fair comparison is done also here so that in the coded case, the energy per transmitted bit will be less than in the uncoded case, i.e., the energy per bit for the i:th code rate is $E_{\mathrm{b},i} = r_i E_{\mathrm{b}}$ [44, 45]. Therefore, each transmitted packet will contain the same amount of energy regardless of the used code rate. Therefore, the bit error probability before decoding can be calculated as [45]

$$P_{\mathrm{b},i} = Q\left(\sqrt{SNR_{\mathrm{DV}}^{i}}\right), \tag{54}$$

where SNR_{DV}^{i} is the signal-to-noise ratio at the decision variable for i:th code rate with $E_{\mathrm{b},i}$.

At the FEC decoder of the receiver, t bit errors will be corrected by the BCH code and the code word error probability for block codes of the form (n,k,t) can be calculated as [44],[45]

$$P_{\mathrm{cw},i} = \sum_{h=t+1}^{n} \binom{n}{h} P_{\mathrm{b},i}^{h} (1 - P_{\mathrm{b},i})^{n-h}. \tag{55}$$

The bit error probability for i:th BCH code rate with r_i can then be approximated as [45]

$$P_{\mathrm{b},i}^{\mathrm{BCH}} = \frac{1}{n} \sum_{h=t+1}^{n} h \binom{n}{h} P_{\mathrm{b},i}^{h} (1 - P_{\mathrm{b},i})^{n-h}. \tag{56}$$

Figure 40 shows the BEP for different BCH code rates and uncoded case as a function of E_{b}/N_0.

The packet error probability can be calculated from BEP as

$$P_{\mathrm{packet},i} = 1 - (1 - P_{\mathrm{b},i}^{\mathrm{BCH}})^{l_i}, \tag{57}$$

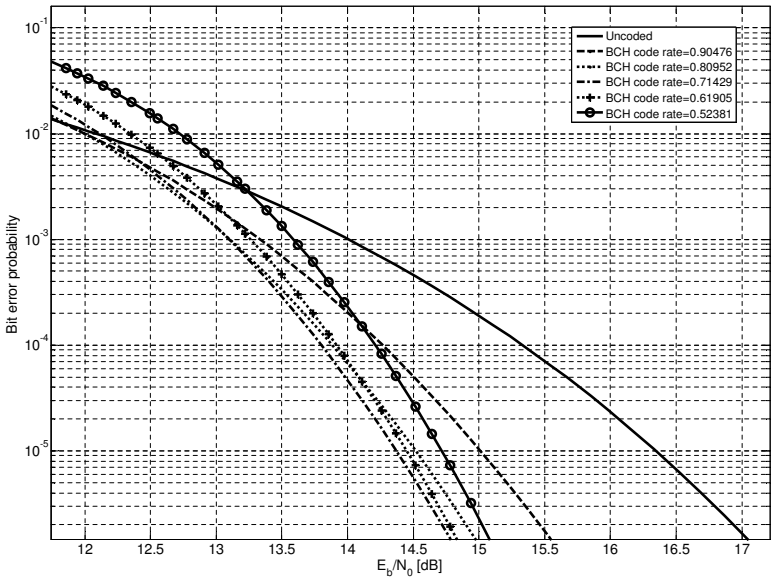

Fig. 40. BEP results for different BCH code rates and uncoded case as a function of E_b/N_0 at the antenna input ([37] ©Springer Science+Business Media 2014).

where l_i is the length of the packet in bits when using the i:th BCH code rate. Therefore, the physical layer success probability for the i:th code rate can be calculated by taking a complement of the packet error probability as

$$P_{\text{succ}}^{\text{PHY}} = 1 - P_{\text{packet},i}. \tag{58}$$

In the coded case, it must be taken into account that packet length will be increased due to the parity bits added by the FEC encoder. For certain payload lengths, there may be also a need for bit filling in order to align with the number of information bits (k) required in the last code word encoding. In the standard [16], it has been defined that the number of code words in a frame is given by

$$N_{\text{CW}}^{i} = \left\lceil \frac{N_{\text{PSDU}}^{'}}{k_i} \right\rceil, \tag{59}$$

where $\lceil \cdot \rceil$ is the ceiling function, $N_{\text{PSDU}}^{'} = 8(N_{\text{MH}} + N_{\text{MFB}} + N_{\text{FCS}})$ is the number of bits in the PSDU, N_{MH} is the number of octets in the MAC header, N_{MFB} is the number of octets in the MAC frame body, N_{FCS} is the number of octets of the frame check sequence (FCS) and k_i is the number of information bits in a code word when using i:th code rate. If the remainder $rem(N_{\text{PSDU}}^{'}, k_i) \neq 0$, the last codeword requires $N_{\text{bs}}^{i} = N_{\text{CW}}^{i} k_i - N_{\text{PSDU}}^{'}$

bits filling before encoding. Therefore, the total number of bits at the encoder input is given by

$$N^i_{\mathrm{PSDU}} = N^{'}_{\mathrm{PSDU}} + N^i_{\mathrm{bs}}. \tag{60}$$

The total number of bits to be transmitted, when using i:th code rate, can be then calculated as

$$N^i_{\mathrm{T}} = N^{'}_{\mathrm{PSDU}} + (n_i - k_i)N^i_{\mathrm{CW}} + N_{\mathrm{pad}}, \tag{61}$$

where N_{pad} is the number of bits needed to align with symbol boundary at modulation. In binary modulation case, there is no need for padding, i.e., $N_{\mathrm{pad}} = 0$.

5.2.2 MAC layer

The MAC layer protocol features will determine the channel access success probability, which affects highly the energy efficiency of wireless communication. Here the studied MAC protocol is S-Aloha, as it is defined to be used with the IR-UWB PHY [16]. In Chapter 3, the MAC layer packet success probability for the slotted Aloha case was defined in (17), which can also be used here to find out the expected number of trials to acquire successful channel access.

The S-Aloha channel access success probability depends on the offered traffic load, G. In order to achieve the maximum success probability, the offered traffic load must be one, which corresponds with a channel competition participation probability $p = 1/N$ for all nodes, when N nodes are competing for channel access. In that case, there is exactly one packet per slot, in average, to be transmitted, and the MAC success probability can be calculated using (19). The standard [16] defines that different channel competition probability values can be used, depending on the user priority value and back-off state, as was introduced in Section 5.1. Here, it is assumed that the offered traffic load is optimal, i.e., the results are given for the S-Aloha best-case scenario. However, the model enables that results for different traffic loads can be calculated as well. Moreover, it has been assumed that in the coded case, the slot length will be increased with respect to coding overhead introduced by the code rate r_i, so that the data frame and ACK can be transmitted during the slot. WBAN standard definitions enable the fulfilment of that assumption because the hub can set the superframe and slot lengths according to the network communication requirements [16].

5.2.3 Energy efficiency

The developed energy consumption model and energy efficiency metric, which enable performance comparison between different code rates and the uncoded case, will be introduced here. The proposed model objective is to explore the energy efficient code rate and payload length selection as a function of communication distance.

The number of required retransmissions for success is the key factor of the communication energy consumption. In the cross-layer analysis used in this work, the number of retransmissions depends on the PHY and MAC layer success probabilities. The average number of transmissions required for a successful packet reception can be calculated for the i:th code rate by using (17) and (58) as

$$N_{\mathrm{tx},i} = \frac{1}{P_{\mathrm{succ}}^{\mathrm{PHY}} P_{\mathrm{succ}}^{\mathrm{MAC}}}. \tag{62}$$

For the calculation of energy consumed during a packet transmission, the duration of frame transmissions must be defined. The transmitted frame duration for the code rate r_i can be calculated as

$$T_{\mathrm{packet}}^{i} = T_{\mathrm{SHR}} + T_{\mathrm{PHR}} + T_{\mathrm{PSDU}}^{i}, \tag{63}$$

where T_{SHR} is the duration of the synchronization header (SHR), T_{PHR} is the duration of the physical layer header (PHR) and T_{PSDU}^{i} is the duration of the PSDU when using the code rate r_i. The length of the synchronization and physical layer header is independent of the code rate. The preamble structure and synchronization method for the IEEE Std 802.15.6. IR-UWB PHY have been analysed in more detail, e.g., in [221]. Forward error correction coding affects the PSDU transmission time, which can be calculated for the i:th code rate as

$$T_{\mathrm{PSDU}}^{i} = \frac{N_{\mathrm{T}}^{i}}{R}, \tag{64}$$

where R is the uncoded bit rate.

The standard [16] defines different options for ACK transmission mechanism. Here, it is assumed that the immediately ACK (I-ACK) mode, in which the ACK will be transmitted right after the successful packet reception, is used. The ACK message is assumed to be always received correctly, i.e., only the erroneous data packets will be retransmitted because ACK will not be transmitted for them. Therefore, after the transmitter has sent the data packet, it will wait for the ACK message for the duration of [16]

$$T_{\mathrm{ACKW}} = pSIFS + T_{\mathrm{SHR}} + T_{\mathrm{PHR}} + T_{\mathrm{ACK}}, \tag{65}$$

where $pSIFS$ is the short interframe spacing time and T_{ACK} is the duration of the ACK packet.

Section 3.4 introduced a general-level energy consumption model, for the transmission period of the star-topology network nodes, which can be used also here. Here, the focus is on the energy consumption of the transmitter−receiver link, therefore the factor $E_{\mathrm{Imp}}^{\mathrm{MAC}}$ of (7) can be neglected. In Section 3.4, $E_{\mathrm{Imp}}^{\mathrm{MAC}}$ is introduced to take account of the idle slot energy consumption when the group of nodes competes for the channel access during the transmission period. Otherwise, the general-level energy consumption factors are the same as in (7), and they are defined here in detail for the WBAN communication link as

$$\begin{aligned} E_{\mathrm{tx}}^{\mathrm{PHY}} &= T_{\mathrm{packet}}^{i}(P_{\mathrm{tx,RF}}^{i} + P_{\mathrm{tx,circ}}) + \varepsilon_{\mathrm{enc}}^{i} \\ E_{\mathrm{tx,f}}^{\mathrm{MAC}} &= T_{\mathrm{ACKW}} P_{\mathrm{rx}} \\ E_{\mathrm{tx,s}}^{\mathrm{MAC}} &= (T_{\mathrm{ACKW}} + T_{\mathrm{ACK}}) P_{\mathrm{rx}} \\ E_{\mathrm{rx}}^{\mathrm{MAC}} &= T_{\mathrm{ACK}}(P_{\mathrm{tx,RF}}^{i} + P_{\mathrm{tx,circ}}) \\ E_{\mathrm{rx}}^{\mathrm{PHY}} &= T_{\mathrm{packet}}^{i} P_{\mathrm{rx}} + \varepsilon_{\mathrm{dec}}^{i}, \end{aligned} \tag{66}$$

where $P_{\mathrm{tx,RF}}^{i}$ is transmitter RF power consumption when using i:th code rate, $P_{\mathrm{tx,circ}}$ is transmitter circuitry power consumption, P_{rx} is receiver power consumption, $\varepsilon_{\mathrm{enc}}^{i}$ and $\varepsilon_{\mathrm{dec}}^{i}$ are the encoding and decoding energies for BCH code rate r_i, respectively. For the uncoded case, $i = 0$, and the code rate $r_0 = 1$. In addition, let's define that $N_{\mathrm{tx}}^{\mathrm{fail}} = N_{\mathrm{tx},i} - 1$ and $N_{\mathrm{tx}}^{\mathrm{succ}} = 1$, since the focus here is on a single link. Therefore, by using (7) and the above definitions, the energy consumption can be calculated for the i:th code rate case as

$$\begin{aligned} E_{\mathrm{link}}^{i} = {} & (N_{\mathrm{tx},i} - 1)\big(T_{\mathrm{packet}}^{i}(P_{\mathrm{tx,RF}}^{i} + P_{\mathrm{tx,circ}}) + \varepsilon_{\mathrm{enc}}^{i} + T_{\mathrm{ACKW}} P_{\mathrm{rx}}\big) + \\ & T_{\mathrm{packet}}^{i}(P_{\mathrm{tx,RF}}^{i} + P_{\mathrm{tx,circ}}) + \varepsilon_{\mathrm{enc}}^{i} + T_{\mathrm{ACK}} P_{\mathrm{rx}} + \\ & N_{\mathrm{tx},i}\big(T_{\mathrm{packet}}^{i} P_{\mathrm{rx}} + \varepsilon_{\mathrm{dec}}^{i}\big) + T_{\mathrm{ACK}}(P_{\mathrm{tx,RF}}^{i} + P_{\mathrm{tx,circ}}). \end{aligned} \tag{67}$$

In this work, the encoding and decoding algorithms of the BCH coding are not discussed in detail. However, the energy consumption of encoding and decoding will be included to the analysis by using the models introduced in previous works [222–224]. The energy consumption of encoding when using i:th BCH code rate can be calculated as [222]

$$\varepsilon_{\mathrm{enc}}^{i} = (2n_i t_i + 2t_i^2)(\varepsilon_{\mathrm{add}} + \varepsilon_{\mathrm{mult}}), \tag{68}$$

where n_i is the code word length, t_i is the error correction capability and the addition ε_{add} and multiplication $\varepsilon_{\text{mult}}$ energy consumptions are for calculating Galois (finite) field (GF($2^{m_{\text{bch}}}$)) elements when $m_{\text{bch}} \geq (n-k)/t$. The generator polynomial of a binary BCH code is specified in terms of its roots from the GF($2^{m_{\text{bch}}}$) [44].

At the BCH decoder, the Berlekamp-Massey (BM) [225],[226] and Chien search [227] algorithm can be used for error-locator and the error-evaluation polynomial generation and location finding [44], [222]. The decoding energy consumption for the i:th code rate can then be calculated as [222]

$$\varepsilon_{\text{dec}}^{i} = (4n_i t_i + 10t_i^2)\varepsilon_{\text{mult}} + (4n_i t_i + 6t_i^2)\varepsilon_{\text{add}} + 3t_i\varepsilon_{\text{inv}}, \tag{69}$$

where ε_{inv} is the energy consumption of inversion operation. From [223] and [224], the following energy consumption values for m_{bch}-bit GF operations can be found

$$\begin{aligned} \varepsilon_{\text{add}} &= 0.4 m_{\text{bch}} \text{ pJ} \\ \varepsilon_{\text{mult}} &= 0.4\left(m_{\text{bch}}^2 + \frac{3(m_{\text{bch}}-1)^2}{2}\right) \text{ pJ} \\ \varepsilon_{\text{inv}} &= 8 m_{\text{bch}} \text{ pJ}. \end{aligned} \tag{70}$$

Energy efficiency metric

An energy efficiency metric (information bits / J) is defined in this work to enable a clear performance comparison of the different code rates when using variable payload lengths as

$$\eta_i = \frac{\lambda}{E_{\text{link}}^{i}}, \tag{71}$$

where λ is the number of information bits and E_{link}^{i} is the energy consumption used for communicating the bits successfully from transmitter to receiver when using the i:th code rate. Energy efficiency definition takes also the transmission reliability into account through E_{link}^{i}, which depends highly on the number of required transmissions for successful detection of a packet. For simple comparison purposes, the energy efficiency can be normalized so that the maximum efficiency value will be one. Here the normalization is done with respect to maximum achievable efficiency as

$$\eta_{norm}^{i}(f) = \frac{\eta_i(f)}{max(\eta(f))} = \frac{\frac{\lambda}{E_{\text{link}}^{i}(f)}}{max\left(\frac{\lambda}{E_{\text{link}}^{0}(f)}, \frac{\lambda}{E_{\text{link}}^{1}(f)}, \ldots, \frac{\lambda}{E_{\text{link}}^{MAXi}(f)}\right)}, \tag{72}$$

where the maximum at denominator is found from η values calculated separately for each code rate $i = 0, 1, \ldots, MAXi$, when uncoded transmission is the case $i = 0$, as a function of parameter of interest f.

It can be deduced that for a given transmission power value, which is high enough to guarantee a successful detection at the receiver, the minimum energy consumption for the link can be achieved with uncoded transmission. The rationale is that uncoded transmission includes a minimum amount of overhead to deliver the λ information bits because in that case there are no redundant parity bits which are required for FEC coded transmission. Therefore, the denominator of (72) can be simplified by eliminating the max -function. Let's then define that the successful detection at the receiver, in the uncoded case, can be achieved in the link whose distance is d_0 when using a given payload length and transmission power. Therefore, the normalized energy efficiency when using the i:th code rate (for uncoded case $i = 0$) and payload length λ for the communication over the link of length d can be derived as

$$\eta^i_{\text{norm}}(d,\lambda) = \frac{\eta_i(d,\lambda)}{\eta_0(d_0,\lambda)} = \frac{\frac{\lambda}{E^i_{\text{link}}(d,\lambda)}}{\frac{\lambda}{E^0_{\text{link}}(d_0,\lambda)}} = \frac{E^0_{\text{link}}(d_0,\lambda)}{E^i_{\text{link}}(d,\lambda)}. \tag{73}$$

Figure 41 shows the normalized energy efficiency results as a function of distance and payload length calculated using (73), i.e., separately for each payload length. The purpose of the 3D figures is to illustrate the trend of the energy efficiency results. As Figure 41 shows, in the longest payload case (255 octets), the uncoded transmission is the most energy efficient when the distance is approximately below 2.65 metres. After that point, the code rate r = 0.9 is the most energy efficient until the point 3.1 metres, after which the code rate r = 0.71 provides the highest energy efficiency. Figure 41 gives results only for these three code rates for clear illustration reasons. As can be observed from the results, the energy efficiency starts to decrease when the communication distance increases, as expected. The reason is simply that a longer distance leads to decrease in received signal power and therefore more retransmissions are required for successful packet reception. As the distance increases, the parity bits of the coded packets starts to be useful and the energy efficiency of coded transmissions starts to be higher than in the uncoded case. Figure 41 also shows the impact of the payload length effect on the energy efficiency ratio between the uncoded case and different code rates. When the payload length is short, the probability for a successful packet reception is higher and therefore the need for coding is lower. As can be seen from the figure, the uncoded case outperforms the coded case also in longer distance cases when the payload

length shortens. For the shortest payload case, 10 octets, the uncoded case is most energy efficient until the distance of 3.1 metres. The results of Figure 41 illustrate that the normalized energy efficiency definition given in (73) is useful for determining the most energy-efficient code rate for certain payload length and communication distance.

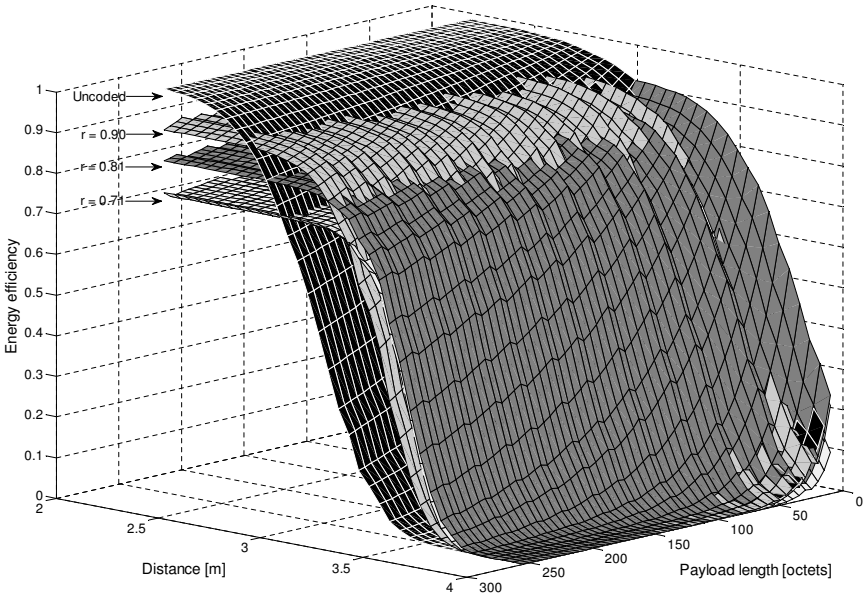

Fig. 41. Normalized energy efficiency calculated separately for each payload length.

In order to enable the efficiency evaluation of particular payload length with respect to overall maximum energy efficiency, the energy efficiency is defined here as

$$\eta^{i}_{\mathrm{ov,norm}}(d,\lambda) = \frac{\eta_i(d,\lambda)}{\eta_0(d_0,\lambda_{\max})} = \frac{\frac{\lambda}{E^{i}_{\mathrm{link}}(d,\lambda)}}{\frac{\lambda_{\max}}{E^{0}_{\mathrm{link}}(d_0,\lambda_{\max})}} = \frac{\lambda}{\lambda_{\max}} \frac{E^{0}_{\mathrm{link}}(d_0,\lambda_{\max})}{E^{i}_{\mathrm{link}}(d,\lambda)}. \qquad (74)$$

Equation (74) enables the evaluation of energy efficiency at distance d with payload length λ in comparison with efficiency that can be achieved with maximum payload λ_{max} over distance d_0 which guarantees the successful detection in the uncoded case. It can be deduced that in the error-free transmission case, the maximum energy efficiency will be achieved when using uncoded transmission and the longest payload length, which consequently minimizes the effect of communication overhead (FEC coding overhead, SHR, PHR and ACK).

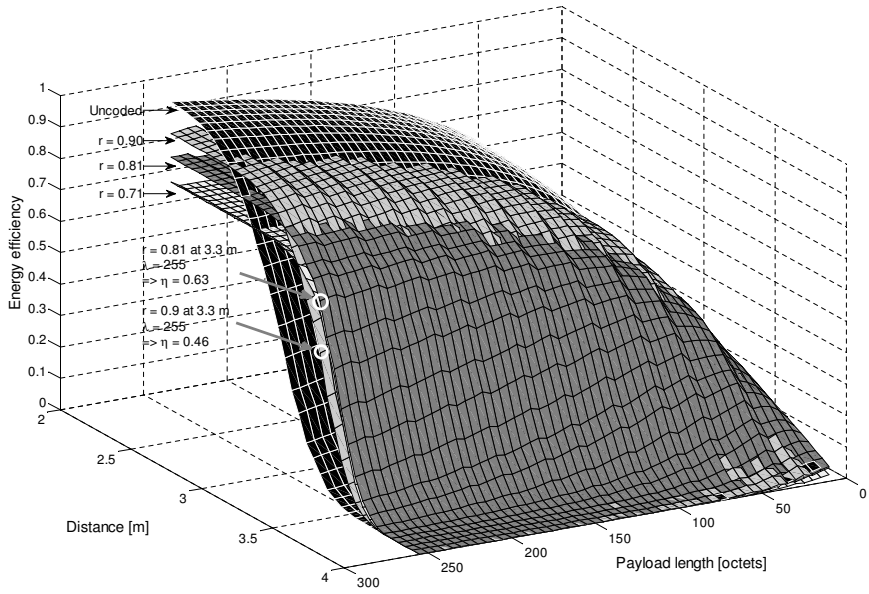

Fig. 42. Energy efficiency calculated by normalizing with respect to maximum overall efficiency value.

Figure 42 shows the energy efficiency as a function of communication distance and payload length when the normalization of energy efficiency has been done with respect to overall maximum energy efficiency by using (74). The overall maximum can be achieved when the communication distance is short enough to guarantee error-free transmission and the maximum payload length is in use to minimize the transmission overhead. Therefore, the maximum energy efficiency ($max(\eta) = 1$) will be achieved by using uncoded transmission with maximum payload length (λ_{max}) and communication distance $d \leq d_0$. As can be seen from Figure 42, from the energy efficiency point of view, it is better to use the maximum payload length if the communication distance is short enough. Figure 42 also shows how far a particular code rate is from the maximum energy efficiency at certain payload length and communication distance point. For example, if the link length $d = 3.3$ metres, code rate $r = 0.9$ would lead to energy efficiency 0.46 when the maximum payload is used. In that case, the payload length should be decreased or stronger code should be used in order to increase the energy efficiency at that communication distance. For example, if the code rate $r = 0.81$ is used with maximum payload at the distance of 3.3 m, then the energy efficiency is 0.63.

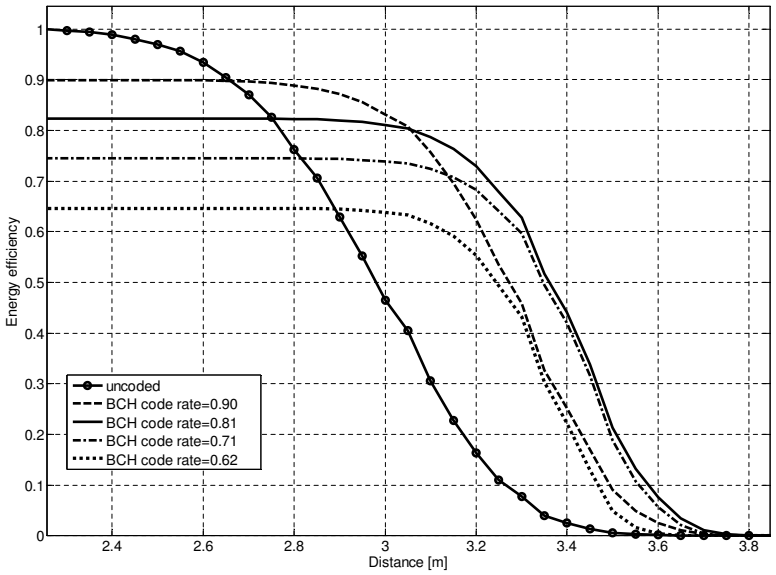

Fig. 43. Energy efficiency versus distance for payload length of 255 octets ([37] ©Springer Science+Business Media 2014).

As can be seen from the figures above, there are remarkable differences in the energy efficiency when using different code rates for different payload and communication distance values. The shown 3D figures illustrate well the trend of the results but they cannot be used for consideration of the results in detail. Therefore, the following figures show more detailed results for specific payload and distance values.

Figure 43 shows the energy efficiency for different code rates versus distance when the payload length is 255 octets. The results clearly illustrate how the most energy-efficient code rate changes when the distance increases. It can also be seen that the code rate 0.61 is not the most energy-efficient at any point. Obviously that code rate has too much redundancy in this case. It can be observed that in the shortest distance case (2.25 metres), the uncoded transmission would provide the highest energy efficiency but the loss in energy efficiency for $r = 0.9$ is only 10% and for $r = 0.81$, the loss is 17.5%. However, if the distance is 3.05 metres, $r = 0.9$ and $r = 0.81$ would provide around 80% of the maximum energy efficiency while in the uncoded case, energy efficiency would be only around 40% of the maximum efficiency. Therefore, the loss in efficiency would be drastic due to the lack of error correction. From this result, one can conclude that it is better to have too strong coding if the distance can change in the range shown in this figure.

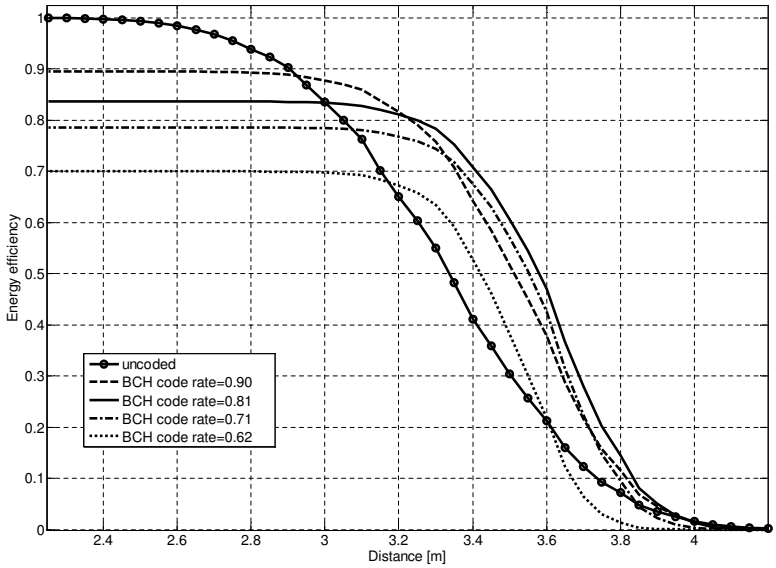

Fig. 44. Energy efficiency versus distance for payload length of 50 octets ([37] ©Springer Science+Business Media 2014).

Figure 44 shows the energy efficiency for different code rate versus distance when the payload length is 50 octets. This figure shows a similar behaviour than in Figure 43 but it can be noticed that the distance until which the uncoded transmission provides the highest efficiency has shifted to 2.9 metres. It can also be noticed that the energy efficiency for the coded cases remains high for longer distances than in the long payload case shown in Figure 43; i.e., shorter packet length enables longer communication distance, and the need for FEC decreases. However, as was noticed in the Figure 42 case, the maximum energy efficiency can be achieved with a combination of the largest payload length and high reliability. By comparing Figure 43 and Figure 44, it can also be noticed how the payload length increases the energy efficiency gap between uncoded and coded cases at distances where FEC is beneficial.

It is also interesting to have a look at the energy efficiency versus the payload length at fixed communication distance point. Figure 45 show results at 3 metres communication distance. The saw tooth effect in these curves originate from the bit filling of the not full code words, as defined in the standard [16]. The code rate 0.9 would be recommended as opposed to this communication distance to enable highest energy efficiency. It can also be noticed that for the uncoded case, the energy efficiency decreases drastically when the payload length increases. From Figure 45, it can be

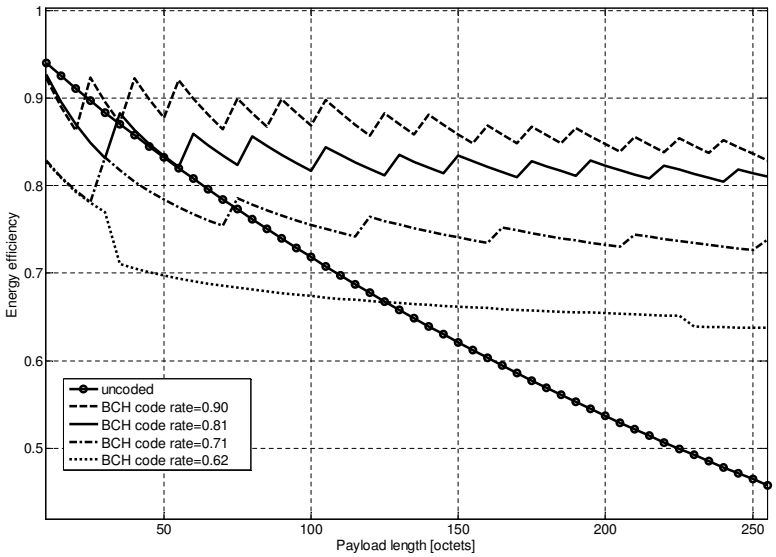

Fig. 45. Energy efficiency with respect to payload length at 3 metres distance ([37] ©Springer Science+Business Media 2014).

observed also how the payload size affects code rate efficiency (saw effect) because some bit filling may be needed to align with the number of information bits needed for code word at the encoding.

Figure 46 shows the energy efficiency averaged over the studied distance values versus the payload length. That figure shows which code rate is the most efficient if communication link distances can vary randomly, according to uniform distribution between the distances from 2.25 to 4.25 metres. As can be seen from the results in Figure 46, for short payload length (below 30 octets) values, the uncoded transmission performs as well as the coded transmission. When the payload is longer, the code rate 0.81 or 0.9 should be chosen.

It is also useful to enable the energy efficiency normalization with respect to the maximum achievable energy efficiency at particular communication distance point. In that way, the most energy-efficient payload and code rate combination at each distance point will be found and other code rate and payload length combinations' energy efficiency can be clearly compared with respect to the performance achieved with the most energy efficient combination. In that case, the maximum achievable energy efficiency must be found for each communication distance point as a function of payload length and code rate. Every other efficiency values calculated for other code rates, as a

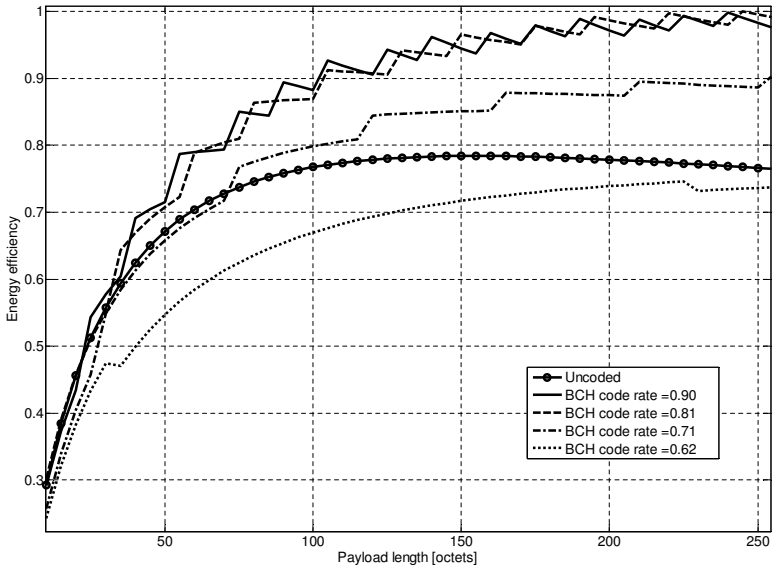

Fig. 46. Energy efficiency averaged with respect to distance values (2.25 - 4.25 m) versus the payload length ([37] ©Springer Science+Business Media 2014).

function of payload, can be then normalized with respect to the maximum achievable energy efficiency at the distance point. Energy efficiency normalization can be done in this case as

$$\eta^{i}_{\mathrm{dis,norm}}(d,\lambda) = \frac{\eta_i(d,\lambda)}{max(\eta(d,[\lambda_1,\lambda_2,\ldots,\lambda_{\max}]))}, \tag{75}$$

where

$$\eta(d,[\lambda_1,\lambda_2,\ldots,\lambda_{\max}])) =$$
$$\eta_0(d,\lambda_1),\eta_0(d,\lambda_2),\ldots,\eta_0(d,\lambda_{\max}),\eta_1(d,\lambda_1),\eta_1(d,\lambda_2),\ldots,\eta_1(d,\lambda_{\max}),\ldots,$$
$$\eta_{MAXi}(d,\lambda_1),\eta_{MAXi}(d,\lambda_2),\ldots,\eta_{MAXi}(d,\lambda_{\max}).$$

Figure 47 shows the normalized energy efficiency results with maximum achievable efficiency at each distance point calculated by using (75). It can be observed that for each communication distance, there is a certain code rate and payload length combination which offers the maximum energy efficiency, ($\eta = 1$). Figure 47 clearly shows such trend that the code rate should be decreased when the communication distance increases in order to maximize the energy efficiency, as expected. It can be observed also that when the communication distance increases, the payload length should be deceased

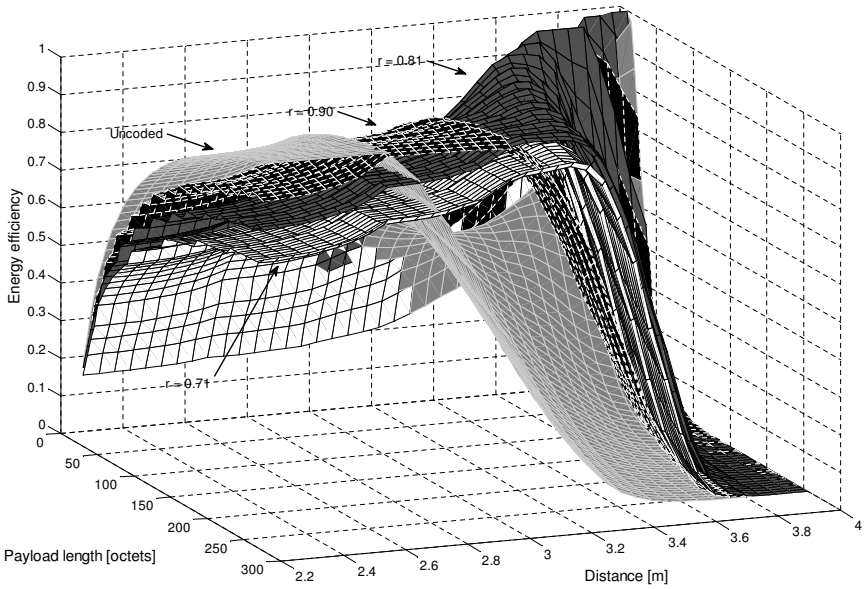

Fig. 47. Energy efficiency normalized with respect to maximum achievable energy efficiency at each distance point, R = 0.975 Mbps.

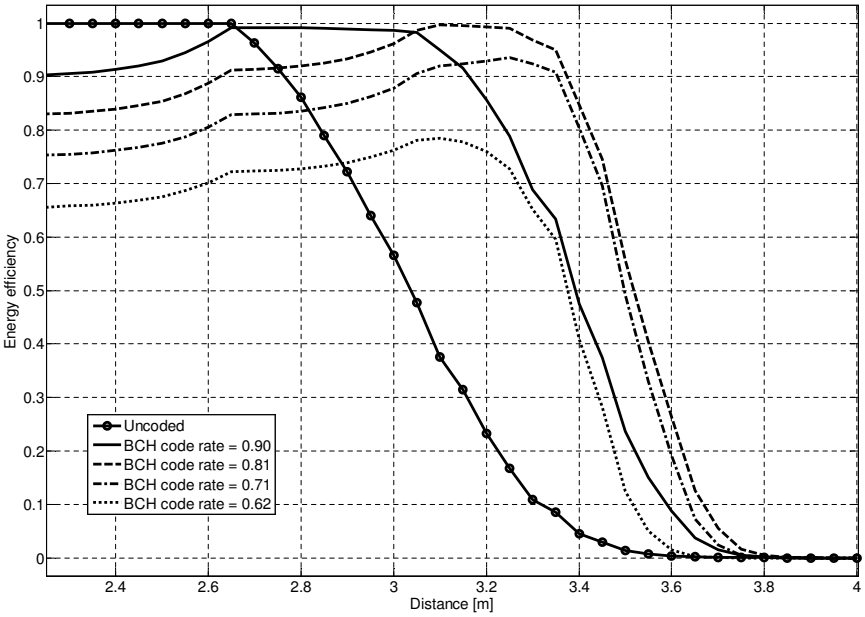

Fig. 48. Energy efficiency normalized with respect to maximum achievable energy efficiency at each distance point, payload length is 255 octets and R = 0.975 Mbps.

in order to achieve maximum energy efficiency. It can be noted also that the code rate $r = 0.71$ is too low from the energy efficiency point of view. Therefore, only the uncoded case and code rates $r = 0.9$ and $r = 0.81$ should be considered for the IEEE Std 802.15.6-based IR-UWB communication with the assumed parameters and channel conditions.

Figure 48 shows, 2D projection of the results shown in Figure 47 for the case of the payload length of 255 octets. From the results, it can be observed how the code rate should be adapted, when the communication distance and consequently the E_b/N_0 changes. The uncoded case provides the highest energy efficiency if the communication distance is shorter than 2.65 metres after which the code rate $r = 0.9$ would provide the highest energy efficiency until the distance increases to 3.05 metres. When the distance is longer than 3.05 metres, the code rate $r = 0.81$ should be selected to achieve highest energy efficiency for this payload length case. Moreover, it can be observed that when the distance is longer than 2.65 metres, the maximum energy efficiency cannot be achieved anymore with this maximum payload length even if the code rate would be adapted as explained. Instead, also the payload length should be decreased jointly with the code rate adaptation. Particularly, when the distance is longer than 3.3 metres the payload should be decreased since energy efficiency starts to decrease drastically when the maximum payload length is used, as can be observed from Figure 48.

The results of Figures 47 and 48 show that the (75) can be used to find out the most energy-efficient code rate and payload length combination as a function of communication distance. That is a very useful information for the code rate and payload length adaptation when the communication distance estimate is available. If the communication distance estimation is not known by the network nodes, the received energy per bit-to-noise value can be used for adaptation purpose as well since the same set of results can be calculated also as a function of E_b/N_0. Table 9 shows the most energy-efficient code rate and payload length values for the case of Figure 47.

Figure 49 shows the normalized energy efficiency results with maximum achievable efficiency at each distance point for the data rate 0.487 Mbps. This result can be compared with Figure 47, and it can be observed that the decrease in data rate affects the feasible distance (increase around 1.25 m). The overall trend of the results is the same, but it can be seen that error correction is more useful when the distance increases. The performance gap between different code rates remains approximately the same, but the gap between uncoded and coded transmission is larger than in the case of Figure 47, where the distance is shorter. The author has done calculations for other data rates

Table 9. The most energy efficient code rate and payload length values with respect to communication distance and E_b/N_0 in the case of Figure 47.

Distance [m]	Energy per bit-to-noise ratio [dB]	Code rate	Payload [oct]
$d < 2.65$	$15.7 < E_b/N_0$	Uncoded	$\lambda = 255$
$2.65 \leq d < 3.1$	$14.4 < E_b/N_0 \leq 15.7$	$r = 0.90$	$\lambda = 240$
$3.1 \leq d < 3.25$	$14.0 < E_b/N_0 \leq 14.4$	$r = 0.81$	$\lambda = 245$
$d = 3.3$	$E_b/N_0 = 13.8$	$r = 0.81$	$\lambda = 195$
$d = 3.4$	$E_b/N_0 = 13.6$	$r = 0.81$	$\lambda = 130$
$d = 3.5$	$E_b/N_0 = 13.4$	$r = 0.81$	$\lambda = 80$
$d = 3.6$	$E_b/N_0 = 13.1$	$r = 0.81$	$\lambda = 60$
$d = 3.7$	$E_b/N_0 = 12.9$	$r = 0.81$	$\lambda = 35$
$d = 3.8$	$E_b/N_0 = 12.7$	$r = 0.81$	$\lambda = 35$
$d = 3.9$	$E_b/N_0 = 12.5$	$r = 0.81$	$\lambda = 15$
$d = 4.0$	$E_b/N_0 = 12.2$	$r = 0.81$	$\lambda = 10$

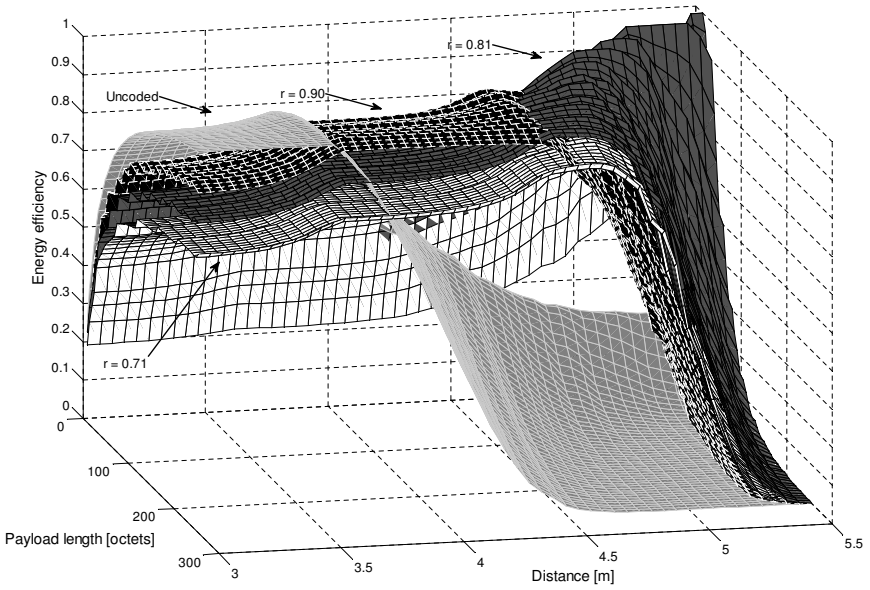

Fig. 49. Energy efficiency normalized with respect to maximum achievable energy efficiency at each distance point, R = 0.487 Mbps.

defined by the standard, and it can be concluded that when the data rate is increased (or decreased), the feasible communication distance will scale down (or up) but the trend of the results remains the same.

Improvement percentage

It is also valuable to know how much the performance would be improved in comparison with the current setting when adapting the code rate or payload. That information can be used for making the decision about the adaptation. For that purpose, in this work, energy efficiency improvement percentage definition

$$\eta[\%] = 1 - \frac{\eta_{\mathrm{r}}}{\eta_i} \tag{76}$$

is used, where η_{r} is the energy efficiency of the reference case and η_i is the energy efficiency for the code rate of interest, r_i.

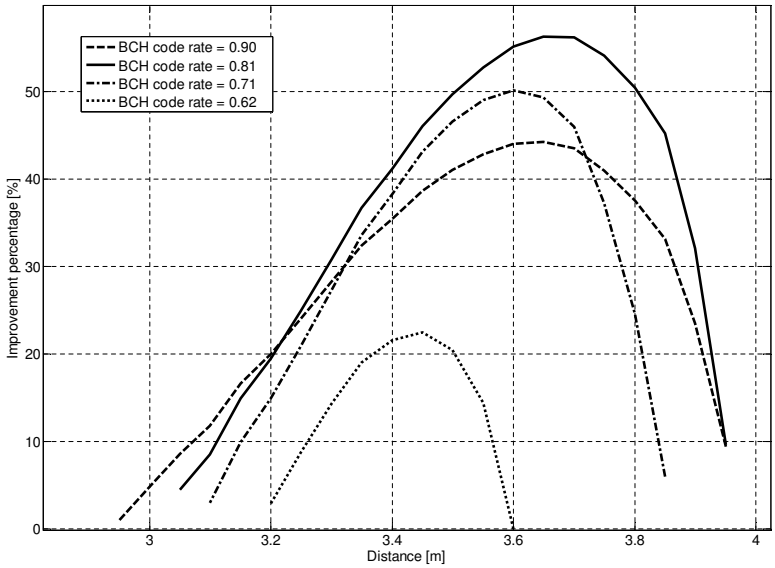

Fig. 50. Energy efficiency improvement percentage with respect to uncoded case, payload length is 50 octets ([37] ©Springer Science+Business Media 2014).

Figure 50 shows the energy efficiency improvement percentage for different code rates with respect to the uncoded case ($\eta_{\mathrm{r}} = \eta_0$). Figure 50 shows that also for a quite short payload length (50 octets in this case), the maximum energy efficiency improvement can be 56%, which is achieved at 3.65 metres point. However, as can be noticed from Figure 44, at that point also the coded case has moderate energy efficiency (0.47) and that should not be the target operating point for the transceiver pair. At 3.4 metres, the code rate 0.9 can provide more than 40% and also the energy efficiency is above 0.7, which can be observed from Figure 44.

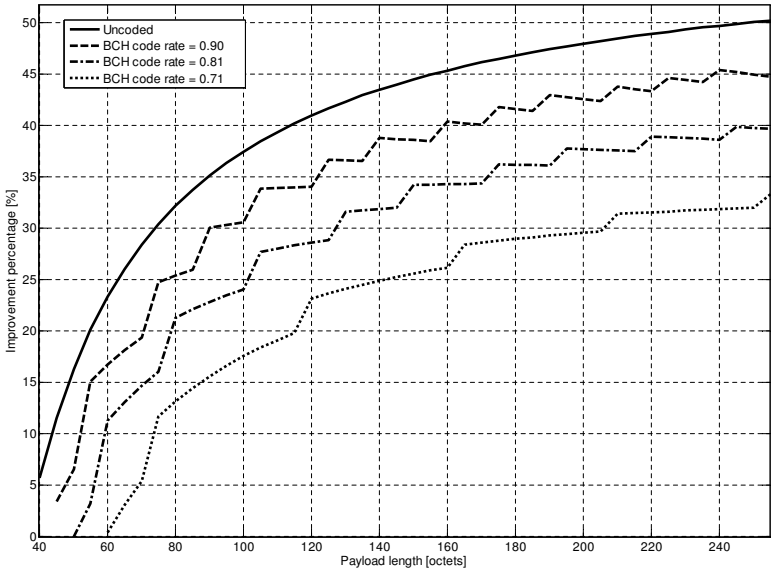

Fig. 51. Energy efficiency improvement percentage with respect to reference parameter setting, code rate $r = 0.81$ and payload $\lambda = 50$ octets at 2.3 metres link.

Let's then consider a reference case that radio is currently using the code rate $r = 0.81$, as defined in the IEEE Std 802.15.6, and the payload length is 50 octets. Assume that the radio estimates that communication distance (or corresponding channel conditions) is now 2.3 metres. Figure 51 shows how much the energy efficiency would be improved in percentage, in comparison with that reference setting, if other code rates and payload lengths would be used for communication at 2.3 metres link. By using (75), it can be found that the uncoded case with 255 octet payload maximizes the energy efficiency for the link of length of 2.3 metres. From Figure 51, it can be observed that the optimal setting (uncoded and 255 octets payload) would provide 50% saving to energy efficiency. From the results, it can also be observed that if only the payload length would be adapted from 50 to 255 octets, the saving would be around 40%. In addition, it can be seen that if only code rate would be adapted, the code rate r = 0.9 and uncoded case would provide around 7% and 16% saving. There are other saving percentage possibilities between these extremes which could be achieved in a real scenario if, for example, the distance estimation is not accurate and the adaptation decision would not be exactly correct. However, it can be observed that remarkable savings are possible to acquire by adapting the code rate and/or payload length even the parameter selection for adaptation would not be optimal.

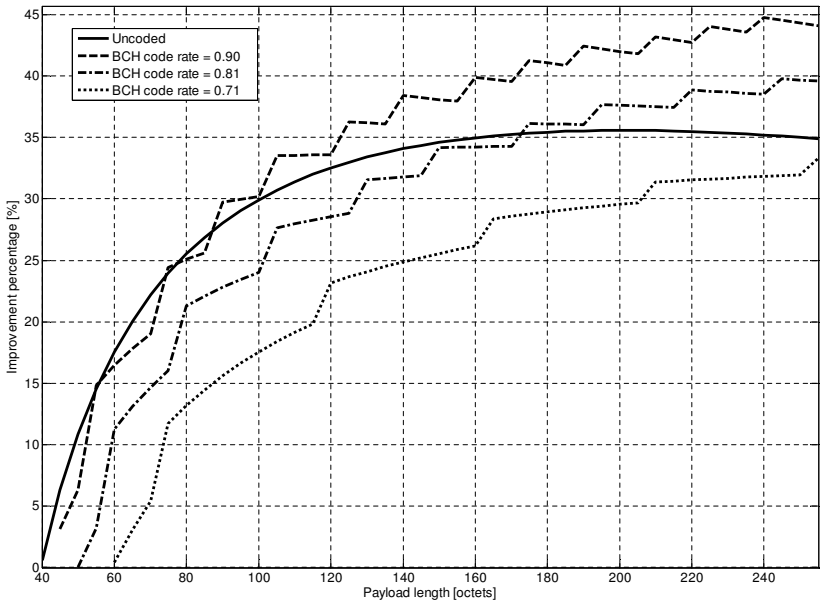

Fig. 52. Energy efficiency improvement percentage with respect to reference parameter setting, code rate $r = 0.81$ and payload $\lambda = 50$ octets at 2.8 metres link.

Figure 52 shows the energy saving improvement percentage as a function of payload length for different code rate in comparison to reference setting $r = 0.81$ and $\lambda = 50$ at 2.8 metres link. It can be observed that in this case the optimal parameters are $r = 0.81$ and $\lambda = 50$, which provide 44% energy efficiency improvement. Also in this case, it can be seen that there are various parameter settings for code rate and payload lengths which can improve the energy efficiency in comparison with the reference setting. The uncoded case would also improve the performance around 35% when increasing the payload to $160 - 255$ octets.

In the Figure 53 case, the same reference setting is used, but the communication distance is assumed to be 3.3 metres. It can be observed that in this case the uncoded case is no longer an option for energy efficiency improvement and also the performance of the code rate $r = 0.9$ is weak, particularly for long payload lengths. In this scenario, the best option would be to keep the code rate the same and increase the payload length to 195 octets, when approximately 27.6% saving would be achieved.

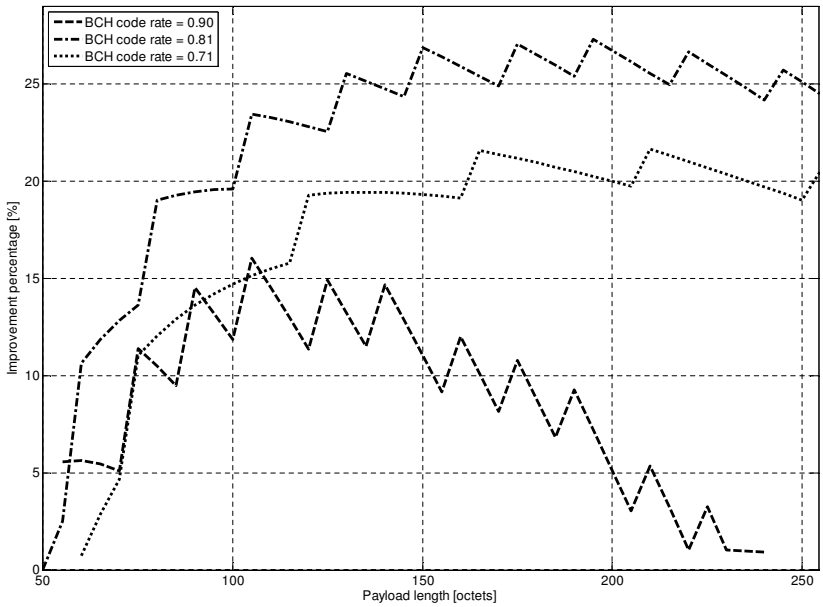

Fig. 53. Energy efficiency improvement percentage with respect to reference parameter setting, code rate $r = 0.81$ and payload $\lambda = 50$ octets at 3.3 metres link.

Figure 54 shows the energy efficiency improvement for adaptive code rate and payload selection versus the IEEE Std 802.15.6 BCH code rate with different payload lengths. The adaptive selection is based on the most energy efficient code rates and payload lengths for different distances according the values shown in Table 9. From Figure 54 it can be observed that the energy efficiency improvement would be 17% when comparing to standard code rate $r = 0.81$ with payload length 255 octets for the communication distance of 2.25 metres. For this communication distance, the most efficient selection is uncoded transmission with payload length 255 octets, as can be seen from Figure 47 and Table 9. When comparing to $r = 0.81$ with 50 octets payload at the communication distance of 2.25 metres, the energy efficiency improvement would be around 53% for the adaptive selection. For the communication distance of 3.6 metres, the adaptive selection would provide approximately 78% improvement in comparison to $r = 0.81$ with 255 octets payload, and only 6% improvement when compared to $r = 0.81$ with 50 octets payload. This figure illustrates that the adaptive selection of code rate and payload length can provide high energy efficiency improvements. From the results of Figure 47, Figure 54 and Table 9, it can be concluded that in the short communication distance case ($\leq$ 3.1 m), it is efficient to use the maximum payload, and

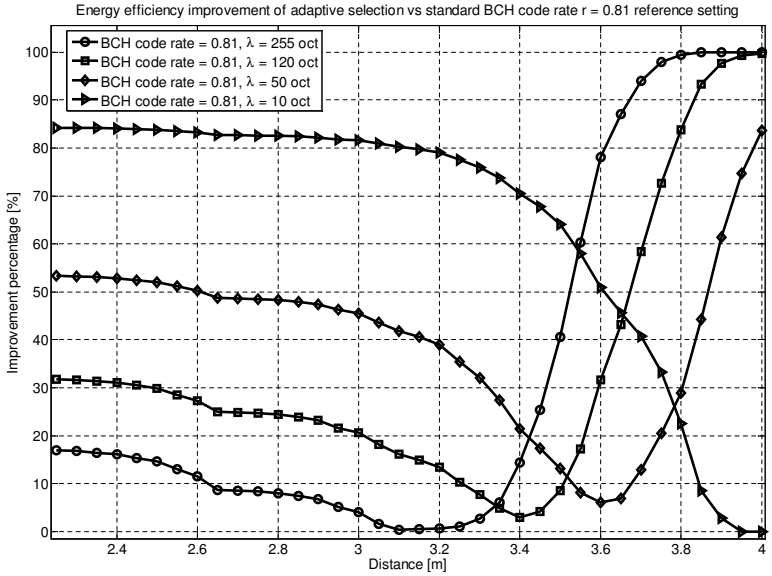

Fig. 54. Energy efficiency improvement percentage for adaptive selection according the values shown in Table 9 versus the reference parameter setting for IEEE Std 802.15.6 code rate $r = 0.81$ with different payload lengths.

code rate adaptation in comparison with the standard setting can provide additional gain. For the longer communication distances (> 3.1 m), the standard code rate is the most energy-efficient, but in that case it is important to adapt the payload length to improve the energy efficiency.

5.3 Adaptation algorithm

There are many possibilities to build code rate and payload length adaptation algorithms based on the introduced model and results. As the results show, the most energy efficient code rate and payload length varies strongly as a function of distance. The code rate and payload length should be therefore selected with respect to the distance between transmitter and receiver to achieve as high energy efficiency as possible. The communication distance value can be used to calculate the estimation of the received signal strength (or E_b/N_0), and vice versa. Therefore, the receiver can also use the received signal strength value for the energy-efficient code rate and payload length selection purposes.

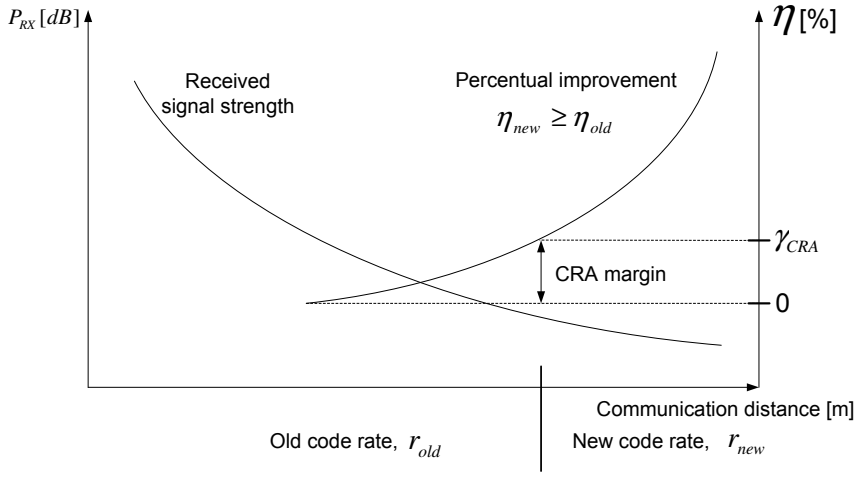

Fig. 55. Code rate adaptation margin (threshold) ([37] ©Springer Science+Business Media 2014).

The WBAN hub can, for example, have a look-up table which includes the most energy-efficient code rate and payload length for the different received signal strength, E_b/N_0 or distance estimate values. In Table 9 were shown the most energy-efficient code rates and payload length values for different communication distance and E_b/N_0 values, which can be used to as a look-up table. If the hub node notices that the received signal strength between the hub and node (or E_b/N_0) changes, then it can send information about the code rate change in order to increase the energy efficiency of communication. The new code rate information can be sent, e.g., as a part of the PHY header, as has been introduced in [159] for the modulation adaptation case. The code rate decision can be done, e.g., based on the threshold about how much the new code rate will improve the energy efficiency percentage, as introduced in Figure 55. In Figure 55, the code rate adaptation (CRA) margin illustrates that the code rate will be adapted when the threshold (γ_{CRA}) is exceed. The purpose of the CRA margin is to ensure that there will not be unnecessary code rate changes due to the channel fluctuations, because the fact is that in WBANs, the channel condition can change rapidly due to the human body movements.

The model introduced in this work provides a tool for a percentage improvement evaluation. The CRA margin can be therefore a certain percentage improvement value which must be met in order to trigger the code rate and/or payload length adaptation.

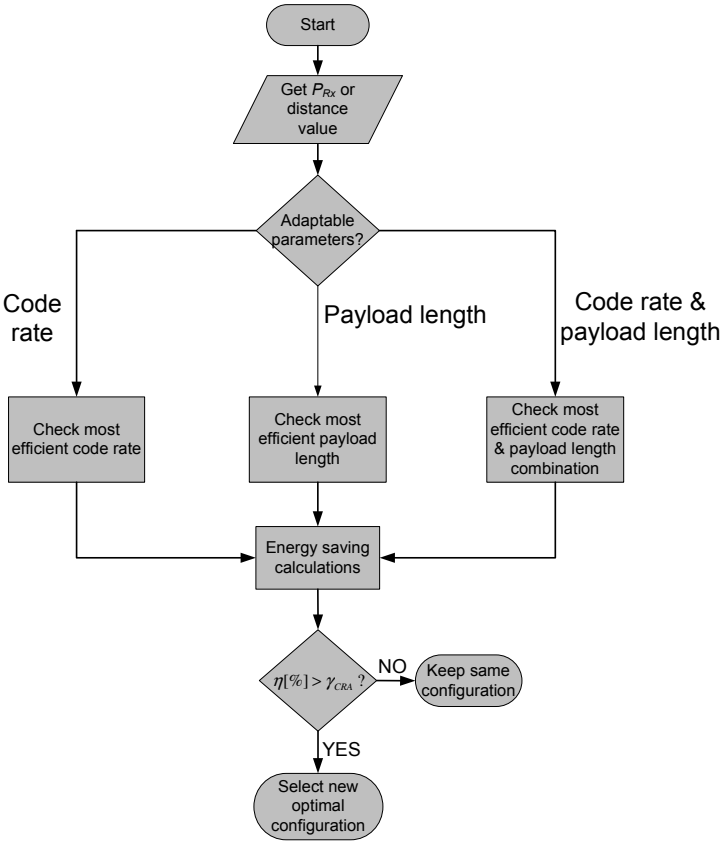

Fig. 56. Code rate and payload length adaptation algorithm ([37] ©Springer Science+Business Media 2014).

In Section 5.2.3, the results for the example scenarios about the energy efficiency percentage improvement that can be achieved by using adaptation were shown.

Different WBAN applications include nodes with varying capabilities. It depends on the node capabilities which parameter configuration can be adapted. In Figure 56, it has been illustrated an example algorithm flowchart for the radio configuration adaptation based on the received signal strength or communication distance value. The WBAN hub should have a possibility to estimate the received signal strength and optionally also to derive the E_b/N_0 estimate or communication distance because the UWB technology enables accurate positioning. In addition, in some applications, the nodes' locations are fixed and known already at the installation phase. Depending on the node capabilities, the hub can try to optimize the code rate or payload length or both. In each case, the hub

selects the most efficient choice from the look-up table and performs energy saving calculation in order to check that the CRA threshold is exceeded with the new choice. If the CRA threshold is exceeded, the hub will send the new configuration information to the node.

5.4 Summary

A novel analytical energy efficiency model for the IEEE Std 802.15.6-based WBAN was introduced in this chapter. The model enables energy efficiency evaluation as a function of communication distance and payload length for different FEC code rates. As was seen from the averaged results of Figure 46, the BCH code rate ($r = 0.81$) chosen for the standard [16] is a good compromise for the range of payload lengths and target communication distance values. However, from the results, it can also be observed that the energy efficiency of different code rates and payload lengths varies highly as a function of received E_b/N_0, which depends on the communication distance.

The model proposed here can be used for payload length and code rate selection at the network planning phase or for real-time adaptation algorithm development purposes to achieve energy efficiency gains. Therefore, the model is useful for an information exploitation-based cross-layer design approach when applied for the PHY and MAC layers. The introduced normalized energy efficiency metrics are not restricted to the studied PHY and MAC protocols, but they can also be used for other communication protocols' performance evaluation. The link energy consumption model must be adjusted to match the particular protocol characteristics, but then the energy efficiency metrics can be used as a useful tool for clear performance comparison and parameter adaptation purposes. Section 5.3 introduced a code rate and payload length adaptation algorithm, which can be implemented based on the introduced model.

6 Conclusions and future work

This thesis focused on a cross-layer analysis of several aspects of communication and networking in WSNs and WBANs. An introduction to wireless sensor networks was provided, and relevant existing works on RF communication energy efficiency improvement were reviewed. In the review part, the cross-layer design approaches were divided into two different categories: merging of layers and information exploitation between layers. In addition, the following definition was proposed therein for the cross-layer design: *Protocol design using information exploitation between the layers of the reference layered architecture either in the design phase or during run-time − with or without merging of layers*. Three different cross-layer models, which were developed in this doctoral research to enable improvement of the communication energy efficiency in WSNs and WBANs, were introduced. A generic wake-up radio-based MAC protocol was proposed to enable energy efficiency by avoiding idle listening, and it was incorporated to the developed models. The GWR-MAC protocol includes a bi-directional wake-up procedure definition and transmission period, which can be implemented using different channel access methods, therefore being scalable to various application scenarios.

First the study proposed a model which takes PHY and MAC layer characteristics jointly into account in a star-topology network transmission period length and energy efficiency analysis for the group of sensor nodes transmitting to the sink node. The model was defined at the general level so that the same approach can be used to evaluate performances of networks based on different PHY and MAC layer protocols. Then the model was used to study the network transmission period length, and energy efficiency for the IR-UWB PHY- and S-Aloha-based transmission period channel access, as a function of error correction code rate, channel competition probability and energy per bit-to-noise ratio. The results showed in which conditions energy savings can be achieved by adapting the code rate and when uncoded transmission should be used instead to maximize the energy efficiency. The model was also applied to energy consumption comparison of the S-Aloha- and TDMA-based MAC when using different code rates for IR-UWB communication. The proposed model enables to perform cross-layer design using the information exploitation approach, which takes advantage

of information exchange between the different layers in order to improve their joint energy efficiency.

Next, a hierarchical architecture was introduced and cross-layer energy consumption evaluation model was proposed for the layered architecture based on either wake-up radios or duty-cycle radios. The studied WUR approach was based on the GWR-MAC protocol proposed in this thesis. The energy efficiency comparison was done for the WUR and DCR approaches as a function of event frequency. The results clearly showed that energy efficiency can be improved when selecting the correct radio type for hierarchical network wake-up mechanisms. The prosed model provides a tool to select the correct radio type in order to enable energy efficiency at the network level, taking into account the physical and MAC layer aspects. In this case, the selection at the physical layer will be done between the WUR and the conventional radios based on duty cycling. That selection then affects the MAC layer design, since when using the WUR for a wake-up mechanism, a duty cycle-based MAC protocol does not need to be used to enable the triggering of the data message exchange.

Finally, a link level analytical cross-layer energy efficiency model was developed for the IEEE Std 802.15.6-based WBAN. The model can be used to select the correct BCH code rate and payload length from the energy efficiency point of view. The results show, as a function of communication distance, which code rate and payload length will lead to the highest energy efficiency. An example method for code rate and payload length adaptation algorithm development purposes was proposed. This model is useful for information exploitation-based cross-layer design since it enables to derive the most energy-efficient code rate and payload length, taking PHY and MAC layer aspects into account.

By introducing three different types of analytical cross-layer models, this thesis provides tools for energy efficiency improvement of low-power communication. The first model focuses on the network nodes' energy efficiency in a star topology WSN. The second model focuses on the hierarchical network-level energy consumption, and the third model can be used to evaluate the link level energy efficiency in WBANs. Because the sensor network application space is very wide, it is very difficult or even impossible to define a model which is sufficient for the analysis of every scenario. However, in the proposed model development, the generality has also been an important design goal. Therefore, the PHY- and MAC-layer energy efficiency model is developed at first at the general level before applying it to study particular protocols. In addition, the same general model is applied to WSN and WBAN scenarios, the former one focusing on

the network total energy consumption and the latter one on link energy consumption. In addition, the proposed GWR-MAC protocol is designed to be scalable to various scenarios and then it has been incorporated for the star topology and hierarchical WSN architectures studied in this thesis. Furthermore, the author has introduced, in [42] and [43], that the GWR-MAC protocol can also be applied to WBAN scenarios. Another important design goal has been that the proposed approaches should not require substantial changes to current standards to take advantage of the research findings. That design goal has been fulfilled by applying the proposed models to study potential energy efficiency gains that can be achieved by simply tuning the protocol parameters, such as FEC code rates and payload lengths. In addition, the hierarchical architecture energy efficiency model enables straightforward selection between the wake-up radios and duty-cycle radios without requiring substantial changes to the transceiver design. The WUR approach requires that two different radio interfaces must be implemented in the nodes. However, the wake-up receivers are fairly simple and do not increase the cost of the nodes remarkably.

In the cross-layer design, there are various interdependencies between different layers to consider and certain assumptions must be done in the performance analysis. Therefore, there always exist improvement possibilities for the proposed models. In the future research, the analysis introduced for the lower layers of the WSN protocol stack can be further developed to take advantage of the introduced model in the context of a hierarchical network. Because there is still room for further energy efficiency optimization in WSNs, a future goal is to apply the proposed general-level approach to study other PHY and MAC protocols, as well as to explore other FEC coding options. In the future, the sensor nodes' computational capabilities will increase, and thus also more complex error correction codes, such as convolutional, LDPC or Turbo codes, could become a feasible option to save energy. In future research, the proposed model can be improved to take more transceiver parameters into account in the analysis and, e.g., by assuming imperfect synchronization. In the architecture energy consumption analysis, it was assumed that the BEP of wireless communication is fixed, since that assumption enabled to perform a straightforward comparison between the WUR- and DCR-based wake-up mechanism, which was the main goal of that analysis. In order to get more exact results in future research, it would be valuable to explore the energy efficiency with more realistic channel models for both data and wake-up signal transmissions. The proposed model is developed so that the channel bit error probability of a target environment can be easily used in the energy efficiency evaluation. The optimal thresholds for the

introduced adaptation algorithm for the IEEE Std 802.15.6-based WBAN should also be explored in the future. The performance evaluation in more realistic channel conditions and with varying offered traffic load values would also be valuable to perform. However, the proposed adaptation algorithm for the IEEE Std 802.15.6-based transceivers is not dependent on the used channel model. In addition, experimental measurements could be performed in the future in order to gain knowledge of the real implementation performance. The proposed GWR-MAC protocol needs to be implemented to verify the functionalities and performance in real scenarios. Wake-up radio-based approaches have remarkable potential to provide energy savings. However, the wake-up radio research area is still quite unexplored, and therefore the purpose of the GWR-MAC protocol is to enable more efficient usage of WURs in WSNs and WBANs, and to foster future research and development.

References

1. Akyildiz IF, Su W, Sankarasubramaniam Y & Cayirci E (2002) A survey on sensor networks. IEEE Communications Magazine 40(8): 102–114.
2. Raghunathan V, Schurgers C, Park S & Srivastava M (2002) Energy-aware wireless microsensor networks. IEEE Signal Processing Magazine 19(2): 40–50.
3. Yick J, Mukherjee B & Ghosal D (2008) Wireless sensor network survey. Elsevier Computer Networks 52(12): 2292–2330.
4. Shelby Z & Bormann C (2010) 6LoWPAN: The Wireless Embedded Internet. Wiley Publishing.
5. Zorzi M, Gluhak A, Lange S & Bassi A (2010) From today's INTRAnet of things to a future INTERnet of things: A wireless- and mobility-related view. IEEE Wireless Communications 17(6): 44–51.
6. Mainetti L, Patrono L & Vilei A (2011) Evolution of wireless sensor networks towards the Internet of Things: A survey. In: Proc. International Conference on Software, Telecommunications and Computer Networks (SoftCOM), pp. 1–6.
7. Lazarescu M (2013) Design of a WSN platform for long-term environmental monitoring for IoT applications. IEEE Journal on Emerging and Selected Topics in Circuits and Systems 3(1): 45–54.
8. Crossbow (2014). TelosB datasheet. URI: www.willow.co.uk/TelosB_Datasheet.pdf.
9. Lu J, Okada H, Itoh T, Harada T & Maeda R (2014) Towards the world smallest wireless sensor nodes with ultra-low power consumption. IEEE Sensors Journal 14(6): 2035–2041.
10. ISO/IEC 7498-1:1994 (1994) Information technology – Open Systems Interconnection – Basic Reference Model: The Basic Model. Standard, International Organization for Standardization.
11. Chonggang W, Sohraby K, Bo L, Daneshmand M & Yueming H (2006) A survey of transport protocols for wireless sensor networks. IEEE Network 20(3): 34–40.
12. DASH7 Alliance (2012). DASH7 alliance webpage. URI: http://www.dash7.org.
13. Z-Wave Alliance (2014). Z-Wave alliance webpage. URI: http://www.z-wavealliance.org.
14. Bluetooth SIG (2013). Bluetooth special interest group webpage. URI: http://www.bluetooth.org.
15. IEEE (2006) IEEE Standard for Local and metropolitan area networks - Part 15.4: Wireless Medium Access Control (MAC) and Physical Layer (PHY) Specifications for Low-Rate Wireless Personal Area Networks (LR-WPANs). Standard, The Institute of Electrical and Electronics Engineers, Inc. IEEE Std. 802.15.4 − 2006, Revision of IEEE Std. 802.15.4 − 2003.
16. IEEE (2012) IEEE Standard for Local and metropolitan area networks - Part 15.6: Wireless Body Area Networks. Standard, The Institute of Electrical and Electronics Engineers, Inc. IEEE Std. 802.15.6 − 2012.
17. IEEE (2007) IEEE Standard for Local and metropolitan area networks - Part 15.4: Wireless Medium Access Control (MAC) and Physical Layer (PHY) Specifications for Low-Rate Wireless Personal Area Networks (WPANs); Amendment 1: Add Alternate PHY. Standard, The Institute of Electrical and Electronics Engineers, Inc. IEEE Std. 802.15.4a - 2007.

18. Oppermann I, Hämäläinen M & Iinatti J (2004) UWB Theory and Applications. John Wiley & Sons, Ltd, The Atrium, Southern Gate, Chichester, West Sussex, England.
19. Gerrits JFM, Farserotu J & Long J (2008) Low-complexity ultra-wide-band communications. IEEE Transactions on Circuits and Systems II: Express Briefs 55(4): 329–333.
20. IEEE (2011) IEEE Standard for Local and metropolitan area networks - Part 15.4: Wireless Medium Access Control (MAC) and Physical Layer (PHY) Specifications for Low-Rate Wireless Personal Area Networks (LR-WPANs). Standard, The Institute of Electrical and Electronics Engineers, Inc. IEEE Std. 802.15.4 – 2011, Revision of IEEE Std 802.15.4-2006.
21. International Organization for Standardization (2014). ISO webpage. URI: http://www.iso.org.
22. Farserotu JR, Gerrits JFM & Rousselot J (2010) Low power and robust PHY-MAC solution for medical BAN. IEICE Transactions on Communications E93-B(4): 802–810.
23. Gerrits JFM, Farserotu J & Long J (2011) Robustness and interference mitigation for FM-UWB BAN radio. In: Proc. International Symposium on Medical Information Communication Technology (ISMICT), pp. 98–102.
24. Gu L & Stankovic JA (2005) Radio-triggered wake-up for wireless sensor networks. Springer Journal on Real-Time Systems 29(2): 157–182.
25. Van der Doorn B, Kavelaars W & Langendoen K (2009) A prototype low-cost wakeup radio for the 868 MHz band. International Journal of Sensor Networks 5(1): 22–32.
26. Ansari J, Pankin D & Mähönen P (2009) Radio-triggered wake-ups with addressing capabilities for extremely low power sensor network applications. International Journal of Wireless Information Networks 16(1): 118–130.
27. Marinkovic SJ & Popovici EM (2011) Nano-power wireless wake-up receiver with serial peripheral interface. IEEE Journal on Selected Areas in Communications 29(8): 1641–1647.
28. Petäjäjärvi J, Karvonen H, Vuohtoniemi R, Hämäläinen M & Huttunen M (2014) Preliminary study of superregenerative wake-up receiver for WBANs. In: Proc. International Symposium on Medical Information and Communication Technology (ISMICT'14), pp. 1–5.
29. Petäjäjärvi J, Karvonen H, Mikhaylov K, Pärssinen A, Hämäläinen M & Iinatti J (2015) WBAN energy efficiency and dependability improvement utilizing wake-up receiver. IEICE Transactions on Communications - Special Issue on Innovation of Medical Information and Communication Technology for Dependable Society E98-B(4). In Press.
30. Pottie GJ & Kaiser WJ (2000) Wireless integrated network sensors. Communications of the ACM 43(5): 51–58. URI: http://doi.acm.org/10.1145/332833.332838.
31. Ares BZ, Park PG, Fischione C, Speranzon A & Johansson KH (2007) On power control for wireless sensor networks: System model, middleware component and experimental evaluation. In: Proc. European Control Conference, pp. 1–8.
32. Hohlt B, Doherty L & Brewer E (2004) Flexible power scheduling for sensor networks. In: Proc. Third International Symposium on Information Processing in Sensor Networks. IPSN 2004, pp. 205–214.
33. Demirkol I, Ersoy C & Alagoz F (2006) MAC protocols for wireless sensor networks: a survey. IEEE Communications Magazine 44(4): 115–121.
34. Anastasi G, Conti M, Francesco MD & Passarella A (2009) Energy conservation in wireless sensor networks: A survey. Ad Hoc Networks 7(3): 537 – 568. URI: http://www.sciencedirect.com/science/article/pii/S1570870508000954.

35. ON World (2014). 802.15.4 & ZigBee: Enabling the Internet of Things. URI: http://www.onworld.com/zigbee/index.htm. A Market dynamics report.
36. Karvonen H, Pomalaza-Ráez CA & Hämäläinen M (2014) A cross-layer optimization approach for lower layers of the protocol stack in sensor networks. ACM Transactions on Sensor Networks 11(1): 1–30. Available at: http://dx.doi.org/10.1145/2590810.
37. Karvonen H, Iinatti J & Hämäläinen M (2014) A cross-layer energy-efficiency optimization model for WBAN using IR-UWB transceivers. Springer Telecommunications Systems Special Issue on Research Advances in Energy-Efficient MAC Protocols for WBANs pp. 1–13. Available at: http://dx.doi.org/10.1007/s11235-014-9900-9.
38. Karvonen H, Suhonen J, Petäjäjärvi J, Hämäläinen M, Hännikäinen M & Pouttu A (2014) Hierarchical architecture for multi-technology wireless sensor networks for critical infrastructure protection. Springer Wireless Personal Communications 76(2): 209–229. Available at: http://dx.doi.org/10.1007/s11277-014-1686-2.
39. Karvonen H & Pomalaza-Ráez C (2006) A cross layer design of coding and awake/sleep periods in WSNs. In: Proc. IEEE International Symposium on Personal, Indoor and Mobile Radio Communications, PIMRC '06, pp. 1–5.
40. Karvonen H, Pomalaza-Ráez C & Hämäläinen M (2006) Cross-layer energy efficiency of FEC coding in UWB sensor networks. In: Proc. IEEE International Conference on Ultra Wideband 2006, ICUWB '06, pp. 357–362.
41. Karvonen H, Iinatti J & Hämäläinen M (2013) Energy efficiency optimization for IR-UWB WBAN based on the IEEE 802.15.6 standard. In: Proc. The Second Ultra Wideband for Body Area Networking Workshop (UWBAN-2013), co-located with the 8th International Conference on Body Area Networks (BodyNets-2013), pp. 575–580.
42. Karvonen H, Petäjäjärvi J, Iinatti J, Hämäläinen M & Pomalaza-Ráez C (2014) A generic wake-up radio based MAC protocol for energy efficient short range communication. In: Proc. IEEE International Symposium on Personal, Indoor and Mobile Radio Communications Workshop: The Convergence of Wireless Technologies for Personalized Healthcare, PIMRC '14, pp. 1–5.
43. Karvonen H, Petäjäjärvi J, Iinatti J & Hämäläinen M (2014) Energy efficient IR-UWB WBAN using a generic wake-up radio based MAC protocol. In: Proc. The Third Ultra Wideband for Body Area Networking Workshop (UWBAN-2014), co-located with the 9th International Conference on Body Area Networks (BodyNets-2014), BodyNets '14, pp. 1–5.
44. Lin S & Costello D (1983) Error Control Coding: Fundamentals and Applications. Prentice-Hall Series in Computer Applications in Electrical Engineering, Englewood Cliffs, N.J., USA.
45. Proakis J (2001) Digital Communications, Fourth Edition. Irwin / McGraw-Hill, New York, USA.
46. Kleinschmidt J, Borelli W & Pellenz M (2007) An analytical model for energy efficiency of error control schemes in sensor networks. In: Proc. IEEE International Conference on Communications, pp. 3895–3900.
47. Karvonen H, Shelby Z & Pomalaza-Ráez C (2004) Coding for energy efficient wireless embedded networks. In: Proc. International Workshop on Wireless Ad-Hoc Networks, IWWAN '04, pp. 300–304.
48. Shelby Z, Pomalaza-Ráez C, Karvonen H & Haapola J (2005) Energy optimization in multihop wireless embedded and sensor networks. International Journal of Wireless Information Networks 12(1): 11–21.

49. Howard SL, Schlegel C & Iniewski K (2006) Error control coding in low-power wireless sensor networks: When is ECC energy-efficient? EURASIP Journal on Wireless Communications and Networking pp. 1–14.
50. Sanchez E, Gandino F, Montrucchio B & Rebaudengo M (2007) Increasing effective radiated power in wireless sensor networks with channel coding techniques. In: Proc. International Conference on Electromagnetics in Advanced Applications, pp. 403–406.
51. Texas Instruments (2014). CC2420 RF transceiver datasheet. URI: http://www.ti.com.cn/cn/lit/ds/symlink/cc2420.pdf.
52. Li L, Maunder RG, Al-Hashimi BM & Hanzo L (2010) An energy-efficient error correction scheme for IEEE 802.15.4 wireless sensor networks. IEEE Transactions on Circuits and Systems II: Express Briefs 57(3): 233–237.
53. Balakrishnan G, Yang M, Jiang Y & Kim Y (2007) Performance analysis of error control codes for wireless sensor networks. In: Proc. Fourth International Conference on Information Technology, pp. 876–879.
54. Morelos-Zaragoza RH (2006) The Art of Error Correcting Coding. John Wiley & Sons.
55. Kashani Z & Shiva M (2006) Channel coding in multi-hop wireless sensor networks. In: Proc. International Conference on ITS Telecommunications Proceedings, pp. 965–968.
56. Chouhan S, Bose R & Balakrishnan M (2009) Integrated energy analysis of error correcting codes and modulation for energy efficient wireless sensor nodes. IEEE Transactions on Wireless Communications 8(10): 5348–5355.
57. Schmidt D, Berning M & Wehn N (2009) Error correction in single-hop wireless sensor networks - a case study. In: Proc. Design, Automation, and Test in Europe Conference & Exhibition, DATE'09, pp. 1296–1301.
58. Agarwal R, Popovici E, De Feo O & O'Flynn B (2007) Energy driven choice of error recovery protocols in embedded sensor network systems. In: Proc. IEEE International Conference on Sensor Technologies and Applications, SensorComm '07, pp. 560–565.
59. Sankarasubramaniam Y, Akyildiz I & McLaughlin S (2003) Energy efficiency based packet size optimization in wireless sensor networks. In: Proc. IEEE International Workshop on Sensor Network Protocols and Applications, pp. 1–8.
60. Bin Qaisar S, Karande S, Misra K & Radha H (2007) Optimally mapping an iterative channel decoding algorithm to a wireless sensor network. In: Proc. IEEE International Conference on Communications, pp. 3283–3288.
61. Agarwal R, Popovici E, De Feo O & O'Flynn B (2006) Adaptive wireless sensor networks: A system design approach to adaptive reliability. In: Proc. 2nd International Conference on Wireless Communication and Sensor Networks, WCSN'06.
62. Yitbarek YH, Yu K, Åkerberg J, Gidlund M & Björkman M (2014) Implementation and evaluation of error control schemes in industrial wireless sensor networks. In: Proc. IEEE International Conference on Industrial Technology, pp. 1–6.
63. Luby M (2002) LT codes. In: Proc. IEEE Symposium on Foundations of Computer Science, pp. 271–280.
64. Shokrollahi A (2006) Raptor codes. IEEE Transactions on Information Theory 52(6): 2551–2567.
65. Eckford A, Chu J & Adve R (2006) Low-complexity cooperative coding for sensor networks using rateless and LDGM codes. In: Proc. IEEE International Conference on Communications, volume 4, pp. 1537–1542.

66. Vellambi BN, Subramanian R, Fekri F & Ammar M (2007) Reliable and efficient message delivery in delay tolerant networks using rateless codes. In: Proc. International MobiSys Workshop on Mobile Opportunistic Networking, MobiOpp '07, pp. 91–98. ACM, New York, NY, USA. URI: http://doi.acm.org/10.1145/1247694.1247712.
67. Hagedorn A, Starobinski D & Trachtenberg A (2008) Rateless deluge: Over-the-air programming of wireless sensor networks using random linear codes. In: Proc. International Conference on Information Processing in Sensor Networks, pp. 457–466.
68. Meghji M & Habibi D (2014) Investigating transmission power control for wireless sensor networks based on 802.15.4 specifications. Springer Telecommunications Systems 56(2): 229–310.
69. Nandi A & Kundu S (2010) Optimal transmit power in wireless sensor networks using MRC space diversity in rayleigh fading channel. In: Proc. International Conference on Industrial and Information Systems (ICIIS), pp. 19–24.
70. Marques A, Wang X & Giannakis G (2008) Minimizing transmit power for coherent communications in wireless sensor networks with finite-rate feedback. IEEE Transactions on Signal Processing 56(9): 4446–4457.
71. Holland M, Wang T, Tavli B, Seyedi A & Heinzelman W (2011) Optimizing physical-layer parameters for wireless sensor networks. ACM Transactions on Sensor Networks 7(4): 28:1–28:20.
72. Qing C & Gursoy M (2009) Energy-efficient modulation design for reliable communication in wireless networks. In: Proc. 43rd Annual Conference on Information Sciences and Systems (CISS), pp. 811–816.
73. Abouei J, Plataniotis K & Pasupathy S (2011) Green modulations in energy-constrained wireless sensor networks. IET Communications 5(2): 240–251.
74. Chehri A & Mouftah H (2010) Energy-aware multi-hop transmission for sensor networks based on adaptive modulation. In: Proc. IEEE International Conference on Wireless and Mobile Computing, Networking and Communications (WiMob), pp. 203–207.
75. Costa F & Ochiai H (2010) A comparison of modulations for energy optimization in wireless sensor network links. In: Proc. IEEE Global Telecommunications Conference (GLOBECOM), pp. 1–5.
76. Rabbachin A (2008) Low complexity UWB receivers with ranging capabilities. Ph.D. thesis, University of Oulu.
77. Wang T, Heinzelman W & Seyedi A (2010) Link energy minimization in IR-UWB based wireless networks. IEEE Transactions on Wireless Communications 9(9): 2800–2811.
78. Zou Z, Mendoza DS, Wang P, Zhou Q, Mao J, Jonsson F, Tenhunen H & Zheng LR (2011) A low-power and flexiple energy detection IR-UWB receiver for RFID and wireless sensor neworks. IEEE Transactions on Circuits and Systems 58(7): 1470–1482.
79. Martelli F, Goratti L & Haapola J (2010) Performance of sensor MAC protocols for medical ICT using IR-UWB technology. In: Proc. Health Informatics, HealthInf '10, pp. 13–20.
80. Niemelä V, Hämäläinen M & Iinatti J (2011) IEEE 802.15.4a UWB receivers in medical applications. International Journal on Ultra Wideband Communications and Systems 2(2): 73–82.
81. ams (2014). ams webpage. URI: http://www.ams.com/.
82. Sample A, Yeager D, Powledge P & Smith J (2007) Design of a passively-powered, programmable sensing platform for UHF RFID systems. In: Proc. IEEE International Conference on RFID, pp. 149–156.

83. Le TN, Magno M, Pegatoquet A, Berder O, Sentieys O & Popovici E (2013) Ultra low power asynchronous MAC protocol using wake-up radio for energy neutral WSN. In: Proc. International Workshop on Energy Neutral Sensing Systems, ENSSys '13, pp. 10:1–10:6. ACM, New York, NY, USA. URI: http://doi.acm.org/10.1145/2534208.2534221.
84. Mahlknecht S & Spinola Durante M (2009) WUR-MAC: Energy efficient wakeup receiver based MAC protocol. In: Proc. IFAC International Conference on Fieldbuses & Networks in Industrial & Embedded Systems, FET 2009, pp. 139–143.
85. Marinkovic S & Popovici E (2011) Power efficient networking using a novel wake-up radio. In: Proc. International Conference on Pervasive Computing Technologies for Healthcare (PervasiveHealth), pp. 139–143.
86. Abramson N (1970) The Aloha system: Another alternative for computer communications. In: Proc. Fall Joint Computer Conference, AFIPS '70 (Fall), pp. 281–285. ACM, New York, NY, USA. URI: http://doi.acm.org/10.1145/1478462.1478502.
87. Roberts LG (1975) Aloha packet system with and without slots and capture. ACM SIGCOMM Computer Communication Review 5(2): 28–42.
88. Tobagi FA (1980) Analysis of a two-hop centralized packet radio network - part I: Slotted ALOHA. IEEE Transactions on Communications 28(2): 196–207.
89. Wan T & Sheikh AU (2000) Performance and stability analysis of buffered slotted ALOHA protocols using tagged user approach. IEEE Transactions on Vehicular Technology 49(2): 582–593.
90. Mendes LDP, Rodriques JJPC, Vasilakos AV & Zhou L (2011) Lifetime analysis of a slotted ALOHA-based wireless sensor network using a cross-layer frame rate adaptation scheme. In: Proc. IEEE International Conference on Communications, ICC'11, pp. 1–5.
91. Kleinrock L & Tobagi F (1975) Packet switching in radio channels: Part I–carrier sense multiple-access modes and their throughput-delay characteristics. IEEE Transactions on Communications 23(12): 1400–1416.
92. Karn P (1990) MACA - a new channel access method for packet radio. In: Proc. of 9th ARRL/CRRL Amateur Radio, Computer Networking Conference, pp. 134–140.
93. Bharghavan V, Demers A, Shenker S & Zhang L (1994) MACAW: A media access protocol for wireless LAN's. In: Proc. Conference on Communications Architectures, Protocols and Applications, SIGCOMM' 94, pp. 212–225.
94. Ye W, Heidemann J & Estrin D (2002) An energy-efficient MAC protocol for wireless sensor networks. In: Proc. Twenty-First Annual Joint Conference of the IEEE Computer and Communications Societies, volume 3 of *INFOCOM'02*, pp. 1567–1576.
95. Ye W, Heidemann J & Estrin D (2004) Medium access control with coordinated adaptive sleeping for wireless sensor networks. IEEE/ACM Transactions on Networking 12(3): 493–506.
96. van Dam T & Langendoen K (2003) An adaptive energy-efficient MAC protocol for wireless sensor networks. In: Proc. International Conference on Embedded Networked Sensor Systems, SenSys '03, pp. 171–180. ACM, New York, NY, USA. URI: http://doi.acm.org/10.1145/958491.958512.
97. Polastre J, Hill J & Culler D (2004) Versatile low power media access for wireless sensor networks. In: Proc. International Conference on Embedded Networked Sensor Systems, SenSys '04, pp. 95–107. ACM, New York, NY, USA. URI: http://doi.acm.org/10.1145/1031495.1031508.

98. El-Hoiydi A & Decotignie JD (2004) WiseMAC: An ultra low power MAC protocol for multi-hop wireless sensor networks. Lecture Notes in Computer Science, Algorithmic Aspects of Wireless Sensor Networks 3121: 18–31.
99. Rousselot J, Farserotu J & Decotignie JD (2008) Reconciling ultra low power consumption, low latency and high throughput communications: the WiseMAC-HA protocol. In: Proc. International Symposium on Wireless Personal Multimedia Communications, WPMC '08, pp. 1–5.
100. Ye W, Silva F & Heidemann J (2006) Ultra-low duty cycle MAC with scheduled channel polling. In: Proc. International conference on Embedded networked sensor systems, volume 3 of *SenSys'06*, pp. 321–334.
101. Aghdasi H & Abbaspour M (2008) ET-MAC: An energy-efficient and high throughput MAC protocol for wireless sensor networks. In: Proc. Annual Communication Networks and Services Research Conference, pp. 526–532.
102. Liao WH, Wang HH & Wu WC (2007) An adaptive MAC protocol for wireless sensor networks. In: Proc. IEEE 18th International Symposium on Personal, Indoor and Mobile Radio Communications, pp. 1–5.
103. Zheng SR & Sarangan V (2005) PMAC: an adaptive energy-efficient MAC protocol for wireless sensor networks. In: Proc. IEEE International Parallel and Distributed Processing Symposium, pp. 65–72.
104. Buettner M, Yee GV, Anderson E & Han R (2006) X-MAC: A short preamble MAC protocol for duty-cycled wireless sensor networks. In: Proc. International Conference on Embedded Networked Sensor Systems, SenSys '06, pp. 307–320. ACM, New York, NY, USA. URI: http://doi.acm.org/10.1145/1182807.1182838.
105. Wang H, Zhang X, Nait-Abdesselam F & Khokbar A (2007) DPS-MAC: An asynchronous MAC protocol for wireless sensor networks. Springer Link Lecture Notes in Computer Science 4873: 393–404.
106. Zhen B, Li HB & Kohno R (2008) Clear channel assessment in ultra-wideband sensor networks. IEICE Transactions on Communications E91.B(4): 998–1005.
107. Haapola J, Rabbachin A, Goratti L, Pomalaza-Ráez C & Oppermann I (2009) Effect of impulse radio-ultrawideband based on energy collection in MAC protocol performance. IEEE Transactions on Vehicular Technology 58(8): 4491–4505.
108. Magno M, Jackson N, Mathewson A, Benini L & Popovici E (2013) Combination of hybrid energy harvesters with MEMS piezoelectric and nano-Watt radio wake up to extend lifetime of system for wireless sensor nodes. In: Proc. International Conference on Architecture of Computing Systems (ARCS), pp. 1–6.
109. Lin EY, Rabaey J & Wolisz A (2004) Power-efficient rendez-vous schemes for dense wireless sensor networks. In: Proc. IEEE International Conference on Communications, volume 7, pp. 3769–3776.
110. Heinzelman WB, Chandrakasan A & Balakrishnan H (2000) Energy-efficient communication protocol for wireless microsensor networks. In: Proc. The Hawaii International Conference on System Sciences, pp. 1–10.
111. Sohrabi K & Pottie G (1999) Performance of a novel self-organization protocol for wireless ad-hoc sensor networks. In: Proc. IEEE Vehicular Technology Conference, volume 2, pp. 1222–1226.
112. Rowe A, Mangharam R & Rajkumar R (2006) RT-Link: A time-synchronized link protocol for energy-constrained multi-hop wireless networks. In: Proc. IEEE Communications

Society on Sensor and Ad Hoc Communications and Networks, volume 2, pp. 402–411.
113. Mangharam R, Rowe A & Rajkumar R (2007) FireFly: a cross-layer platform for real-time embedded wireless networks. Real-Time Systems (37): 183–231.
114. IEEE (2011) IEEE Standard for Information Technology–Telecommunications and information exchange between systems–Local and metropolitan area networks–Specific requirements Part 11: Wireless LAN Medium Access Control (MAC) and Physical Layer (PHY) specifications Amendment 10: Mesh Networking. Standard, The Institute of Electrical and Electronics Engineers, Inc. IEEE Std. 802.11s − 2011.
115. Rhee I, Warrier A, Aia M, Min J & Sichitiu M (2008) Z-MAC: A hybrid MAC for wireless sensor networks. IEEE/ACM Transactions on Networking 16(3): 511–524.
116. Pei H, Li X, Soltani S, Mutka M & Ning X (2013) The evolution of MAC protocols in wireless sensor networks: A survey. IEEE Communications Surveys Tutorials 15(1): 101–120.
117. Gobriel S, Mosse D & Cleric R (2009) TDMA-ASAP: Sensor network TDMA scheduling with adaptive slot-stealing and parallelism. In: Proc. IEEE International Conference on Distributed Computing Systems, pp. 458–465.
118. Rajendran V, Obraczka K & Garcia-Luna-Aceves JJ (2006) Energy-efficient, collision-free medium access control for wireless sensor networks. Wireless Networks 12(1): 63–78. URI: http://dx.doi.org/10.1007/s11276-006-6151-z.
119. Paso T, Tanaka H, Hämäläinen M, Chin W, Matsuo R, Subramani S & Haapola J (2015) An overview of ETSI TC SmartBAN MAC protocol. In: Proc. International Symposium on Medical Information and Communication Technology (ISMICT'15), pp. 1–5. Accepted for publication.
120. ETSI TC (2014) Smart body area networks (SmartBAN): Low compexity MAC for SmartBAN. Technical specification, ETSI Technical Committee. TS DTS/SmartBAN-005 V1.1.1 draft.
121. Al-Karaki J & Kamal A (2004) Routing techniques in wireless sensor networks: a survey. IEEE Wireless Communications 11(6): 6–28.
122. ZigBee Alliance (2014). ZigBee Alliance webpage. URI: http://www.zigbee.org.
123. Pantazis N, Nikolidakis S & Vergados D (2013) Energy-efficient routing protocols in wireless sensor networks: A survey. IEEE Communications Surveys Tutorials 15(2): 551–591.
124. Srivastava V & Motani M (2005) Cross-layer design: a survey and the road ahead. IEEE Communications Magazine 43(12): 112–119.
125. Jurdak R (2007) Wireless Ad Hoc and Sensor Networks: A Cross-layer Design Perscpective. Springer Science+Business Media, LLC, Springer Street 233, New York, NY 10013, USA.
126. Vuran MC & Akyildiz IF (2010) XLP: A cross-layer protocol for efficient communication in wireless sensor networks. IEEE Transactions on Mobile Computing 9(11): 1578–1691.
127. Park P, Fischione C, Bonivento A, Johansson K & Sangiovanni-Vincent A (2011) Breath: An adaptive protocol for industrial control applications using wireless sensor networks. IEEE Transactions on Mobile Computing 10(6): 821–838.
128. Cui S, Madan A, Goldsmith A & Lall S (2007) Cross-layer energy and delay optimization in small-scale sensor networks. IEEE Transactions on Wireless Communications 6(10): 3688–3699.
129. Yi S, Hou Y, Sherali H & Midkiff S (2006) Optimal routing for UWB-based sensor networks. IEEE Journal on Selected Areas in Communications 24(4): 857–863.

130. Almi'ani K, Selvakennedy S & Viglas A (2008) RMC: An energy-aware cross-layer data-gathering protocol for wireless sensor networks. In: Proc. International Conference on Advanced Information Networking and Applications, pp. 410–417.
131. Rajendran V, Garcia-Luna-Aveces J & Obraczka K (2005) Energy-efficient, application-aware medium access for sensor networks. In: Proc. IEEE International Conference on Mobile Adhoc and Sensor Systems Conference, pp. 1–8.
132. Kawadia V & Kumar P (2005) Principles and protocols for power control in wireless ad hoc networks. IEEE Journal on Selected Areas in Communications 23(1): 76–88.
133. Kawadia V & Kumar P (2003) Power control and clustering in ad hoc networks. In: Proc. Twenty-Second Annual Joint Conference of the IEEE Computer and Communications., volume 1, pp. 459–469 vol.1.
134. Gao Q, Zhang J, Shen XS & Larish B (2007) A cross-layer optimization approach for energy efficient wireless sensor networks: Coalition-aided data aggregation, cooperative communication, and energy balancing. Advances in Multimedia .
135. van der Schaar M & Sai Shankar N (2005) Cross-layer wireless multimedia transmission: challenges, principles, and new paradigms. IEEE Wireless Communications 12(4): 50–58.
136. Haapola J, Shelby Z, Pomalaza-Raez C & Mähonen P (2005) Cross-layer energy analysis of multihop wireless sensor networks. In: Proc. European Workshop on Wireless Sensor Networks, pp. 33–44.
137. Kulkarni S, Iyer A & Rosenberg C (2006) An address-light, integrated MAC and routing protocol for wireless sensor networks. IEEE/ACM Transactions on Networking 14(4): 793–806.
138. Suh C, Ko YB & Son DM (2006) An energy efficient cross-layer MAC protocol for wireless sensor networks. Springer Link Lecture Notes in Computer Science 3842: 410–419.
139. Xiong Z, Yang Z, Liu W & Feng Z (2006) A lightweight FEC algorithm for fault tolerant routing in wireless sensor networks. In: Proc. International Conference on Wireless Communications, Networking and Mobile Computing, pp. 1–4.
140. Charfi Y, Wakamiya N & Murata M (2007) Adaptive and reliable multi-path transmission in wireless sensor networks using forward error correction and feedback. In: Proc. IEEE Wireless Communications and Networking Conference, pp. 3681–3686.
141. Ruzzelli AG, O'Hare GMP & Jurdak R (2008) MERLIN: cross-layer integration of MAC and routing for low duty-cycle sensor networks. Ad Hoc Networks pp. 1–20.
142. Jurdak R, Baldi P & Lopes C (2007) Adaptive low power listening for wireless sensor networks. IEEE Transactions on Mobile Computing 6(8): 988–1004.
143. Jurdak R, Baldi P & Lopes C (2005) State-driven energy optimization in wireless sensor networks. In: Proc. Systems Communications, pp. 356–363.
144. Vuran MC & Akyildiz I (2007) A-MAC: Adaptive medium access control for next generation wireless terminals. IEEE/ACM Transactions on Networking 15(3): 574–587.
145. Cho J, Kim S, Nam H & An S (2007) An energy-efficient mechanism using CLMAC protocol for wireless sensor networks. In: Proc. Third International Conference on Networking and Services, pp. 1–5.
146. Rossi M & Zorzi M (2007) Integrated cost-based MAC and routing techniques for hop count forwarding in wireless sensor networks. IEEE Transactions on Mobile Computing 6(4): 434–448.
147. Du S, Saha A & Johnson D (2007) RMAC: A routing-enhanced duty-cycle MAC protocol for wireless sensor networks. In: Proc. IEEE International Conference on Computer

Communications, pp. 1478–1486.
148. Cunha F, Mini R & Loureiro A (2012) Sensor-MAC with dynamic duty cycle in wireless sensor networks. In: Proc. IEEE Global Communications Conference (GLOBECOM), pp. 530–536.
149. Vuran MC & Akyildiz IF (2009) Error control in wireless sensor networks: A cross layer analysis. IEEE/ACM Transactions on Networking 17(4): 1186–1199.
150. Memsic Inc (2014). MICAz and MICA2 RF transceiver datasheet. URI: www.memsic.com.
151. Jeong J (2009) Evaluation of network stack optimization techniques for wireless sensor networks. Int. J. Communications, Network and System Sciences 2(8): 720–731.
152. Texas Instruments (2014). CC1000 RF transceiver datasheet. URI: http://www.ti.com/lit/ds/symlink/cc1000.pdf.
153. Naderi MY, Rebiee HR, Khansari M & Salehi M (2012) Error control for multimedia communications in wireless sensor networks: A comparative performance analysis. Elsevier Ad Hoc Networks Journal 10(6): 1028–1042.
154. Kumar V, Raghuvansi AS & Tiwari S (2010) Performance study of beacon-enabled IEEE 802.15.4 standard in WSNs with clustering. In: Proc. International Conference on Power, Control and Embedded Systems (ICPCES), pp. 1–5.
155. Ahn JS, Hong SW & Heidemann J (2005) An adaptive FEC code control algorithm for mobile wireless sensor networks. Journal of Communications and Networks 7(4): 489–499.
156. Garzás JE, Calzón C & Armada A (2007) An energy-efficient adaptive modulation suitable for wireless sensor networks with SER and throughput constraints. EURASIP Journal on Wireless Communications and Networking pp. 1–7.
157. Salameh HB, Shu T & Krunz M (2007) Adaptive cross-layer MAC design for improved energy-efficiency in multi-channel wireless sensor networks. Ad Hoc Networks 5(6): 844–854. URI: http://dx.doi.org/10.1016/j.adhoc.2007.02.011.
158. Huan W, Qiuling T, Xiuyu Y & Tuanfa Q (2009) Cross-layer energy efficiency of orthogonal modulations in TDMA-based wireless sensor networks. In: Proc. International Conference on Computer Science Education (ICCSE), pp. 404–407.
159. Paso T, Niemelä V, Haapola J & Iinatti J (2012) Novel modulation adaptation techniques for IEEE 802.15.4a UWB system. In: Proc. International Symposium on Medical Information and Communication Technology (ISMICT).
160. Messier G, Hartwell J & Davies R (2008) A sensor network cross-layer power control algorithm that incorporates multiple-access interference. IEEE Transactions on Wireless Communications 7(8): 2877–2883.
161. Gajjar S, Pradhan S & Dasgupta K (2011) Wireless sensor network: Application led research perspective. In: Proc. Recent Advances in Intelligent Computational Systems (RAICS), 2011 IEEE, pp. 25–30.
162. Kawadia V & Kumar P (2005) A cautionary perspective on cross-layer design. IEEE Wireless Communications 12(1): 3–11.
163. Melodia T, Vuran MC & Pompili D (2006) The state of the art in cross-layer design for wireless sensor networks. In: Proc. International Conference on Wireless Systems and Network Architectures in Next Generation Internet, EURO-NGI'05, pp. 78–92.
164. Freedman D (1983) Markov Chains. Springer-Verlag, New York, NY, USA.
165. Bianchi G (2000) Performance analysis of the IEEE 802.11 distributed coordination function. IEEE Journal on Selected Areas in Communications 18(3): 535–547.

166. Pollin S, Ergen M, Ergen S, Bougard B, Der Perre L, Moerman I, Bahai A, Varaiya P & Catthoor F (2008) Performance analysis of slotted carrier sense IEEE 802.15.4 medium access layer. IEEE Transactions on Wireless Communications 7(9): 3359–3371.
167. Faridi A, Palattella M, Lozano A, Dohler M, Boggia G, Grieco L & Camarda P (2010) Comprehensive evaluation of the IEEE 802.15.4 MAC layer performance with retransmissions. IEEE Transactions on Vehicular Technology 59(8): 3917–3932.
168. Park P, Di Marco P, Soldati P, Fischione C & Johansson K (2009) A generalized Markov chain model for effective analysis of slotted IEEE 802.15.4. In: Proc. IEEE 6th International Conference on Mobile Adhoc and Sensor Systems, 2009. MASS '09., pp. 130–139.
169. Mišić J, Shafi S & Mišić VB (2005) The impact of MAC parameters on the performance of 802.15.4 PAN. Ad Hoc Networks 3(5): 509–528. URI: http://dx.doi.org/10.1016/j.adhoc.2004.08.002.
170. Cassioli D, Win M & Molisch AF (2002) The ultra-wide bandwidth indoor channel: From statistical model to simulations. IEEE Journal on Selected Areas in Communications 20(6): 1247–1257.
171. Molisch AF, Cassioli D, Chong CC, Emami S, Fort A, Balakrishnan K, Karedal J, Kunisch J, Schantz HG, Siwiak K & Win MZ (2006) A comprehensive standardized model for ultrawideband propagation channels. IEEE Transactions on antennas and propagation 54(11): 3151–3166.
172. Rycaert J, Desset C, Fort A, Badaroglu M, De Heyn V, Wambacq P, Van der Plas G, Donnay S, Van Poucke B & Gyselinckxs B (2005) Ultra-wide-band transmitter for low-power wireless body area networks: Design and evaluation. IEEE Transactions on Circuits and Systems 52(12): 2515–2525.
173. Daly DC, Mercier PP, Bhardwaj M, Stone AL, Aldworth ZN, Daniel TL, Voldman J, Hildebrand JG & Chandrakasan AP (2010) A pulsed UWB receiver SoC for insect motion control. IEEE Journal on Solid State Circuits 45(1): 153–166.
174. FCC (2002) First Reports and Order in the Matter of Revision of Part 15 of the Commission's Rules Regarding Ultra-Wideband Transmission Systems. Recommendation, ET−Docket 98−153, FCC 02−48.
175. Taylor J (1995) Introduction to ultra-wideband radar systems. CRC Press, Boca Raton, FL USA.
176. DecaWave (2013). Decawave company webpage. URI: http://www.decawave.com.
177. Zebra Technologies (2014). Zebra technologies webpage. URI: http://www.zebra.com.
178. Ubisense (2014). Ubisense company webpage. URI: http://www.ubisense.net.
179. Niemelä V, Haapola J, Hämäläinen M & Iinatti J (2012) Integration interval and threshold evaluation for an energy detector receiver with PPM and OOK modulations. In: Proc. International Conference on Body Area Networks, BodyNets '12, pp. 242–248. ICST (Institute for Computer Sciences, Social-Informatics and Telecommunications Engineering), ICST, Brussels, Belgium, Belgium. URI: http://dl.acm.org/citation.cfm?id=2442691.2442747.
180. Hämäläinen M, Niemelä V, Iinatti J & Kohno R (2012) Performance of UWB receivers using IEEE802.15.4a's minimum burst lengths. In: Proc. International Symposium on Medical Information and Communication Technology (ISMICT), pp. 1–4.
181. Nakagami M (1960) The m-distribution - a general formula of intensity distribution of rapid fading. Statistical Methods of Radio Wave Propagation, Pergamon Press pp. 3–36.
182. Tarique M & Hasan T (2011) Impact of Nakagami-m fading model on multi-hop mobile ad hoc network. International Journal of Computer Applications 26(2): 5–12.

183. Quek TQS & Win MZ (2005) Analysis of UWB transmitted-reference communication systems in dense multipath channels. IEEE Journal on Selected Areas in Communications 23(9): 1863–1874.
184. Karvonen H & Goratti L (2010) Optimal code rate for wireless sensor networks using IR-UWB and non-coherent detection. In: Proc. IEEE International Conference on Mobile Ad-hoc and Sensor Systems (MASS'10), pp. 492–500.
185. Demirkol I, Ersoy C, Alagöz F & Delic H (2009) The impact of a realistic packet traffic model on the performance of surveillance wireless sensor networks. Elsevier Computer Networks Journal 53(3): 382–399.
186. Taylor H & Karlin S (1988) An Introduction to Stochastic Modeling. Academic Press, An Imprint of Elsevier, 525 B St., Suite 1900, San Diego, California 92101-4495, USA, 3rd. edition.
187. Tanenbaum AS & Wetherall DJ (2011) Computer Networks. Pearson Education, Inc., publishing as Prentice Hall, 501 Boylston Street, Suite 900, Boston, Massachusetts 02116, USA, 5th. edition.
188. Jiang J & Narayanan KR (2006) Iterative soft-input soft-output decoding of Reed-Solomon codes by adapting the parity-check matrix. IEEE Transactions on Information Theory 52(8): 3746–3756.
189. Koetter R & Vardy A (2003) Algebraic soft-decision decoding of Reed-Solomon codes. IEEE Transactions on Information Theory 49(11): 2809–2825.
190. Bellorado J & Kavcic A (2010) Low-complexity soft-decoding algorithms for Reed-Solomon codes-part I: An algebraic soft-in hard-out chase decoder. IEEE Transactions on Information Theory 56(3): 945–959.
191. Gross WJ, Kschischang FR, Koetter R & Gulak PG (2006) Applications of algebraic soft-decision decoding of Reed-Solomon codes. IEEE Transactions on Communications 54(7): 1224–1234.
192. Buratti C & Verdone R (2008) A hybrid hierarchical architecture: From a wireless sensor network to the fixed infrastructure. In: Proc. Wireless Conference, EW 2008.
193. Khan Z, Catalot D & Thiriet J (2009) Hierarchical wireless network architecture for distributed applications. In: Proc. Wireless and Mobile Communications, ICWMC '09, pp. 70–75.
194. Yang J, Gao Y & Zhang Z (2011) Cluster-based routing protocols in wireless sensor networks: A survey. In: Proc. International Conference on Computer Science and Network Technology, volume 3 of *ICCSNT '11*, pp. 1659–1663.
195. Kumar D, Aserib TC & Patelc RB (2009) EEHC: Energy efficient heterogeneous clustered scheme for wireless sensor networks. Journal of Computer Communications 32.
196. Wu M & Collier M (2011) Extending the lifetime of heterogeneous sensor networks using a two-level topology. In: Proc. IEEE International Conference on Computer and Information Technology, pp. 499–504.
197. Slimane JB, Song YQ, Koubâa A & Frikha M (2009) A three-tiered architecture for large-scale wireless hospital sensor networks. In: Proc. The International Workshop on Mobilizing Health Information to Support Healthcare-related Knowledge Work, MobiHealthInf 2009, pp. 1–12.
198. Zhang M, Song J & Zhang Y (2005) Three-tiered sensor networks architecture for traffic information monitoring and processing. In: Proc. Intelligent Robots and Systems, IROS 2005, pp. 2291–2296.

199. Kulkarni P, Ganesan D, Shenoy P & Lu Q (2005) SensEye: A multitier camera sensor network. In: Proc. ACM International Conference on Multimedia, MM '05, pp. 229–238.
200. Lopes CER, Linhares FD, Santos MM & Ruiz LB (2007) A multi-tier, multimodal wireless sensor network for environmental monitoring. Springer Link Lecture Notes in Computer Science 4611: 589–598.
201. Zatout Y, Campo E & Llibre JF (2009) WSN-HM: Energy-efficient wireless sensor network for home monitoring. In: Proc. International Conference on Intelligent Sensors, Sensor Networks and Information Processing, ISSNIP '09, pp. 367–372.
202. Stefanov A & Stojanovic M (2010) Hierarchical underwater acoustic sensor networks. In: Proc. ACM International Workshop on UnderWater Networks, WUWNet'10, pp. 1–4.
203. The ISA100 Committee (2014). The ISA100 Standards, Wireless Systems for Automation. URI: http://www.isa.org/isa100.
204. Suhonen J, Kivelä O, Laukkarinen T & Hännikäinen M (2012) Unified service access for wireless sensor networks. In: International Workshop on Software Engineering for Sensor Network Applications, SESENA 2012, pp. 49–55.
205. FriendlyARM (2014). FriendlyARM Mini6410 specification. URI: http://www.friendlyarm.net/products/mini6410.
206. Kuorilehto M, Kohvakka M, Suhonen J, Hämäläinen P, Hännikäinen M & Hämäläinen T (2007) *Ultra-Low Energy Wireless Sensor Networks in Practice: Theory, Realization and Deployment*. John Wiley & Sons.
207. Cattani M, Zuniga M, Woehrle M & Langendoen K (2014) SOFA: communication in extreme wireless sensor networks. In: Proc. Wireless Sensor Networks - 11th European Conference, EWSN 2014, pp. 100–115.
208. Pak W, Cho KT, Lee J & Bahk S (2008) W-MAC: Supporting ultra low duty cycle in wireless sensor networks. In: Proc. IEEE Global Telecommunications Conference, IEEE GLOBECOM 2008., pp. 1–5.
209. Boulis A, Smith D, Miniutti D, Libman L & Tselishchev Y (2012) Challenges in body area networks for healthcare: the MAC. IEEE Communications Magazine 50(5): 100–106.
210. Dargie W, Chao X & Denko MK (2009) Modelling the energy cost of a fully operational wireless sensor network. Springer Telecommunication Systems Journal 44(1-2): 3–15.
211. Garcia M, Sendra S, Lloret J & Canovas A (2011) Saving energy and improving communications using cooperative group-based wireless sensor networks. Springer Telecommunication Systems Journal 52(4): 2489–2502.
212. Cheng L, Jiao W, Chen M, Chen C & Ma J (2011) Wait, focus and spray: efficient data delivery in wireless sensor networks with ubiquitous mobile data collectors. Springer Telecommunication Systems Journal 52(4): 2501–2517.
213. Ullah S, Higgins H, Braem B, Latre B, Blondia C, Moerman I, Saleem S, Rahman Z & Kwak KS (2012) A comprehensive survey of wireless body area networks. Springer Medical Systems 36(3): 1065–1094.
214. Sthapit P & Pyun JY (2011) Medium reservation based sensor MAC protocol for low latency and high energy efficiency. Springer Telecommunication Systems Journal 52(4): 2387–2395.
215. Ullah S & Kwak KS (2011) Throughput and delay limits of IEEE 802.15.6. In: Proc. IEEE Wireless Communications & Networking Conference (WCNC).
216. Tachtatzis C (2010) An energy analysis of IEEE 802.15.6 scheduled access modes. In: Proc. IEEE Global Communications Conference (GLOBECOM).

217. Rashwand S, Misic J & Khazaei H (2011) IEEE 802.15.6 Under Saturation: Some Problems to Be Expected. IEEE Communications Magazine 13(2): 142–148.
218. Rashwand S & Misic J (2011) Performance evaluation of IEEE 802.15.6 under non-saturation condition. In: Proc. IEEE Global Communications Conference (GLOBECOM).
219. Hernandez M & Kohno R (2011) UWB on-off waveform coded modulation for body area networks. In: Proc. IEEE International Conference on Ultra-Wideband (ICUWB).
220. IEEE P80215 (2009) IEEE P802.15 Working Group for WBANs - Channel Model for Body Area Network (BAN). Technical report, The Institute of Electrical and Electronics Engineers, Inc.
221. Dotlic I & Kohno R (2011) Preamble structure and synchronization for IEEE 802.15.6 impulse-radio ultra-wideband physical layer. In: Proc. International Symposium on Medical Information and Communication Technology (ISMICT).
222. Goel M & Shanbhag NR (1999) Low power channel coding via dynamic reconfiguration. In: Proc. IEEE International Conference on Acoustic, Speech, and Signal Processing (ICASSP).
223. Biard L & Noguet D (2008) Reed-Solomon codes for low power communications. Journal of Communications, Academy publisher 3(2).
224. Desset C & Fort A (2003) Selection of channel coding for low-power wireless systems. In: Proc. IEEE Vehicular Technology Conference (VTC).
225. Berlekamp E (1968) Nonbinary BCH decoding. IEEE Transactions on Information Theory 14(2).
226. Massey J (1969) Shift-register synthesis and BCH decoding. IEEE Transactions on Information Theory, 15(1): 122–127.
227. Chien R (1964) Cyclic decoding procedures for Bose-Chaudhuri-Hocquenghem codes. IEEE Transactions on Information Theory 10(4): 357–363.

504. Rezazadegan Tavakoli, Hamed (2014) Visual saliency and eye movement : modeling and applications

505. Tuovinen, Tommi (2014) Operation of IR-UWB WBAN antennas close to human tissues

506. Vasikainen, Soili (2014) Performance management of the university education process

507. Jurmu, Marko (2014) Towards engaging multipurpose public displays : design space and case studies

508. Namal, Suneth (2014) Enhanced communication security and mobility management in small-cell networks

509. Huang, Xiaohua (2014) Methods for facial expression recognition with applications in challenging situations

510. Ala-aho, Pertti (2014) Groundwater-surface water interactions in esker aquifers : from field measurements to fully integrated numerical modelling

511. Torabi Haghighi, Ali (2014) Analysis of lake and river flow regime alteration to assess impacts of hydraulic structures

512. Bordallo López, Miguel (2014) Designing for energy-efficient vision-based interactivity on mobile devices

513. Suopajärvi, Hannu (2014) Bioreducer use in blast furnace ironmaking in Finland : techno-economic assessment and CO_2 emission reduction potential

514. Sobocinski, Maciej (2014) Embedding of bulk piezoelectric structures in Low Temperature Co-fired Ceramic

515. Kulju, Timo (2014) Utilization of phenomena-based modeling in unit operation design

516. Karinkanta, Pasi (2014) Dry fine grinding of Norway spruce (*Picea abies*) wood in impact-based fine grinding mills

517. Tervo, Valtteri (2015) Joint multiuser power allocation and iterative multi-antenna receiver design

518. Jayasinghe, Laddu Keeth Saliya (2015) Analysis on MIMO relaying scenarios in wireless communication systems

519. Partala, Juha (2015) Algebraic methods for cryptographic key exhange

Book orders:
Granum: Virtual book store
http://granum.uta.fi/granum/

UNIVERSITY OF OULU P.O. Box 8000 FI-90014 UNIVERSITY OF OULU FINLAND

ACTA UNIVERSITATIS OULUENSIS

UNIVERSITY of OULU
OULUN YLIOPISTO

ISBN 978-952-62-0749-0 (Paperback)
ISBN 978-952-62-0750-6 (PDF)
ISSN 0355-3213 (Print)
ISSN 1796-2226 (Online)